UNIVERSIDADE DE SÃO PAULO
INSTITUTO DE QUÍMICA DE SÃO CARLOS
DEPARTAMENTO DE QUÍMICA E FÍSICA MOLECULAR

João Victor Basolli Borsatto

Avaliação e aplicação de fases estacionárias derivadas de grafeno em cromatografia líquida

São Carlos
2023

João Victor Basolli Borsatto

Avaliação e aplicação de fases estacionárias derivadas de grafeno em cromatografia líquida

Tese apresentada ao Instituto de Química de São Carlos da Universidade de São Paulo como requisito necessário para a obtenção do título de Doutor em Ciências.

Área de concentração: Química Analítica e Inorgânica

Orientador: Prof. Dr. Fernando Mauro Lanças

São Carlos
2023

Assinatura: João Victor Basolli Borsatto
Data: 29 de Outubro de 2023

Ficha Catalográfica elaborada pela Seção de Referência e Atendimento ao Usuário do SBI/IQSC

Borsatto, João Victor Basolli
Avaliação e aplicação de fases estacionárias derivadas de grafeno em cromatografia líquida / João Victor Basolli Borsatto. — São Carlos, 2023.
138 f.

Tese (Doutorado em Química Analítica e Inorgânica) — Instituto de Química de São Carlos / Universidade de São Paulo, 2023.
Edição revisada

Orientador: Prof. Dr. Fernando Mauro Lanças

1. Fases estacionárias. 2. Cromatografia líquida. 3. SiGO-C18ec. 4. Derivados de grafeno. 5. LC miniaturizada. I. Título.

Wilneide do C. M. Maiorano - CRB: 3978/8

Agradecimentos

À minha família pelo apoio incondicional durante esse período, em especial à minha mãe, Lisete C. B. Borsatto, meu pai, João Borsatto Filho, e meu irmão, Lucas B. Borsatto.

Ao Prof. Dr. Fernando M. Lanças pela orientação durante o doutorado.

Ao Prof. Dr. Alejandro Cifuentes pela supervisão durante o doutorado-sanduíche.

À M.Sc Elaine A. A. F. Gobato e ao Dr. Guilherme, M. Titato por toda a ajuda e dedicação durante o período de mestrado.

À Prof. Dr. Elena Ibáñez e ao Prof. Dr. José A. M. León por toda ajuda durante o doutorado-sanduíche.

Ao Instituto de Química de São Carlos, São Carlos, Brasil e a Universidade de São Paulo por me permitirem realizar o doutorado.

Ao Instituto de Investigación en Ciencias de la Alimentación, Madrid, Espanha por me permitir realizar o doutorado-sanduíche.

Aos meus colegas de grupo do Croma pela ajuda e colaboração durante esse período, em especial, à Dr. Juliana S. S. Burato, pela colaboração cientifica e Dr. Edivaldo. S. V. Maciel pelas colaborações cientificas e por ter gentilmente cedido as fases utilizadas durante esse doutorado.

Aos colegas do grupo Foodomics pela ajuda e colaboração durante o período de doutorado-sanduíche.

A todos os funcionários do IQSC, técnicos de equipamentos, da seção de pós-graduação, da biblioteca e demais setores por toda ajuda fornecida durante o doutorado.

Ao Conselho Nacional de Desenvolvimento Científico (CNPq) pela bolsa de doutorado concedida (Processos 142513/2019-9 e 142396/2018-4).

À Coordenação de Aperfeiçoamento de Pessoal de Nível Superior (CAPES) pela bolsa de doutorado-sanduíche concedida (Processo 88887.695324/2022-00).

À Fundação de Amparo à Pesquisa do estado de São Paulo (FAPESP) pelo apoio indireto à pesquisa realizada no doutorado (Processos 2019/22724-7 e 2017/02147-0)

Ao Ministério de Ciência e Inovação Espanhol pelo apoio indireto à pesquisa realizada no doutorado (Projeto PID2020-113050RB-I00)

Resumo

O grafeno e seus derivados são materiais com crescente aplicação em química analítica, especialmente no seu uso como sorventes. Na última década, derivados de grafeno vêm sendo aplicados com sucesso como sorventes nas etapas de preparo de amostras, tanto em técnicas off-line quanto em técnicas online. Devido ao sucesso nessa área, também se acreditou que esse tipo de material poderia ser aplicado como fase estacionária em cromatografia líquida; essa expectativa vem sendo continuamente confirmada com os recentes avanços descritos na literatura. Este trabalho visa contribuir com os estudos sobre a aplicação de fases estacionárias compostas por materiais baseados em grafeno em cromatografia líquida, especialmente no uso de partículas de óxido de grafeno funcionalizadas com octadecilsilano fixadas sobre partículas de sílica e submetidas ao processo de endcapping (SiGO-C18ec). Para tal, foram selecionadas diversas aplicações, tanto em análises quantitativas quanto em análises qualitativas. Pesticidas, fármacos, hormônios e outros tipos de compostos foram selecionados para realizar as avaliações. Separações em modos isocráticos e gradiente foram aplicadas e estudadas. Em resumo, observou-se que fases de SiGO-C18ec possuem seletividade diferente das fases de C18 convencional. Além disso, observou-se que o diâmetro da partícula utilizada afeta a performance da separação. As colunas de SiGO-C18ec podem ser utilizadas como alternativas às colunas de C18 para determinados casos e, também, não são um fator limitante, permitindo análises qualitativas e quantitativas bem-sucedidas. A vida útil dessas colunas não foi determinada, continuando operacionais após mais de 300 separações. Adicionalmente, limitações do uso desse tipo de coluna são descritas.

Esta tese apresenta uma coletânea de artigos que discutem a aplicação de materiais derivados de grafeno como fase estacionária em cromatografia líquida. O primeiro capítulo dessa tese aborta uma introdução que fundamenta os conceitos básicos de sorventes de grafeno e cromatografia líquida, os quais são os principais temas abordados nessa tese. O segundo capítulo explica as razões para a seleção de cada trabalho para compor essa tese. O terceiro capítulo apresenta uma revisão do estado-da-arte do uso de sorventes de grafeno em análises de alimentos por cromatografia líquida, explorando aplicações recentes e tendências futuras. O quarto capítulo discute a utilização de colunas capilares em cromatografia líquida acoplada a espectrometria de massas, mencionando as bases teóricas utilizadas para planejar as séries experimentais e analisar os resultados. O quinto capítulo apresenta os resultados do emprego de partículas de SiGO-C18ec como fase estacionária em colunas capilares analíticas, comparando seu desempenho e seletividade com uma coluna empacotada com partículas de C18. O sexto capítulo aborda a aplicação das fases de SiGO-C18ec para a análise de hormônios em amostras de urina, utilizando um sistema column-switching. Já o sétimo capítulo apresenta a técnica de extração líquida online (OLE) para análise de lipídios em amostras naturais, mostrando que a coluna de SiGO-C18ec apresentou melhor desempenho do que uma coluna de C18 convencional. O oitavo capítulo discute a construção de um sistema bidimensional composto exclusivamente por colunas empacotadas com fases baseadas em grafeno, aplicado na análise de pesticidas em refrigerantes de laranja. Por fim, o nono capítulo conclui a tese apresentando as principais observações realizadas e apontando possíveis ramificações desse trabalho.

Abstract

Graphene and its derivatives are materials with increasing application in analytical chemistry, especially in their use as sorbents. In the last decade, graphene derivatives have been successfully applied as sorbents in the stages of sample preparation, both in offline and online techniques. Due to the success in this area, it was also believed that this type of material could be applied as a stationary phase in liquid chromatography; this expectation has been continuously confirmed with the recent advances described in the literature. This work aims to contribute to the studies on the application of stationary phases composed of graphene-based materials in liquid chromatography, especially in the use of graphene oxide particles functionalized with octadecylsilane fixed on silica particles and subjected to the endcapping process (SiGO-C18ec). For this, various applications were selected, both in quantitative and qualitative analyses. Pesticides, drugs, hormones and other types of compounds were selected to conduct the evaluations. Separations in isocratic and gradient modes were applied and studied. In summary, it was observed that SiGO-C18ec phases have different selectivity from conventional C18 phases. In addition, it was observed that the diameter of the particle used affects the performance of the separation. The SiGO-C18ec columns can be used as alternatives to C18 columns for certain cases and are also not a limiting factor, allowing successful qualitative and quantitative analyses. The lifespan of these columns was not determined, remaining operational after more than 300 separations. Additionally, limitations of the use of this type of column are described.

This thesis presents a collection of articles that discuss the application of graphene-derived materials as a stationary phase in liquid chromatography, especially in the use of octadecylsilane-functionalized graphene oxide particles fixed on silica particles and subjected to the endcapping process (SiGO-C18ec). The first chapter presents an introduction that lays the foundation for the basic concepts of graphene sorbents and liquid chromatography, which are the main topics addressed in this thesis. The second chapter explains the reasons for selecting each work to compose this thesis. The third chapter presents a review of the state-of-the-art use of graphene sorbents in analytical methods, exploring recent applications and future trends. Chapter 4 discusses the use of capillary columns in liquid chromatography coupled to mass spectrometry, mentioning the theoretical bases used to plan experimental series and analyze results. Chapter 5 presents the results of the use of SiGO-C18ec particles as a stationary phase in analytical capillary columns, comparing their performance and selectivity of this phase with a column packed with C18 particles. Chapter 6 addresses the application of SiGO-C18ec phases for the analysis of hormones in urine samples, using a column-switching system. Chapter 7 presents the online liquid extraction (OLE) technique for lipid analysis in natural samples, showing that the SiGO-C18ec column performed better than a conventional C18 column. Chapter 8 discusses the construction of a two-dimensional system composed exclusively of columns packed with graphene-based phases, applied to the analysis of pesticides in orange flavored soft drinks. Finally, Chapter 9 concludes the thesis by presenting the main observations made and pointing out possible ramifications of this work.

Sumário

Capítulo 1

Introdução

1.1. O grafeno e seus derivados

Recentemente, o grafeno e seus derivados têm atraído grande interesse na área de pesquisa e desenvolvimento (JOSHI et al., 2021; JUSTINO et al., 2017; SITKO; ZAWISZA; MALICKA, 2013; YU et al., 2020). Esses materiais são constituídos predominantemente de átomos de carbono hibridizados SP2, organizados em uma rede hexagonal planar por meio de ligações covalentes σ e π paralelas (JOSHI et al., 2021) (Figura 1). Apesar de relativamente novos, cujas primeiras aplicações relatam do início desse século, o grafeno e seus derivados têm sido largamente empregados em química analítica, devido às suas características intrínsecas (SITKO; ZAWISZA; MALICKA, 2013). Entre estas, destacam-se alta condutividade elétrica, resistência mecânica, baixa densidade, alto rendimento de dispersão de luz e, portanto, excelente aplicabilidade em sensores e detectores (JUSTINO et al., 2017). Ademais, a grande área superficial desses materiais implica em alta capacidade de adsorção, o que resultou em diversas pesquisas no desenvolvimento de catalisadores e adsorventes (LIU; SHI; JIANG, 2012). Consequentemente, materiais derivados de grafeno são cada vez mais utilizados em preparação de amostras e cromatografia, tornando-se destaque na última década (DE TOFFOLI et al., 2018; LI; XIA, 2012).

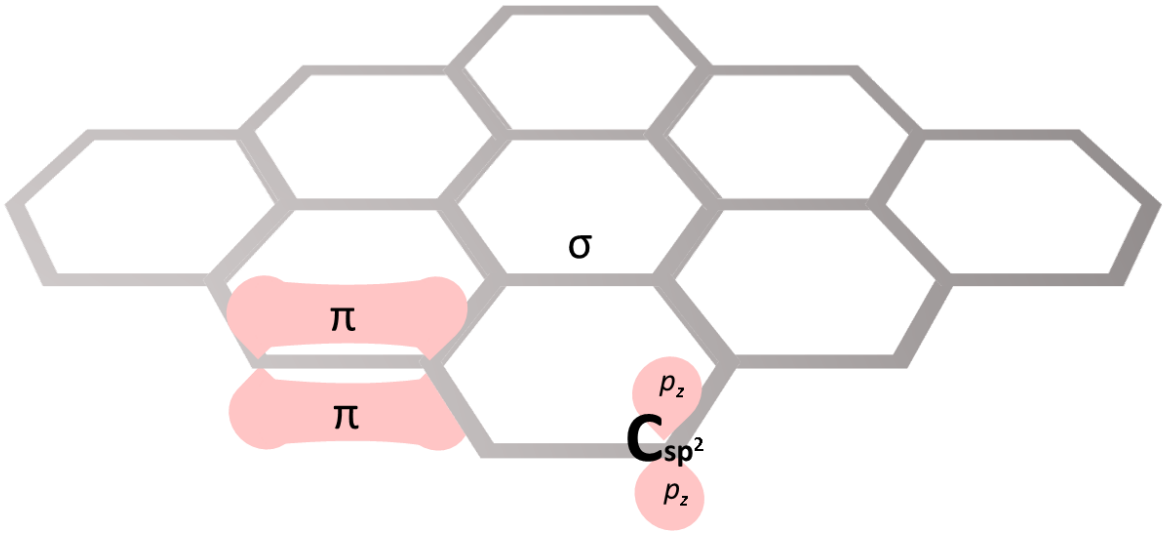

Figura 1. Ilustração representando a estrutura de uma folha de grafeno. Fonte: Autoria própria.

1.2. A produção de derivados de grafeno

Embora o grafeno tenha um grande potencial de aplicação devido às suas qualidades únicas, a fabricação em escala industrial ainda representa um obstáculo para sua ampla implementação em diversas áreas (KUMAR et al., 2021). Isso ocorre porque um dos métodos de fabricação mais comuns é o processo de esfoliação mecânica do grafite por fita adesiva, o qual possui como principal limitação a alta dependência de manipulação humana (NOVOSELOV et al., 2004). Esse processo ocorre exatamente como o nome sugere: uma barra de grafite é esfoliada utilizando fita adesiva, manualmente, de forma que as folhas de grafeno fiquem presas ao adesivo. Esse processo é repetido sucessivas vezes a fim de se obter camadas cada vez mais finas de grafite até a formação de folhas de grafeno (NOVOSELOV et al., 2004). Devido a essas limitações, rotas alternativas para produzir grandes quantidades de folhas de grafeno de alta qualidade são exploradas (KUMAR et al., 2021). Dentre as rotas alternativas, a esfoliação química tem mostrado resultados interessantes, sendo uma forma prática e relativamente menos manual de obter esse material (YU et al., 2020), a qual inclui o método de Hummers, (HUMMERS; OFFEMAN, 1958). O método de Hummers é um processo químico que pode ser usado para gerar óxido de grafite através da adição de permanganato de potássio a uma solução de grafite, nitrato de sódio e ácido sulfúrico (HUMMERS; OFFEMAN, 1958). Após a obtenção das folhas de derivados de grafeno, esse material pode ser modificado sucessivas vezes para a formação de novos materiais que podem ser empregados em diferentes aplicações (JOSHI et al., 2021; YU et al., 2020). A Figura 2 ilustra a rota mais comum para a obtenção de derivados de grafeno para uso em química analítica.

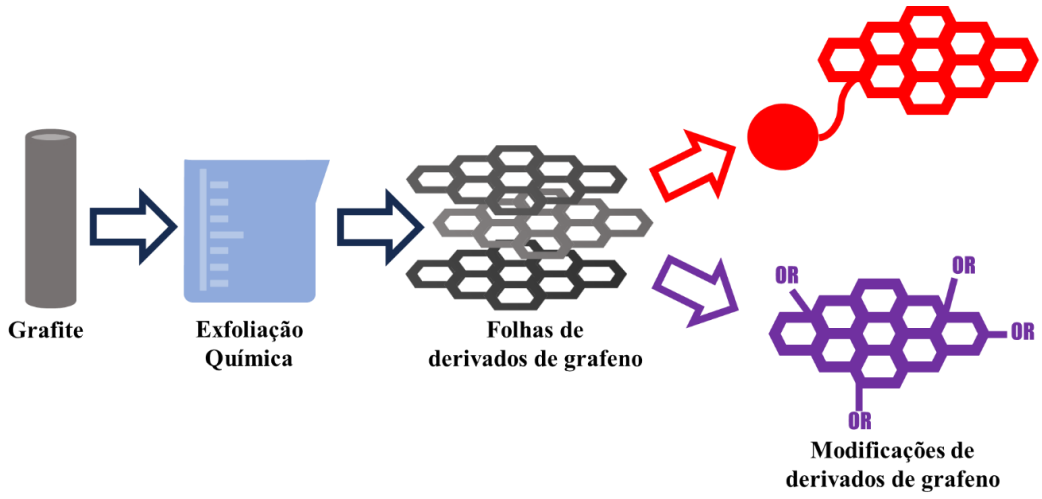

Figura 2. Representação simplificada do processo de produção de derivados de grafeno. Fonte: Autoria própria.

1.3. O grafeno como sorvente

Uma das mais interessantes aplicações de materiais baseados em grafeno está no seu uso como sorvente (LANÇAS et al., 2021). Isso ocorre porque as folhas de grafeno e seus derivados possuem características bidimensionais, o que significa que uma pequena quantidade de massa apresenta uma grande área superficial (DE TOFFOLI et al., 2018; SITKO; ZAWISZA; MALICKA, 2013). Consequentemente, quanto maior a área superficial de um material, maior sua capacidade de sorção (AUGUSTO et al., 2010). Diversos materiais baseados em grafeno vêm sendo aplicados no preparo de amostra para uma grande gama de aplicações (LIU; SHI; JIANG, 2012). Entre essas aplicações, pode-se destacar seu uso em técnicas como: (i) *stir bar sorptive extraction* (extração por sorção em barra magnética) - SBSE (MADEJ et al., 2019), uma técnica na qual uma barra magnética recoberta por fase de extração é inserida em uma solução contendo a amostra; (ii) *dispersive solid phase micro-extraction* (micro-extração por fase sólida dispersiva) - d-SPME (SONG et al., 2022), uma técnica na qual a fase de extração na forma de pó é inserida na solução de amostra; (iii) hollow-fiber solid phase microextraction (micro-extração por fase sólida em fibra oca) - HF-SPME (MA et al., 2014), uma técnica na qual a fase de extração é fixada na parede interna de um capilar, formando uma fibra oca, e então inserida na solução de amostra; (iv) solid phase extraction (extração por fase sólida) - SPE (WANG; LU; CUI, 2021), uma técnica na qual a fase de extração é empacotada em uma um cartucho, no qual a amostra é percolada; e (v) *pipett tip solid phase micro-extraction* (micro-extração por fase sólida em ponta de pipeta) - PT-SPME (ZHANG et al., 2021a), uma técnica na qual a fase de extração é empacotada em uma ponta de pipeta a fim de formar um cartucho, no qual a amostra e percolada. A Figura 3 ilustra os dispositivos de SPE e SBSE para preparo de amostra. Usualmente, os materiais derivados de grafeno usados em técnicas de preparo de amostras apresentam alguma modificação, seja essa na estrutura do grafeno, como óxido de grafeno (GOLZARI AQDA et al., 2019) ou grafeno reduzido (ZHANG et al., 2021b), ou na sua fixação, como partículas de sílica (MEJÍA-CARMONA; LANÇAS, 2020) ou em *zeólitos* (ZHANG et al., 2021a), por exemplo.

Figura 3. Representação de dispositivos de preparo de amostras produzidos com derivados de grafeno. Fonte: Autoria própria.

1.4 O óxido de grafeno

Dentre os derivados mais interessantes de grafeno para ser usado como sorvente, está o óxido de grafeno (GO). Este material possui grupos OH em sua superfície, permitindo sua funcionalização com diferentes grupos funcionais (YU et al., 2020). Ao fixar covalentemente folhas de óxido de grafeno a uma partícula ou superfície de um capilar, ocorre um grande aumento nas possibilidades de aplicação (GOLZARI AQDA et al., 2019; JOSHI et al., 2021). Por exemplo, folhas de óxido de grafeno não fixadas a suportes não podem ser utilizadas em cartuchos de extração por fase sólida porque a passagem de fluxo faz com que essas folhas soltas se acumulem na extremidade dos cartuchos e entupam o sistema. No entanto, quando o óxido de grafeno é fixado a partículas de sílica (SiGO), esse material pode ser empacotado em cartuchos e colunas sem o risco de entupimento (MEJÍA-CARMONA; LANÇAS, 2020). Destaque especial pode ser dado às funcionalizações de partículas de SiGO com C18 e *endcapping* (SiGO-C18ec). Esse material combina o potencial sorvente dos anéis aromáticos das folhas de grafeno (material inovador) com o potencial sorvente das cadeias alifáticas do C18 (tradicional em fases de extração) (BORSATTO; MACIEL; LANÇAS, 2022). A Figura 4 mostra um exemplo de partículas de SiGO-C18ec utilizadas nesse trabalho. Nessa figura, é possível ver a diversidade de materiais presentes no meio de empacotamento, incluindo partículas recobertas por óxido de grafeno e folhas de oxido de grafeno não ligadas.

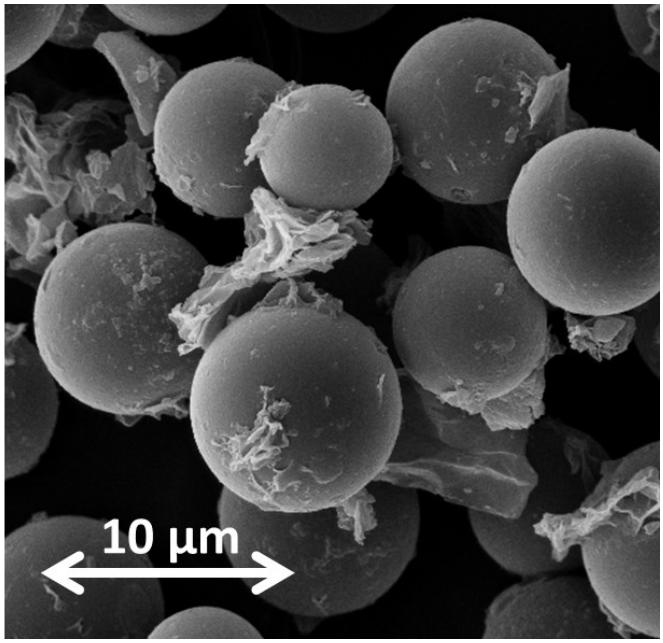

Figura 4. Micrografia obtida através de microscopia eletrônica de varredura (MEV) para um conjunto de partículas de SiGO-C18ec de 10 µm de diâmetro. Fonte: Autoria própria.

1.5 O grafeno em cromatografia líquida

Além das aplicações em preparo de amostras, materiais derivados de grafeno também estão sendo aplicados na produção de colunas para cromatografia líquida (LC). Essas aplicações ocorrem tanto em colunas analíticas quanto em colunas de extração para métodos de preparo de amostra online. In-tube SPME (IT-SPME), também conhecida como *column-switching*, é uma técnica de preparo de amostra *online* na qual duas colunas são utilizadas, sendo a primeira uma coluna de extração e a segunda uma coluna analítica. Esse método é bastante interessante, pois automatiza o preparo de amostras, reduzindo as chances de erros humanos, uma das fontes de erro mais comuns em química analítica (TECHNICAL ANALYTICAL METHODS COMMITTEE BRIEFS, 2013). Adicionalmente, os métodos *column-switching* possibilitam a pré-concentração de compostos a serem analisados na coluna de extração, permitindo assim reduzir os limites de quantificação e detecção do método (BORREY et al., 2007; DE TOFFOLI; FUMES; LANÇAS, 2018), ou seja, analisar compostos presentes em baixas quantidades nas amostras. Colunas de extração produzidas com GO já foram usadas para diversas aplicações, incluindo análises de alimentos, fármacos e contaminantes (Tabela 1). As características que permitem o uso de derivados de grafeno para a sorção de diversas classes de moléculas para preparo de amostra *online* também podem permitir a separação desses compostos em uma coluna analítica em cromatografia líquida. Materiais baseados em grafeno aplicados como sorvente como fases estacionárias são descritos na literatura (Tabela 1), porém ainda há poucas publicações sobre esse tema. Essa é uma lacuna que ainda precisa ser preenchida.

Tabela 1: Exemplos de aplicação de derivados de óxido de grafeno em cromatografia líquida descritos na literatura.

	Suporte	**Modificação**	**Aplicação**	**Compostos analisados**	**Matriz**	**Ano**	**Ref.**
Fases extratoras	Si	Sem modificação	IT-SPME	Antibióticos β-lactâmicos	Água	2023	(MACIEL; VARGAS-MEDINA; LANCAS, 2023)
	Si	Sem modificação	IT-SPME	Hidrocarbonetos aromáticos policíclicos	Mel	2021	(SUN et al., 2021a)
	Si	C18 and *end-capping*	IT-SPME	Xantinas	Café	2020	(MEJÍA-CARMONA; LANÇAS, 2020)
Fases estacionárias	Tubular aberta	Albumina sérica bovina	Separação enantiomérica	Enantiômeros	Sem matriz	2014	(LIANG et al., 2014)
	Monolítica	Sem modificação	Eletrocromatografia capilar	Compostos aromáticos	Sem matriz	2012	(WANG; YAN, 2012)
	Si	C18	LC em fase reversa	Diversas classes	Sem matriz	2012	(LIANG et al., 2012)
	Si	C18 and *end-capping*	LC em fase reversa	Pesticidas, drogas e hormônios	Sem matriz	2022	(BORSATTO; MACIEL; LANÇAS, 2022)

1.6. A cromatografia líquida

A cromatografia líquida é uma técnica de grande importância na área de pesquisa e desenvolvimento, em especial nas áreas de farmacêutica, química, biotecnológica e ambiental (JORGENSON, 2010; MASIÁ et al., 2016; RIGANO et al., 2019). A LC é utilizada com duas principais funções: purificação (GUIOCHON, 2002) e análise de compostos químicos (DI STEFANO et al., 2012; PITT, 2009). Dentre as principais aplicações da LC para purificação de compostos está o isolamento de compostos bioativos em produtos naturais (LATIF; SARKER, 2012), como plantas, algas, e fungos, e a purificação de compostos farmacologicamente ativos de subprodutos de síntese (WARREN; VELLA, 1995). Dentre as aplicações de LC como ferramenta analítica, pode-se destacar o uso dessa técnica para determinar contaminantes em águas e alimentos (KIM et al., 2018; TOLOSA et al., 2016) e para o monitoramento de biomarcadores a partir de amostras de fluidos biológicos (AHONEN et al., 2010; BRUCE et al., 2009). A LC teve um salto tecnológico importante em meados do século passado com o estabelecimento da cromatografia líquida em alta pressão (*high pressure liquid chromatography)* ou também chamada de cromatografia líquida de alta eficiência (*high performance liquid chromatography)* (TOUCHSTONE, 1993); em ambos os casos a abreviação convencionalmente utilizada é HPLC. Essa técnica consiste em utilizar um cromatógrafo líquido de alta pressão (também abreviado por uso da sigla HPLC) composto por um conjunto de bombas de alta pressão, um sistema de injeção de amostra, um módulo de controle de temperatura (opcional), uma coluna, e um sistema de detecção (espectrômetro de massas, por exemplo). A Figura 5 ilustra um equipamento típico de HPLC. Outro interessante salto tecnológico recente na LC foi a popularização e emprego LC miniaturizada. A LC miniaturizada não consiste na redução do tamanho do equipamento, como poderia ser deduzido erroneamente, mas na redução do diâmetro da coluna, no volume das tubulações do sistema e da vazão utilizada (VARGAS MEDINA et al., 2020).

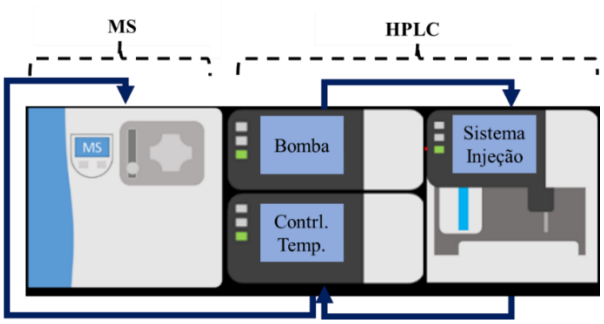

Figura 5. Ilustração de um sistema HPLC acoplado a um MS. As setas representam o sentido do fluxo. Fonte: Autoria própria.

1.7 A separação cromatográfica

A separação cromatografia de compostos em cromatografia líquida ocorre devido à diferença de tempo em que os compostos ficam retidos na coluna (SNYDER, 1970). De forma simplificada, as moléculas dos compostos solubilizadas na fase móvel entram em contato com a superfície da fase estacionária e atingem um equilíbrio, com uma fração das moléculas dos compostos distribuídas em cada fase; esse processo é chamado de transferência de massa (GRITTI; GUIOCHON, 2010a). Para diferentes compostos, a proporção entre as frações solubilizadas na fase móvel e sorvida na fase estacionária é diferente (FAUSNAUGH; REGNIER, 1986; SUN et al., 2005). Como o sistema cromatográfico em LC está em fluxo, ou seja, com a fase móvel fluindo em uma direção, a fração das moléculas solubilizadas na fase móvel é deslocada de forma a entrar em contato com uma nova região da fase estacionária sem moléculas sorvidas, assim, deslocando o equilíbrio químico no sentido da sorção dos compostos nessa região (FALLAS et al., 2010; ZHANG et al., 2013). O mesmo ocorre com a região da fase estacionária na qual a fração das moléculas está sorvida; essa entra em contato com uma região da fase móvel sem moléculas solubilizadas, descolando o equilíbrio na direção da transferência de moléculas dos compostos da fase estacionária para a fase móvel. Esse processo de movimento das moléculas pela coluna é chamado de eluição. Idealmente, a eluição das moléculas de um mesmo composto ocorreria simultaneamente (em escala de tempo), porém em separações reais isso não ocorre (NIESSEN; VAN VLIET; POPPE, 1985). Algumas moléculas são carregadas mais rapidamente pela coluna, estando "mais a frente", outras, mais lentamente, "estando mais atrás" e um grande contingente das moléculas são carregadas "no meio". Por causa desse fenômeno, o pico cromatográfico apresenta a forma de uma gaussiana. A Figura 6 ilustra a separação de dois diferentes compostos em uma coluna de LC e a formação do pico cromatográfico.

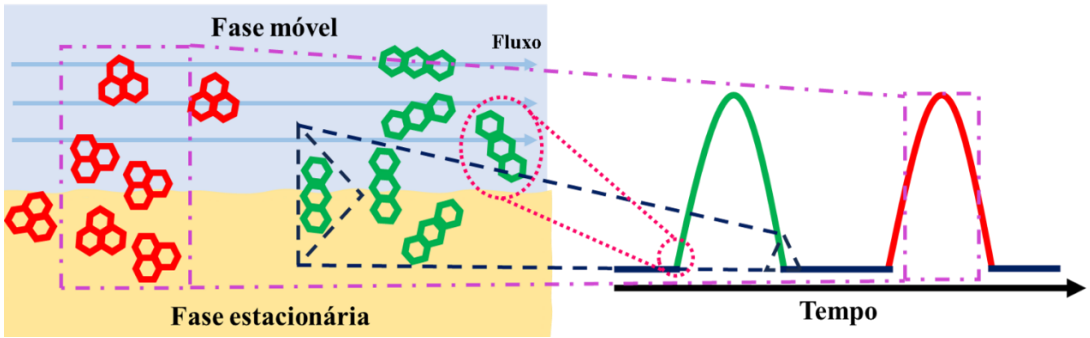

Figura 6. Representação da separação cromatográfica. Fonte: Autoria própria.

1.8 Colunas para cromatografia líquida

Em LC, há três tipos principais de colunas: (i) monolíticas (NESTERENKO, 2018), (ii) tubulares abertas (KUCERA; GUIOCHON, 1984) e (iii) empacotadas (GUAN; ZHOU; SHANG, 1992; MAJORS, 1973a). A Figura 7 ilustra esses tipos de coluna. As colunas monolíticas são formandas por um único bloco contínuo de material, convencionalmente nomeado de monólito (GÜNYEL et al., 2021; ZHAO et al., 2016). Esse monólito apresenta poros de diferentes tamanhos pelos quais as fases estacionárias percola a coluna (NESTERENKO, 2018; NÚÑEZ; NAKANISHI; TANAKA, 2008). As fases estacionárias monolíticas são comumente produzidas utilizando-se estruturas de sílica, polímeros orgânicos ou híbridas (ROZENBRAND; VAN BENNEKOM, 2011). Esse tipo de coluna pode ser utilizada tanto para LC convencional, quanto para LC miniaturizada. Já as colunas tubulares abertas para cromatografia líquida são exclusivamente aplicadas a LC miniaturizada (VARGAS MEDINA et al., 2021). Essas colunas são formadas por um capilar cuja parede interna é recoberta com um filme fino de fase estacionaria, podendo ser um filme líquido ou uma camada porosa (DESMET et al., 2015). Colunas tubulares abertas com fase porosa, conhecidas como *porous layer open tubular* (PLOT) *columns,* são as mais comuns em LC, uma vez que apresentam características bastante interessantes para o processo de transferência de massa entre as fases (DA SILVA BURATO; BASOLLI BORSATTO; LANÇAS, 2023; VARGAS MEDINA et al., 2022). Assim como as colunas monolíticas, as colunas PLOT também podem apresentar estruturas baseadas em sílica ou polímeros orgânicos (DA SILVA BURATO; BASOLLI BORSATTO; LANÇAS, 2023; HARA et al., 2018). As colunas empacotadas, compostas por partículas esférica, são as colunas mais aplicadas a HPLC (MAJORS, 1973a) e LC capilar (FRANC et al., 2014). As próximas duas subseções são dedicadas a composição e produção dessas colunas.

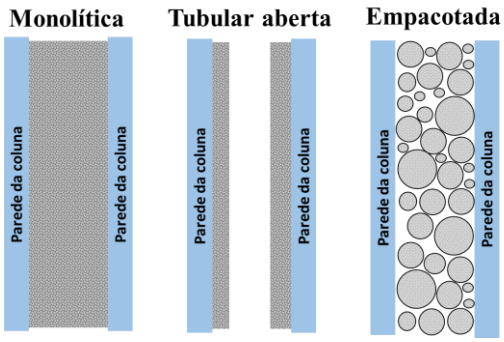

Figura 7. Ilustração de coluna monolítica, tubular aberta e empacotada para LC. Fonte: Autoria própria.

1.9 Fases estacionárias para colunas empacotadas

Em geral, as fases estacionárias de colunas empacotadas modernas são formadas por partículas esféricas para se obter o empacotamento mais homogêneo e diminuir o alargamento de banda causado pelo efeito dos múltiplos caminhos. Usualmente, as fases estacionárias para a HPLC moderna são produzidas a partir de esferas de sílica porosa funcionalizadas com diversos grupos, como C18, fenil, CN e óxido de grafeno, por exemplo. Outros tipos de partículas também podem ser utilizadas, como partículas formadas por polímeros ou do tipo *core-shell*, contendo um núcleo sólido e uma camada porosa (HAYES et al., 2014). Partículas *core-shell*, também conhecidas por partículas superficialmente porosas, foram responsáveis por um significativo aumento de performance na HPLC nesse século devido à minimização do efeito dos múltiplos caminhos que ocorre nos poros das partículas, e por permitir operar colunas com partículas menores em pressões mais baixas (BRUNS; TALLAREK, 2011; TANAKA; MCCALLEY, 2016). A Figura 8 ilustra uma coluna empacotada e os tipos de partículas totalmente porosas e superficialmente porosas. Embora seja bem estabelecido que a redução dos diâmetros das partículas aumente a performance da HPLC convencional (MAZZEO et al., 2005), isso não é observado em LC capilar. Em LC capilar, reduzir o diâmetro da partícula não representa, necessariamente, aumento na performance das colunas. (GRITTI, 2018).

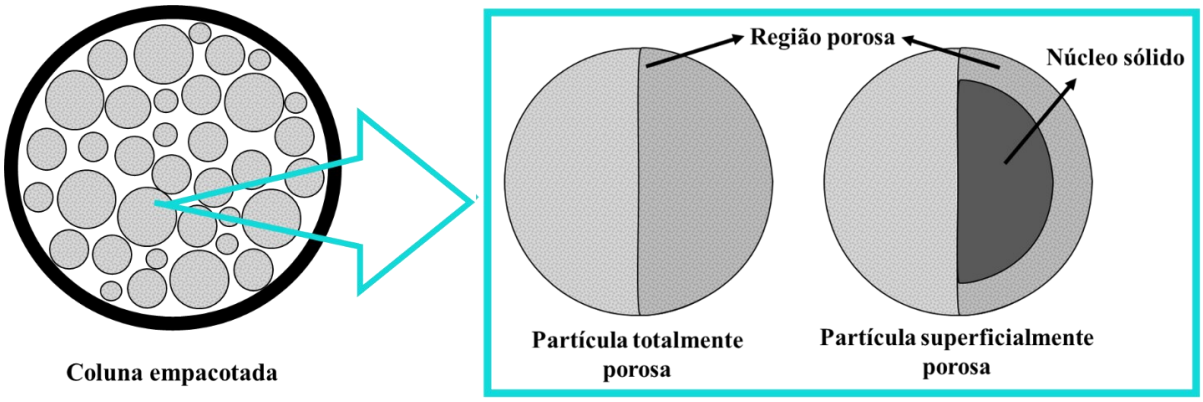

Figura 8. Ilustração representando uma coluna empacotada e os tipos de partículas totalmente porosas e superficialmente porosas. Fonte: Autoria própria.

1.10 A produção de colunas empacotadas

O empacotamento de uma coluna cromatográfica para LC é fundamental para garantir o desempenho da coluna (WAHAB et al., 2017). A forma mais comum de empacotar uma coluna é por meio da assistência de um líquido carregado por uma bomba, o qual empurra o material que formará a fase estacionária para dentro da coluna. Usualmente, o processo de empacotamento segue os seguintes passos: (i) o material sólido que será utilizado como fase estacionaria é suspenso em uma solução, chamada de suspensão de empacotamento; (ii) em paralelo, a câmara de empacotamento, dispositivo no qual a suspensão de empacotamento será inserida, é conectada no dispositivo que comporá a coluna; (iii) a suspensão de empacotamento é adicionada a câmara de empacotamento; (iv) a camada de empacotamento e o dispositivo que comporá a coluna são conectados na bomba de empacotamento; (v) a bomba é ativada e se inicia o processo de empacotamento. A Figura 9 ilustra o sistema de empacotamento. A pressão de empacotamento e a composição dos solventes da suspensão de empacotamento são fatores fundamentais para garantir uma boa coluna (WAHAB et al., 2017). Quanto maior for a pressão, e mais compactada é a fase, melhor será a coluna (ver subseção sobre o efeito dos múltiplos caminhos), porém, caso a pressão exceda a resistência mecânica das partículas da fase estacionária, essas podem se romper, perdendo desempenho. O efeito da composição dos solventes da solução de empacotamento não pode ser explicado com correlações simples, mas está relacionado a aglomeração dessas partículas na suspensão (WAHAB et al., 2017). A aglomeração das partículas da fase estacionária na suspensão pré-empacotamento é determinada pelas forças eletroestáticas de superfície, as quais podem ser controladas ajustando a proporção dos solventes presentes na suspensão. Por exemplo, o desempenho de colunas capilares empacotadas com fase normal melhora quando as partículas estão mais dispersas na suspensão de empacotamento, enquanto o desempenho de colunas de C18 melhoram à medida que as partículas na suspensão de empacotamento estão mais aglomeradas (WAHAB et al., 2017).

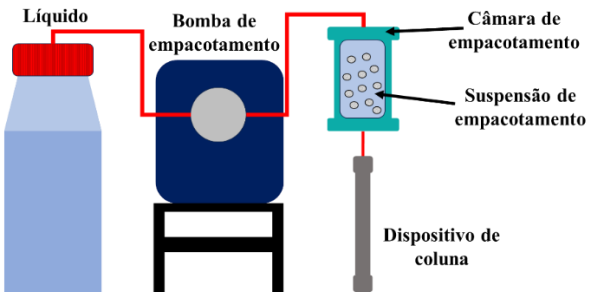

Figura 9. Ilustração do sistema de empacotamento. Fonte: Autoria própria.

1.11 Colunas para cromatografia líquida miniaturizada

As colunas para LC miniaturizada podem ser classificadas em dois tipos, : as capilares, e as nano-capilares (VARGAS MEDINA et al., 2020). As colunas nano-capilares são bastante particulares, geralmente apresentam diâmetros internos inferiores a 0,1 mm e operam de uma faixa de vazão limitada, usualmente abaixo de 1 µL/min (GÜNYEL et al., 2021). Colunas capilares para cromatografia geralmente apresentam dimensões entre 0,5 mm e 0,1 mm de diâmetro interno (MEJÍA-CARMONA et al., 2020). Essa escala é bastante interessante, pois, dependendo das características da coluna, elas podem ser aplicadas em uma ampla faixa de vazão, podendo ir de 0,5 mL/min (operacional em HPLCs convencionais) a 0,5 µL/min (operacional em HPLCs capilares) (DESMET; EELTINK, 2013). Adicionalmente, as colunas em escala capilar são de produção considerada simples, similar a colunas empacotadas convencionais, e utilizam materiais amplamente disponíveis no mercado (WAHAB et al., 2017). Colunas capilares são ideais para investigar novos materiais, pois são empacotadas com pouca massa de fase estacionária (WAHAB et al., 2017). Atualmente, as colunas capilares são tão confiáveis quanto as colunas convencionais em cromatografia líquida. Outro atrativo das colunas capilares é sua compatibilidade com a "química verde" (DOMINGUES NAZARIO et al., 2018). Por permitir análises em baixas vazões, a LC capilar consome pouca quantidade de solvente tóxicos por análise, resultando em um ganho ambiental significativo ao fim de uma longa série analítica. A figura 10 mostra um exemplo da coluna capilar utilizada.

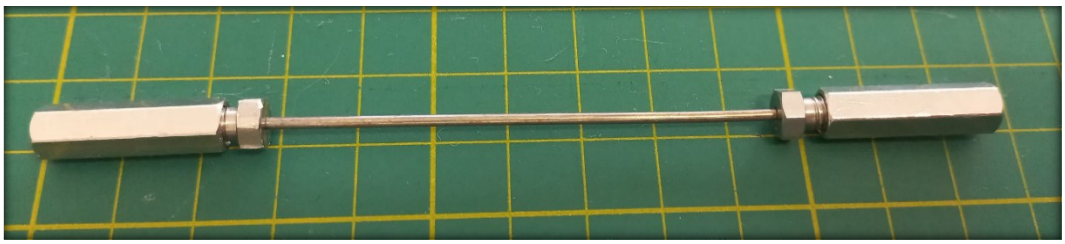

Figura 10. Fotografia de uma das colunas capilares produzidas, essa empacotada com partículas de 3 µm de diâmetro. Fonte: Autoria própria.

1.12 Fatores importantes em LC

De forma geral, colunas empacotadas capilares e convencionais são afetadas similarmente por parâmetros que afetam a performance das colunas (GRITTI et al., 2011; KNOX, 2002). Quando os efeitos que afetam a performance da análise ocorrem dentro da coluna, são chamados de efeito intra-coluna (KNOX; PARCHER, 1969); já efeitos que ocorrem no sistema cromatográfico não relacionados a coluna são chamados de fatores extra-coluna (DESMET; BROECKHOVEN, 2019). A performance de um sistema cromatográfico é avaliada na forma da largura dos picos cromatográficos obtidos (KNOX; PARCHER, 1969). Ou seja, quanto mais fino os picos, melhor é a performance (Figura 11). Em cromatografia, convencionalmente, chamamos o efeito do pico alargar durante uma análise por HPLC de "alargamento de banda". O alargamento de banda intra-coluna foi estudado, principalmente, por van Deemter (VAN DEEMTER; ZUIDERWEG; KLINKENBERG, 1956), o qual dividiu os fatores causadores do alargamento de banda em três categorias: alargamento causado pelos múltiplos caminhos; alargamento por difusão longitudinal e alargamento causado pela transferência de massa (ALVAREZ-SEGURA et al., 2019; HETZEL et al., 2016). Já os fatores de alargamento de banda extra-coluna ocorrem, principalmente, nas tubulações do sistema cromatográfico e nos detectores (FEKETE; FEKETE, 2011).

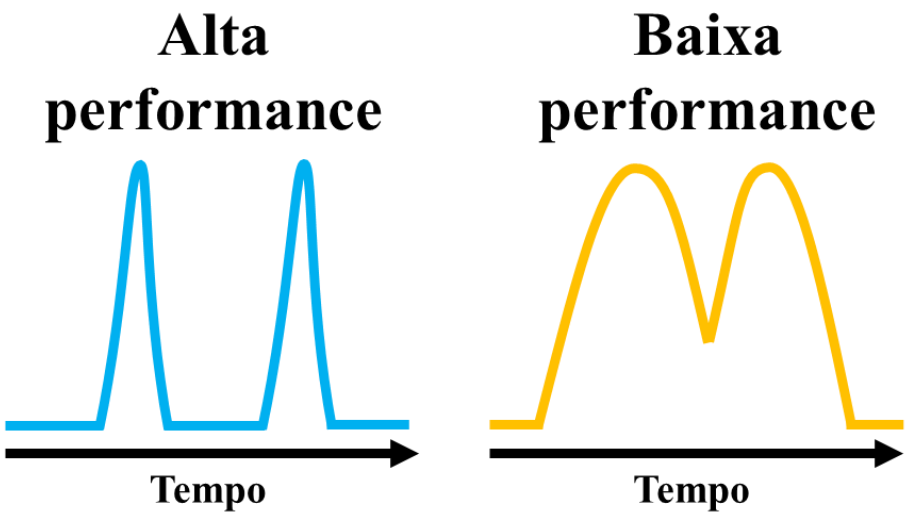

Figura 11. Representações de cromatogramas com alta e baixa performance. Fonte: Autoria própria.

1.13 O efeito dos múltiplos caminhos

O efeito dos múltiplos caminhos, citado anteriormente, é um dos principais fatores causadores do alargamento de banda (MAJORS, 1973b). Esse efeito, também conhecido por difusão turbulenta ("*Eddy diffusion*") (GIDDINGS, 1959), compreende as diferentes possibilidades de caminhos para um conjunto de moléculas percorrer na coluna. O preenchimento da coluna com a fase estacionária gera uma grande possibilidade de caminhos os quais as moléculas podem percorrer. Estatisticamente, a maioria das moléculas percorrera caminhos de distâncias semelhantes, porém algumas percorreram caminhos mais longos e outras mais curtos. Quanto mais heterogêneo for o leito empacotado (o interior da coluna), maior será a possibilidade de múltiplos caminhos, portanto maior será o alargamento de banda. Esse efeito inclui cinco componentes: (i) difusão trans-coluna (GRITTI; GUIOCHON, 2010b), ocorrendo entre as paredes da coluna; (ii) difusão trans-partícula (MAJORS, 1973b), ocorrendo nos poros das partículas; (iii) difusão trans-canal (MAJORS, 1973b), ocorrendo nos interstícios formados pelo empacotamento e as difusões inter-canais (iv) de curtas (MAJORS, 1973b) e (v) de longas distâncias (MAJORS, 1973b), resultantes de defeitos na homogeneidade do leito empacotado. A figura 12 ilustra esse efeito.

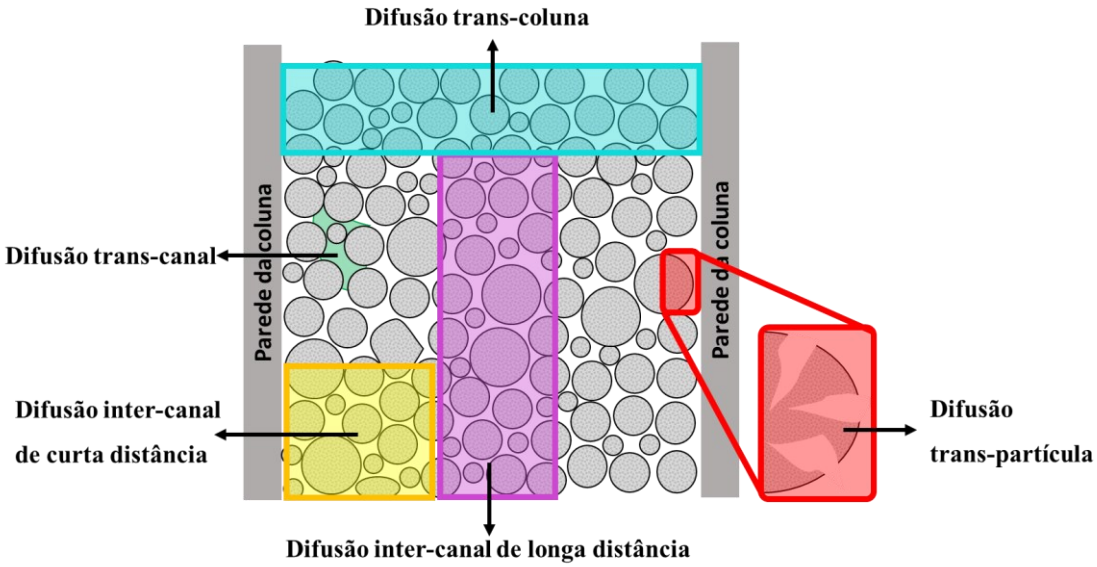

Figura 12. Representação das regiões nas quais ocorrem a difusão devido aos efeitos dos múltiplos caminhos. Fonte: Autoria própria.

1.14 A difusão longitudinal

O alargamento de banda por difusão longitudinal ocorre devido ao espalhamento das moléculas dos compostos na fase móvel (VAN DEEMTER; ZUIDERWEG; KLINKENBERG, 1956). Uma analogia bastante simples que pode ser feita sobre esse fenômeno é o espalhamento de uma gota de tinta em um copo de água, ; porém, em LC, o sistema está em fluxo. A difusão longitudinal é um efeito que depende apenas da constante de difusão das moléculas dos compostos na fase móvel (VAN DEEMTER; ZUIDERWEG; KLINKENBERG, 1956). A temperatura também tem um efeito indireto sobre o alargamento, uma vez que a mudança de temperatura altera a viscosidade da fase móvel e a constante de difusão dos compostos nela (VANHOENACKER; SANDRA, 2006). O efeito da difusão longitudinal no alargamento de banda é mais perceptível em vazões baixas (VAN DEEMTER; ZUIDERWEG; KLINKENBERG, 1956). Em vazões mais elevadas as moléculas dos compostos ficam pouco tempo no sistema cromatográfico e, portanto, a difusão longitudinal é pouco percebida. Em vazões menores, as moléculas ficam mais tempo no sistema cromatográfico, permitindo que as moléculas se espalhem mais na fase móvel. A Figura 13 A ilustra o efeito do alargamento de banda pela difusão longitudinal em relação ao tempo e a Figura 13 B efeito do alargamento de banda pela difusão longitudinal em relação à vazão.

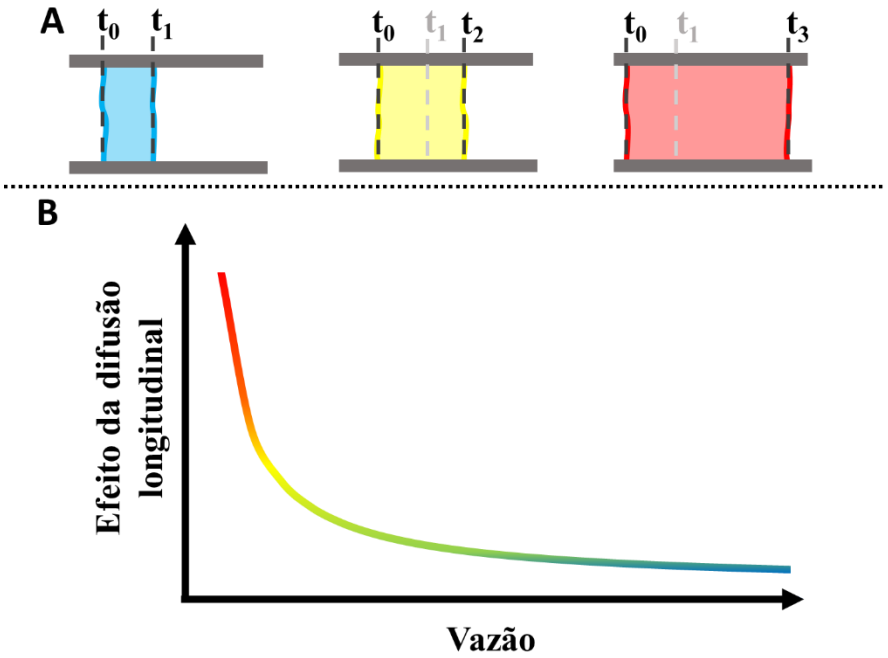

Figura 13. (A) Efeito do alargamento de banda pela difusão longitudinal em relação ao tempo e (B) efeito do alargamento de banda pela difusão longitudinal em relação à vazão. Fonte: Autoria própria.

1.15 A transferência de massas

Como mencionado anteriormente, o processo de separação cromatografia ocorre devido à transferência de massas entre a fase móvel e a fase estacionária (GRITTI; GUIOCHON, 2010a; VAN DEEMTER; ZUIDERWEG; KLINKENBERG, 1956). Embora essencial para a cromatografia, alguns efeitos no processo de transferência de massas podem causar alargamento de banda. A transferência de massa pode ser influenciada por algumas variáveis que afetam a dinâmica da partição das moléculas dos compostos entre as fases móvel e estacionária. A principal dessas variáveis é a vazão da fase móvel (VAN DEEMTER; ZUIDERWEG; KLINKENBERG, 1956). Uma vazão muito alta pode levar a uma transferência de massa insuficiente devido o pouco tempo de interação entre as moléculas dos compostos solubilizadas na fase móvel com a fase estacionária. A temperatura da coluna é uma variável que pode influenciar significativamente a transferência de massa porque afeta a constante de equilíbrio da distribuição das moléculas dos compostos entre as fases (VANHOENACKER; SANDRA, 2008). Usualmente, é considerado que elevar a temperatura favorece a performance da separação, porém esse fato não é verdadeiro para todos os casos (ISSAQ et al., 1987). A Figura 14 ilustra o efeito de transferência de massas.

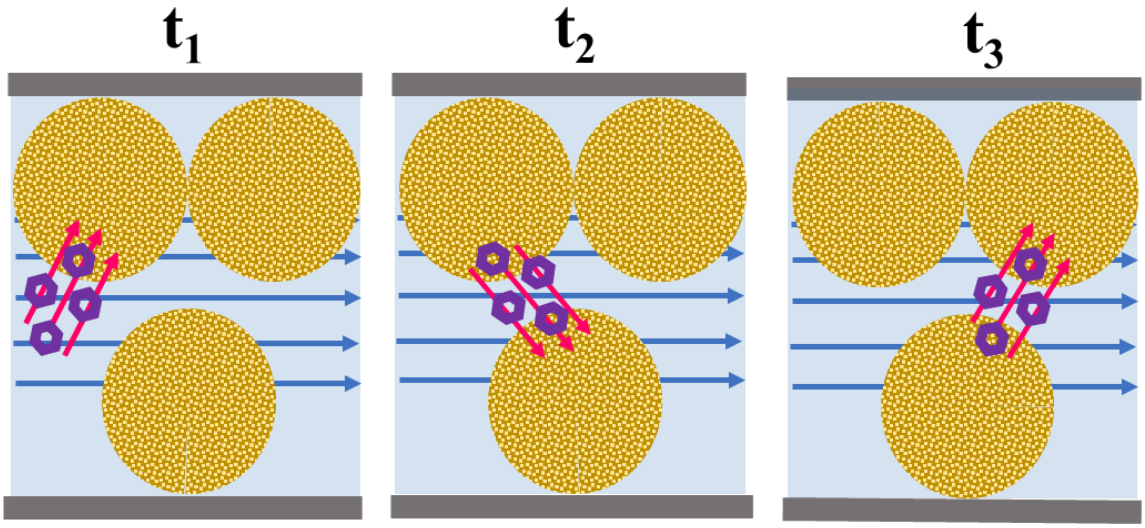

Figura 14. Representação da transferência de massas entre fases. Fonte: Autoria própria.

1.16 A equação de van Deemter

Os fatores descritos nas subsecções anteriores foram sumarizados por van Deemter e então relacionados, quantitativamente, a performance da coluna (Van Deemter, Zuiderweg, & Klinkenberg, 1956). Esses estudos foram primeiramente realizados para a cromatografia gasosa e posteriormente aplicados a cromatografia líquida (Gritti & Guiochon, 2010a). Para ambas as técnicas, as condições determinadas por van Deemter permanecem válidas. Esses estudos resultaram na famosa "equação de van Deemter" (equação 1), a qual é um dos pilares nas técnicas de avaliação de performance de separações. Van Deemter estabeleceu uma relação fundamental entre o alargamento da banda intra-coluna e a altura equivalente a um prato, representada pela letra "H" na equação de Van Deemter. A altura do prato (H) é inversamente proporcional a eficiência, ou seja, quanto menor H mais eficiente é a separação porque menor será o alargamento da banda. De forma geral, a eficiência da coluna está intrinsecamente ligada ao fluxo da análise, sendo representada pela velocidade linear da fase móvel (μ) na equação de van Deemter. A equação de Van Deemter, na sua forma mais simples (Equação 1), engloba os principais parâmetros que influenciam a eficiência da separação cromatográfica.

$$H = A + \frac{B}{\mu} + C\mu \qquad \text{(Equação 1)}$$

-H → Altura do Prato

-A → Efeito dos Múltiplos Caminhos

-B → Difusão Longitudinal:

-C → Resistência à Transferência de Massa

-μ → Velocidade Linear da Fase Móvel

1.17 Picos assimétricos

Um cromatograma ideal apresenta picos gaussianos, completamente simétricos e finos, ; porém em análises reais, os picos podem apresentar formas assimétricas não gaussianas. Essas formas podem apresentar distorções na parte da frente do pico, chamada *fronting*, ou na parte de trás do pico, chamada *tailing* ou caudas (Figura 15). O *fronting* pode ocorrer por sobrecarga da coluna (massa de injeção em excesso na coluna) ou um erro na instalação da coluna, formando um espaço vazio de volume grande entre a tubulação e a coluna (BROGLÉ et al., 1999). Outra causa possível para o *fronting* é a incompatibilidade do diluente da amostra e a fase móvel (SHALLIKER; SAMUELSSON; FORNSTEDT, 2016). Por exemplo, em análises em fase reversa, quando a amostra está solubilizada em um teor maior de solvente orgânico do que a coluna está condicionada, o solvente da amostra pode carregar uma fração das moléculas dos compostos por uma certa distância, causando o *fronting*. Já o *tailing* ocorre por dois principais fatores, um físico e outro químico. O fator físico do *tailing* está relacionado diretamente ao efeito dos múltiplos caminhos e ao alargamento de banda extra-coluna. Simplificadamente, quando as moléculas no sistema cromatográfico encontram um espaço aberto, elas ocupam esse volume. Como o sistema está em fluxo, esse conjunto de moléculas é carregada pelo sistema, porém poucas ainda permanecem na região anterior. Esse efeito torna-se mais pronunciado quando há mudanças buscas de volume no sistema, causando turbulência no fluxo (FELINGER, 2008). Já o fator químico do *tailing* é causado pela interação de grupos aceptores ou doadores de elétrons na fase estacionaria com grupos ácidos ou básicos dos compostos analisados. Fases baseadas em partículas de sílica, muito comum em HPLC, podem apresentar grupos Si-OH em sua superfície, e assim interagir por de hidrogênio com grupos básicos de moléculas analisadas (NAWROCKI, 1997). Por exemplo, a separação de compostos básicos em colunas contendo C18 como fase estacionária, podem apresentar *tailing*.

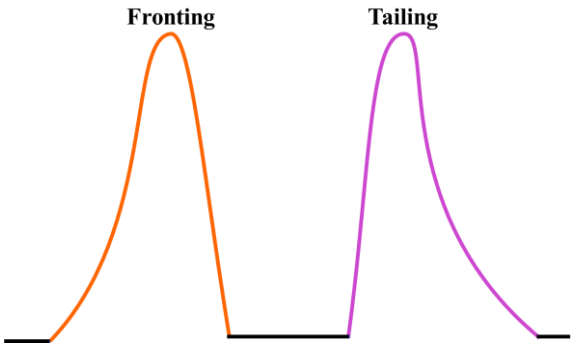

Figura 15. Ilustração representando os efeitos de *fronting* e *tailing* nos picos cromatográficos. Fonte: Autoria própria.

1.18 Métodos de avaliação da performance de colunas

A melhor forma de se avaliar e comparar performances de diferentes métodos cromatográficos ou de diferentes colunas é através de métodos gráficos de análise (DESMET; CABOOTER; BROECKHOVEN, 2015). Gráficos são ferramentas interessantes, pois permitem comparar facilmente muitos dados de uma forma eficiente, porém simples. Atualmente, as curvas cinéticas, também conhecidas por *knetic plots*, são a principal forma de avaliação (BROECKHOVEN et al., 2010; HETZEL et al., 2016, 2017). Curvas cinéticas nada mais são do que um gráfico que apresenta um parâmetro de performance em um dos eixos e um parâmetro de tempo em outro. A Figura 16 mostra um exemplo de curva cinética. Embora seja uma ferramenta importantíssima na cromatografia moderna e tenham se popularizado recentemente, as curvas cinéticas não são novidades. As curvas de Poppe foram desenvolvidas em meados do século passado e são consideradas as primeiras curvas cinéticas (POPPE, 1997). Adicionalmente, existem outras formas de se avaliar a performance das colunas (ALVAREZ-SEGURA et al., 2019; DESMET; CABOOTER; BROECKHOVEN, 2015; VANDERHEYDEN et al., 2013). O Capítulo 4 "*Trends In Graphene-Based Sorbents For LC Analysis Of Food And Environmental Water*" dessa tese apresenta, mais detalhes sobre outras formas de avaliar e comparar métodos e colunas cromatográficas.

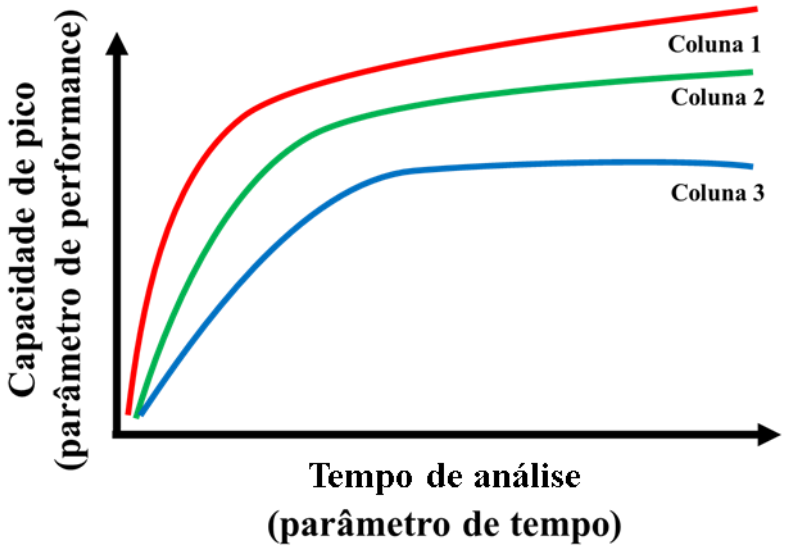

Figura 16. Exemplo de curva cinética, essa apresentando capacidade de pico como parâmetro de performance e tempo de retenção como parâmetro de tempo. Fonte: Autoria própria.

2. Objetivos do doutorado

Objetivo geral

Desenvolver e avaliar colunas capilares empacotadas para cromatografia líquida (LC) com materiais baseados em grafeno.

Objetivos específicos

- Realizar revisões da literatura envolvendo a aplicação de materiais derivados de grafeno como sorventes em análises por cromatografia líquida.
- Realizar revisões da literatura envolvendo fundamentos e características sobre cromatografia líquida miniaturizada.
- Investigar e comparar a seletividade de colunas empacotadas com SiGO-18ec com colunas empacotadas com C18, assim como comparar a seletividade de colunas empacotadas com partículas de SiGO-C18ec de diferentes diâmetros
- Investigar o efeito do diâmetro das partículas de SiGO-C18ec no desempenho das colunas empacotadas.
- Investigar a aplicabilidade de colunas de SiGO-C18ec na análise quantitativa de hormônios.
- Aplicar colunas de SiGO-C18ec em análises qualitativas e quantitativas.
- Avaliar a aplicação de SiGO-C18ec em sistemas de extração e separação hifenados, como o sistema de extração líquida online (*online liquid extraction*) – OLE-LC.
- Avaliar as limitações e capacidades de um sistema *column -switching* composto exclusivamente por colunas empacotadas com materiais baseados em grafeno.
- Avaliar a vida-útil das colunas produzidas nesse trabalho.

Referências

AHONEN, L. L.; HAAPALA, M.; SAARELA, V.; FRANSSILA, S.; KOTIAHO, T.; KOSTIAINEN, R. Feasibility of capillary liquid chromatography/microchip atmospheric pressure photoionization mass spectrometry in analyzing anabolic steroids in urine samples. **Rapid Communications in Mass Spectrometry**, Hoboken, v. 24, n. 7, p. 958–964, 2010. DOI: 10.1002/rcm.4468

ALVAREZ-SEGURA, T.; CABO-CALVET, E.; BAEZA-BAEZA, J. J.; GARCÍA-ALVAREZ-COQUE, M. C. Study of the column efficiency using gradient elution based on Van Deemter plots. **Journal of Chromatography A**, Amsterdam, v. 1584, p. 126–134, 2019. DOI: 10.1016/j.chroma.2018.11.042.

AUGUSTO, F.; CARASEK, E.; SILVA, R. G. C.; RIVELLINO, S. R.; BATISTA, A. D.; MARTENDAL, E. New sorbents for extraction and microextraction techniques. **Journal of Chromatography A**, Amsterdam, v. 1217, n. 16, p. 2533–2542, 2010. DOI: 10.1016/j.chroma.2009.12.033.

BORREY, D.; MOERMAN, E.; COCKX, A.; ENGELRELST, V.; LANGLOIS, M. R. Column-switching LC-MS/MS analysis for quantitative determination of testosterone in human serum. **Clinica Chimica Acta**, *Amsterdam,* v. 382, n. 1–2, p. 134–137, 2007. DOI: 10.1016/j.cca.2007.03.019.

BORSATTO, J. V. B.; MACIEL, E. V. S.; LANÇAS, F. M. Investigation of the applicability of silica-graphene hybrid materials as stationary phases for capillary liquid chromatography. **Journal of Chromatography A**, Amsterdam, v. 1685, p. 463618, 2022. DOI: 10.1016/j.chroma.2022.463618.

BROECKHOVEN, K.; CABOOTER, D.; LYNEN, F.; SANDRA, P.; DESMET, G. The kinetic plot method applied to gradient chromatography: theoretical framework and experimental validation. **Journal of Chromatography A,** Amsterdam, v. 1217, n. 17, p. 2787–2795, 2010. DOI: 10.1016/j.chroma.2010.02.023.

BROGLÉ, K.; ORNAF, R. M.; WU, D.; PALERMO, P. J. Peak fronting in reversed-phase high-performance liquid chromatography: a study of the chromatographic behavior of oxycodone hydrochloride. **Journal of Pharmaceutical and Biomedical Analysis**, Amsterdam, v. 19, n. 5, p. 669–678, 1999. DOI: 10.1016/S0731-7085(98)00290-8.

BRUCE, S. J.; TAVAZZI, I.; PARISOD, V.; REZZI, S.; KOCHHAR, S.; GUY, P. A. Investigation of human blood plasma sample preparation for performing metabolomics using ultrahigh performance liquid chromatography/mass spectrometry. **Analytical Chemistry**, Washington, v. 81, n. 9, p. 3285–3296, 2009. DOI: 10.1021/ac8024569.

BRUNS, S.; TALLAREK, U. Physical reconstruction of packed beds and their morphological analysis: Core-shell packings as an example. **Journal of Chromatography A**, Amsterdam, v. 1218, n. 14, p. 1849–1860, 2011. DOI: 10.1016/j.chroma.2011.02.013.

DA SILVA BURATO, J. S.; BASOLLI BORSATTO, J. V.; LANÇAS, F. M. Practical aspects of preparation, optimization, and evaluation of poly(styrene-divinylbenzene)porous-layer open tubular (PLOT) columns for capillary liquid chromatography. **Talanta**, Amsterdam, v. 253, p. 124106, 2023. DOI: 10.1016/j.talanta.2022.124106.

DE TOFFOLI, A. L.; FUMES, B. H.; LANÇAS, F. M. Packed in-tube solid phase microextraction with graphene oxide supported on aminopropyl silica: Determination of target triazines in water samples. **Journal of Environmental Science and Health, Part B**, Abingdon-on-Thames, v. 53, n. 7, p. 434–440, 2018. DOI: 10.1080/03601234.2018.1438831.

DE TOFFOLI, A. L.; MACIEL, E. V. S.; FUMES, B. H.; LANÇAS, F. M. The role of graphene-based sorbents in modern sample preparation techniques. **Journal of Separation Science**, Weinheim, 2018. DOI: 10.1002/jssc.201700870.

DESMET, G.; BROECKHOVEN, K. Extra-column band broadening effects in contemporary liquid chromatography: causes and solutions. **TrAC Trends in Analytical Chemistry**, Amsterdam, v. 119, p. 115619, 2019. DOI: 10.1016/j.trac.2019.115619.

DESMET, G.; CABOOTER, D.; BROECKHOVEN, K. Graphical data representation methods to assess the quality of LC Columns. **Analytical Chemistry,** Washington, v. 87, p. 8593–8602, 2015. DOI: 10.1021/ac504473p.

DESMET, G.; CALLEWAERT, M.; OTTEVAERE, H.; DE MALSCHE, W. Merging Open-Tubular and packed bed liquid chromatography. **Analytical Chemistry**, Washington, v. 87, n. 14, p. 7382–7388, 2015. DOI: 10.1021/acs.analchem.5b01579.

DESMET, G.; EELTINK, S. Fundamentals for LC miniaturization. **Analytical Chemistry**, Washington, v. 85, n. 2, p. 543–556, 2013. DOI: 10.1021/ac303317c.

DI STEFANO, V.; AVELLONE, G.; BONGIORNO, D.; CUNSOLO, V.; MUCCILLI, V.; SFORZA, S.; DOSSENA, A.; DRAHOS, L.; VÉKEY, K. Applications of liquid chromatography–mass spectrometry for food analysis. **Journal of Chromatography A**, Amsterdam, v. 1259, p. 74–85, 2012. DOI: 10.1016/j.chroma.2012.04.023.

DOMINGUES NAZARIO, C. E.; FUMES, B. H.; DA SILVA, M. R.; LANÇAS, Fernando Mauro. Miniaturized column liquid chromatography. **Nanomaterials in Chromatography,** Amsterdam: Elsevier, v.1, n.1, p. 359-385, 2018. DOI: 10.1016/b978-0-12-812792-6.00013-3.

FALLAS, M. M.; NEUE, U. D.; HADLEY, M. R.; MCCALLEY, D. V. Further investigations of the effect of pressure on retention in ultra-high-pressure liquid chromatography. **Journal of Chromatography A**, Amsterdam, v. 1217, n. 3, p. 276–284, 2010. DOI: 10.1016/j.chroma.2009.11.041.

FAUSNAUGH, J. L.; REGNIER, F. E. Solute and mobile phase contributions to retention in hydrophobic interaction chromatography of proteins. **Journal of Chromatography A**, Amsterdam, v. 359, n. C, p. 131–146, 1986. DOI: 10.1016/0021-9673(86)80068-1.

FEKETE, S.; FEKETE, J. The impact of extra-column band broadening on the chromatographic efficiency of 5cm long narrow-bore very efficient columns. **Journal of Chromatography A**, Amsterdam, v. 1218, n. 31, p. 5286–5291, 2011. DOI: 10.1016/j.chroma.2011.06.045.

FELINGER, A. Molecular dynamic theories in chromatography. **Journal of Chromatography A**, Amsterdam, v. 1184, n. 1–2, p. 20–41, 2008. DOI: 10.1016/j.chroma.2007.12.066.

FRANC, M.; SOBOTNÍKOVÁ, J.; COUFAL, P.; BOSÁKOVÁ, Z. Comparison of different types of outlet frits in slurry-packed capillary columns. **Journal of Separation Science**, Weinheim, v. 37, n. 17, p. 2278–2283, 2014. DOI: 10.1002/jssc.201400434.

GIDDINGS, J. C. Eddy diffusion in chromatography. **Nature**, London, v. 184, n. 4683, p. 357–358, 1959. DOI: 10.1038/1871023a0.

GOLZARI AQDA, T.; BEHKAMI, S.; RAOOFI, M.; BAGHERI, H. Graphene oxide-starch-based micro-solid phase extraction of antibiotic residues from milk samples. **Journal of chromatography. A**, Amsterdam, v. 1591, p. 7–14, 2019. DOI: 10.1016/j.chroma.2018.11.069.

GRITTI, F. A stochastic view on column efficiency. **Journal of Chromatography A**, Amsterdam, v. 1540, p. 55–67, 2018. DOI: 10.1016/j.chroma.2018.02.005.

GRITTI, F.; FARKAS, T.; HENG, J.; GUIOCHON, G. On the relationship between band broadening and the particle-size distribution of the packing material in liquid chromatography: Theory and practice. **Journal of Chromatography A**, Amsterdam, v. 1218, n. 45, p. 8209–8221, 2011. DOI: 10.1016/j.chroma.2011.09.034.

GRITTI, F.; GUIOCHON, G. Mass transfer mechanism in liquid chromatography columns packed with shell particles: would there be an optimum shell structure? **Journal of Chromatography A**, Amsterdam, v. 1217, n. 52, p. 8167–8180, 2010. a. DOI: 10.1016/j.chroma.2010.10.075.

GRITTI, F.; GUIOCHON, G. Relationship between trans-column eddy diffusion and retention in liquid chromatography : Theory and experimental evidence. **Journal of Chromatography A**, Amsterdam, v. 1217, n. 41, p. 6350–6365, 2010. b. DOI: 10.1016/j.chroma.2010.07.029.

GUAN, Y.; ZHOU, L.; SHANG, Z. Dry-packed capillary columns for micro HPLC. **Journal of High Resolution Chromatography**, New Jersey, v. 15, n. 7, p. 434–436, 1992. DOI: 10.1002/jhrc.1240150706.

GUIOCHON, G. Preparative liquid chromatography. **Journal of Chromatography A**, Amsterdam, v. 965, n. 1–2, p. 129–161, 2002. DOI: 10.1016/S0021-9673(01)01471-6.

GUIOCHON, G; GRITTI, F. Shell particles, trials, tribulations and triumphs. **Journal of Chromatography A**, Amsterdam, v. 1218, n. 15, p. 1915–1938, 2011. DOI: 10.1016/j.chroma.2011.01.080.

GÜNYEL, Z.; ASLAN, H.; DEMIR, N.; AYDOĞAN, C. Nano-liquid chromatography with a new nano-structured monolithic nanocolumn for proteomics analysis. **Journal of Separation Science**, New Jersey, v. 44, n. 21, p. 3996–4004, 2021. DOI: 10.1002/jssc.202100454.

HARA, T.; IZUMI, Y.; NAKAO, M.; HATA, K.; BARON, G. V.; BAMBA, T.; DESMET, G. Silica-based hybrid porous layers to enhance the retention and efficiency of open tubular capillary columns with a 5 μm inner diame9ter. **Journal of Chromatography A**, Amsterdam, v. 1580, p. 63–71, 2018. DOI: 10.1016/j.chroma.2018.10.023.

HAYES, R.; AHMED, A.; EDGE, T.; ZHANG, H. Core-shell particles: Preparation, fundamentals and applications in high performance liquid chromatography. **Journal of Chromatography A**, Amsterdam ,v. 1357, p. 36–52, 2014. DOI: 10.1016/j.chroma.2014.05.010.

HETZEL, T.; BLAESING, C.; JAEGER, M.; TEUTENBERG, T.; SCHMIDT, T. C. Characterization of peak capacity of microbore liquid chromatography columns using gradient kinetic plots. **Journal of Chromatography A**, Amsterdam, v. 1485, p. 62–69, 2017. DOI: 10.1016/j.chroma.2017.01.018.

HETZEL, T.; LOEKER, D.; TEUTENBERG, T.; SCHMIDT, T. C. Characterization of the efficiency of microbore liquid chromatography columns by van Deemter and kinetic plot analysis. **Journal of Separation Science**, New Jersey, v. 39, n. 20, p. 3889–3897, 2016. DOI: 10.1002/jssc.201600775.

HUMMERS, W. S.; OFFEMAN, R. E. Preparation of graphitic oxide. **Journal of the American Chemical Society**, Washington, v. 80, n. 6, p. 1339–1339, 1958. DOI: 10.1021/ja01539a017.

ISSAQ, H. J.; FOX, S. D.; LINDSEY, K.; MCCONNELL, J. H.; WEISS, D. E. Effect of temperature on HPLC separations using C1, C4, C8, and C18 alkyl chain bonded silica columns. **Journal of Liquid Chromatography**, Abingdon-on-Thames, v. 10, n. 1, p. 49–70, 1987. DOI: 10.1080/01483918708074191.

JORDAN-SINISTERRA, M.; LANÇAS, F. M. Microextraction by packed sorbent of selected pesticides in coffee samples employing ionic liquids supported on graphene nanosheets as extraction phase. **Analytical and Bioanalytical Chemistry**, New York, v. 414, n. 1, p. 413–423, 2022. DOI: 10.1007/s00216-021-03245-3.

JORGENSON, J. W. Capillary Liquid chromatography at ultrahigh pressures. **Annual Review of Analytical Chemistry**, Palo Alto, v. 3, n. 1, p. 129–150, 2010. DOI: 10.1146/annurev.anchem.1.031207.113014.

JOSHI, D. J.; KODURU, J. R.; MALEK, N. I.; HUSSAIN, C. M.; KAILASA, S. K. Surface modifications and analytical applications of graphene oxide: A review. **TrAC Trends in Analytical Chemistry**, Amsterdam, v. 144, p. 116448, 2021. DOI: 10.1016/j.trac.2021.116448.

JUSTINO, C. I. L.; GOMES, A. R.; FREITAS, A. C.; DUARTE, A. C.; ROCHA-SANTOS, T. A. P. Graphene based sensors and biosensors. **TrAC - Trends in Analytical Chemistry**, Amsterdam, v. 91, p. 53–66, 2017. DOI: 10.1016/j.trac.2017.04.003.

KIM, C.; RYU, H. D.; CHUNG, E. G.; KIM, Y.; LEE, J. A review of analytical procedures for the simultaneous determination of medically important veterinary antibiotics in environmental water: Sample preparation, liquid chromatography, and mass spectrometry. **Journal of Environmental Management**, Amsterdam, v. 217, p. 629–645, 2018. DOI: 10.1016/j.jenvman.2018.04.006.

KNOX, J. H. Band dispersion in chromatography - a universal expression for the contribution from the mobile zone. **Journal of Chromatography A**, Amsterdam, v. 960, n. 1–2, p. 7–18, 2002. DOI: 10.1016/S0021-9673(02)00240-6.

KNOX, J. H.; PARCHER, J. F. Effect of the column to particle diameter ratio on the dispersion of unsorbed solutes in chromatography. **Analytical Chemistry**, *Washington,* v. 41, n. 12, p. 1599–1606, 1969. DOI: 10.1021/ac60281a009.

KUCERA, P.; GUIOCHON, G. Use of open-tubular columns in liquid chromatography. **Journal of Chromatography A**, Amsterdam, v. 283, n. C, p. 1–20, 1984. DOI: 10.1016/S0021-9673(00)96238-1.

KUMAR, N.; SALEHIYAN, R.; CHAUKE, V.; JOSEPH BOTLHOKO, O.; SETSHEDI, K.; SCRIBA, M.; MASUKUME, M.; SINHA RAY, S. Top-down synthesis of graphene: A comprehensive review. **FlatChem**, Amsterdam, v. 27, p. 100224, 2021. DOI: 10.1016/j.flatc.2021.100224.

LANÇAS, F. M.; MEDINA, D. A. V.; PEREIRA DOS SANTOS, N. G.; SINISTERRA, M. J. Graphene-based sorbents for modern magnetic solid-phase extraction techniques. In:

HUSSAIN, C. M. (ed.). **Analytical applications of functionalized magnetic nanoparticles,** Cambridge: Royal Society of Chemistry, 2021. p. 174–199. DOI: 10.1039/9781839162756-00174.

LATIF, Z.; SARKER, S. D. Isolation of natural products by preparative high performance liquid chromatography (prep-HPLC). In: SARKER, S. D.; NAHAR, L. (org.). **Natural products isolation**. Nova York: Springer, 2012. v. 864p. 255–274. DOI: 10.1007/978-1-61779-624-1_10.

LI, Z. J.; XIA, Q. f. Recent advances on synthesis and application of graphene as novel sensing materials in analytical chemistry. **Reviews in analytical chemistry**, Berlin: De Gruyter, 2012. DOI: 10.1515/revac-2011-0039.

LIANG, R. P.; MENG, X. Y.; LIU, C. M.; WANG, J. W.; QIU, J. D. Enantiomeric separation by open-tubular capillary electrochromatography using bovine-serum-albumin-conjugated graphene oxide–magnetic nanocomposites as stationary phase. **Microfluidics and Nanofluidics**, New York, v. 16, n. 1–2, p. 195–206, 2014. DOI: 10.1007/s10404-013-1235-4.

LIANG, X.; WANG, S.; LIU, S.; LIU, X.; JIANG, S. A novel octadecylsilane functionalized graphene oxide/silica composite stationary phase for high performance liquid chromatography. **Journal of Separation Science**, New Jersey, v. 35, n. 16, p. 2003–2009, 2012. DOI: 10.1002/jssc.201200258.

LIU, Q.; SHI, J.; JIANG, G. Application of graphene in analytical sample preparation. **TrAC Trends in Analytical Chemistry**, Amsterdam v. 37, p. 1–11, 2012. DOI: 10.1016/j.trac.2012.03.011.

MA, X.; WANG, J.; WU, Q.; WANG, C.; WANG, Z. Extraction of carbamate pesticides in fruit samples by graphene reinforced hollow fibre liquid microextraction followed by high performance liquid chromatographic detection. **Food Chemistry**, Amsterdam, v. 157, p. 119–124, 2014. DOI: 10.1016/j.foodchem.2014.02.007.

MACIEL, E. V. S.; VARGAS-MEDINA, D. A.; LANCAS, F. M. Analyzes of β-lactam antibiotics by direct injection of environmental water samples into a functionalized graphene oxide-silica packed capillary extraction column online coupled to liquid chromatography tandem mass spectrometry. **Talanta Open**, Amsterdam, v. 7, n. October 2022, p. 100185, 2023. DOI: 10.1016/j.talo.2023.100185.

MADEJ, K.; JONDA, A.; BORCUCH, A.; PIEKOSZEWSKI, W.; CHMIELARZ, L.; GIL, B. A novel stir bar sorptive-dispersive microextraction in combination with magnetically modified graphene for isolation of seven pesticides from water samples. **Microchemical Journal**, Amsterdam, v. 147, p. 962–971, 2019. DOI: 10.1016/j.microc.2019.04.002.

MAJORS, Ronald E. Techniques for liquid chromatographic columns packed with small porous particles. A**nalytical Chemistry**, Washington, v. 45, n. 4, p. 755–762, 1973. a. DOI: 10.1021/ac60326a020.

MAJORS, R. E. Effect of particle size on particle eddy diffusivity. **Journal of Chromatographic Science**, Oxford, v. 11, p. 88–95, 1973.

MASIÁ, A.; SUAREZ-VARELA, M. M.; LLOPIS-GONZALEZ, A.; PICÓ, Y. Determination of pesticides and veterinary drug residues in food by liquid chromatography-mass spectrometry: A review. **Analytica Chimica Acta**, Amsterdam, v. 936, p. 40–61, 2016. DOI: 10.1016/j.aca.2016.07.023.

MAZZEO, J. R.; NEUE, U.; KELE, M.; PLUMB, R. S. Advancing LC Performance with smaller particles and higher pressure. **Analytical Chemistry**, Washington, v. 77, n. 23, p. 460 A-467 A, 2005. DOI: 10.1021/ac053516f.

MEJÍA-CARMONA, K.; LANÇAS, F. M. Modified graphene-silica as a sorbent for in-tube solid-phase microextraction coupled to liquid chromatography-tandem mass spectrometry. determination of xanthines in coffee beverages. **Journal of Chromatography A**, Amsterdam, v. 1621, 2020. DOI: 10.1016/j.chroma.2020.461089.

MEJÍA-CARMONA, K.; SOARES DA SILVA BURATO, J.; BORSATTO, J. V. B; DE TOFFOLI, A. L.; LANÇAS, F. M. Miniaturization of liquid chromatography coupled to mass spectrometry: 1. current trends on miniaturized lc columns. **TrAC - Trends in Analytical Chemistry**, Amsterdam, v. 122, 2020. DOI: 10.1016/j.trac.2019.115735.

NAWROCKI, J. The silanol group and its role in liquid chromatography. **Journal of Chromatography A**, Amsterdam, v. 779, n. 1–2, p. 29–71, 1997. DOI: 10.1016/S0021-9673(97)00479-2.

NESTERENKO, E. P. **Liquid Chromatography :** monolithic columns. 3. ed. Amstderdam: Elsevier, 2018. DOI: 10.1016/B978-0-12-409547-2.13991-5.

NIESSEN, W. M. A.; VAN VLIET, H. P. M.; POPPE, H. Studies on external peak broadening in open-tubular liquid chromatography systems using the exponentially modified Gaussian model. **Chromatographia**, New York, v. 20, n. 6, p. 357–363, 1985. DOI: 10.1007/BF02269062.

NOVOSELOV, K. S.; GEIM, A. K.; MOROZOV, S. V.; JIANG, D.; ZHANG, Y.; DUBONOS, S. V.; GRIGORIEVA, I. V.; FIRSOV, A. A. Electric field effect in atomically thin carbon films. **Science**, Washington, v. 306, n. 5696, p. 666–669, 2004. DOI: 10.1126/science.1102896.

NÚÑEZ, O.; NAKANISHI, K.; TANAKA, N. Preparation of monolithic silica columns for high-performance liquid chromatography. **Journal of Chromatography A**, Amsterdam, 2008. DOI: 10.1016/j.chroma.2008.02.029.

PITT, J. J. Principles and applications of liquid chromatography-mass spectrometry in clinical biochemistry. **The Clinical biochemistry Reviews**, Alexandria, v. 30, n. 1, p. 19–34, 2009.

POPPE, H. Some reflections on speed and efficiency of modern chromatographic methods. **Journal of Chromatography A**, *Amsterdam*, v. 778, n. 1–2, p. 3–21, 1997. DOI: 10.1016/S0021-9673(97)00376-2.

RIGANO, F.; TRANCHIDA, P. Q.; DUGO, P.; MONDELLO, L. High-performance liquid chromatography combined with electron ionization mass spectrometry: a review. **TrAC - Trends in Analytical Chemistry**, Amsterdam, v. 118, p. 112–122, 2019. DOI: 10.1016/j.trac.2019.05.032.

ROZENBRAND, J.; VAN BENNEKOM, W. P. Silica-based and organic monolithic capillary columns for LC: Recent trends in proteomics. **Journal of Separation Science**, New Jersey, v. 34, n. 16–17, p. 1934–1944, 2011. DOI: 10.1002/jssc.201100294.

SHALLIKER, R. A.; SAMUELSSON, J.; FORNSTEDT, T. Sample introduction for high performance separations. **TrAC Trends in Analytical Chemistry**, Amsterdam, v. 81, p. 34–41, 2016. DOI: 10.1016/j.trac.2016.01.004.

SITKO, R.; ZAWISZA, B.; MALICKA, E. Graphene as a new sorbent in analytical chemistry. **TrAC Trends in Analytical Chemistry**, Amsterdam, v. 51, p. 33–43, 2013. DOI: 10.1016/j.trac.2013.05.011.

SNYDER, L. R. Comparisons of normal elution, coupled-columns, and solvent, flow or temperature programming in liquid chromatography. **Journal of Chromatographic Science**, *Oxford,* v. 8, n. 12, p. 692–705, 1970. DOI: 10.1093/chromsci/8.12.692.

SONG, X. L.; LV, H.; WANG, D. D.; LIAO, K. C.; WU, Y. Y.; LI, G. M.; CHEN, Y. Graphene oxide composite microspheres as a novel dispersive solid-phase extraction adsorbent of bisphenols prior to their quantitation by HPLC–mass spectrometry. **Microchemical Journal**, Amsterdam, v. 172, p. 106920, 2022. DOI: 10.1016/j.microc.2021.106920.

SUN, M.; HAN, S.; MALOKO LOUSSALA, H.; FENG, J.; LI, C.; JI, X.; FENG, J.; SUN, H. Graphene oxide-functionalized mesoporous silica for online in-tube solid-phase microextraction of polycyclic aromatic hydrocarbons from honey and detection by high performance liquid chromatography-diode array detector. **Microchemical Journal**, Amsterdam*,* v. 166, n. October 2020, p. 106263, 2021. a. DOI: 10.1016/j.microc.2021.106263.

SUN, X.; DING, Y.; NIU, B.; CHEN, Q. Evaluation of a composite nanomaterial consist of gold nanoparticles and graphene-carbon nitride as capillary electrochromatography stationary phase for enantioseparation. **Microchemical Journal**, Amsterdam, v. 169, p. 106613, 2021. b. DOI: 10.1016/j.microc.2021.106613.

SUN, Y.; CABOVSKA, B.; EVANS, C. E.; RIDGWAY, T. H.; STALCUP, A. M. Retention characteristics of a new butylimidazolium-based stationary phase. **Analytical and Bioanalytical Chemistry**, New York*,* v. 382, n. 3, p. 728–734, 2005. DOI: 10.1007/s00216-004-3051-x.

TANAKA, N.; MCCALLEY, D. V. Core-Shell, Ultrasmall Particles, Monoliths, and Other Support Materials in High-Performance Liquid Chromatography. **Analytical Chemistry**, Washington, v. 88, n. 1, p. 279–298, 2016. DOI: 10.1021/acs.analchem.5b04093.

TECHNICAL ANALYTICAL METHODS COMMITTEE BRIEFS. Analytical methods. what causes most errors in chemical analysis? London: Royal Society of Chemistry, 2013. DOI: 10.1039/C3AY90035E.

TOLOSA, J.; FONT, G.; MAÑES, J.; FERRER, E. Multimycotoxin analysis in water and fish plasma by liquid chromatography-tandem mass spectrometry. **Chemosphere**, Amsterdam, v. 145, p. 402–408, 2016. DOI: 10.1016/j.chemosphere.2015.11.085.

TOUCHSTONE, J. C. History of Chromatography. **Journal of Liquid Chromatography**, Abingdon-on-Thames, v. 16, n. 8, p. 1647–1665, 1993. DOI: 10.1080/10826079308021679.

VAN DEEMTER, J. J.; ZUIDERWEG, F. J.; KLINKENBERG, A. Longitudinal diffusion and resistance to mass transfer as causes of nonideality in chromatography. **Chemical Engineering Science**, Amsterdam, v. 5, n. 6, p. 271–289, 1956. DOI: 10.1016/0009-2509(56)80003-1.

VANDERHEYDEN, Y.; CABOOTER, D.; DESMET, G.; BROECKHOVEN, K. Isocratic and gradient impedance plot analysis and comparison of some recently introduced large size core-shell and fully porous particles. **Journal of Chromatography A**, Amsterdam, v. 1312, p. 80–86, 2013. DOI: 10.1016/j.chroma.2013.09.009.

VANHOENACKER, G.; SANDRA, P. Elevated temperature and temperature programming in conventional liquid chromatography - Fundamentals and applications. **Journal of Separation Science**, New Jersey, v. 29, n. 12, p. 1822–1835, 2006. DOI: 10.1002/jssc.200600160.

VANHOENACKER, G.; SANDRA, P. High temperature and temperature programmed HPLC: possibilities and limitations. **Analytical and Bioanalytical Chemistry**, London, v. 390, n. 1, p. 245–248, 2008. DOI: 10.1007/s00216-007-1671-7.

VARGAS MEDINA, D. A.; BURATO, J. S. S.; BORSATTO, J. V. B.; LANÇAS, Fernando M. Porous layer open tubular nano liquid chromatography directly coupled to electron ionization mass spectrometry. **Journal of Chromatography A**, Amsterdam, v. 1674, p. 463143, 2022. DOI: 10.1016/j.chroma.2022.463143.

VARGAS MEDINA, D. A.; PEREIRA DOS SANTOS, N. G.; DA SILVA BURATO, J. S.; BORSATTO, J. V. B.; LANÇAS, F. M. An overview of open tubular liquid chromatography with a focus on the coupling with mass spectrometry for the analysis of small molecules. **Journal of Chromatography A**, Amsterdam, v. 1641, p. 461989, 2021. DOI: 10.1016/j.chroma.2021.461989.

VARGAS MEDINA, D. A.; SOARES MACIEL, E. V.; LÚCIA DE TOFFOLI, A.; LANÇAS, F. M. Miniaturization of liquid chromatography coupled to mass spectrometry. 2. Achievements on modern instrumentation for miniaturized liquid chromatography coupled to mass spectrometry. **TrAC Trends in Analytical Chemistry**, Amsterdam, v. 128, p. 115910, 2020. DOI: 10.1016/j.trac.2020.115910.

WAHAB, M. F.; PATEL, D. C.; WIMALASINGHE, R. M.; ARMSTRONG, D. W. Fundamental and practical insights on the packing of modern high-efficiency analytical and capillary columns. **Analytical Chemistry,** Washington, v. 89, p. 8177–8191, 2017. DOI: 10.1021/acs.analchem.7b00931.

WANG, M. M.; YAN, X. P. Fabrication of graphene oxide nanosheets incorporated monolithic column via one-step room temperature polymerization for capillary electrochromatography. **Analytical Chemistry**, Washington, v. 84, n. 1, p. 39–44, 2012. DOI: 10.1021/ac202860a.

WANG, N.; LU, Y.; CUI, B. Preparation and Application of β-Cyclodextrin Functionalised graphene oxide-grafted silica sorbents for solid-phase extraction (spe) of polycyclic aromatic hydrocarbons from fried food using a box-behnken design. **Food Analytical Methods**, New York, v. 14, n. 8, p. 1577–1589, 2021. DOI: 10.1007/s12161-021-02013-4.

WARREN, W. J.; VELLA, G. Principles and methods for the analysis and purification of synthetic deoxyribonucleotides by high-performance liquid chromatography. **Molecular Biotechnology**, New York, v. 4, n. 2, p. 179–199, 1995. DOI: 10.1007/BF02921611.

YU, W.; SISI, L.; HAIYAN, Y.; JIE, L. Progress in the functional modification of graphene/graphene oxide: a review. **RSC Advances**, London, v. 10, n. 26, p. 15328–15345, 2020. DOI: 10.1039/D0RA01068E.

ZHANG, J.; YU, C.; CHEN, Z.; LUO, X.; ZHAO, H.; WU, F. Zeolitic imidazolate framework-8/ fluorinated graphene coated SiO2 composites for pipette tip solid-phase extraction of chlorophenols in environmental and food samples. **Talanta**, Amsterdam, v. 228, p. 122229, 2021. a. DOI: 10.1016/j.talanta.2021.122229.

ZHANG, Q.; YOU, L.; CHEN, B.; HE, M.; HU, B. Reduced graphene oxide coated nickel foam for stir bar sorptive extraction of benzotriazole ultraviolet absorbents from environmental water. **Talanta**, *Amsterdam*, v. 231, p. 122332, 2021. b. DOI: 10.1016/j.talanta.2021.122332.

ZHANG, X.; CHEN, S.; HAN, Q.; DING, M. Preparation and retention mechanism study of graphene and graphene oxide bonded silica microspheres as stationary phases for high performance liquid chromatography. **Journal of Chromatography A**, Amsterdam, v. 1307, p. 135–143, 2013. DOI: 10.1016/j.chroma.2013.07.106.

ZHAO, H.; WANG, Y.; CHENG, H.; SHEN, Y. Graphene oxide decorated monolithic column as stationary phase for capillary electrochromatography. **Journal of Chromatography A**, *Amsterdam,* v. 1452, p. 27–35, 2016. DOI: 10.1016/j.chroma.2016.05.001.

Capítulo 2

Coletânea de artigos

A Coletânea de artigos

Essa tese é apresentada no formato de coletânea de artigos. Esse capítulo sumariza os artigos relacionados nessa tese e discute a relação de cada trabalho com a tese. Foram obtidas as permissões legais para os usos desses trabalhos nessa tese junto as revistas nas quais os artigos encontram-se publicados.

Capítulo 3 - "Trends in graphene-based sorbents for LC. Analysis of food and environmental water"

Nesse trabalho de revisão é apresentado o estado-da-arte do uso de materiais derivados de grafeno como sorventes para métodos analíticos visando análises de alimentos e águas por meio de cromatografia líquida. São apresentadas aplicações recentes (entre 2019 e 2023) relacionando o uso desses sorventes como fases de extração e fases estacionárias s. Também são relacionadas as tendências e vacâncias a serem preenchidas futura para aplicação de materiais em análises de alimentos.

Capítulo 4 – "Miniaturization of liquid chromatography coupled to mass spectrometry 1. Current trends on miniaturized LC columns"

Esse trabalho de revisão apresenta os fundamentos e principais aspectos práticos da utilização de colunas capilares em cromatografia líquida, em especial no acoplamento com espectrometria de massas. Esse trabalho apresenta, também, as bases teóricas utilizadas para planejar as séries experimentais e analisar os resultados de performance cromatográficas para as colunas de grafeno estudadas.

Capítulo 5 – "Investigation of the applicability of silica-graphene hybrid materials as stationary phases for capillary liquid chromatography".

Nesse capítulo são apresentados os primeiros resultados do emprego de partículas de SiGO-C18ec como fase estacionária em colunas capilares analíticas para cromatografia líquida. Esse estudo faz um comparativo da performance de colunas empacotadas com partículas SiGO-C18ec de três diâmetros diferentes (3, 5 e 10 μm) assim como as compara com uma coluna empacotada com partículas de C18 com 3 μm de diâmetro. Para essa comparação, usou-se um

conjunto de sondas (compostos) de diferentes classes, incluindo fármacos, pesticidas e toxinas. Nesse mesmo estudo também é apresentada uma comparação da seletividade das fases de SiGO-C18ec de diferentes diâmetros, e com a coluna de C18. DOI: 10.1016/j.chroma.2022.463618.

Capítulo 6 - "Application of an in-house packed octadecylsilica-functionalized graphene oxide column for capillary liquid chromatography analysis of hormones in urine samples".

Esse trabalho visou a aplicação das fases de SiGO-C18ec para a separação de hormônios. Nesse estudo, duas frentes foram abordadas. A primeira foi a otimização das condições experimentais do HPLC para o uso de partículas de SiGO-C18ec em colunas empacotadas e a seleção de qual diâmetro de partícula seria utilizado nas análises subsequentes. A segunda abrange a aplicação dessas fases em um método analítico, utilizando um sistema *column-switching,* para a determinação de biomarcadores em amostras de urina. Também é importante mencionar que resultados parciais relacionados a esse trabalho foram apresentados na forma de pôster no *5th International Conference on Applied Surface Science*, em Palma de Maiorca, Espanha.

Capítulo 7 – "Online extraction followed by LC–MS/MS analysis of lipids in natural samples: a proof-of-concept profiling lecithin in seeds".

Nesse capítulo é abordada a aplicação de análises de lipídios por meio de extração líquida online (OLE), técnica na qual a amostra solida é colocada em um dispositivo antes da coluna, permitindo assim a "injeção de amostra solida". Esse trabalho apresenta uma novidade intrigante, a coluna de SiGO-C18ec apresentou melhor desempenho do que uma coluna de C18 convencional para o método aplicado. Esse resultado é bastante interessante, pois não se esperava que seria encontrada uma aplicação na qual as colunas de SiGO-C18ec seriam mais adequadas do que colunas de C18 tão rapidamente devido ao estágio inicial de desenvolvimento. Adicionalmente, esse é o primeiro estudo utilizando clorofórmio como fase móvel para uma coluna empacotada com fase de SiGO-C18ec.

Capítulo 8 – "Applicability and limitations of a capillary-LC column-switching system using hybrid graphene-based stationary phases".

Nesse capítulo é abordada a construção de um sistema bidimensional composto exclusivamente por colunas empacotadas com fases baseadas em grafeno. O sistema bidimensional foi construído para operar no modo *column-switching.* Esse sistema foi aplicado na análise de pesticidas em refrigerantes de laranja. Segundo o que conhecemos da literatura, trata-se da primeira avaliação das capacidades e limitações de um sistema bidimensional composto exclusivamente com colunas empacotadas com fases baseadas em grafeno. O sistema apresentou resultados satisfatórios na quantificação de piriproxifen na faixa de concentração entre 0,5 e 25µg/mL. No entanto, a análise quantitativa de abamectina B1a não foi possível. Além disso, a composição da matriz afetou a área observada para o piriproxifen.

Apoio

O presente trabalho foi realizado com apoio do Conselho Nacional de Desenvolvimento Científico e Tecnológico – CNPq.

O presente trabalho foi realizado com apoio da Coordenação de Aperfeiçoamento de Pessoal de Nível Superior – Brasil (CAPES) – Código de Financiamento 001.

Capítulo 3

Trends in graphene-based sorbents for LC analysis of food and environmental water

Borsatto, João V. B.; Lanças, Fernando M. Recent Trends in Graphene-Based Sorbents for LC Analysis of Food and Environmental Water Samples. **Molecules**, *[S. l.]*, v. 28, n. 13, p. 5134, 2023. DOI: 10.3390/molecules28135134. Disponível em: https://www.mdpi.com/1420-3049/28/13/5134.

molecules

MDPI

Review

Recent Trends in Graphene-Based Sorbents for LC Analysis of Food and Environmental Water Samples

João V. B. Borsatto and Fernando M. Lanças *

Laboratory of Chromatography, Institute of Chemistry at Sao Carlos, University of Sao Paulo, P.O. Box 780, São Carlos 13566-590, Brazil
* Correspondence: flancas@iqsc.usp.br

Abstract: This review provides an overview of recent advancements in applying graphene-based materials as sorbents for liquid chromatography (LC) analysis. Graphene-based materials are promising for analytical chemistry, including applications as sorbents in liquid chromatography. These sorbents can be functionalized to produce unique extraction or stationary phases. Additionally, graphene-based sorbents can be supported in various materials and have consequently been applied to produce various devices for sample preparation. Graphene-based sorbents are employed in diverse applications, including food and environmental LC analysis. This review summarizes the application of graphene-based materials in food and environmental water analysis in the last five years (2019 to 2023). Offline and online sample preparation methods, such as dispersive solid phase microextraction, stir bar sorptive extraction, pipette tip solid phase extraction, in-tube solid-phase microextraction, and others, are reviewed. The review also summarizes the application of the columns produced with graphene-based materials in separating food and water components and contaminants. Graphene-based materials have been reported as stationary phases for LC columns. Graphene-based stationary phases have been reported in packed, monolithic, and open tubular columns and have been used in LC and capillary electrochromatography modes.

Keywords: liquid chromatography; graphene-based sorbents; sample preparation; food analysis; water analysis; graphene; stationary phase

Citation: Borsatto, J.V.B.; Lanças, F.M. Recent Trends in Graphene-Based Sorbents for LC Analysis of Food and Environmental Water Samples. *Molecules* **2023**, *28*, 5134. https://doi.org/10.3390/molecules28135134

Academic Editors: Gavino Sanna, Pengxiang Hou and Maoshuai He

Received: 5 June 2023
Revised: 22 June 2023
Accepted: 22 June 2023
Published: 30 June 2023

1. Introduction

Graphene and graphene derivates are emerging materials in research and development [1], including in material science, chemistry, physics, and many other fields (Figure 1A). Graphene-based materials mainly comprise SP2 hybridized carbons organized in a hexagonal flat web formed by σ covalent bonds and parallel π bonds, the base graphene structure [2]. Although graphene and its derivatives are relatively new materials, they have a great diversity of applications in analytical chemistry due to their intrinsic characteristics [2]. Among such characteristics, the high electrical conductivity, mechanical resistance, low density, and high light scattering yield can be highlighted, making it an excellent candidate for applications in sensors and detectors [3]. Furthermore, its large surface area also results in a high adsorption capacity, making it a promising material for catalysts and sorbents [4,5]. Due to these characteristics, graphene-based materials have gained prominence in the last decade in sample preparation and chromatography (Figure 1B). The literature presents reviews that cover the physico-chemical characteristics of graphene and graphene-based materials, as well the application of those materials [6–8].

Despite the potential for graphene and its derivates as a highly suitable material, the manufacturing obstacle hinders its adoption on an industrial scale. The mechanical exfoliation of graphite through adhesive tape is a practical way to produce graphene-based materials [9,10]. This procedure, also called the Geim–Novoselov scotch method, involves an adhesive tape, which is pressed onto a piece of graphite and lifted off, taking

a layer of graphite with it [11]. The process is repeated several times to obtain thinner and thinner layers of graphite. The mechanical force applied by the tape causes the layers to separate, leaving behind clean, smooth surfaces [10]. However, this process is highly dependent on human manipulation, and is laborious. Because of these limitations, efforts have been directed to develop alternative routes to produce large quantities of high-quality graphene-based materials [12]. Among the alternative routes, chemical exfoliation, such as Hummer's method, provides exciting results, being a practical and relatively less manual way of obtaining this material [13–17]. Also, other methods to produce graphene and graphene-based materials have been described in the literature [18]. Chemical vapor deposition [19,20], electrochemical exfoliation [21,22], and unzipping carbon nanotubes [23] are examples of alternative routes to produce graphene and its derivates. Though different preparation procedures for graphene-based materials are described in the literature, they usually follow a general route for application as sorbents [24]. Firstly, the graphite material is oxidated to form graphite oxide. After the graphite oxide has been obtained, this material is sonicated to separate the layers that compose the graphite oxide, forming graphene oxide (GO) sheets. The GO obtained produces reduced graphene oxide or is functionalized with diverse bindings (Figure 1C).

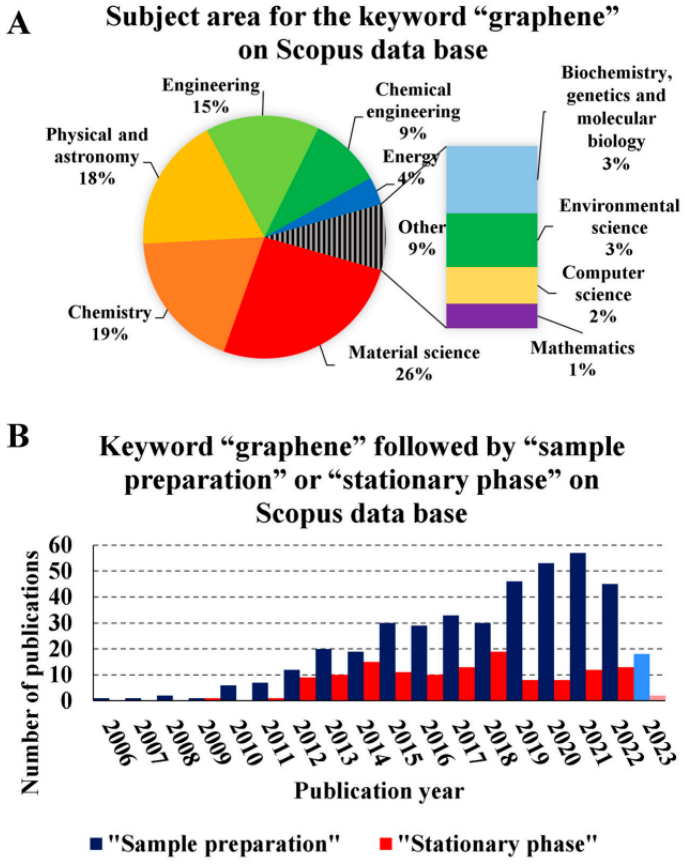

Figure 1. *Cont.*

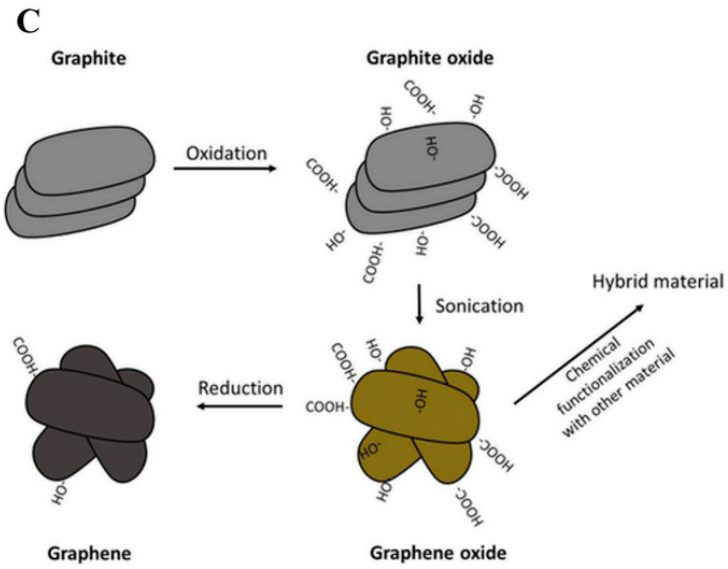

Figure 1. (**A**) Subject area for the keyword "graphene" on the Scopus database. (**B**) The number of publications per year in the database from the keyword search "graphene" followed by "sample preparation" or "stationary phase" on the Scopus database. (**C**) General route to obtain graphene-based materials. Figure 1C is reproduced with permission from J. Sep. Sci., 41, de Toffoli, A.L.; Maciel, E.V.S.; Fumes, B.H.; Lanças, The Role of Graphene-Based Sorbents in Modern Sample Preparation Techniques, Pages 288–302, Copyright (2018), John Wiley and Sons [24].

The diversity of potential functionalizations of graphene-based materials allows for a wide range of applications in separation science. These applications include the use of techniques such as stir bar sorptive extraction (SBSE) [25,26], dispersive solid phase extraction (d-SPME) [27,28], fiber solid phase microextraction (Fiber-SPME) [29,30], in-tube solid-phase microextraction (IT-SPME), and others [2,24] in sample preparation methods. Additionally, graphene-based materials have been explored as packing materials for analytical columns in LC, including using graphene oxide (GO) fixed to silica particles functionalized with C18, graphene (G) fixed to silica particles modified with gold nanoparticles, and reduced graphene oxide (rGO) coated with cellulose fixed to silica particles [31–34]. The variety of analytes that can be analyzed using these phases is as diverse as applying graphene-based sorbents in analytical techniques. Proteins [35], hormones [30], aromatic contaminants [36], pharmaceutical compounds [37,38], and others [2,39] are examples of analytes separated in columns composed by the graphene-based stationary phase.

The present review investigates the applications of graphene-based materials in food and water analysis, including their utilization as sorbents for sample preparation and analytical columns for LC, in a time frame from 2019 until 2023. The escalating necessity for enhanced analytical processes in food and water analysis has stimulated interest in using graphene-based materials as efficient and trustworthy solutions. Therefore, this review article aims to illuminate the current state and potential prospects for graphene-based sorbents in food and water analysis.

2. Offline Sample Preparation for Liquid Chromatography

Offline sample preparation techniques are the most common strategy in the analytical chemistry field. They consist of preparing the sample for analysis while disconnected from the instrument or application. Some advantages of this strategy are the simple procedure, which is usually not dependent on complex instrumentation set-up, and the possibility of analyzing sample fractions prepared with different analytical techniques. This section

summarizes offline extraction techniques in which graphene-based sorbents have been employed recently.

2.1. Graphene-Based Materials as Dispersive Sorbents

Dispersive solid phase extraction (d-SPE) and microextraction (d-SPME) are examples of sample preparation techniques that involve graphene-based materials as dispersive sorbents [40]. This sample preparation procedure involves (i) adding a solid phase extraction material, usually a powder, to the matrix, (ii) stirring the suspension, (iii) removing the extraction phase from the matrix, (iv) washing the extraction phase material to remove the residue of the matrix in the solid phase particles surface, and (v) eluting the analytes from the extraction phase with a suitable solvent before analysis.

Graphene-based materials have been employed in d-SPE and d-SPME, and mainly supported in magnetic nanoparticles [41]. Magnetic particles are helpful because they allow a magnet to remove the solid phase material from the matrix without filtration [41]. Furthermore, magnetic graphene-based d-SPME sorbents present an interesting advantage over non-magnetic graphene-based d-SPME sorbents. When inserted into an aqueous sample, the graphene-based materials tend to accumulate due to the hydrophobic characteristics of the graphene sheets, reducing their total surface area and, consequentially, reducing their absorption capacity [41]. The presence of the magnetic particles minimizes the accumulation and benefits the adsorption capacity of the extraction phase [41]. Different methods of preparing graphene-based magnetic sorbents are reported in the literature; they can be divided into three main routes. The first route to be cited is physical adsorption [42]. In this route, the graphene-based material and the magnetic particles are produced separately, then mixed in a solution under stirring or sonication. The graphene sheets are then fixed over the magnetic particles by physical adsorption [42]. This method is simple to perform but usually produces single-use sorbents. Another interesting route to produce magnetic graphene-based sorbents is via the in situ growth of magnetic materials [43]. This method is based on the co-precipitation of magnetic particles and graphene-based material sheets [44]. Also, the solvothermal method is a possibility for this route [45]. Covalent bonding is the third possible route to produce graphene-based magnetic particles [46]. In this method, the graphene is covalently bonded to the magnetic particles by modifying them with linker groupers, such as silane groups, binding them to the graphene-based material [47]. The application of d-SPME and d-SPE graphene-based sorbents is also a trend in food and water analysis. For example, the d-SPE phase composed of magnetic graphene oxide (GO) tert-butylamine (TBA) fixed in the magnetic particles' (GO/Fe_3O_4/TBA) nanocomposite was successfully applied in the determination of herbicides in vegetables and water samples [48]. The GO/Fe_3O_4/TBA sorbent was prepared by co-precipitating GO and Fe_3O_4 particles. After the obtention of the GO/Fe_3O_4 particles, they were functionalized with TBA using ethylene glycol to form covalent bonds. A d-SPME method using the GO/Fe_3O_4/TBA to quantify 2,4-dichlorophenoxyacetic acid presented limit of detection (LOD) and limit of quantitation (LOQ) values lower than 0.02 $\mu g \cdot mL^{-1}$, and the recovery range was between 88.0 and 94.0%. Another graphene-based magnetic phase that has been successfully applied to the analysis of contaminants in vegetables is the GO-Fe_3O_4 nanoparticles functionalized with maltodextrin (MD) and β-cyclodextrin (β-CD), which was used for the investigation of triazole and triazine pesticides in corn, tomato, and potato [49]. Co-precipitating the GO with the Fe_3O_4 magnetic particles produced this magnetic extraction phase. After the obtention of the GO-Fe_3O_4, this material was functionalized with MD and β-CD using epichlorohydrin as a linker. The LODs obtained for determining the pesticides in the vegetables ranged from 0.01 to 0.08 $\mu g \cdot L^{-1}$ and recovery was between 88.4 and 112.0%. Metal-organic frameworks (MOF) have also been used to functionalize graphene-based sorbents. MOFs are porous crystalline materials formed by assembling metal ions and organic ligands with large surface areas, high porosity, and controllable pore structures. As a recent example, in d-SPME, Fe_3O_4 particles functionalized with GO sheets and UiO-66 (a Zr-based MOF) have been used as a sorbent for the determination of food dyes in soft

drinks, candies, and pastilles [28]. This interesting phase was produced by co-precipitating GO and Fe_3O_4, followed by the addition of $ZrOCl_2 \cdot 8H_2O$ and terephthalic acid into a GO-Fe_3O_4 suspension in order to produce the magnetic GO/UIO-66 sorbent. The s-SPME method employing the GO/UIO-66 sorbent presented LODs less than 0.218 $ng \cdot mL^{-1}$, LOQs lower than 9.368 $ng \cdot mL^{-1}$, and recovery ranging from 95.01 to 106.33%. The interaction mechanism between the MOF-based sorbent and the food dye analytes was attributed to multiple mechanisms, including n–π/π–π interactions, Yoshida/dipole–dipole hydrogen bonds, and electrostatic interactions. Though magnetic particles are the primary support for sample preparation in d-SPME and d-SPE in food and water analysis, no magnetic materials have been used. For example, GO-coating polystyrene (PS) microspheres were applied to extract bisphenol endocrine disruptors in environmental water samples [27]. To produce GO-PS sorbents, PS colloid templates were first activated to present a positively charged surface. This material was reacted with a suspension of GO in order to form the desired extraction phase. This GO-PS sorbent was employed in the d-SPME method to determine bisphenol A, bisphenol B, bisphenol AF, and tetrabromobisphenol A, presenting LODs between 0.02 and 0.11 $\mu g \cdot L^{-1}$ and LOQs of 0.07–0.37 $\mu g \cdot L^{-1}$ and recovering in a range from 71.1% to 104.8%. The retention mechanism of this GO-PS extraction phase was attributed to the π–π interactions and hydrogen interactions between the sorbent and the analytes. Another interesting variation of the d-SPME using graphene-based sorbents applied in food analysis is the "rotating flat surface solid phase microextraction (RFS-SPME)" method. This strategy consists of suspending and stirring foams of the stationary phase, instead of powder material, in the matrix, and after the end of the stirring the foam can be removed with forceps [50]. The RFS-SPME sample preparation method was employed to analyze sulfonamides in animal-based food using an innovative material, the 3D GO/La fixed in Ni foams [50]. To produce the sorbent, GO and lanthanum nitrate were mixed and sonicated in water, followed by the immersion of nickel foam pieces in order to form the extraction phase. The 3D GO/La Ni foams could be applied in the RFS-SPME sample preparation method, which presented LODs lower than 0.14 $\mu g \cdot L^{-1}$, LOQs lower than 0.475 $\mu g \cdot L^{-1}$, and recoveries over 90.0% The evaluated 3D GO/La Ni foams' extraction phase presented an extraction mechanism sorbent–sorbate combining π–π interaction, hydrogen bonding, and electrostatic interaction.

2.2. Graphene-Based Materials as Coating Sorbents

Coating techniques involve sample preparation strategies where the sorbent is coated over, typically, a non-sorptive surface. For example, stir bar sorptive extraction (SBSE) and fiber solid phase microextraction (fiber-SPME) are techniques in which the sorbent is fixed over an inert surface. Usually, the sample preparation process using these techniques involves (i) immersing the device coated with sorbent in a matrix solution, (ii) stirring the solution for a specific time, (iii) removing and washing the device to remove the matrix, and finally (iv) desorbing the analyst in an appropriated solvent before analysis.

SBSE and related techniques are simple and effective ways to extract analytes from the matrix. SBSE devices are usually produced by chemically or physically adhering the sorbent to an inert material [51]. Graphene-based materials have been explored in SBSE using this strategy [26,52]. For example, a Ni bar coated with reduced graphene oxide (rGO) was recently used to evaluate benzotriazole ultraviolet absorbents from environmental water [26]. The SBSE bar was produced through covalent bonding between GO and the Ni foam, forming the rGO-Ni foam sorbent. The formed material was then shaped in a stir bar format. This device could be used as an SBSE sample preparation method to determine the analytes at LODs of 0.33–0.50 $\mu g \cdot L^{-1}$ and recovery in a range of 83% to 112%. The rGO-Ni SBSE bar presented an attributed extraction mechanism based on π–π interaction and hydrophobic interactions [26]. Moreover, SBSE bars can be produced by covering cheap magnetic materials, such as coating a wire with sorbent. Graphene-based materials have been used to prepare SBSE devices using this strategy. For example, an SBSE bar produced with stainless steel (SS) wire covered with graphene oxide frameworks

(GOF) was employed to extract and analyze dyes in water samples [52], presenting LODs of 0.15 to 0.3 ng·mL^{-1}, LOQs of 0.5 to 1.0 ng·mL^{-1}, and a recovery range of 89.38–108.54%. To produce this device, it was first necessary to activate the SS wire surface to allow the chemical binding of the GO. To do that, the SS wire was submitted to a sequence of reactions until the polydopamine-SS wire was formed. The GO was suspended in a solution and then reacted with the polydopamine-SS wire forming the GOF-SS wire SBSE bar [52]. Another way to produce SBSE bars is by magnetic fixation of the sorbent to the stirring bar [25]. This bar type is used in a sample preparation technique called stir bar sorptive-dispersive microextraction (SBSDμE). As the name suggests, this technique introduces the coated magnetic bar into the sample solution, and under fast stirring the sorbent is dispersed in the solution. After the end of the stirring, the magnetic bar attracts the sorbent forming against the coated bar, which can be removed by plastic forceps [25]. A recent application of this technique using graphene-based materials for water analysis was the use of an SBSDμE device composed of a neodymium stir bar coated by graphene (G) fixed on Fe_3O_4 particles' sorbent (G-Fe_3O_4) in the determination of seven pesticides in water [25]. The magnetic G-Fe_3O_4 particles were produced by the co-precipitation method, similar to that previously described in the d-SPME section. This SBSDμE method presented a recovery range between 20% and 75%, with a LOQ between 5 ng·mL^{-1} and 9.5 ng·mL^{-1}. Another interesting sample preparation technique based on the sorbent phase coating a surface was fiber solid phase microextraction (fiber-SPME). Fiber-SPME consists of the sorbent coating a capillary's inner or outer surface, forming the extraction fiber. Commonly, fiber-SPME devices are filled with monolithic extraction phases, including the ones modified with graphene-based materials. Graphene-based materials as fiber-SPME sorbents have also been explored for food and water LC analysis in the last five years. For example, a composite prepared with GO, MOF zeolitic imidazolate framework 8 (ZIF-8), and molecularly imprinted polymers (MIP) deposited in fiber was used to evaluate sterol and steroid hormones in white meat, egg yolks, and vegetables [30]. The fiber-SPME device was prepared by first producing the GO-MOF sorbent via the solvothermal method. The GO-MOF material was then reacted with a functional monomer (methacrylic acid), a cross-linking agent (ethylene glycol dimethacrylate), and an initiator of the imprinting polymerization (azo (bis)-isobutyronitrile) inside a capillary in order to form the MIP-GO-MO fiber. Applying this fiber-SPME device in the sample preparation method resulted in LODs ranging from 3 to 5 ng·L^{-1} and recovery ranging from 95.0% to 101.0%. This sorbent presented a mixed interaction mechanism, primarily attributed to the MIP efficient imprinting effect and the differences in size, functional group type, and position of the analytes and polar interactions, hydrogen bonds, and electrostatic interactions [30]. Another interesting application of graphene-based sorbents in food analysis is the combination of multiple fibers for the sample preparation procedure [29]. Using multiple SPME fibers increases the surface area of the extraction device, and consequently enhances the extraction. In food and water analysis, a multifiber-SPME device consisting of G embedded in a poly 4-vinylpyridine-co-ethylene glycol dimethacrylate (VP-co-EGDMA) monolith was used to extract and determine phenoxy acetic acid herbicides in water and rice samples [29]. LODs lower than 0.66 μg·L^{-1} and LOQs lower than 2.27 μg·L^{-1} were obtained, and a recovery of range between 70.0 and 117% was reported using this sample preparation method.

Hollow fiber solid phase microextraction (HF-SPME) is a variation of the fiber-SPME in which the sorbent coats the inner wall of a capillary, forming an open channel in the device's core [53]. Unfortunately, graphene-based sorbents applied on HF-SPME has been underexplored in food and water LC analysis in the last five years. Though underexplored, a recent example can be found in the literature, comprising an LC analysis of food and water samples. An HF-SPME device was prepared by using a MIL-101(Cr) MOF linked to GO and fixed in a polypropylene (PP) fiber to investigate organophosphorus compounds in tomato, cucumber, and agricultural water samples [54]. The hydrothermal method produced MIL-101(Cr) MOF linked to GO. Lately, the material formed has been immobilized on the wall of the PP fiber. Applying the HF-SPME method in determining

organophosphorus compounds in vegetables presented LODs lower than 0.27 $\mu g \cdot L^{-1}$ and LOQs lower than 0.91 $\mu g \cdot L^{-1}$. This extraction phase presented an interesting proposed interaction mechanism in which hydrogen bonding participates. However, the adsorption process also influences the interaction of π-electrons of the analyte with the Cr and back donation from the sorbent material into the molecular anti-bonding π∗ orbital [54].

2.3. Graphene-Based Materials as Packed Sorbent

Packed sorbent techniques are sample preparation techniques that use a solid adsorbent material packed in a cartridge, a column, or a pipette. The sample preparation procedure of these techniques comprises the following steps: (i) equilibrate the sorbent by flushing a suitable solvent through the cartridge, (ii) load the sorbent with the sample by flushing it through the cartridge (for SPE), (iii) wash the sorbent to remove the matrix, and (iv) elute and collect the analytes using a proper solvent.

Sorbents packed on cartridges are a usual approach for producing SPE devices. Silica particles are frequently used as a support for graphene-based sorbents due to their capacity to provide a stable structure and prevent blockages in cartridges [54]. Additionally, suppose that unbonded graphene, GO, or reduced (rGO) sheets are packed. In that case, they can accumulate and block the SPE device. When graphene-based sheets are bonded to Si particles, the covalent bond prevents the accumulation of free graphene-based sheets and avoids blocking. For example, GO sheets covalently bonded to Si particles (SiGO) and modified with β-CD were packed in a cartridge and used for the extraction and analysis of polycyclic aromatic hydrocarbons (PAHs) from fried food [55]. This strategy resulted in an LOD range of 0.1–0.3 $\mu g \cdot L^{-1}$ and a recovery range from about 55 to 90%. This stationary phase presents a complex interaction mechanism between the sorbent and the analytes due to the participation of π–π stacking, hydrophobic interaction, and size complementarity interactions. Another interesting graphene-based material packed in an SPE sample preparation cartridge is a zwitterionic sorbent modified with graphene (G) and fixed over Si particles [56]. This sorbent is prepared based on three steps. A sol solution is prepared to form the substrate in the first step. In the second step, the G is added to the previously formed material, forming a sol-gel G composite monolith. In the third step, this material is submitted to a synthesis route to produce the zwitterionic sorbent modified with (G). This combination of materials allowed intermolecular and interionic interactions such as dipole–dipole, ion exchange, and π–π interactions. The zwitterionic sorbent modified with the graphene (G) SPE cartridge was used to determine benzothiazoles, benzotriazoles, and benzenesulfonamides contaminants in environmental water [56], presenting LODs and LOQs lower than 20 $ng \cdot L^{-1}$ and a recoveries range from 48 to 85%. Though graphene-based materials are usually fixed over support, SPE cartridges can be packed with graphene sheets that are not fixed in support. As mentioned above, this kind of packing presents limitations, such as blocking the frits caused by the accumulation of the graphene sheets, but it is still possible. For example, it was reported that rGO sheets packed on SPE cartridges were used to extract aflatoxins from food samples [57]. It was possible to obtain LODs lower than 0.83 $ng \cdot g^{-1}$, LOQs lower than 2.83 $ng \cdot g^{-1}$, and relative recoveries ranging from 70 to 113% using this cartridge. Another interesting example of an SPE sorbent not supported in particles is 3D reduced graphene oxide (3D-rGO), a self-supported material [58]. In this configuration, the rGO material formed a 3D framework with a high content of carbon at the surface and some residual oxygen-containing groups. This sorbent was formed via hydrothermal reaction, using GO as a starting material. The 3D-rGO SPE devices were employed to determine diclofenac in water and effluent samples, presenting a recovery of about 80% [58]. A sorbent–sorbate interaction based mainly on π–π interactions and possibly on hydrogen bonding interactions was attributed to the 3D-rGO sorbent.

Pipet tip SPME (PT-SPME) can be considered a variation of the SPE because the sorbent packed on a pipet tip forms a device similar to a cartridge. Si particles have also been used as a sorbent support for PT-SPME sample preparation. As a recent example, GO sheets fixed on Si particles have reportedly been packed in PT-SPME devices and applied to determine

herbicides in sugarcane-derived foods [59]. The SiGO particles were prepared via covalent bonding between the GO and the Si particle, as is usual for this phase. This method showed acceptable LODs of 1.0–5.0 ng·mL^{-1} for juice and 5.0–25.0 ng·g^{-1} for candy and syrup. Additionally, recoveries ranging from 48 to 69%, 34 to 89%, and 28 to 76% were obtained for juice, candy, and syrup, respectively. MOF materials modified with graphene-base materials have also been reported as sorbents for PT-SPME. Si microspheres covalently bonded to fluorinated graphene (FG) and functionalized with ZIF-8 nanocrystals were packed in a PT-SPME device and applied to determine chlorophenols in tap water, honey, and black tea [60]. About 83.7% to 97.7% were for the chlorophenol compounds, with LOQs of 4.76 µg·kg^{-1} and LOQs of 15.9 µg·kg^{-1}. This extraction phase presented multi-interaction mechanisms, including π-stacking and hydrophobic and hydrogen-bonding interactions between the adsorbent and the compounds. Though Si particles are standard, other types of particles can be used as supports for graphene-based materials in PT-SPME and have been applied in LC analyses of foods. For example, the nanocomposite GO-starch-polyacrylamide was packed in PT-SPME devices and used to determine antibiotic residues in cow's milk [14]. The sorbent was produced by copolymerizing GO and polyacrylamide using CCO_3 to form the porous material. The PT-SPME method presented LODs of 2.7–5.0 µg·kg^{-1} and a recovery range of 88–102%. This extraction phase presented an adsorption mechanism mainly based on hydrogen bond interactions between the analytes and the sorbent [14].

2.4. Trends in Graphene-Based Offline Sample Preparation

In the last five years, graphene-based sorbents have successfully been employed in diverse sample preparation techniques for food and water analysis. Water, milk, vegetables, cereals, and meat are examples of the diversity of samples that graphene-based sorbents could prepare recently (Table 1). The diversity of the variety of the matrix represents the diversity of analytes that graphene-based sorbents can analyze. Pesticides, dyes, toxins, drugs, and hormones can be extracted using graphene-based sorbents. Dispersive solid phase extraction and packed sorbent devices, such as SPE cartridges and PT-SPE, are the most common applications of graphene-based sorbents. It has also been observed that GO and rGO sheets are the most usual type of graphene-based material used for the sorbents, and Hummer's method is the most usual way to obtain graphene-based material. Usually, graphene-based sorbents for sample preparation are prepared with no functionalization, or functionalization with MOF. The supporting material of the graphene-based sorbents is also important because it directly affects the application of those materials. In dispersive solid phase extraction, magnetic supports are receiving the most attention; for coated techniques (SBSE and fiber-SPME), a variety of supports has been presented; and for packed columns, Si particles have been the most-used support in recent years.

Table 1. Examples of graphene-based materials in offline sample preparation followed by liquid chromatography analysis since 2019.

Graphene-Based Material	Support	Modification	Techniques	Analytes	Matrix	Year	Ref.
GO	Fe_3O_4 particles	TBA	d-SPME	2,4-Dichlorophenoxyacetic acid	Environmental water, lettuce, celery, tomato, and cucumber	2020	[48]
GO	Fe_3O_4 particle	MD and β-CD	d-SPE	Triazole, and triazine	Corn, tomato, and potato	2021	[49]
GO	Fe_3O_4 particle	MOF/UIO-66	d-SPE	Sunset yellow, tartrazine, allura red	Soft drinks, candies, and pastilles	2023	[28]
GO	PS particle	Not modified	d-SPE	Bisphenol A, bisphenol B, bisphenol AF, tetrabromobisphenol A	Drinking water, tap water, and river water	2022	[27]

Table 1. *Cont.*

Graphene-Based Material	Support	Modification	Techniques	Analytes	Matrix	Year	Ref.
GO	Ni foam	La nanoparticles	RFS-SPME	Sulfadiazine, sulfamethoxazole, sulfamethazine	Fresh egg, cow meat, chicken meat, and fish	2022	[50]
GO	SS wire	GOF	SBSE	Sudan G, sudan I, sudan II, and sudan III (dyes)	Water and fruit juice	2019	[52]
GO	Ni bar	Not modified	SBSE	Benzotriazole	Environmental water	2021	[26]
G	Nd bar	Fe_3O_4-G	SBSDμE	Boscalid, chlorpyrifos, deltamethrin, dimethenamid-P, dimoxystrobin, metazachlor and tebuconazol	Water	2019	[25]
GO	MIP monolith	MOF/ZIF-8	Fiber-SPME	Sterols: progesterone, testosterone, β-sitosterol, cholesterol, and campesterol	White meat, egg yolks, and vegetables	2019	[30]
GO	VP-co-EGDMA monolith	Not modified	Fiber-SPME	Phenoxyacetic acid, 4-chloro-2-methylphenoxyacetic acid, 2,4-dichlorophenoxyacetic acid, 2-nitrophenoxyacetic acid, and 4-chlorophenoxyacetic acid	Water and rice	2019	[29]
GO	PP monolith	MOF/MIL-101	HF-SPME	Diazinon and chlorpyrifos	Tomato, cucumber, and agricultural water	2020	[54]
GO	Si particles	β-CD	SPE	Benzanthracene, benzofluoranthene, benzo(a)pyrene (bap), anthracene	Fried chicken	2021	[55]
G	Si particles	ZIF-8	SPE	Benzothiazoles, benzotriazoles, benzenesulfonamides.	River water, effluent wastewater, and influent wastewater	2023	[56]
rGO	Not supported	Not modified	SPE	Aflatoxin B1, B2, G1, and G2	Rice and wheat	2019	[57]
rGO	Self-supported	rGO 3D structured	SPE	Diclofenac	Environmental waters	2021	[58]
GO	Starch	Starch	PT-SPME	Amoxicillin, ampicillin, cloxacillin	Milk	2019	[14]
GO	Si particles	Not modified	PT-SPME	Simazine, metribuzin, atrazine, ametryn, tebuthiuron, clomazone, hexazinone, acetochlor, Alachlor, metolachlor, oxyfluorfen	Candy, juice, and syrup	2023	[59]
FG	Si particles	MOF/ZIF-8	PT-SPME	2-chlorophenol, 2,3-dichlorophenol, 2,4-dichlorophenol, 2,5-dichlorophenol, 2,6-dichlorophenol, and 2,4,6-trichlorophenol	Tap water, honey, and black tea	2021	[60]

3. Online Sample Preparation for Liquid Chromatography

The online sample preparation strategy presents a significant advantage over offline techniques; the automation process minimizes the chance of human error, one of the most common error sources in analytical methods [61,62]. Though it has advantages over offline techniques, the need for more expensive and specialized equipment limits its wide adoption [62,63]. In-tube SPME (IT-SPME), also referred to as a synonym of column-switching, is the most-used strategy for online sample preparation in LC. This technique consists of (i) loading the extraction column with the samples with the help of a weak mobile phase (usually pure water), while a valve directs the flow after the extraction column to waste, (ii) stopping the load and switching the valve to connect the extraction

column to the analytical column (second column), and (iii) starting the elution and LC separation. Figure 2 shows a regular online IT-SPME analysis.

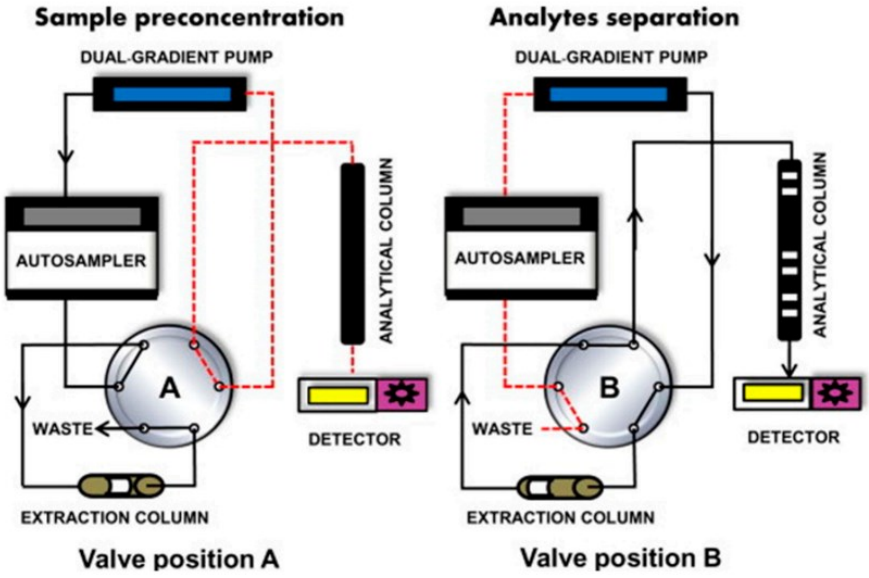

Figure 2. General scheme of a column switching (online IT-SPME) liquid chromatography approach. Valve position A represents the extraction procedure, and valve position B represents the elution and separation procedure. Reproduced with permission from TrAC Trends Anal. Chem., 62, Fernández-Ramos, C.; Šatínský, D.; Šmídová, B.; Solich, P., Analysis of Trace Organic Compounds in Environmental, Food and Biological Matrices Using Large-Volume Sample Injection in Column-Switching Liquid Chromatography, Pages 69–85, Copyright (2014), Elsevier [63].

Graphene-based materials fixed over silica particles are an interesting sorbent for this application. For example, GO supported into the Si particles' (SiGO) sorbent was packed inside a fused silica capillary to produce a miniaturized extraction column employed in the extraction of β-lactam antibiotics from environmental water samples [13]. This method presented LODs lower than 0.3 $\mu g \cdot L^{-1}$ and recovery between 70.4 and 91.6%. In-tube SPME also utilized SiGO particles' functionalization with other bindings. For example, SiGO particles functionalized with C18 and end-capped were used for the online sample preparation of coffee samples, targeting the determination of xanthines [64]. LOQs of about 0.3 to 1.0 $\mu g \cdot L^{-1}$ and recoveries between 73 and 109% were obtained. Both works above employed a similar route to prepare the SiGO particle or its functionalized derivate with C18 and end-capping. Briefly, GO sheets, produced by Hummer's method, were covalently bonded to the Si particle's surface. For the functionalization with C18 and end-capping, the SiGO particles formed were reacted with chlorodimethyl-n-octadecylsilane and trimethylchlorosilane in separate steps [64]. Monoliths can also be a support for graphene-based materials for IT-SPME. A simple way to produce graphene-based monoliths is to suspend graphene-based materials in a polymerization mixture and insert it into the extraction column hardware [65]. After polymerization, the graphene is fixed together in a monolithic structure. An example of graphene-based monoliths' applications in online IT-SPME analysis in foods is the use of GO incorporated in an ethylene glycol dimethacrylate (EDMA) monolithic column to extract and analyze 16 sulfonamides in chicken muscle and milk samples [65]. The in situ polymerization of Go and EDMA inside a 10 mm × 2.1 mm stainless steel capillary produced the monolithic column. LODs of 0.3 $\mu g \cdot kg^{-1}$ for milk and 0.6 $\mu g \cdot kg^{-1}$ in chicken muscle and recoveries of about 70.3 to 98.5% and 79.0 to 108.0% for each matrix, respectively, were obtained [65]. Coated bars

inserted inside LC tubing are also an alternative for preparing IT-SPME devices [66]. An interesting recent example of this strategy is to apply a device composed of stainless steel (SS) wire coated with SiGO mesoporous structure and place it inside a PEEK tube to analyze PAH in honey samples [66]. This IT-SPME device was produced by coating a wire with epoxy resin and attaching the sorbent powder material. The SiGO mesopore material was prepared with a hydrothermal reaction [66] This IT-SPME approach could detect PAH from honey, which presented a LOD of 0.25 $ng \cdot g^{-1}$.

Headspace in-tube solid phase microextraction (HS-SPME) using a graphene-based sorbents is another sample preparation strategy that has been applied recently, hyphenated to LC. This strategy consists of introducing the sample in a vail and inserting the HS-SPME device into the space above the liquid surface; after the extraction procedure, the HS-SPME system is connected online to LC equipment. A recently reported application of graphene-based sorbents in the HS-SPME technique for food analysis was performed, utilizing a stainless steel tubing coated with a composite formed by GO and ionic liquid (IL) for the analyses of the headspace of naphthalene, a volatile PAH, in honey samples [67]. The GO-IL sorbent was prepared by reacting GO and 1-methyl imidazole. The prepared material was then electrochemically deposited on an SS tube, forming the HS-SPME device [67]. The sample preparation method presented a LOD of 0.1 $ng \cdot mL^{-1}$, a LOQ of 0.3 $ng \cdot mL^{-1}$, and a recovery range between 90.0 and 106.5%.

In short, a trend exists to employ GO as the graphene-based sorbent in online sample preparation (Table 2). The fixation of the GO sheets in Si does not allow the movement of the sheets, and the sequential blocking of the column is caused by the accumulation of the GO sheets in the column frit. These characteristics make the packing of extraction columns with graphene-based phases viable. As mentioned in the previous section, wide possibilities for functionalizing GO materials are available, and some of them are interesting for online approaches. There is space for advancements using specialized materials in IT-SPME and HS-SPME, and their exploration might result in significant improvements in the detection of contaminants in food and water samples. Though IT-SPME is the most popular approach for online sample preparation in liquid chromatography, graphene-based materials are also possible in other techniques, such as the needle-sleeve-based online hyphenation of solid-phase microextraction and liquid chromatography [68]. However, to our knowledge, these approaches have not been applied to food and environmental water analysis.

Table 2. Examples of graphene-based materials in online sample preparation followed by liquid chromatography analysis since 2019.

Graphene-Based Material	Support	Modification	Techniques	Analytes	Matrix	Year	Ref.
GO	Si particles	Not modified	IT-SPME	Benzylpenicillin, cefalexin, cefoperazone, and ceftiofur	Water	2023	[13]
GO	Si particles	C18 and end-capping	IT-SPME	Xanthines: theophylline, theobromine, and caffeine	Coffee	2020	[64]
GO	EDMA monolith	Not modified	IT-SPME	Sulfamethoxazole, sulfamoxole, sulfadoxine, sulfamethizole, sulfadimidine, sulfameter, sulfamethoxypyridazine, sulfisoxazole, sulfapyridine, sulfabenzamide, sulfamerazine, sulfamonomethoxine, sulfachloropyridazine, sulfaquinoxaline, sulfadimethoxine, and sulfaphenazole	Milk and muscle	2019	[65]
GO	SS wire	Mesopore Si	IT-SPME	Naphthalene, acenaphthylene, acenaphthene, fluorene, phenanthrene, anthracene, fluoranthene, and pyrene	Honey	2021	[66]
GO	SS tubing	IL/1-methyl imidazole	HS-SPME	Naphthalene	Honey	2020	[67]

4. Stationary Phase for Liquid Chromatography

Graphene-based materials have also been used as stationary phases for liquid chromatography columns. These sorbents have been employed in packed, monolithic, and open tubular (OT) columns, the three most common types of LC columns (Figure 3). These sorbents have also been used in capillary electrochromatography (CEC), a hybrid between LC and capillary electrophoresis [69,70]. This section discusses the application of graphene-based sorbents as a stationary phase for separating usual food and environmental water contaminants in packed, monolithic, and OT columns in LC and CEC.

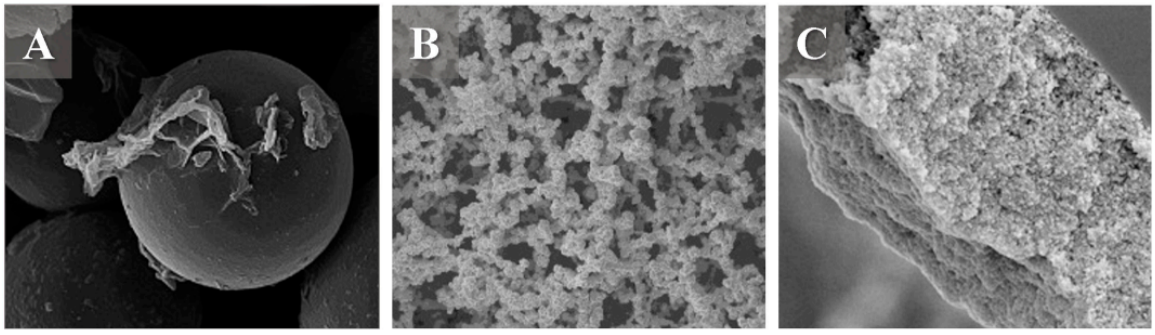

Figure 3. (**A**) Example of the SiGO-C18ec sorbent used as a sorbent for a packed column. Reproduced with permission from J. Chromatogr. A, 1685, Borsatto, J.V.B.; Maciel, E.V.S.; Lanças, F.M., Investigation of the Applicability of Silica-Graphene Hybrid Materials as Stationary Phases for Capillary Liquid Chromatography., Starting page 463618, Copyright (2022), Elsevier [71]. (**B**). Example of the poly (GO-co-TAIC-co-MMA) sorbent used as a sorbent for a monolithic column. Reproduced with permission from J. Chromatogr. B, Anal. Technol. Biomed. Life Sci. 1203, Guo, Y.; Si, H.; Li, H.; Zhao, X.; Zhao, Y.; Li, S.; Wang, Q.; Zhu, B., Graphene Oxide-Based a Network Porous Poly (Trially Isocyanurate-Co-Methacrylate) Monolithic Column for HPLC Separation of Aromatic Molecular and Lipopeptide Antibiotics., Starting page 123310, Copyright (2022), Elsevier [38]. (**C**). Example of the poly (MGONPs) sorbent used as a sorbent for an open tubular column. Reproduced with permission from J. Chromatogr. A, 1667, Şeker, S.; Alharthi, S.; Aydoğan, C., Open Tubular Nano-Liquid Chromatography with a New Polylysine Grafted on Graphene Oxide Stationary Phase for the Separation and Determination of Casein Protein Variants in Milk., Starting page 462885, Copyright (2022), Elsevier [35].

4.1. Packed Columns

Packed columns are the standard types of columns in LC. They comprise particles of the stationary phase packed inside a tubing (or capillary tubing). This type of column is easy to produce given its production procedures demand only a pump that allows the packing of the stationary phase in the column hardware [72]. The simplicity of the production makes packed columns a straightforward strategy for evaluating new stationary phases. Graphene-based sorbents are in an early development stage as a stationary phase for LC column, but some examples are present in the literature [34,73,74]. Usually, graphene-based materials, such as GO sheets, are fixed over silica particles once it is easily the packing procedure [34,73,74]. GO is the most present in the LC column among the graphene-based materials [31,32,73,74], but graphene quantum dots (GQD) are also commonly used in graphene-based sorbents [75–79]. Diverse functionalizations of GO sheets are reported in the literature. β-CD-functionalized graphene-based materials are interesting materials being explored when focusing on separating chiral mixtures [78,80]. Other functionalizations with gold [31], IL [81], C18 [71], and cellulose [32] are examples reported in the literature.

Graphene-based packed LC columns are still underexplored for food and water analysis. However, some applications reported in the last five years are described in the literature. In seed samples, a capillary column packed with a SiGO-C18ec stationary phase, produced

by the functionalization of SiGO particles with C18 followed by end-caping (as previously mentioned), was employed to separate lecithin, a common phospholipid component in foods. This study evaluated the viability of applying an online liquid extraction (OLE) system coupled with an LC-MS to evaluate the hyphenated extraction and separation of lecithin from the pounder of seeds [82]. The SiGO-C18ec column presented a better separation than a conventional C18 column in reversed-phase (RP) separation mode for this application. Graphene-based packed LC columns have also been used to separate contaminants in food and water. For example, sulfonamides, frequently detected antibiotics in food and water samples [83], have recently been the focus of separation studies utilizing graphene-based stationary phases. LC columns packed with porous graphene (PG), fixed over Si particles, have been employed for the separation of sulfanilamide, sulfamethazine, sulfamerazine, sulfasalazine, sulfadiazine, and sulfamethoxazole in HILIC mode [37]. PG materials are graphene-based materials with random or highly stable carbon atom vacancies in the sheet [37]. To produce the PG-Si sorbent, (3-aminopropyl)triethoxysilane is used to link the PG material to the Si particles. Sulfonamides have also been separated in HILIC mode using GQD fixed on Si particles (Si-GQD) modified with octadecyl amine and serine; this column has also separated nucleosides in HILIC mode [84]. To prepare this material, the GQD, produced by the solvothermal method, was factionalized with octadecylamine and serine to present hydrophilic and hydrophobic groups in its structure. Lately, the functionalized GQD has been bonded to Si particles using (3-isocyanatopropyl)triethoxysilane as a linker [84]. The same column could also be applied for the RP separation mode, which effectively separated alkylbenzenes and PAHs [84]. Another interesting application of the GQDS-derived material is the application of poly(N-isopropyl acrylamide) (PNIPAAm) functionalized Si-GQDs particles as a stationary phase for the multiclass separation of water-soluble compounds, including contaminants, alkylbenzenes, PAHs, biphenyls, nucleosides/nucleobases, phenols, and anilines [76]. The material was produced by functionalizing Si particles with (3-Aminopropyl)triethoxysilane as a liker. Lately, the Si-GQD particles have been functionalized by the covalent bonding of the PNIPAAm to the GQD. The GQDs were prepared by hydrothermal synthesis using GO as starting material. Also, capillary columns packed with the SiGO-C18ec particles prepared similarly to [82] have been reported to separate a multiclass mixture presenting a different selectivity from the conventional C18 column among the separated compounds, including pesticides such as carbofuran, hexazinone, and clomazone [71].

4.2. Monolithic Column

Monolithic columns are another popular type of LC column composed of a monolith of the stationary phase, usually inside a capillary tubing. These columns are, conventionally, produced by the in situ polymerization of polymer-based [85] and silica-based [86] monoliths. In addition, monolithic graphene-based columns have been used in LC and capillary electrochromatography (CEC) columns [85,87]. These types of columns have been reported to be adequate for the separation of small molecules, such as alkylbenzenes, polycyclic aromatics, phenols, and anilines [87,88], and long molecules, such as proteins and peptides [88,89].

Graphene-based monolithic columns have been used in LC and CEC modes, but recent food and water analysis applications present few reported examples. In LC, a monolithic column prepared by the polymerization of 3-chloro-2-hydroxypropylmethacrylate (HPMA-Cl) and ethylene dimethacrylate (EDMA), followed by the fixation of GO, was used recently for the determination of chloramphenicol (CAP), a veterinarian antibiotic, and chloramphenicol glucuronide (CAPG), a metabolite from CAP, in honey and milk samples [15]. Another interesting application of graphene-based monolithic columns evaluated five ingredients in *Schisandra*, a purple-red berry typically used in traditional Chinese medicine [38]. For this study, a column produced by the co-polymerization of GO with triallyl isocyanurate (TAIC) and methyl methacrylate (MMA) was employed to separate schizandrol A, schizandrol B, schisandra A, schisandra B, and schisandra C in

reversed-phase LC [38]. The CEC mode has also employed graphene-based monolithic sorbents to separate usual water contaminants. In a recent example, a monolithic column was produced by the co-polymerization of GO with polydopamine (PDA) in the enantiomeric separation of ephedrine and pseudoephedrine isomers [90]. These compounds might contaminate environmental waters [91].

4.3. Open Tubular Columns

Open tubular columns have gained popularity in liquid chromatography due to their intrinsic advantages over packed columns, such as low pressures, and their theoretically higher performance [92–94]. This type of column presents lower solvent consumption, meeting green chemistry requirements [95]. Additionally, the open channel inside OT columns reduces the multi-path diffusion of the analytes [96]. Open tubular columns consist of a small-diameter capillary, usually coated with a stationary phase. Porous layer open tubular columns (PLOT), wall-coated open tubular columns (WCOT), and bare open tubular columns (BOT) are examples of OT column types [97–99]. Open tubular columns were reborn after Karger's work, and since then they have been widely explored for the separation of large molecules [100–103].

Nevertheless, the separation of small molecules on OT columns has also been described [96,104,105]. The general procedure of the production of OT columns involves modifying the capillary inner surface with a stationary phase using chemical reaction or physical adsorption methods [106]. Graphene-based OT stationary phases have been employed in LC and CEC separation modes for diverse applications such as pharmaceutical, food, and environmental analysis [35,106–109].

Graphene-based OT-LC columns have not received much attention for food and environmental water analysis. Very few works explore graphene-based OT columns in food and water analysis. An example reported in the last five years is the separation of casein protein variants from milk samples using an OT column produced with Poly-L-Lysine (PLL) grafted on a methacryloyl graphene oxide nanoparticles (MGONPs) stationary phase [35]. In CEC, examples of graphene-based columns in foods and environmental analysis are more common than in LC, but they are still rare. An interesting example is using molybdenum disulfide and GO composite (GO-MoS_2) as stationary phases for determining sulfonamides in environmental water [109]. The column was produced by inserting a GO-MoS_2 dispersion into a fused-silica capillary and leaving it overnight for the GO-MoS_2 to bond in the fused-silica capillary wall [109]. The separation of other pharmaceutical products that might be found in environmental water has also been reported using graphene-based OT columns in CEC mode [110]. For example, a CEC-OT column produced with a nanocomposite of gold nanoparticles and graphene-carbon nitride was used in the enantioseparation of metoprolol, bisoprolol, propranolol chlorpheniramine, and amlodipine [110]. The enantioseparation of pharmaceutical products in CEC mode has also been reported using the CEC-OT column using GO modified with maltodextrin as a chiral selective phase for the analysis of nefopam, amlodipine, citalopram hydrobromide, econazole, ketoconazole, and cetirizine hydrochloride [107].

4.4. Trends Observed in Graphene-Based Stationary Phases in LC Columns

Graphene sorbents have been employed in diverse analytical column configurations in the last five years. Packed, monolithic, and open tubular are the three most common column types, and all present examples are of graphene-based materials as stationary phases (Table 3). In food and environmental analysis, graphene-based stationary phases have been employed in the analysis of food components, such as lecithin, caseins, and schizandrols, and environmental water contaminants, such as antibiotics, alkylbenzenes, PAHs, and others. It was observed that GO is the most usual type of graphene base material for the stationary phase, being most frequently employed with no modifications. While in packed columns Si particles are described as the most common support for GO, and in a monolith organic polymers are the most employed support for the fixation of GO, in the

OT column, the GO is directly bonded to the capillary wall or fixed with the assistance of an organic polymer. It can be inferred that the use of graphene-based stationary phases in food and water analysis tends to expand, probably with a diversification of the application of packed columns in LC analysis and OT columns in CEC analysis. In LC, graphene-based sorbents present π–π interactions as the primary separation mechanism [34,75]. For some sorbents and analytes, it is also possible for hydrogen bonding to participate in the interaction mechanism. When aliphatic chains are present in the functionalization of the sorbent, hydrophobic interaction might also participate in the retention process. In CEC, it has also been reported that hydrogen bonding, π–π, and hydrophobic interactions participate in the retention process [70]. GO should remain the preferred choice as the primary component in graphene-based LC stationary phases because of its molecular characteristics, facilitating functionalization. Moreover, the functionalization of graphene-based materials with different bindings tends to increase, finding specific functionalization for specific problems.

Table 3. Examples of graphene-based material as a stationary phase for liquid chromatography analysis since 2019.

Graphene-Based Material	Support/Column Type	Surface Modification	Techniques/Separation Mode	Analytes	Matrix	Year	Ref.
GO	Si particles/Packed column	C18 and end-capping	OLE-LC/RP	Lecithin	Seeds	2023	[82]
GP	Si particles/Packed column	Not modified	LC/HILIC	Sulfonamides	-	2019	[37]
GQD	Si particle/Packed column	Octadecylamine and serine	LC/HILIC and LC/RP	Sulfonamides and nucleosides and alkylbenzenes and PAHs	-	2022	[84]
GQD	Si particle/Packed column	PNIPAAm	LC/HILIC and LC/RP	Alkylbenzenes, PAHs, biphenyls, nucleosides/nucleobases, phenols, anilines, water-soluble vitamins, and amino acids	-	2021	[76]
GO	Si particles/Packed column	C18 and end-capping	LC/RP	Carbofuran, clomazone, hexazinone, carbamazepine, citalopram, clomipramine, desipramine, and ochratoxin A	-	2022	[71]
GO	HPMA-Cl and EDMA/Monolith	Not modified	LC/RP	CAP and CAPG	Honey and milk	2022	[15]
GO	TAIC and MMA/Monolith	Not modified	LC/RP	Schizandrol A, schizandrol B, schisandra A, schisandra B, and schisandra C	*Schisandra*	2022	[38]
GO	PDA/Monolith	Not modified	CEC	Ephedrine and pseudoephedrine	-	2019	[90]
GO	MGONPs/OT	PLL	LC/RP	Casein	Milk	2022	[35]
GO	MoS_2/OT	Not modified	CEC	Sulfisomidine, sulfathiazole, sulfamerazine, phthalylsulfathiazole and sulfacetamide, ulfamonomethoxine and sulfachloropyridazine	Environmental water	2020	[109]
G	Gold nanoparticles/OT	C_3N_4	CEC	Metoprolol, bisoprolol, propranolol chlorpheniramine, and amlodipine	-	2021	[110]
GO	Directly coated over fused-silica capillary wall/OT	Not modified	CEC	Nefopam, amlodipine, citalopram hydrobromide, econazole, ketoconazole, and cetirizine hydrochloride	-	2020	[107]

5. Conclusions

Graphene-based sorbents are becoming more popular year after year in diverse applications. In food and environmental water LC analysis, graphene-based materials have been underexplored in the last five years. However, a trend in the diversification of the application of those materials is also being observed. In offline sample preparation, dispersive solid phase extraction receives the most attention for the application of graphene-based sorbents in food and environmental water LC analysis, but other techniques, such as SBSE, Fiber-SPME, SPE, HF-SPME, and others, could employ graphene-based sorbents with success. Hence, graphene-based sorbents are in an early stages of development, and the number and variety of sample preparation techniques using these materials is tending to increase. In online sample preparation methods, IT-SPME is the most common application of graphene sorbents in food and environmental water analysis. This kind of online sample preparation allows an easy connection to LC analysis, which has been a great advantage of these techniques.

Additionally, the extraction column might be packed with a wide variety of graphene-based sorbents and can deal with a high diversity of samples. Graphene-based sorbents have also been used for analytical LC columns. These sorbents have been utilized in packed, monolithic, and open tubular columns. Graphene oxide bonded to Si particles is the most common graphene-based sorbent used as stationary phases. Graphene-based sorbents have been used as stationary phases in the analysis of food components such as caseins, lecithin, and schizandrols. Graphene-based sorbents have also been employed in separating water contaminants such as alkylbenzenes and antibiotics. The future of graphene-based stationary phases in food and water analyses is promising, with packed columns becoming more frequent for LC and OT columns for CEC analysis. GO should remain the most preferred graphene-based material due to its molecular characteristics, allowing it to be functionalized. Functionalizing these materials with different bindings should be encouraged to find solutions to specific problems.

Graphene-based sorbents present advantages and disadvantages in analyzing food and water samples through liquid chromatography. One significant advantage is the versatility of these sorbents in extracting various analytes while being compatible with different sample preparation techniques. Furthermore, functionalizing GO, and other graphene-based materials, offers a range of possibilities for online approaches. In contrast, as its main disadvantage, these phases are relatively new and may present a lower scope of applications than conventional commercially available extraction phases. In other words, graphene-based materials are not multipurpose, which means that for some applications it is crucial to select an adequate material to extract specific analytes. Another advantage of graphene-based materials is that they can be used as stationary phases in packed, monolithic, and open tubular chromatographic columns. Conversely, detachment followed by the accumulation of graphene sheets in the column outlet can again hinder effectiveness and limit the column's lifetime. Nonetheless, the functionalization of graphene-based materials with different bindings for specific applications presents intriguing opportunities for improving the diversity of applications for food and water analysis.

Author Contributions: Conceptualization, J.V.B.B. and F.M.L.; writing—original draft preparation, J.V.B.B.; writing—review and editing, J.V.B.B. and F.M.L.; supervision, F.M.L. administration, F.M.L.; funding acquisition, F.M.L. All authors have read and agreed to the published version of the manuscript.

Funding: The authors are grateful for financial support from (i) the Coordination for the Improvement of Higher Education Personnel (CAPES—Brazil, Finance Code 001 and Proc. 88887.695324/2022-00); (ii) the São Paulo Research Foundation (FAPESP—Brazil, Grants 2019/22724-7, 2017/02147-0); and (iii) the National Council for Scientific and Technological Development (CNPq—Brazil, 307293/2014-9; 308843/2019-3; Proc. 142513/2019-9).

Institutional Review Board Statement: Not applicable.

Informed Consent Statement: Not applicable.

Data Availability Statement: Not applicable.

Acknowledgments: Figure 1C—Reproduced with permission from John Wiley and Sons, Copyright (2018). Figure 2—Reproduced with permission from Elsevier, Copyright (2014). Figure 3A—Reproduced with permission from Elsevier, Copyright (2022). Figure 3B—Reproduced with permission from Elsevier, Copyright (2022). Figure 3C—Reproduced with permission from Elsevier, Copyright (2022).

Conflicts of Interest: The authors declare that they have no known competing financial interests or personal relationships that could have appeared to influence the work reported in this paper.

References

1. Mbayachi, V.B.; Ndayiragije, E.; Sammani, T.; Taj, S.; Mbuta, E.R.; Khan, A. Ullah Graphene Synthesis, Characterization and Its Applications: A Review. *Results Chem.* **2021**, *3*, 100163. [CrossRef]
2. Lanças, F.M.; Medina, D.A.V.; Pereira Dos Santos, N.G.; Sinisterra, M.J. Graphene-Based Sorbents for Modern Magnetic Solid-Phase Extraction Techniques. In *Analytical Applications of Functionalized Magnetic Nanoparticles*; The Royal Society of Chemistry: London, UK, 2021; pp. 174–199.
3. Justino, C.I.L.; Gomes, A.R.; Freitas, A.C.; Duarte, A.C.; Rocha-Santos, T.A.P. Graphene Based Sensors and Biosensors. *TrAC Trends Anal. Chem.* **2017**, *91*, 53–66. [CrossRef]
4. Wang, X.; Liu, B.; Lu, Q.; Qu, Q. Graphene-Based Materials: Fabrication and Application for Adsorption in Analytical Chemistry. *J. Chromatogr. A* **2014**, *1362*, 1–15. [CrossRef]
5. Grajek, H.; Jonik, J.; Witkiewicz, Z.; Wawer, T.; Purchała, M. Applications of Graphene and Its Derivatives in Chemical Analysis. *Crit. Rev. Anal. Chem.* **2020**, *50*, 445–471. [CrossRef] [PubMed]
6. Huang, H.; Shi, H.; Das, P.; Qin, J.; Li, Y.; Wang, X.; Su, F.; Wen, P.; Li, S.; Lu, P.; et al. The Chemistry and Promising Applications of Graphene and Porous Graphene Materials. *Adv. Funct. Mater.* **2020**, *30*, 1909035. [CrossRef]
7. Tiwari, S.K.; Sahoo, S.; Wang, N.; Huczko, A. Graphene Research and Their Outputs: Status and Prospect. *J. Sci. Adv. Mater. Devices* **2020**, *5*, 10–29. [CrossRef]
8. Yu, W.; Sisi, L.; Haiyan, Y.; Jie, L. Progress in the Functional Modification of Graphene/Graphene Oxide: A Review. *RSC Adv.* **2020**, *10*, 15328–15345. [CrossRef] [PubMed]
9. Park, S.; Ruoff, R.S. Chemical Methods for the Production of Graphenes. *Nat. Nanotechnol.* **2009**, *4*, 217–224. [CrossRef]
10. Bohr, J. Adhesive Tape Exfoliation: Why It Works for Graphene. *EPL (Europhys. Lett.)* **2015**, *109*, 58004. [CrossRef]
11. Novoselov, K.S.; Geim, A.K.; Morozov, S.V.; Jiang, D.; Zhang, Y.; Dubonos, S.V.; Grigorieva, I.V.; Firsov, A.A. Electric Field Effect in Atomically Thin Carbon Films. *Science* **2004**, *306*, 666–669. [CrossRef]
12. Gengler, R.Y.N.; Spyrou, K.; Rudolf, P. A Roadmap to High Quality Chemically Prepared Graphene. *J. Phys. D Appl. Phys.* **2010**, *43*, 374015. [CrossRef]
13. Maciel, E.V.S.; Vargas-Medina, D.A.; Lancas, F.M. Analyzes of β-Lactam Antibiotics by Direct Injection of Environmental Water Samples into a Functionalized Graphene Oxide-Silica Packed Capillary Extraction Column Online Coupled to Liquid Chromatography Tandem Mass Spectrometry. *Talanta Open* **2023**, *7*, 100185. [CrossRef]
14. Golzari Aqda, T.; Behkami, S.; Raoofi, M.; Bagheri, H. Graphene Oxide-Starch-Based Micro-Solid Phase Extraction of Antibiotic Residues from Milk Samples. *J. Chromatogr. A* **2019**, *1591*, 7–14. [CrossRef]
15. Demir, N.; Aydoğan, C. ProFlow Nano-Liquid Chromatography with a Graphene Oxide-Functionalized Monolithic Nano-Column for the Simultaneous Determination of Chloramphenicol and Chloramphenicol Glucuronide in Foods. *J. Food Sci.* **2022**, *87*, 1721–1730. [CrossRef]
16. Gu, S.; Hsieh, C.-T.; Chiang, Y.-M.; Tzou, D.-Y.; Chen, Y.-F.; Gandomi, Y.A. Optimization of Graphene Quantum Dots by Chemical Exfoliation from Graphite Powders and Carbon Nanotubes. *Mater. Chem. Phys.* **2018**, *215*, 104–111. [CrossRef]
17. Hummers, W.S.; Offeman, R.E. Preparation of Graphitic Oxide. *J. Am. Chem. Soc.* **1958**, *80*, 1339. [CrossRef]
18. Kumar, N.; Salehiyan, R.; Chauke, V.; Joseph Botlhoko, O.; Setshedi, K.; Scriba, M.; Masukume, M.; Sinha Ray, S. Top-down Synthesis of Graphene: A Comprehensive Review. *FlatChem* **2021**, *27*, 100224. [CrossRef]
19. Deng, B.; Liu, Z.; Peng, H. Toward Mass Production of CVD Graphene Films. *Adv. Mater.* **2019**, *31*, 1800996. [CrossRef]
20. Jia, K.; Zhang, J.; Zhu, Y.; Sun, L.; Lin, L.; Liu, Z. Toward the Commercialization of Chemical Vapor Deposition Graphene Films. *Appl. Phys. Rev.* **2021**, *8*, 041306. [CrossRef]
21. Munuera, J.M.; Paredes, J.I.; Enterría, M.; Pagán, A.; Villar-Rodil, S.; Pereira, M.F.R.; Martins, J.I.; Figueiredo, J.L.; Cenis, J.L.; Martínez-Alonso, A.; et al. Electrochemical Exfoliation of Graphite in Aqueous Sodium Halide Electrolytes toward Low Oxygen Content Graphene for Energy and Environmental Applications. *ACS Appl. Mater. Interfaces* **2017**, *9*, 24085–24099. [CrossRef]
22. Coroş, M.; Pogăcean, F.; Roşu, M.-C.; Socaci, C.; Borodi, G.; Mageruşan, L.; Biriş, A.R.; Pruneanu, S. Simple and Cost-Effective Synthesis of Graphene by Electrochemical Exfoliation of Graphite Rods. *RSC Adv.* **2016**, *6*, 2651–2661. [CrossRef]
23. Song, Z.; Mu, X.; Luo, T.; Xu, Z. Unzipping of Carbon Nanotubes Is Geometry-Dependent. *Nanotechnology* **2016**, *27*, 015601. [CrossRef]
24. de Toffoli, A.L.; Maciel, E.V.S.; Fumes, B.H.; Lanças, F.M. The Role of Graphene-Based Sorbents in Modern Sample Preparation Techniques. *J. Sep. Sci.* **2018**, *41*, 288–302. [CrossRef]
25. Madej, K.; Jonda, A.; Borcuch, A.; Piekoszewski, W.; Chmielarz, L.; Gil, B. A Novel Stir Bar Sorptive-Dispersive Microextraction in Combination with Magnetically Modified Graphene for Isolation of Seven Pesticides from Water Samples. *Microchem. J.* **2019**, *147*, 962–971. [CrossRef]
26. Zhang, Q.; You, L.; Chen, B.; He, M.; Hu, B. Reduced Graphene Oxide Coated Nickel Foam for Stir Bar Sorptive Extraction of Benzotriazole Ultraviolet Absorbents from Environmental Water. *Talanta* **2021**, *231*, 122332. [CrossRef] [PubMed]
27. Song, X.-L.; Lv, H.; Wang, D.-D.; Liao, K.-C.; Wu, Y.-Y.; Li, G.-M.; Chen, Y. Graphene Oxide Composite Microspheres as a Novel Dispersive Solid-Phase Extraction Adsorbent of Bisphenols Prior to Their Quantitation by HPLC–Mass Spectrometry. *Microchem. J.* **2022**, *172*, 106920. [CrossRef]

28. Arabkhani, P.; Sadegh, N.; Asfaram, A. Nanostructured Magnetic Graphene Oxide/UIO-66 Sorbent for Ultrasound-Assisted Dispersive Solid-Phase Microextraction of Food Colorants in Soft Drinks, Candies, and Pastilles Prior to HPLC Analysis. *Microchem. J.* **2023**, *184*, 108149. [CrossRef]
29. Pei, M.; Shi, X.; Wu, J.; Huang, X. Graphene Reinforced Multiple Monolithic Fiber Solid-Phase Microextraction of Phenoxyacetic Acid Herbicides in Complex Samples. *Talanta* **2019**, *191*, 257–264. [CrossRef] [PubMed]
30. Mirzajani, R.; Kardani, F.; Ramezani, Z. A Nanocomposite Consisting of Graphene Oxide, Zeolite Imidazolate Framework 8, and a Molecularly Imprinted Polymer for (Multiple) Fiber Solid Phase Microextraction of Sterol and Steroid Hormones Prior to Their Quantitation by HPLC. *Microchim. Acta* **2019**, *186*, 129. [CrossRef]
31. Liang, X.; Wang, X.; Ren, H.; Jiang, S.; Wang, L.; Liu, S. Gold Nanoparticle Decorated Graphene Oxide/Silica Composite Stationary Phase for High-Performance Liquid Chromatography. *J. Sep. Sci.* **2014**, *37*, 1371–1379. [CrossRef]
32. Li, Y.; Li, Q.; Zhu, N.; Gao, Z.; Ma, Y. Cellulose Type Chiral Stationary Phase Based on Reduced Graphene Oxide@silica Gel for the Enantiomer Separation of Chiral Compounds. *Chirality* **2018**, *30*, 996–1004. [CrossRef]
33. Maciel, E.; Borsatto, J.V.B.; Mejia-Carmona, K.; Lanças, F.M. Application of an In-House Packed Octadecylsilica-Functionalized Graphene Oxide Column for Capillary Liquid Chromatography Analysis of Hormones in Urine Samples. *Anal. Chim. Acta* **2023**, *1239*, 340718. [CrossRef] [PubMed]
34. Liang, X.; Wang, S.; Liu, S.; Liu, X.; Jiang, S. A Novel Octadecylsilane Functionalized Graphene Oxide/Silica Composite Stationary Phase for High Performance Liquid Chromatography. *J. Sep. Sci.* **2012**, *35*, 2003–2009. [CrossRef] [PubMed]
35. Şeker, S.; Alharthi, S.; Aydoğan, C. Open Tubular Nano-Liquid Chromatography with a New Polylysine Grafted on Graphene Oxide Stationary Phase for the Separation and Determination of Casein Protein Variants in Milk. *J. Chromatogr. A* **2022**, *1667*, 462885. [CrossRef]
36. Tong, Y.; Li, S.; Wu, Y.; Guo, J.; Zhou, B.; Zhou, Q.; Jiang, L.; Niu, J.; Zhang, Y.; Liu, H.; et al. Graphene Oxide Modified Magnetic Polyamidoamide Dendrimers Based Magnetic Solid Phase Extraction for Sensitive Measurement of Polycyclic Aromatic Hydrocarbons. *Chemosphere* **2022**, *296*, 134009. [CrossRef]
37. Song, L.; Zhang, H.; Cai, T.; Chen, J.; Li, Z.; Guan, M.; Qiu, H. Porous Graphene Decorated Silica as a New Stationary Phase for Separation of Sulfanilamide Compounds in Hydrophilic Interaction Chromatography. *Chin. Chem. Lett.* **2019**, *30*, 863–866. [CrossRef]
38. Guo, Y.; Si, H.; Li, H.; Zhao, X.; Zhao, Y.; Li, S.; Wang, Q.; Zhu, B. Graphene Oxide-Based a Network Porous Poly (Trially Isocyanurate-Co-Methacrylate) Monolithic Column for HPLC Separation of Aromatic Molecular and Lipopeptide Antibiotics. *J. Chromatogr. B Anal. Technol. Biomed. Life Sci.* **2022**, *1203*, 123310. [CrossRef] [PubMed]
39. Hou, X.; Tang, S.; Wang, J. Recent Advances and Applications of Graphene-Based Extraction Materials in Food Safety. *TrAC Trends Anal. Chem.* **2019**, *119*, 115603. [CrossRef]
40. Ghorbani, M.; Aghamohammadhassan, M.; Chamsaz, M.; Akhlaghi, H.; Pedramrad, T. Dispersive Solid Phase Microextraction. *TrAC Trends Anal. Chem.* **2019**, *118*, 793–809. [CrossRef]
41. Li, N.; Jiang, H.-L.; Wang, X.; Wang, X.; Xu, G.; Zhang, B.; Wang, L.; Zhao, R.-S.; Lin, J.-M. Recent Advances in Graphene-Based Magnetic Composites for Magnetic Solid-Phase Extraction. *TrAC Trends Anal. Chem.* **2018**, *102*, 60–74. [CrossRef]
42. Luo, Y.-B.; Shi, Z.-G.; Gao, Q.; Feng, Y.-Q. Magnetic Retrieval of Graphene: Extraction of Sulfonamide Antibiotics from Environmental Water Samples. *J. Chromatogr. A* **2011**, *1218*, 1353–1358. [CrossRef] [PubMed]
43. Liu, Q.; Shi, J.; Jiang, G. Application of Graphene in Analytical Sample Preparation. *TrAC Trends Anal. Chem.* **2012**, *37*, 1–11. [CrossRef]
44. Zhao, G.; Song, S.; Wang, C.; Wu, Q.; Wang, Z. Determination of Triazine Herbicides in Environmental Water Samples by High-Performance Liquid Chromatography Using Graphene-Coated Magnetic Nanoparticles as Adsorbent. *Anal. Chim. Acta* **2011**, *708*, 155–159. [CrossRef] [PubMed]
45. Wu, Q.; Feng, C.; Wang, C.; Wang, Z. A Facile One-Pot Solvothermal Method to Produce Superparamagnetic Graphene–Fe3O4 Nanocomposite and Its Application in the Removal of Dye from Aqueous Solution. *Colloids Surf. B Biointerfaces* **2013**, *101*, 210–214. [CrossRef] [PubMed]
46. Raghu, M.S.; Yogesh Kumar, K.; Prashanth, M.K.; Prasanna, B.P.; Vinuth, R.; Pradeep Kumar, C.B. Adsorption and Antimicrobial Studies of Chemically Bonded Magnetic Graphene Oxide-Fe_3O_4 Nanocomposite for Water Purification. *J. Water Process Eng.* **2017**, *17*, 22–31. [CrossRef]
47. Zhang, R.; Su, P.; Yang, Y. Microwave-Assisted Preparation of Magnetic Nanoparticles Modified with Graphene Oxide for the Extraction and Analysis of Phenolic Compounds. *J. Sep. Sci.* **2014**, *37*, 3339–3346. [CrossRef]
48. Mohammadnia, M.; Heydari, R.; Sohrabi, M.R. Determination of 2,4-Dichlorophenoxyacetic Acid in Food and Water Samples Using a Modified Graphene Oxide Sorbent and High-Performance Liquid Chromatography. *J. Environ. Sci. Health Part B* **2020**, *55*, 293–300. [CrossRef]
49. Majd, M.; Nojavan, S. Magnetic Dispersive Solid-Phase Extraction of Triazole and Triazine Pesticides from Vegetable Samples Using a Hydrophilic-Lipophilic Sorbent Based on Maltodextrin- and β-Cyclodextrin-Functionalized Graphene Oxide. *Mikrochim. Acta* **2021**, *188*, 380. [CrossRef]
50. Shirani, M.; Parandi, E.; Nodeh, H.R.; Akbari-adergani, B.; Shahdadi, F. Development of a Rapid Efficient Solid-Phase Microextraction: An Overhead Rotating Flat Surface Sorbent Based 3-D Graphene Oxide/Lanthanum Nanoparticles @ Ni Foam for Separation and Determination of Sulfonamides in Animal-Based Food Products. *Food Chem.* **2022**, *373*, 131421. [CrossRef]

51. Hasan, C.K.; Ghiasvand, A.; Lewis, T.W.; Nesterenko, P.N.; Paull, B. Recent Advances in Stir-Bar Sorptive Extraction: Coatings, Technical Improvements, and Applications. *Anal. Chim. Acta* **2020**, *1139*, 222–240. [CrossRef]
52. Zhou, J.; Wang, R.; Chen, Z. Stir Bar Sorptive Extraction with a Graphene Oxide Framework-Functionalized Stainless-Steel Wire for the Determination of Sudan Dyes in Water Samples. *Anal. Methods* **2019**, *11*, 2050–2056. [CrossRef]
53. Zheng, J.; Huang, J.; Yang, Q.; Ni, C.; Xie, X.; Shi, Y.; Sun, J.; Zhu, F.; Ouyang, G. Fabrications of Novel Solid Phase Microextraction Fiber Coatings Based on New Materials for High Enrichment Capability. *TrAC Trends Anal. Chem.* **2018**, *108*, 135–153. [CrossRef]
54. Darvishnejad, F.; Raoof, J.B.; Ghani, M. MIL-101 (Cr) @ Graphene Oxide-Reinforced Hollow Fiber Solid-Phase Microextraction Coupled with High-Performance Liquid Chromatography to Determine Diazinon and Chlorpyrifos in Tomato, Cucumber and Agricultural Water. *Anal. Chim. Acta* **2020**, *1140*, 99–110. [CrossRef] [PubMed]
55. Wang, N.; Lu, Y.; Cui, B. Preparation and Application of β-Cyclodextrin Functionalised Graphene Oxide-Grafted Silica Sorbents for Solid-Phase Extraction (SPE) of Polycyclic Aromatic Hydrocarbons from Fried Food Using a Box-Behnken Design. *Food Anal. Methods* **2021**, *14*, 1577–1589. [CrossRef]
56. Moral, A.; Borrull, F.; Fourton, K.G.; Kabir, A.; Marcé, R.M.; Fontanals, N. Extraction of Selected Benzothiazoles, Benzotriazoles and Benzenesulfonamides from Environmental Water Samples Using a Home-Made Sol-Gel Silica-Based Mixed-Mode Zwitterionic Sorbent Modified with Graphene. *Talanta* **2023**, *256*, 124315. [CrossRef] [PubMed]
57. Feizy, J.; Jahani, M.; Beigbabaei, A. Graphene Adsorbent-Based Solid-Phase Extraction for Aflatoxins Clean-Up in Food Samples. *Chromatographia* **2019**, *82*, 917–926. [CrossRef]
58. de Gomes, R.S.; Thesing, A.; Santos, J.F.L.; Fernandes, A.N. Self-Supported 3D Reduced Graphene Oxide for Solid-Phase Extraction: An Efficient and Low-Cost Sorbent for Environmental Contaminants in Aqueous Solution. *Talanta* **2021**, *235*, 122750. [CrossRef]
59. Oliveira, T.C.; Lanças, F.M. Determination of Selected Herbicides in Sugarcane-Derived Foods by Graphene-Oxide Based Disposable Pipette Extraction Followed by Liquid Chromatography-Tandem Mass Spectrometry. *J. Chromatogr. A* **2023**, *1687*, 463690. [CrossRef]
60. Zhang, J.; Yu, C.; Chen, Z.; Luo, X.; Zhao, H.; Wu, F. Zeolitic Imidazolate Framework-8/Fluorinated Graphene Coated SiO_2 Composites for Pipette Tip Solid-Phase Extraction of Chlorophenols in Environmental and Food Samples. *Talanta* **2021**, *228*, 122229. [CrossRef]
61. Analytical Methods Committee. Technical Analytical Methods Committee Briefs What Causes Most Errors in Chemical Analysis? *Anal. Methods* **2013**, *5*, 2914–2915. [CrossRef] [PubMed]
62. Pan, J.; Zhang, C.; Zhang, Z.; Li, G. Review of Online Coupling of Sample Preparation Techniques with Liquid Chromatography. *Anal. Chim. Acta* **2014**, *815*, 1–15. [CrossRef] [PubMed]
63. Fernández-Ramos, C.; Šatínský, D.; Šmídová, B.; Solich, P. Analysis of Trace Organic Compounds in Environmental, Food and Biological Matrices Using Large-Volume Sample Injection in Column-Switching Liquid Chromatography. *TrAC Trends Anal. Chem.* **2014**, *62*, 69–85. [CrossRef]
64. Mejía-Carmona, K.; Lanças, F.M. Modified Graphene-Silica as a Sorbent for in-Tube Solid-Phase Microextraction Coupled to Liquid Chromatography-Tandem Mass Spectrometry. Determination of Xanthines in Coffee Beverages. *J. Chromatogr. A* **2020**, *1621*, 461089. [CrossRef] [PubMed]
65. Chen, X.-L.; Ai, L.-F.; Cao, Y.-Q.; Nian, Q.-X.; Jia, Y.-Q.; Hao, Y.-L.; Wang, M.-M.; Wang, X.-S. Rapid Determination of Sulfonamides in Chicken Muscle and Milk Using Efficient Graphene Oxide-Based Monolith On-Line Solid-Phase Extraction Coupled with Liquid Chromatography–Tandem Mass Spectrometry. *Food Anal. Methods* **2019**, *12*, 271–281. [CrossRef]
66. Sun, M.; Han, S.; Maloko Loussala, H.; Feng, J.; Li, C.; Ji, X.; Feng, J.; Sun, H. Graphene Oxide-Functionalized Mesoporous Silica for Online in-Tube Solid-Phase Microextraction of Polycyclic Aromatic Hydrocarbons from Honey and Detection by High Performance Liquid Chromatography-Diode Array Detector. *Microchem. J.* **2021**, *166*, 106263. [CrossRef]
67. Seidi, S.; Abolhasani, H.; Razeghi, Y.; Shanehsaz, M.; Manouchehri, M. Electrochemically Deposition of Ionic Liquid Modified Graphene Oxide for Circulated Headspace In-Tube Solid Phase Microextraction of Naphthalene from Honey Samples Followed by on-Line Liquid Chromatography Analysis. *J. Chromatogr. A* **2020**, *1628*, 461486. [CrossRef]
68. da Silva, L.F.; Vargas Medina, D.A.; Lanças, F.M. Automated Needle-Sleeve Based Online Hyphenation of Solid-Phase Microextraction and Liquid Chromatography. *Talanta* **2021**, *221*, 121608. [CrossRef]
69. Wei, Z.H.; Mu, L.N.; Pang, Q.Q.; Huang, Y.P.; Liu, Z.S. Preparation and Characterization of Grafted Imprinted Monolith for Capillary Electrochromatography. *Electrophoresis* **2012**, *33*, 3021–3027. [CrossRef]
70. Qu, Q.; Gu, C.; Hu, X. Capillary Coated with Graphene and Graphene Oxide Sheets as Stationary Phase for Capillary Electrochromatography and Capillary Liquid Chromatography. *Anal. Chem.* **2012**, *84*, 8880–8890. [CrossRef]
71. Borsatto, J.V.B.; Maciel, E.V.S.; Lanças, F.M. Investigation of the Applicability of Silica-Graphene Hybrid Materials as Stationary Phases for Capillary Liquid Chromatography. *J. Chromatogr. A* **2022**, *1685*, 463618. [CrossRef] [PubMed]
72. Wahab, M.F.; Patel, D.C.; Wimalasinghe, R.M.; Armstrong, D.W. Fundamental and Practical Insights on the Packing of Modern High-Efficiency Analytical and Capillary Columns. *Anal. Chem.* **2017**, *89*, 8177–8191. [CrossRef] [PubMed]
73. Zhang, X.; Chen, S.; Han, Q.; Ding, M. Preparation and Retention Mechanism Study of Graphene and Graphene Oxide Bonded Silica Microspheres as Stationary Phases for High Performance Liquid Chromatography. *J. Chromatogr. A* **2013**, *1307*, 135–143. [CrossRef] [PubMed]

74. Liang, X.; Liu, S.; Song, X.; Zhu, Y.; Jiang, S. Layer-by-Layer Self-Assembled Graphene Oxide/Silica Microsphere Composites as Stationary Phase for High Performance Liquid Chromatography. *Analyst* **2012**, *137*, 5237. [CrossRef]
75. Zhou, Y.; Qu, Z.B.; Zeng, Y.; Zhou, T.; Shi, G. A Novel Composite of Graphene Quantum Dots and Molecularly Imprinted Polymer for Fluorescent Detection of Paranitrophenol. *Biosens. Bioelectron.* **2014**, *52*, 317–323. [CrossRef]
76. Luo, Q.; Zhong, Z.; Zheng, Y.; Gao, D.; Xia, Z.; Wang, L. Preparation and Evaluation of a Poly(N-Isopropylacrylamide) Derived Graphene Quantum Dots Based Hydrophilic Interaction and Reversed-Phase Mixed-Mode Stationary Phase for Complex Sample Analysis. *Talanta* **2021**, *224*, 121869. [CrossRef] [PubMed]
77. Wu, Q.; Chen, L.; Gao, J.; Dong, S.; Li, H.; Di, D.; Zhao, L. Graphene Quantum Dots-Functionalized C18 Hydrophobic/Hydrophilic Stationary Phase for High Performance Liquid Chromatography. *Talanta* **2019**, *194*, 105–113. [CrossRef]
78. Wu, Q.; Gao, J.; Chen, L.; Dong, S.; Li, H.; Qiu, H.; Zhao, L. Graphene Quantum Dots Functionalized β-Cyclodextrin and Cellulose Chiral Stationary Phases with Enhanced Enantioseparation Performance. *J. Chromatogr. A* **2019**, *1600*, 209–218. [CrossRef]
79. Luo, Q.; Wan, M.; Zhou, J.; Dai, X.; Yang, H.; Zu, F.; Zheng, Y.; Wang, L. Preparation and Evaluation of a Double-Hydrophilic Interaction Stationary Phase Based on Bovine Serum Albumin and Graphene Quantum Dots Modified Silica. *J. Chromatogr. A* **2022**, *1669*, 462933. [CrossRef]
80. Li, Y.; Wei, M.; Chen, T.; Zhu, N.; Ma, Y. Self-Assembled Cyclodextrin-Modified Gold Nanoparticles on Silica Beads as Stationary Phase for Chiral Liquid Chromatography and Hydrophilic Interaction Chromatography. *Talanta* **2016**, *160*, 72–78. [CrossRef]
81. Liu, H.; Guo, Y.; Wang, X.; Liang, X.; Liu, X. Amino-Terminated Ionic Liquid Modified Graphene Oxide Coated Silica Composite Stationary Phase for Hydrophilic Interaction Chromatography. *RSC Adv.* **2014**, *4*, 37381–37388. [CrossRef]
82. Borsatto, J.V.B.; Maciel, E.V.S.; Cifuentes, A.; Lanças, F.M. Online Extraction Followed by LC–MS/MS Analysis of Lipids in Natural Samples: A Proof-of-Concept Profiling Lecithin in Seeds. *Foods* **2023**, *12*, 281. [CrossRef] [PubMed]
83. Xie, X.; Huang, S.; Zheng, J.; Ouyang, G. Trends in Sensitive Detection and Rapid Removal of Sulfonamides: A Review. *J. Sep. Sci.* **2020**, *43*, 1634–1652. [CrossRef] [PubMed]
84. Zhao, C.; Yan, S.; Liu, J.; Xiong, Z.; Zhao, L. Octadecylamine and Serine-Derived Carbon Dots-Modified Silica Gel for Reversed Phase/Hydrophilic Interaction Liquid Chromatography. *Microchem. J.* **2022**, *183*, 107987. [CrossRef]
85. Zhao, H.; Wang, Y.; Cheng, H.; Shen, Y. Graphene Oxide Decorated Monolithic Column as Stationary Phase for Capillary Electrochromatography. *J. Chromatogr. A* **2016**, *1452*, 27–35. [CrossRef]
86. Xu, S.; Mo, R.; Jin, C.; Cui, X.; Bai, R.; Ji, Y. Mesoporous Silica Nanoparticles Incorporated Hybrid Monolithic Stationary Phase Immobilized with Pepsin for Enantioseparation by Capillary Electrochromatography. *J. Pharm. Biomed. Anal.* **2017**, *140*, 190–198. [CrossRef] [PubMed]
87. Li, Y.; Qi, L.; Ma, H. Preparation of Porous Polymer Monolithic Column Using Functionalized Graphene Oxide as a Functional Crosslinker for High Performance Liquid Chromatography Separation of Small Molecules. *Analyst* **2013**, *138*, 5470. [CrossRef] [PubMed]
88. Lin, Z.; Wang, J.; Yu, R.; Yin, X.; He, Y. Incorporation of Graphene Oxide Nanosheets into Boronate-Functionalized Polymeric Monolith to Enhance the Electrochromatographic Separation of Small Molecules. *Electrophoresis* **2015**, *36*, 596–606. [CrossRef]
89. Günyel, Z.; Aslan, H.; Demir, N.; Aydoğan, C. Nano-liquid Chromatography with a New Nano-structured Monolithic Nanocolumn for Proteomics Analysis. *J. Sep. Sci.* **2021**, *44*, 3996–4004. [CrossRef]
90. Tang, Y.; Cui, X.; Zhang, Y.; Ji, Y. Preparation and Evaluation of a Polydopamine-Modified Capillary Silica Monolith for Capillary Electrochromatography. *New J. Chem.* **2019**, *43*, 1009–1016. [CrossRef]
91. Rice, J.; Proctor, K.; Lopardo, L.; Evans, S.; Kasprzyk-Hordern, B. Stereochemistry of Ephedrine and Its Environmental Significance: Exposure and Effects Directed Approach. *J. Hazard. Mater.* **2018**, *348*, 39–46. [CrossRef]
92. Ishii, D.; Tsuda, T.; Hibi, K.; Takeuchi, T.; Nakanishi, T. Study of Open-Tubular Micro-Capillary Liquid Chromatography. *J. High Resolut. Chromatogr.* **1979**, *2*, 371–377. [CrossRef]
93. Knox, J.H.; Gilbert, M.T. Kinetic Optimization of Straight Open-Tubular Liquid Chromatography. *J. Chromatogr. A* **1979**, *186*, 405–418. [CrossRef]
94. Desmet, G.; Eeltink, S. Fundamentals for LC Miniaturization. *Anal. Chem.* **2013**, *85*, 543–556. [CrossRef]
95. Sagandykova, G.; Szumski, M.; Buszewski, B. How Much Separation Sciences Fit in the Green Chemistry Canoe? *Curr. Opin. Green Sustain. Chem.* **2021**, *30*, 100495. [CrossRef]
96. Vargas Medina, D.A.; dos Santos, N.G.P.; da Silva Burato, J.S.; Borsatto, J.V.B.; Lanças, F.M. An Overview of Open Tubular Liquid Chromatography with a Focus on the Coupling with Mass Spectrometry for the Analysis of Small Molecules. *J. Chromatogr. A* **2021**, *1641*, 461989. [CrossRef]
97. Vargas Medina, D.A.; da Burato, J.S.S.; Borsatto, J.V.B.; Lanças, F.M. Porous Layer Open Tubular Nano Liquid Chromatography Directly Coupled to Electron Ionization Mass Spectrometry. *J. Chromatogr. A* **2022**, *1674*, 463143. [CrossRef] [PubMed]
98. Wang, X.; Wang, S.; Veerappan, V.; Byun, C.K.; Nguyen, H.; Gendhar, B.; Allen, R.D.; Liu, S. Bare Nanocapillary for DNA Separation and Genotyping Analysis in Gel-Free Solutions without Application of External Electric Field. *Anal. Chem.* **2008**, *80*, 5583–5589. [CrossRef] [PubMed]
99. Chen, H.; Zhu, Z.; Lu, J.J.; Liu, S. Charging YOYO-1 on Capillary Wall for Online DNA Intercalation and Integrating This Approach with Multiplex PCR and Bare Narrow Capillary–Hydrodynamic Chromatography for Online DNA Analysis. *Anal. Chem.* **2015**, *87*, 1518–1522. [CrossRef]

100. Yue, G.; Luo, Q.; Zhang, J.; Wu, S.L.; Karger, B.L. Ultratrace LC/MS Proteomic Analysis Using 10-Mm-i.d. Porous Layer Open Tubular Poly(Styrene-Divinylbenzene) Capillary Columns. *Anal. Chem.* **2007**, *79*, 938–946. [CrossRef]
101. Luo, Q.; Yue, G.; Valaskovic, G.A.; Gu, Y.; Wu, S.; Karger, B.L. On-line 1D and 2D porous layer open tubular/LC-ESI-MS using 10-µm-id poly (styrene-divinylbenzene) columns for ultrasensitive proteomic analysis. *Anal. Chem.* **2007**, *79*, 6549–6556. [CrossRef]
102. Luo, Q.; Rejtar, T.; Wu, S.L.; Karger, B.L. Hydrophilic Interaction 10 Mm I.D. Porous Layer Open Tubular Columns for Ultratrace Glycan Analysis by Liquid Chromatography-Mass Spectrometry. *J. Chromatogr. A* **2009**, *1216*, 1223–1231. [CrossRef] [PubMed]
103. Hustoft, H.K.; Vehus, T.; Brandtzaeg, O.K.; Krauss, S.; Greibrokk, T.; Wilson, S.R.; Lundanes, E. Open Tubular Lab-on-Column/Mass Spectrometry for Targeted Proteomics of Nanogram Sample Amounts. *PLoS ONE* **2014**, *9*, e106881. [CrossRef] [PubMed]
104. Niu, X.; Ding, S.; Wang, W.; Xu, Y.; Xu, Y.; Chen, H.; Chen, X. Separation of Small Organic Molecules Using Covalent Organic Frameworks-LZU1 as Stationary Phase by Open-Tubular Capillary Electrochromatography. *J. Chromatogr. A* **2016**, *1436*, 109–117. [CrossRef] [PubMed]
105. da Silva, M.R.; Brandtzaeg, O.K.; Vehus, T.; Lanças, F.M.; Wilson, S.R.; Lundanes, E. An Automated and Self-Cleaning Nano Liquid Chromatography Mass Spectrometry Platform Featuring an Open Tubular Multi-Hole Crystal Fiber Solid Phase Extraction Column and an Open Tubular Separation Column. *J. Chromatogr. A* **2017**, *1518*, 104–110. [CrossRef]
106. Ahmed, M.A.; Yu, R.B.; Quirino, J.P. Recent Developments in Open Tubular Liquid Chromatography and Electrochromatography from 2019–2021. *TrAC Trends Anal. Chem.* **2023**, *164*, 117045. [CrossRef]
107. Ma, M.; Xi, Y.; Du, Y.; Yang, J.; Ma, X.; Chen, C. Maltodextrin-Modified Graphene Oxide for Improved Enantiomeric Separation of Six Basic Chiral Drugs by Open-Tubular Capillary Electrochromatography. *Microchim. Acta* **2020**, *187*, 55. [CrossRef]
108. Ye, N.; Li, J. Determination of Dopamine, Epinephrine, and Norepinephrine by Open-Tubular Capillary Electrochromatography Using Graphene Oxide Molecularly Imprinted Polymers as the Stationary Phase. *J. Sep. Sci.* **2014**, *37*, 2239–2247. [CrossRef]
109. Cai, Z.; Hu, X.; Zong, R.; Wu, H.; Jin, X.; Yin, H.; Huang, C.; Xiang, Y.; Ye, N. A Graphene Oxide-Molybdenum Disulfide Composite Used as Stationary Phase for Determination of Sulfonamides in Open-Tubular Capillary Electrochromatography. *J. Chromatogr. A* **2020**, *1629*, 461487. [CrossRef]
110. Sun, X.; Ding, Y.; Niu, B.; Chen, Q. Evaluation of a Composite Nanomaterial Consist of Gold Nanoparticles and Graphene-Carbon Nitride as Capillary Electrochromatography Stationary Phase for Enantioseparation. *Microchem. J.* **2021**, *169*, 106613. [CrossRef]

Capítulo 4

Miniaturization of liquid chromatography coupled to mass spectrometry 1. Current trends on miniaturized LC columns

Mejía-Carmona, Karen; Soares Da Silva Burato, Juliana; **Borsatto, João Victor Basolli;** De Toffoli, Ana Lúcia; Lanças, Fernando Mauro. Miniaturization of liquid chromatography coupled to mass spectrometry: 1. Current trends on miniaturized LC columns. **TrAC - Trends in Analytical Chemistry**, *[S. l.]*, v. 122, 2020. DOI: 10.1016/j.trac.2019.115735.

Trends in Analytical Chemistry 122 (2020) 115735

Contents lists available at ScienceDirect

Trends in Analytical Chemistry

journal homepage: www.elsevier.com/locate/trac

Miniaturization of liquid chromatography coupled to mass spectrometry
1. Current trends on miniaturized LC columns

Karen Mejía-Carmona , Juliana Soares da Silva Burato , João Victor Basolli Borsatto , Ana Lúcia de Toffoli , Fernando Mauro Lanças *

São Carlos Institute of Chemistry, University of São Paulo, 13560-970 São Carlos, SP, Brazil

ARTICLE INFO

Article history:
Available online 21 November 2019

Keywords:
Miniaturized liquid chromatography
Particle packed capillary column
Monolithic capillary columns
Open-tubular columns
Wall coated open-tubular columns
Porous layer open tubular columns
Mass spectrometry

ABSTRACT

Over the last decade, the use of miniaturized columns in liquid chromatography (LC) has seen intense growth in a wide range of research areas. This report brings an overview of the current developments and applications of miniaturized columns in LC, focused on the type of columns used. Following a short introductory section on some theoretical aspects, the fundamental bases on their design and fabrication, new stationary phases and incorporated materials, performance evaluation/characterization, main advantages, and recent applications of filled capillary and open tubular (OT) capillary columns are introduced and critically discussed. Prospects on the different types of miniaturized columns and their hyphenation with mass spectrometry (MS) reported in the last years are also introduced and discussed.

1. Introduction

Liquid chromatography (LC) has become a widespread analytical technique used in many fields of natural and health sciences [1–3]. Following the current trends in analytical chemistry, miniaturization is among the main LC innovation areas along the last ten years [4].

Horvárth et al. [5] were one of the pioneers in LC miniaturization. In 1967 they compared a stainless-steel uncoated capillary tubing of inner diameter (i.d.) of 0.3 mm with a 50 μm pellicular particle packed capillary of 1.0 mm i.d. for the separation of nucleotides. This study drove the authors to the conclusion that packed small-bore capillaries were more efficient than uncoated capillary ones. One decade later, Tsuda and Novotny [6,7] established the required equipment for working with capillary LC, by miniaturizing the overall capillary LC system. They diminished the column i.d. to 50–200 μm, and the particle size down to ~30–10 μm, as well as have implemented modifications on conventional injection and detector systems aiming to reduce the band-broadening effects. At the same time, Ishii et al. [8] worked in the development of a micro-high performance liquid chromatography (MHPLC) system, successfully applied to both packed [9] and open tubular (OT) capillary columns. These seminal works were an essential contribution that allowed miniaturized LC to significantly advance in the 80's, along with other techniques as capillary electrophoresis and capillary supercritical fluid chromatography, waking up the interest of researchers from different fields [10]. Recently, Novotny et al. [10] reported a comprehensive review of the historical aspects, advances, and efforts of capillary LC developments from the beginning until the present.

Nowadays, the separation in miniaturized LC is performed in capillary columns similar to those used in high-resolution gas chromatography. As a result of all the developments made in miniaturized LC, it is possible now to find commercially available capillary and nano liquid chromatography systems (capillary-LC and nano-LC), including —and principally— using ESI-MS as a detector.

One of the most important advantages offered by miniaturized LC is the viability to work in applications were just a small sample volume may be collected and analyzed, covering areas such as forensic, clinical, and omics. Besides, the low flow rate employed means lower solvent consumption, allowing the use of specialized solvents, and leading to enhanced detection as a result of the lower chromatographic dilution [11,12].

Miniaturized LC is a general term employed for describing liquid chromatography using i.d. columns below to 1.0 mm. In practice, to

* Corresponding author. Fax: +55 16 3373 9984.
E-mail address: flancas@iqsc.usp.br (F.M. Lanças).

https://doi.org/10.1016/j.trac.2019.115735
0165-9936/

Abbreviations

β-CD	β-cyclodextrin
capillary-LC	capillary liquid chromatography
CLSM	confocal laser scanning microscopy
CTCs	circulating tumor cells
d_p	particle diameter
ESI	electrospray ionization
EI	electron ionization
FP	fully porous particles
GC	gas chromatography
h	reduced plate height
H	plate height
HILIC	hydrophilic interaction chromatography
HIC	hydrophobic interaction chromatography
HPLC	high-performance liquid chromatography
i.d.	inner diameter
KPL	kinetic performance limits plots
LC	liquid chromatography
MS	mass spectrometry
MS/MS	tandem mass spectrometry
nano-ESI	nano-electrospray ionization
nano-LC	nano liquid chromatography
NP	non-porous particles
OT	open tubular
PDMS	polydimethylsiloxane
PLOT	porous layer open tubular
SEM	scanning electron microscopy
SP	superficially porous particles
TMOS	tetramethoxysilane
UHPLC	ultra-high pressure liquid chromatography
υ	reduced linear velocity
WCOT	wall coated open tubular

make an accurate description of this approach, it is necessary to consider both the internal column diameter and the mobile phase flow rate used [13]. In general terms, for practical purposes, capillary-LC employs capillary columns with i.d. between 100 and 500 μm, and flow rates of 1–10 μL/min, while nano-LC employs capillary columns with i.d. < 100 μm with flow rates from 10 to 1000 nL/min [2].

The design of the columns has been one of the main drivers on LC miniaturization, as exposed by Desmet et al. [11]. There are two main types of capillary columns: filled capillary columns and open tubular capillary columns (Fig. 1). The former can be filled with a particle bed or a monolith, and the second has a thin layer of stationary phase attached to the inner surface of the column, leaving an open tubular space.

Particle packed capillary columns commonly use the same particles employed in conventional HPLC columns; silica-based particles are the most employed. Silica particles can be prepared in different ways, producing unique characteristics, resulting in a wide range of packed capillary columns commercially available [12]. In LC, it is known that reducing the particle size and the internal diameter of columns improves the separation performance; the use of sub-2 μm particles enables greater efficiency at faster flows, reducing analysis time [14]. Nevertheless, this advantage is limited by the high back-pressure generated, requiring specialized instrumentation similar to that used in ultra-high pressure liquid chromatography (UHPLC) [15]. Additional information about particles and support materials, as well as packing capillary columns methods, can be found in several reviews [2,14–17].

Monolithic capillary columns —another way to prepare filled columns— since their introduction in the early 90's, have gained particular interest because of their easy *in-situ* preparation and high permeability that decrease the back-pressure when compared to particle packed capillary columns. A monolithic column consists of a continuous polymeric block structure made from either silica-based or organic-based polymers that fill the whole capillary tube [1]. Capillaries with i.d. ranging from 20 to 500 μm are commonly employed. The efficiency of monolithic columns depends on the stationary phase morphology, macropore size, uniform skeleton, and kind of polymers employed. Improvements in the efficiency —similarly by that obtained by the reduction particle sizes in packed columns— can be achieved by controlling both the external porosity and pore size [14]. Currently, the synthesis of a wide range of monolithic materials containing metallic nanoparticles, metal-organic frameworks, carbon-based nanomaterials, as well as monoliths functionalized with boronic acid, zwitterionic monomers and other functionalities [18], extended the range of applications of capillary LC.

On the other hand, open tubular (OT) columns, firstly introduced for gas chromatography (GC) in 1958 by Golay [19], became an unique type of column which have a thin layer of stationary

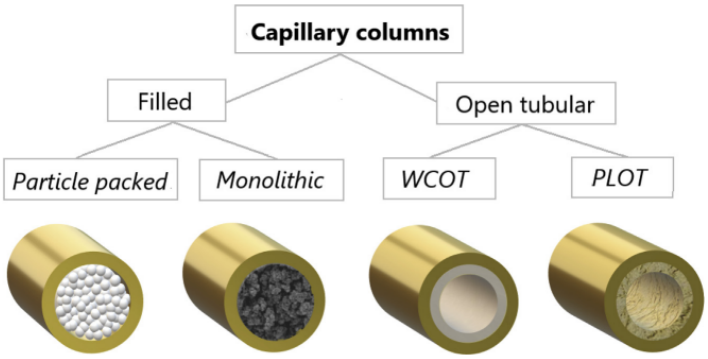

Fig. 1. Classification of capillary columns based on the arrangement of packing material inside the column.

phase on the inner wall of the capillary. By the late 1970s, Tsuda et al. [20] explored the OT concept in LC studies, including the design, theory, and practical aspects of the technique. However, the research interest decayed quickly, mainly due to its lower performance compared to particle packed columns, and the lack of suitable miniaturized instrumentation and detectors at the time. Recently, with the commercial availability of highly sensitive detectors, reduced volume injectors, and micro and nanoflow LC instruments, the interest in applications and fundamental research in OT columns emerged again.

In contrast to particle packed columns, the most critical advantages of OT columns is the exclusion of eddy dispersion contribution —counting roughly to one-half of band-broadening in packed columns— and their high permeability, which allows the use of longer columns [11]. However, to achieve a high chromatographic efficiency are required columns with downsized inner diameters (~5 μm), a fact that severely compromises the backpressure and column length [21]. OT columns are classified into two main types: wall coated open tubular (WCOT), and porous layer open tubular (PLOT).

Although WCOT is the most employed in GC, consisting of a thin cover film of non-porous stationary phase, these columns were poorly explored in LC because of their lower sample capacity and efficiency, mainly due to their non-porous film. Later efforts aiming to obtain thicker films and increase their sample capacity were made, employing multilayer coatings and unique chemical bonding processes. Despite this, WCOT columns were overshadowed by a new type of open tubular LC column termed PLOT columns, once they showed to be superior to the LC purposes at that time [1]. In practice, LC-type WCOT capillary columns have been to the moment employed more successfully in capillary electrochromatography (CEC) than in micro and nano-LC [22].

In a PLOT column, also initially developed for GC, the stationary phase is a porous material that offers a higher surface area and better retention capacity compared to WCOT columns. Among the stationary phases employed, organic polymeric or silica polymeric-based materials are the most utilized. Polystyrene (PS), polydivinylbenzene (DVB), and polymethacrylate (PMMA) are the current phases applied to proteomic analyses. Thin layer polymeric stationary phases are usually deposited by the free-radical polymerization method, either by thermal or photo-initiation approaches, yielding several layer structures and morphologies by modifying such as the energy supplied through the polymerization time [3,23,24].

The last generation of silica-based PLOT columns was recently obtained by the sol-gel method, as reported by Förster et al. [25]. They employed a solution of tetramethoxysilane (TMOS), urea and polyethylene oxide (PEO) as progeny agent in preparing fused silica capillaries of 10–100 μm i.d. The authors obtained PLOT columns with a good mass loadability that provided high-efficiency separations (>170,000 plates), successfully applied to normal phase separations [25,26]. Recently, Hara et al. [27] demonstrated that capillary columns with 5 μm of i.d. coated with mesoporous silica, 550 nm layer width and 2.6 m length, achieved ~950,000 plates.

In this first review of a series on coupling miniaturized LC columns to mass spectrometry (MS), we provide an overview of the recent advances on capillary-LC and nano-LC, focused on the capillary columns, stationary-phases synthesis and packing methods, and their recent applications with particular emphasis on the coupling to mass spectrometry (MS). In a second review, we will discuss the miniaturized instrumentation, hyphenation with mass spectrometry, and the current status of chip-based systems.

2. Theoretical aspects

The behavior of the analyte's molecules inside a column and how it affects the analysis performance have been one of the most important topics to be understood in all chromatography techniques. The main fundaments were first developed for GC and further transferred to LC. Among the researchers that have developed the theory of chromatography in the last century, J. J. van Deemter and coworkers receive the main attention. In their work, the authors described how the molecules of analytes are distributed along the column during the separation based on three terms [28]. The first term (A-term), also called eddy diffusion, demonstrates how the molecules of analytes spread by flowing through the column. It is independent of the flow but depends on the column morphology (particle diameter (d_p) for packed columns and i.d. for OT columns, as an example). The second term (B-term) is related to the longitudinal diffusion and depends on the diffusion coefficient of the mobile phase, but also on the flow rate. The last term, (C-term) called the mass transfer resistance, depends on the transference of the analytes between the mobile and stationary phase and presents a linear dependence on the flow rate. Those terms were used to correlate the plate height and the flow rate of analysis generating Equation (1) (Table 1). The plate height (H) (Equation (2), Table 1), an important metric to be considered in the evaluation of the separation performance, is defined as the rate of increase of the peak variance per unit of length of the column. The lower the H, the better the separation performance. The van Deemter equations not only brought a deeper view of the chromatography fundamentals but also resulted in a powerful tool to evaluate the performance of the columns. The so-called van Deemter plots have been applied for generations of scientists to evaluate the performance of the chromatographic separation in combination with other graphical representation methods to be mentioned later in this topic.

Giddings proposed dimensionless metrics in order to correlate the performance of different forms of chromatography [29]. The dimensionless metrics were denominated as reduced terms. The reduced plate height (h) and the reduced linear velocity (υ) take into account the particle diameters of the packing material (Equations (5) and (6), Table 1). Knox and Parcher [30] proposed that by plotting log h as a function of log υ, a powerful tool to assay the packing quality would be available. This relationship, known latter as the Knox equation (Equation (4), Table 1), correlated the h and the υ in a way similar to the van Deemter equation. The major difference between the equations is related to the dependence of the multipath term on the υ (see Equations (1) and (4) to compare). At low υ values, the multipath diffusion tends to have a lower impact on h until it reaches a constant value at high υ values. The longitudinal diffusion and the mass transfer resistance present the same behavior as proposed by van Deemter.

Recently, the kinetic plots are receiving more attention in order to characterize columns and separation performances. A kinetic plot is a graphical representation method that expresses a metric of separation quality (efficiency, peak capacity, resolution, and others) as a function of a metric of time (retention time, analysis time, dead time, and others). The initial concepts of kinetic plots were proposed by Giddings in his work comparing the theoretical efficiency limits of GC and LC [31], which was followed by a report by Poppe in the 90's, proposing the use of the now called Poppe plots to correlate speed and efficiency of the modern liquid chromatography techniques [32]. The kinetic plots started to be used as a valuable tool to evaluate separation and assay column performance in the works reported by Desmet [33,34]. The kinetic plots can be applicable in both isocratic and gradient analysis; due to this reason, it presents a series of uses and applications [35–37]. Among

Table 1
Highlight parameters and related equations for column evaluation in liquid chromatography.

	Equation No.	Equations/metric name	Equation
Classical terms	1	van Deemter	$H = A + \frac{B}{\mu} + C\mu$
	2	Plate height (H)	$H = \frac{L}{N} = \frac{\sigma^2}{L}$
	3	Linear velocity (μ)	$\mu = \frac{L}{t_0}$
Reduced terms	4	Knox	$h = A\nu^{0.33} + \frac{B}{\upsilon} + C\upsilon$
	5	Reduced plate height (h)	$h = \frac{H}{d_p}$
	6	Reduced linear velocity (υ)	$\upsilon = \frac{\mu d_p}{D_m}$
Kinetic Performance limit terms	7	*KPL* correction factor (λ)	$\lambda = \frac{\Delta P_{max}}{\Delta P_{exp}}$
	8	Efficiency *KPL* (N_{KPL})	$N_{KPL} = \lambda . N$
	9	Peak capacity KPL ($n_{P,KPL}$)	$n_{p,KPL} = 1 + \sqrt{\lambda} . (n_p - 1)$
	10	Dead time *KPL* ($t_{0,\ KPL}$)	$t_{0,KPL} = \lambda . t_0$
	11	Retention time *KPL* ($t_{R,KPL}$)	$t_{R,KPL} = \lambda . t_R$
Additional parameters in LC	12	Resolution (R_s)	$R_S = \frac{2(\Delta t_R)}{W_{0.5AB}}$
	13	Efficiency (N)	$N = 5,545\left(\frac{t_R}{W_{0.5}}\right)^2$
	14	Impedance (E)	$E = h^2\phi$
	15	Flow resistance (ϕ)	$\phi = \frac{d_p^2}{K}$
	16	Permeability (K)	$K = \frac{\mu\eta L}{\Delta P}$

L, column length; t_0, dead time; d_p, particle diameter; D_m, diffusion coefficient of the analyte in the mobile phase; ΔP_{max}, maximum pressure; ΔP_{exp}, experimental pressure drop; $w_{0.5}$: Half peak width at 50% of the peak height; η, mobile phase viscosity.

the main kinetic plots used today, kinetic performance limits plots (KPL) receives particular attention. This type of plot represents an imaginary set of columns of various lengths operating under conditions in which their performances are maximum [38]. Although the KPL plot represents an imaginary set of columns, it is constructed using experimental data transformed by a correction factor (see Table 1, Equations (6) to (11) to the more usual kinetic plots metrics). The correction factor (Equation (7), Table 1) takes into account the pressure drop of the column, which makes it useful to compare columns of different lengths, diameters, particle diameters, and even filled with different supports.

Another critical factor for capillary columns is the internal diameter of the capillary. Although it has no direct effect on the interaction with the analyte, smaller diameters result in higher linear velocities because the smaller cross-section forces the flow to be more intense. The column i.d. effect has been a focus of the investigation since the beginning of the instrumentation development for chromatography. It was observed that when the size is reduced to the capillary and nanoscale, the i.d. influences the column performance (Fig. 2A).

Bruns and coworkers [39,40] published a series of papers on the evaluation of column porosity by using confocal laser scanning microscopy (CLSM) and packing profile of the particles close to the wall, and its consequences over the separation. The observation showed that the i.d. of the capillary affects the packing porosity closer to the wall. Columns with larger i.d. presented higher porosity on the wall region and consequently lower performance. Adversely, smaller columns i.d. presented lower porosity and better results (Fig. 2B). The CLSM also demonstrated that columns of smaller i.d. presents more homogenous packing than larger i.d. columns [41]. Additionally, Gritti has demonstrated that for certain combinations of i.d. and d_p, some conditions of poor packing are formed, reducing the efficiency (Fig. 2C) [42].

The thermal effects are also minimized in the miniaturized packed columns. The viscous heating, generated by the friction of the mobile phase with the particles, is easily dissipated in capillary columns. The heating distribution inside the column is not homogenous; the center of the column becomes hotter than the walls, generating band dispersion. For columns packed with particles of $d_p = 1.0$ μm operating at 2000 bar, a regular column of 4.6 mm i.d. produces 2.8 W (at 820 μL/min) of heating. For the same conditions, a capillary column of 0.1 mm i.d. generates 1.3 mW (at 380 nL/min) and a nano column of 0.05 mm i.d. results in only 0.33 mW (at 96 nL/min) of power dissipation [43].

Miniaturized liquid chromatography has as its most notable advantage over conventional HPLC, better compatibility with MS, especially the electrospray ionization (ESI) interface. The small column diameters allow reduced mobile phase flow rates, which are more compatible with the optimal values of flow for the ESI-MS. The sampling efficiency increases significantly at low flow rates for ESI sources (Fig. 2D) [44]. Additionally, works have been carried out to allow the coupling of miniaturized LC with electron ionization (EI) sources, which is practically impossible to be achieved with conventional LC due to the high flow rates used and the back-pressures generated [45].

3. Packed columns

Packed columns represent the most significant slice of columns used in liquid chromatography, being the most popular kind of commercial column available in all scales (conventional and miniaturized LC). Other types of LC columns, such as the monolithic and OT columns are still in the state-of-the-art; its main characteristics are described and explored in the following sections of this review. Packed LC columns can be obtained in a large variety of stationary phases commercially available, operating in several chromatographic separation modes, including (i) reversed-phase, (ii) normal phase, (iii) hydrophilic interaction chromatography (HILIC), (iv) hydrophobic interaction chromatography (HIC), (v) ion-exchange chromatography, and others varieties. The primary particles used

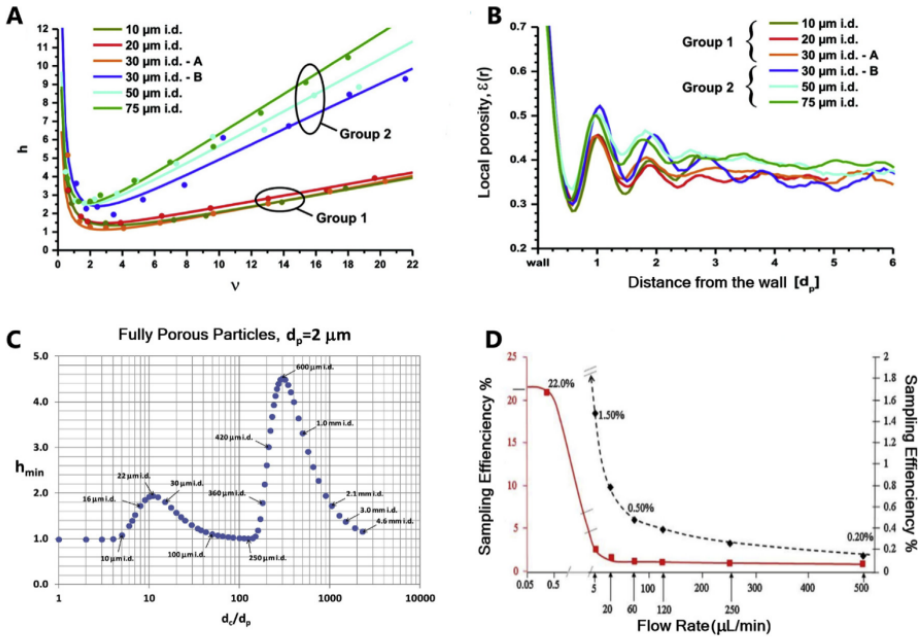

Fig. 2. (A) Plot of the reduced plate height for hydroquinone as a function of the reduced velocity for six different column diameters (2.0 µm d_p particles). (B) Radially resolved profiles of the interparticle void volume fraction or porosity for the wall region of the reconstructed column packing of the same columns presented in the A. (A and B) Reprinted with permission from Ref. [41], Copyright 2012, American Chemical Society. (C) Prediction by the stochastic model of trans-column eddy dispersion regarding the variation of the minimum for columns packed with 2 µm. Reprinted with permission of [42], Copyright 2018, Elsevier B.V. (D) Sampling efficiency versus flow rate. The data in the upper dashed trace (black), read from the right (black) Y-axis, is an expansion of the data in the lower solid trace (red) read from the left (red) Y-axis. Reprinted with permission of [44], Copyright 2009, Wiley Periodicals, Inc.

in LC can be produced using silicates-like structures generating phases such as C18, C8, cyano, amino, and bare silica particles, or be produced as organic resins. The particles' morphology can be divided into three types: (i) the fully porous (FP) particles, which is, as its name describe, a fully porous sphere; (ii) the superficially porous (SP) particles, which is a sphere of solid (non-porous) core surrounded by a thin porous layer; and (iii) the non-porous particles (NP), that is a non-porous sphere of the stationary phase. Majors summarized those and other more types of column packing for LC [46].

A significant advancement in columns for LC was the optimization of the packing material, in particular, the reduction of particle size. The reduction in particle diameter (d_p) resulted in a more significant performance incensement due to the considerable improvement in the mass transfer between the phases and the reduction in trans-particle and trans-channel diffusions. On the other hand, these small d_p demands a higher mobile phase pressure to percolate along its packed bed [47]. To overcome the limitation of the higher back-pressure produced by the stationary phase, more powerful equipment were developed, resulting in the UHPLC concept. Some commercially available models can withstand pressures higher than 1500 bar.

The SP particles, also known as core-shell, porous-shell, or fused-core particles, were developed as an alternative to the UHPLC system. The presence of a solid core reduces the trans-porous diffusion because the porous layer is thinner than in the FP particles. This reduction in the porous structure allows to bigger SP particles to reach comparable efficiency as smaller FP particles. NP particles are also availed but are less used than FP and SP particles.

The packed columns are composed of three main parts: (i) the column tubing, (ii) the packed stationary phase, and (iii) the frits (responsible for retaining the stationary phase inside the column). The type of frit used affects the separation performance and detection possibilities. Franc and coworkers have evaluated the performance of several types of frit for capillary columns produced with different materials in columns of 0.32 and 0.25 mm i.d [48]. Four different types of frits were produced (Fig. 3). The type A frit

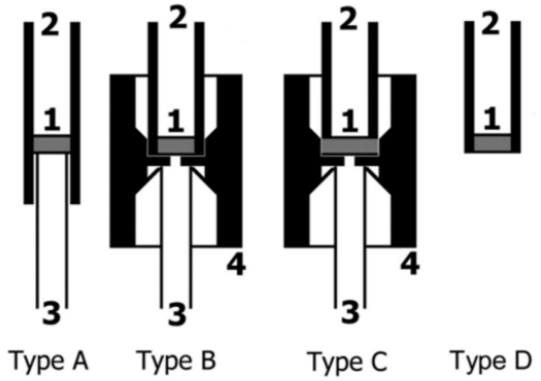

Fig. 3. Most used frit designs for miniaturized packed columns LC (see text for detailed information). Reprinted with permission of [48], Copyright 2014, Wiley-VCH.

was composed of a glass wool filter frit placed inside the column capillary and secured by a smaller i.d. outlet capillary emended with epoxy resin. The type B frit used the same glass wool frit but secured by a polyether ether ketone (PEEK) union. The type C frit was produced by placing a glass wool frit, stainless steel, or titanium frit inside the union and then secure the frit by pressing the capillary. Type D was produced with different monolithic frits, which allows on-column detection. It was concluded that both the material and the frit type affect the separation efficiency significantly and must be taken into account when preparing the column based on the experiment target. For an analysis not demanding on-column detection, the type A frit is recommended. The coupling of packed capillary columns to MS detection requires a capillary tubing connecting the column outlet to the MS inlet. A highlighted work concerning capillary columns is presented by Santos-Neto and coworkers, who used a fully operational system consisting of a capillary column switching restricted-access media-liquid chromatography-electrospray ionization-tandem mass spectrometry system to analyze drugs in biofluids [49]. The use of nano-LC columns coupled with MS has increasing relevance in the field of metabolomics; Chetwynd and David summarized several examples in a recent review [50].

The interface between miniaturized columns and MS is so relevant that several groups (and companies) are making substantial efforts to produce LC chips that replace the conventional columns [51]. Independently of the company that produces, the chip column has as an essential characteristic, its placement very close to the ionization source (and in some cases, it may contain an ESI tip) [52,53]. This approach is used to reduce the post-column band diffusion significantly.

The packing procedure well performed is vital to ensure highly efficient columns. The most used type of column packing procedure is the slurry packing, which consists of a dispersion of the stationary phase in a solvent (the slurry solvent) been flushed through the column. The slurry solvent nature and slurry concentration play an essential role in column packing. The nature of the solvent used affects the distribution of the particles in the slurry. It was found that the most aggregated solution produces the most efficient columns for the packing of 0.03 mm i.d. columns with particles of 1.1 μm d_p [54]. Similar results were found by Wahab and coworkers [16].

Different packing approaches are employed to pack columns using slurry solutions. The simplest, but very effective system, is prepared in a set up very similar to the one employed for packing regular HPLC columns. In this setup, the slurry reservoir is connected directly to an air driven-liquid pump, and the column is connected to the slurry reservoir by using an empty capillary tube (Fig. 4A). Though it is expected to produce pressure pulses during the packing, the columns produced by this system result in efficient columns [49,55]. An alternative set up was proposed for packing capillary columns, avoiding pressure pulses (Fig. 4B). In this setup, the slurry is placed in the chamber and stirred during the application of the high pressure; a microscope can be used to evaluate the packing process [16]. Berg and coworkers used a similar approach in which the chamber is filled with the slurry solution, but nitrogen gas is used to flow the material through the capillary [56].

Dry packing and supercritical fluid packing are also alternatives to pack columns. The dry packing procedure is straightforward; the particles are deposited in the reservoir, and then a gas (usually nitrogen) is flushed through the system resulting in the packed bed [57]. The supercritical fluid packing combines the best of the slurry and dry packing methods, using supercritical CO_2 as a solvent. The setup of supercritical fluid packing is different from dry or slurry packing because the outlet of the column is connected to a vacuum pump [58]. Other possibilities of packing procedures are described and discussed by a practical viewpoint by Lanças and coworkers [17].

Alternatives to packing are also presented in the literature. The pillar array columns (μPAC) are produced by milling pillars on silicon, followed by the functionalization with the stationary phase. The significant advantage of this layout is that the milled pillars result in a high ordinated filling, which allows a more homogenous flow inside the column and a reduction on the multipath diffusion [59,60]. 3D printing has also been investigated as a way to produce ordinated fillings for columns. Although it seems to be promissory, mainly because they use of 3D manufacturing allows the construction of different geometry for the inner part of the column, the instrumental (3D printers) limitations are still the bottleneck for this use [61].

4. Monolithic columns

Monolithic columns consist of a small i.d. tubing, all filled with a robust porous polymer. The polymeric phase consists of pores of different sizes that provide retention and separation selectivity. The porous skeleton of the monolithic columns gives the mobile phase high permeability and low back pressure, which enables the use of high flow rates allowing faster mass transport when compared to particle-filled columns. Therefore, the central positive aspect claimed in favor of monolithic columns is their ability to maintain a proper separation efficiency at high flow rates [62].

The monolithic columns stationary phases are made of polymers that may have inorganic, organic, or hybrid characteristics. Silica monoliths from inorganic stationary phases have a porosity higher than 80%, resembling silica particle packed columns. Thus, the main advantages related to the use of silica monoliths are the high separation efficiency associated with low backpressure. Also, the main disadvantage is the sensitivity to pH variations characteristic of silica-based materials.

A general procedure for producing monolithic columns with silica polymer phase employs the sol-gel approach, consisting in the hydrolysis and polycondensation processes catalyzed by tetraalkoxysilanes acids in the presence of an inert compound that acts as a porogenic agent. Such a reaction results in a continuous silica mesh with a defined pore structure that can be modified according to the reactant concentration, temperature, and polymerization time. It is also possible to perform interventions on the surface of the polymeric phase through washing with solutions containing modifiers, in order to improve selectivity and extend the application of these columns [63].

Due to the high porosity characteristics of silica monoliths, these phases are ideal for the separation of small molecules. Thus, monolithic columns with inorganic stationary phases are generally used in the separation of environmental, forensic, natural products, and pharmaceutical samples, among others [64].

Another aspect that stands out in the use of monolithic columns containing inorganic stationary phases is their high efficiency at flow rates higher than the theoretically expected value, without loss of separation efficiency. This ability to perform quick separations qualifies it to be used for multidimensional LC separations, proving to be an excellent tool for separating complex samples. As an example, Espina-Benitez et al. developed an in-line coupling of a monolithic boronate extracting column with a monolithic silica-based analytical column to analyze uridine, cytidine, adenosine, and guanosine. The monolithic silica analytical column had its activated surface functionalized by thiol-one photo click [65].

In turn, organic monoliths are extensively used due to their qualities, such as easier preparation and stability at high

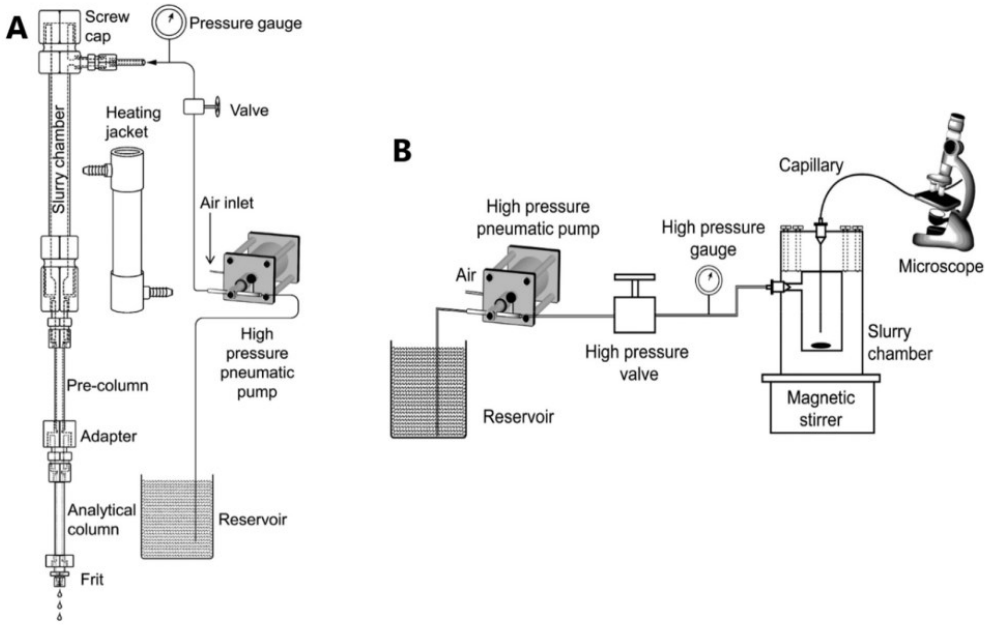

Fig. 4. (A) Scheme of a slurry packing system employed for packing analytical columns (also applicable to capillary columns). (B) Scheme of a high-pressure upward slurry packing system for capillary columns. The microscope can be used for examining the bed as the capillary is being packed (A and B). Reprinted with permission of [16], Copyright 2018, American Chemical Society.

temperatures and pH variations. As a disadvantage, the low mechanical strength stands out.

The general procedure for producing an organic polymeric phase for monolithic columns is to subject a solution containing functional organic monomers, porogenic solvents, and a radical initiator to either heat or a light source to release free radicals which will trigger the monolith formation. The morphology of the formed monolith is a consequence of the reagent concentration, temperature or light intensity, and polymerization time. As in silica monoliths, organic monoliths can be surface modified to increase stationary phase selectivity. It is noteworthy that, besides the mentioned thermal initiation method, there are also other techniques such as polycondensation, emulsion polymerization, and ring-opening metathesis [66].

Organic monoliths have a nonporous granular characteristic interspersed with large pores, as can be observed by scanning electron microscopy (SEM) (Fig. 5) [67]. In this type of monolith, the pores are too miniaturized, making it impossible to separate small molecules. Thus, this stationary phase is ideal for the separation of large molecules, such as proteins and other biomolecules, as the passage pores retain these analytes. However, there are scientific advances aimed at the development of organic monoliths capable of separating small molecules. Initial efforts are focused on pore morphology changes through studies that adapt the polymerization time and reagent concentration. Also, post-polymerization modifications and the addition of nanostructures to the polymer may be performed [68].

Echevarría et al. developed monolithic capillary columns with organic stationary phase coated with tris cellulose (3,5-dimethyl phenyl carbamate) for the separation of several compounds such as β-blockers and pesticides. The synthesis of the stationary phase was done by thermal polymerization of 2-hydroxyethyl

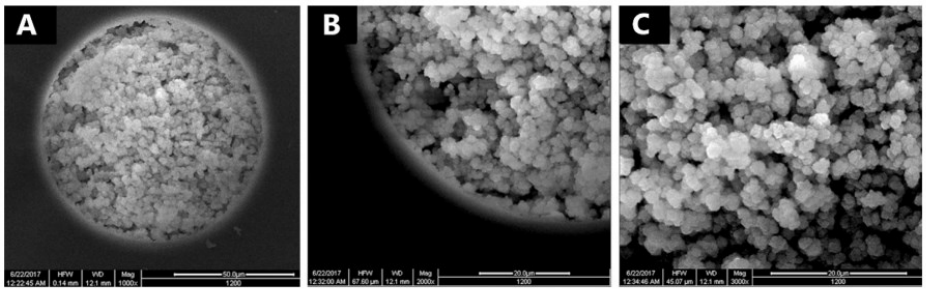

Fig. 5. Representative SEM images of poly(p-MAPHA-co-PETA) monolithic column prepared in a 100 μm i.d. capillary (A: ×1000; B: ×2000; C: ×3000). Reprinted with permission of [67], Copyright 2018, Elsevier.

methacrylate and ethylene glycol dimethacrylate in the presence of a porogenic mixture [69].

Monolithic columns consisting of hybrid stationary phase combine the advantages shown by organic polymer-based and silica-based monolithic columns. As such, they have a high surface area and mesoporous structure, such as the inorganic ones, and stability at a higher temperature and pHs, like organic ones, still retaining the general advantages of monolithic columns that are low flow resistance. Sol-gel or ring-opening methodologies can prepare most such monoliths, which have a wide range of applications depending on the analytes of interest.

Recently, Zhao et al. used a monolithic column consisting of hybrid characteristics aiming at the separation of inorganic arsenic. The thiol functionalized organic-inorganic phase was synthesized using a unique ternary weak basic solvent system by a sol-gel process [70]. Other application examples encompassing inorganic, organic, and hybrid monoliths have been selected and are included at the application table in the following sections.

Monolithic columns, after its laboratory preparation, can be evaluated by physical, chemical, and chromatographic means. The phase characterization is made by physical evaluation through SEM photos and methods able to evaluate the porosity and dimensions of the polymers. In turn, the chemical and chromatographic analyses are obtained through chromatographic runs to evaluate the selectivity and separation power of the produced column.

The use of capillary monolithic columns in LC is growing and is being established as a great alternative to packed columns, as they often have superior results. The main advantages of both organic and silica polymeric stationary phases for monolithic columns are its ease synthesis, rapid analysis, no need for use frits, and a variety of stationary phases that can be available. The existence of mass spectrometry coupled micro/nano-LC systems also represents a gain for miniaturized monolithic columns to analyze samples with small volumes and excellent detection efficiency [62]. Therefore, it is expected that the miniaturized monolithic column in LC will continuously be further explored, and phases will continue to be developed in order to increase the selectivity of analyzing specific compounds.

5. Porous Layer Open Tubular Columns (OT-PLOT)

The technological advances in the miniaturization of LC and the commercial availability of adequate instrumentation made it possible to explore the use of OT analytical columns, allowing its successful coupling to mass spectrometry using nano-electrospray ionization (nano-ESI) or electron ionization (EI) sources.

The use of open tubular columns in LC is theoretically advantageous compared to the use of filled columns. Desmet et al. [11] comparing the kinetic efficiency of OT-PLOT columns with packed columns found that at any retention time, OT analytical columns have at least ten times more theoretical plates, as can be seen in Fig. 6. Other advantages of using OT-PLOT LC over conventional LC columns include the ability to use higher flow rates without significant column pressure increase; column efficiency increase; lower mobile phase and sample consumptions; lower waste generation —all in accordance to the green chemistry principles— and ease of coupling to MS [3].

Among the open tubular columns, PLOT columns present more compatibility with LC at present. The porous nature of the stationary phase enables a larger surface area of contact, which promotes a more significant interaction of the stationary phase with the analytes and, consequently, increases the retention factor making the chromatographic separation more efficient.

It is noteworthy that after production, PLOT columns can be evaluated by physical, chemical, and chromatographic

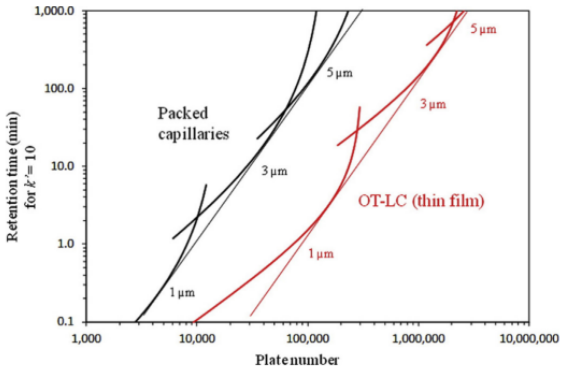

Fig. 6. Kinetic-performance limit curves calculated for packed-bed capillaries and open-tubular capillaries coated with a thin film. For both cases, 1, 3, and 5 µm particles or capillary diameter are considered. The black and red straight lines represent the Knox and Saleem-limit of the packed-bed and OT-LC capillaries, respectively. Reprinted with permission of [11], Copyright 2013, American Chemical Society.

parameters. The physical parameters refer to the stationary phase morphology; SEM is one of the main tools in this type of evaluation, as it provides information on the thickness, uniformity, and adhesion of the stationary phase to the tube wall. Fig. 7 shows three SEM images corresponding to three OT-PLOT columns prepared by Hara et al. having 5 µm i.d. with a thin layer of mesoporous silica [27]. These columns, produced utilizing a sol-gel process, fundamentally differ one from the other in the amount of TMOS utilized. From the SEM figures, it is possible to determinate for each column the layer thickness and the flow-throw diameter, as exemplified in Fig. 7A. It is also noticed in this figure that the layer thickness increased with increasing the amount of TMOS employed [27]. The chemical analysis aims to verify the selectivity of the developed column and is performed by comparing the chromatograms resulting from the separation of analytical standards injected into a regular column with those obtained by an OT-PLOT column. The chromatographic analyses are performed by applying dimensionless or reduced parameters such as impedance (E), reduced plate height (h), flow resistance (ϕ), and reduced linear velocity (υ) (Table 1).

In the last decade, there has been significant progress in the production of OT-PLOT LC columns. However, to date, there is no general protocol that can be used to synthesize the coating phase utilized in such columns, in part due to the vast diversity of stationary phases that can be used. Though, there are three fundamental steps in the fabrication of any OT-PLOT column: (i) a pre-treatment of the inner wall of the tube, followed by (ii) its silanization for use as a support for the porous layer, and (iii) the final polymerization or adsorption of the stationary phase.

The pre-treatment and silanization steps refer to the preparation of the inner wall of the PLOT column support assembly, which generally consists of a fused silica material. These steps are significant because the characteristics of the internal wall of the capillary are the governing factors in the formation of adequate immobilized stationary phases since a secure connection of the stationary phase to the capillary wall is necessary - otherwise, the coating bleeding will occur.

The polymerization or adsorption of the stationary phase into the inner wall is considered as a central topic involving the development of PLOT columns at present. In polymerization, a fused silica capillary is filled with a polymeric mixture, its ends are sealed, and the supply of heat or light causes the polymerization reaction. Such processes are respectively called thermal initiation

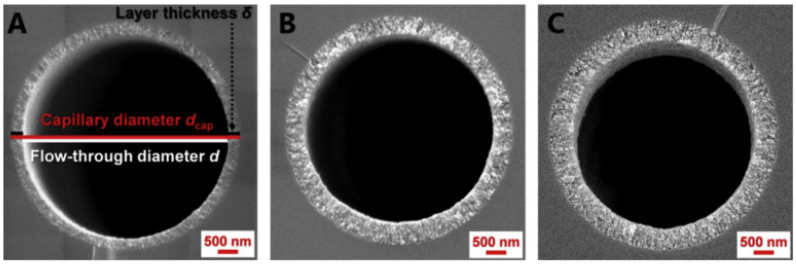

Fig. 7. Scanning electron micrographs of 5 μm i.d. capillary columns produced with (A) 5.0 mL of TMOS, (B) 6.4 mL of TMOS, and (C) 7.2 mL of TMOS, respectively. The measurements were carried out at 10 000-fold magnification, and the scale bars correspond to 500 nm. Reprinted with permission of [27], Copyright 2016, American Chemical Society.

and photoinitiation, and both give rise to stationary phases linked to the capillary wall by covalent bonding.

OT-PLOT LC columns developed using thermal initiation are the most used, after Luo et al. reintroduced the use of OT-PLOT in LC in 2007. They demonstrated the development and application of a stationary phase based on poly (styrene-divinylbenzene) (PS-DVB) in a 10 μm internal diameter column for peptide separation, awakening the interest of other researchers [71]. More recently, Knob et al. used thermal initiation on small diameter columns to make OT-PLOT analytical columns and suggested that the polymeric stationary phase morphology is significantly impacted by internal diameters lower than 10 μm [72].

The stationary phase can also be adhered to the capillary wall by adsorptive processes. In these cases, they are termed as physically adsorbed stationary phases, being connected, like layers, to the capillary wall through electrostatic and hydrophobic interactions. Just a single layer can be adsorbed, forming a monolayer, or several overlapping layers can be built, called the "layer by layer" (LbL) approach. The application of several overlapping layers against the monolayer has the advantages of increased durability, stability, and loadability.

Kubáň et al. have developed a column containing as a stationary phase a multilayer structure of methylamine (MA) and 1,4-butanedioldiglycidyl ether (BDDE) copolymer (MA-BDDE) demonstrating its usability by separating inorganic anions [73]. Another example was the work reported by Wang et al. in which the researchers describe the development of a stationary phase based on hydroxypropyl cellulose (HPC) monolayer in an OT-PLOT column employed to separate proteins [74].

Depending on the nature of the polymerization reagents, the stationary phase formed in PLOT columns may be organic or inorganic. Similar to monolithic columns, PLOT columns made up of organic polymers are the most used in miniaturized LC. This fact might be explained by considering that this type of stationary phase was the first to be developed, and therefore was the most reproduced, to date. The main advantages related to the use of these phases are the synthesis simplicity, control of material porosity, stability against extreme pH conditions, high thermal stability, and the possibility of making modifications to its surface with several active groups. As a disadvantage, the low mechanical strength stands out. In turn, the stationary phases of most inorganic polymers are formed by silica-based polymers. This type of stationary phase has a higher surface area and mechanical resistance than must organic polymer phases. However, they are more sensitive to sudden pH variations [3].

There are also "less conventional" stationary phases that envision the incorporation of new materials capable of providing higher selectivity. The primary new materials used for the preparation of OT-PLOT LC columns are based on different metal oxides, ion exchange materials, molecularly imprinted polymers, and hybrid materials, which contain both organic and inorganic characters [3].

Peng et al. developed a new zwitterionic stationary phase (ZIC) by thermal initiation for HILIC separations [75]. Also, Aydoğan developed a stationary phase based on β-cyclodextrin (β-CD) reporting enantioseparation with high theoretical plate numbers - up to 26 000 plates/m [76].

In short, the use of OT-PLOT analytical columns in LC has not yet reached its climax. However, it has shown great potential and is increasingly being the focus of the interest of different research groups. There is a wide variety of new stationary phases preparation techniques under development. Also, the natural compatibility for coupling these miniaturized columns with MS evidences the full potential of OT-PLOT-LC-MS.

6. Wall Coated Open Tubular Columns (WCOT)

Another type of open tubular column is termed as "wall coated open tubular" (WCOT). These columns have as a stationary phase a non-porous thin film adhered to the interior of the tube, which is often made of fused silica. This coating is obtained after extensive treatments of the tubing interior surface, enabling the immobilization of the film on the column wall through cross-linking processes [77–79].

Nowadays, WCOT columns with capillary dimensions are consolidated in gas chromatography and have many advantages over packed columns such as high durability, superior performance, more inertness, ease of use, and from the theoretical perspective, the highest chromatographic potential [80].

However, for miniaturized LC, there are few reports in the literature employing OT columns [81–83]. One of the main reasons would be the fact that these columns present low sample capacity because of their low surface area of contact, reducing the interaction of the analyte with the stationary phase. As a consequence, it is more instrument demanding than all other forms of miniaturized LC [84].

Although this type of column has promoted highly efficient separations in GC, it has still been little exploited in miniaturized LC. WCOT columns were first successfully used in LC by Hibi et al. [8] in 1978, when the authors were promoted highly efficient separations of polynuclear aromatic hydrocarbons (PAHs) using 15 cm long and 0.5 mm i.d. polytetrafluoroethylene (PTFE), introducing the term "micro-LC".

The preparation of WCOT-LC columns is meticulous and requires great care to obtain a uniform stationary phase that tightly adheres to the column tube wall. The initial step in preparing a WCOT column consists of leaching the fused silica capillary. This process consists in preparing the capillary wall to receive the phase of interest. Leaching can be done in an acidic or basic medium, and its

efficiency depends on the solution concentration, temperature, and treatment time. In the second stage, the tube is dehydrated by heating it in an oven while passing through its interior a gentle and controlled flow of nitrogen [85,86].

Following the silica tube treatment procedures described above, the treated tubes are usually subjected to a further persilylation step using a compound capable of producing the appropriate "wettability" for the subsequent coating, which will result in the formation of a thin film inside of the tube. For the persilylation process, a silica capillary tubing is filled with a proper silanizing solution, its ends are closed, and the capillary is placed into an oven. The most used silanizing agents are hexamethyldisilazane (HMDS), tetraphenyldimethyldisilazane (TPDMDS), and diphenyltetramethyldisilazano (DPTMDS).

After the persilylation process, the capillary is covered with the stationary phase of interest. The most employed WCOT stationary phases used so far to produce WCOT-LC columns follow the same trends used for GC, with polydimethylsiloxane (PDMS) and its various modifications being the most used liquid polymer evaluated to date. By inserting distinct functional groups into the pendant siloxane groups, it is possible to obtain a variety of new stationary phases (modified polysiloxanes). The most frequently inserted functional groups are phenyl and cyano. In addition to PDMS, other stationary phases have been investigated, including GeO_2-PDMS, 3-mercaptopropyltrimethoxylanosilica, polypyrrole, TiO_2-PDMS, and β-CD [87,88]. Besides, the sol-gel process, as well as alternative procedures, may render different stationary phases for the coating process.

The interior wall of the tube can be covered with the stationary phase in two different ways: static coating or dynamic coating. In the dynamic process, the stationary phase solution containing the stationary phase is pushed with the aid of gas through the capillary tube, forming a thin film on the tube wall. Although it is an easy and straightforward technique, it results in a smaller phase ratio. In the static coating, the tube is kept at a high temperature so that the phase solution solvent evaporates, and steam is displaced out of the column with the aid of vacuum exerted at one end of the column [85].

The static coating procedure has gained prominence and is the most used coating type, allowing the use of higher molar mass phases. Moreover, with this methodology, it is possible to more accurately predict the thickness of the stationary phase film by varying the concentration of the polymer in solution.

After the coating process, a cross-linking step is performed to immobilize the stationary phase on the tubing wall, preventing its detachment during the chromatographic run. The cross-linking process is usually done by using compounds such as azo-tert-butane (ATB) or azo-tert-octane (ATO), among others.

Fig. 8 shows a schematic drawing representing the capillary filling system with the solutions of interest (Fig. 8A), coating tube set up (Fig. 8B), and the static coating resulting process inside the tube of a capillary column (Fig. 8C).

Table 2 shows the characteristics of some commercially available stationary phases derived from polydimethylsiloxane, which are the most used materials to prepare WCOT columns to date.

After the WCOT LC column is prepared, some chromatographic parameters should be evaluated to verify the performance and quality of the developed columns. Generally, aromatic polycyclic hydrocarbons, such as naphthalene, phenanthrene, anthracene, and pyrene, as well as alkylbenzenes, such as toluene, ethylbenzene, propylbenzene, butyl benzene, and pentyl benzene, are the most commonly used analytical standards to evaluate these columns [16,89–91].

Despite showing several advantages, these columns still have been little explored in LC, primarily due to some instrumental

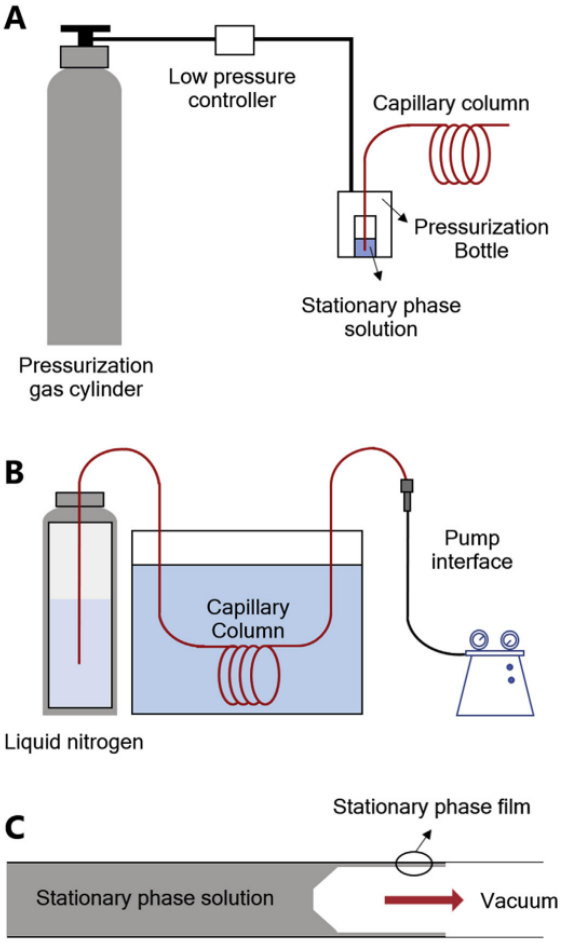

Fig. 8. Main steps required for the preparation of WCOT-LC columns (A) capillary filling system, (B) coating tube set up, and (C) the resulting static coating process.

limitations as a function of their reduced sample capacity, requiring the use of particular sample inlet systems and detectors with reduced cell volumes. Besides that, the preparation of the right WCOT column still involves several steps that are not yet completely understood and should be further studied and evaluated before this miniaturized LC mode can become more popular.

The use of WCOT columns in LC is still a poorly explored area to obtain high-performance nanocolumns for the analysis of complex matrices. Few studies have been performed, most of them dedicated exclusively to the analysis of macromolecules as proteins (omic sciences).

At the same time, no significant steps have been recently pursued to investigate the potentiality of small molecules analysis using WCOT LC columns, which makes this area of research very attractive from the scientific point of view. Moreover, with the recent advances achieved in the miniaturization of LC instrumentation, along with their unique and inherent characteristics, WCOT columns became an exciting alternative for mass spectrometric coupling (using either nano-ESI or EI) and high-efficiency analysis of small quantities of samples. Besides that, it is a trend that these

Table 2
Chemical composition, USP specification and commercial code of some polydimethylsiloxane derived commercial stationary phases used to prepare WCOT-LC columns.

Composition	USP code	Manufacturer code
50% Phenyl - 50% Dimethyl polysiloxane	G3	OV-17
5% Phenyl - 95% Dimethyl polysiloxane	G27	OV-5
35% Phenyl - 65% Dimethyl vinylsiloxane	G42	OV-1701
6% Cyanopropyl phenyl - 94% Dimethyl polysiloxane	G43	OV-1301
14% Cyanopropyl phenyl - 86% Methyl polysiloxane	G46	OV-35

columns will be in the future the most used ones in both liquid and gas chromatography [7,92].

7. Recent applications of miniaturized LC

Miniaturized LC applications are present in the pharmaceutical, food, forensic, environmental, and proteomic areas [13,93,94]. Proteomic applications are the most studied area, taking advantage of the low sample availability, and the small amount needed to be analyzed by miniaturized LC. Currently, MS has become the preferred detector used for the analysis of complex samples due to its selectivity, matrix effect reduction, and enhanced signal detection [94].

Recent reviews introduce a vast and comprehensive sum up of several miniaturized LC applications. Lynch et al. [93] and Blue et al. [95] reported some general applications of various types of columns in miniaturized LC and capillary UHPLC systems. Regarding filled columns, Tofolli et al. [2] present some applications using particle packed columns, and Aydoğan and co-workers [68] reviewed organic polymer monolithic capillary columns materials

Table 3
Recent applications involving capillary-LC and nano-LC separated by column type (2015–2019).

Column type	i.d. (μm)	Length (cm)	Flow rate (μL/min)	Stationary phase or coated material	LC mode-detector	Application	Ref.
Particle packed	500	25	20	Fully porous C18 particles, 4 μm, 90 Å	Cap-LC-MS	Antidepressants in human blood	[105]
	150	10	2.55	C18 particles, 1.8 μm	Cap-LC- MS/MS	Tienilic acid and other metabolites in rat urine	[106]
	75	25	0.15	C18 particles, 3 μm	Nano-LC-EI-MS	Free fatty acid in mussel	[107]
	75	25	10	C18 particles, 2.2 μm, 100 Å	Nano-LC-MS/MS	Bioactive peptides of soybean seeds and milk proteins	[108]
	75	15	0.20	C18 particles, 3 μm, 100 Å	Nano-LC-MS/MS	Veterinary drugs in food (honey, egg, milk and beef muscle)	[109]
	75	15	0.20	C18 particles, 3 μm	Nano-LC-MS/MS	Pesticides in virgin olive oil	[110]
	75	15	0.30	C18 particles, 2 μm, 100 Å	Nano-LC-MS/MS	Peptide biomarkers of Anisakids (a fish-borne parasite)	[111]
	75	10.1	0.3	C18 particles, 3 μm	Nano-LC-MS/MS	Phenolic compounds in cranberry syrups	[112]
	50	15–30	0.130	Core-shell C18 particles, 2.6 μm, 80 Å	Nano-LC-MS/MS	Peptides biomarkers of CYP27A1 enzyme in CTCs	[56]
	50	4.5	0.3	C18 particles, 5 μm	Cap-LC-MS/MS	Neuropeptides in rat brain (*in-vivo* microdialysis samples)	[97]
Monolithic	100	37	0.1–4.0	Octakis (3-mercaptopropyl) octasilsesquioxane polyacrylate hybrid monolith	Cap-LC-MS/MS	Phenolic compounds, anilines, antibiotics and peptides from BSA tryptic digestion	[113]
	100	27	0.200	Mesoporous carbon nanomaterial-based butyl-silica hybrid monolith	Cap-LC-MS/MS	Alkylbenzenes, proteins and peptides from BSA tryptic digestion	[98]
	75	33.6	0.270	Hybrid monolith of 1,3-diethynyltetramethyl-disiloxane (DYDS) and 2SH, 3SH and 4SH thiol monomers	Cap-LC-MS/MS	Phenols, alkylbenzenes, and peptides from BSA tryptic digestion	[114]
	75	30	1.0	Hydrophilic organic-silica hybrid monolith (HILIC) modified with thiols	Cap-LC-MS/MS	Methylated ribonucleosides (m6A and 5-mC) in RNA from human blood	[115]
	75	10	0.800	Multiwalled carbon nanotubes (MWCNT) incorporated in 3-chloro-2-hydroxypropyl methacrylate (HPMACl) monolith	Nano-LC-MS/MS	Antibiotics and pesticides in honey and milk	[116]
	250	20	23	Poly (glycidyl methacrylate-co-ethylene dimethacrylate) monolith	Nano-LC-UV	Pharmaceutical drugs in commercial preparations	[117]
	150	15	0.3	Hydrophilic organic hybrid monolith (HILIC) carboxyethyl acrylate and polyethylene glycol dimethacrylate based	Nano-LC-UV	Nitrogenous bases, amides and acrylamides	[118]
	100	30	0.358	Polyhedral oligomeric silsesquioxane methacryl (POSS-MA) modified amino acid (Cys) and ionic liquid hybrid monolith	Nano-LC-UV	Alkylbenzenes, amides, glycoproteins, and TARG1 protein.	[119]
	100	15	0.5	Alkyl and polyfluoroalkyl organo-silica monolithic	Cap-LC-UV	Alkylbenzenes, phenols, and planar aromatic compounds	[120]

(*continued on next page*)

Table 3 (*continued*)

Column type	i.d. (μm)	Length (cm)	Flow rate (μL/min)	Stationary phase or coated material	LC mode-detector	Application	Ref.
Open tubular	100	500	1.7–16.7	Aptamer immobilized in biotin-avidin system gold modified OT column	Nano-LC-MS/MS	Capturing and analysis of target CTCs	[101]
	10	300	0.01	ODS coated	Nano-LC-MS	Lipids and OHCs in exosomes, peptides of AXIN1 protein in mouse embryonic stem cells, and intact proteins USP-1 standard	[102]
	25	1120	0.16–0.20	Metal-organic frameworks (NH_2-UiO-66 nanoparticles) bonded to the brushes of chain polymer poly(glycidylmethacrylate)	Cap-LC-UV	Alkylbenzenes, phenols, anilines, and flavonoids from licorice	[121]
	2	2.7	12–320 (before split)	ODS coated	Cap-LC-LIF	Trypsin digested cytochrome C and peptides	[103]
	2	27–155	$\upsilon = 79$ mm/s	ODS coated	Cap-LC-LIF	Pepsin/trypsin digested *E. coli* lysates	[104]

SA, Bovine serum albumin; Cap-LC, capillary-LC; CTCs, circulating tumor cells; Cys, L-cysteine; LIF, Laser-induced fluorescence detector; m6A, N6-methyladenosine; ODS, Octadecylsilane; OHCs, hydroxycholesterols; USP-1, universal protein standard; υ, linear velocity of the mobile phase; 2SH, 1,6-hexanedithiol; 3SH, trimethylolpropanetris (3-mercaptopropionate); 4SH, pentaerythriol tetrakis (3-mercaptopropionate); 5-mC, 5-methylcytosine.

applied in foods analysis and their coupling with MS detectors. Lam et al. [3] covered the progress and applications of OT-LC capillary columns from 2007 to 2018. Ahmed et al. [83] recently published a review focused on OT columns reported from 2014 to 2018, according to the capillary i.d. and coating thickness (CID/CT) ratio and developments in new stationary phases. Li et al. [23] focused on applications employing narrow inner diameter capillaries (≤25 μm). In specific reviews, for instance, Yi and co-workers [94], summarized the recent advances in micro and nanoscale separations and their application in proteomic analysis. Fanali [96] reviewed enantiomeric separations in nano-LC employing chiral selectors as cyclodextrins, polysaccharides, and glycopeptide antibiotics, mainly bonded or supported on silica-based particles and monolith phases.

Table 3 highlights some of the most recent applications of different capillary column types, principally coupled to MS detectors, from 2015 to 2019. These applications were not discussed in the reviews above cited.

Wilson et al. [97] described an on-line capillary-LC-MS/MS to collect, label, and analyze two neuropeptides, leu-enkephalin e met-enkephalin, in rat brain *in-vivo* microdialysis. The authors used a two-column approach, employing a home-packed fused-silica capillary column containing 3 μm C18 particles (75 μm i.d. x 20 mm) as a precolumn and an analytical column of 5 μm C18 particles (50 μm i.d. x 45 mm). The use of a pre-column (where on-column demethylation of the neuropeptides and their preconcentration is carried out) and its online coupling to the analytical column brought perceived advantages over conventional methods. These include the reduction of the labeling reagents volume and labeling time, which means lower cost and greater closeness with real-time measurements. The use of a 2D capillary approach improves the columns' lifetime, the reproducibility, and the linearity of the method. Additionally, the method minimized potential losses due to sample handling and enabled the analysis of *in-vivo* small samples and the quantification of the neuropeptides at low concentration levels.

The utilization of nanomaterials to prepare hybrid monoliths is another exciting approach recently reported. The physicochemical properties of nanocarbon based materials such as their large surface area, hydrophobicity, high sorption capacities, and ease functionalization make these an excellent sorbent material recently explored. Liu et al. [98] prepared via cross-linking a capillary column containing a hybrid organic monolith-mesoporous carbon material suitable for the separation of small and large molecules (alkylbenzenes, amines, peptides, and proteins). The inclusion of the nanocarbon material in the monolithic structure was advantageous over the monolith absence, including improvements in the separation efficiency, monolith morphology and pore changes, high stability, and reproducible analyses.

Circulating tumor cells (CTCs) are cancer cells released and circulated in the blood that can migrate to other tissues promoting metastasis or the growth of other cancer cells [99]. The isolation and analysis of these CTCs is a challenge since they are mixed with blood cells [100]. Liu et al. [101] immobilized aptamers into an OT capillary column of 100 μm i.d. using gold particles bound to streptavidin to anchor biotin modified aptamer, which is capable of capturing CTCs. The stability and specificity of the aptamer allowed to capture and identify SMMC-7721 human hepatoma cells with a 50–70% of efficiency and enrichment factor of 3.0, value high compared to interfering cells, showing a preference immobilization of the target cells.

Another significant advance on OT columns involves studies utilizing extremely narrow i.d. (<10 μm) capillaries. Vehus et al. [102], for instance, proposed the use of a monolithic trap column and a 10 μm OT column coupled to an LC-Orbitrap MS aiming to enhance the sensitivity, separation efficiency, and repeatability in the analysis from small molecules to proteins. This design increased the sample loadability and the possibility to be applied in simple and complex mixture samples, obtaining separations and sensitivity with approximately 100 times improvement compared to the conventional nano-LC-MS systems. Recently, Xiang et al. [103,104] reported the preparation of 2 μm i.d. OT columns and their application to the analysis of small molecules and peptides. This new approach, using extremely narrow open tubular (NOT) columns, on-column detection, and without requiring ultrahigh elution pressures, allowed the authors to achieve low detection limits (in the range of attomoles) requiring small sample volumes, in the order of picoliters. Also, it showed ultrahigh efficiency separations of amino acids in milliseconds, and ultrahigh-resolution in the analysis of pepsin/trypsin digested *E. coli* lysates with a high peak capacity of 2000 in just 160 min.

8. Concluding remarks

The miniaturization of liquid chromatography is one of the current trends in modern analytical chemistry and has been significantly highlighted in recent years. Capillary and nano liquid chromatography have attracted attention from various fields of analysis due to its high application potential. This technique offers several advantages over conventional diameter LC systems such as the reduction of samples and solvents consumption, increased chromatographic efficiency, use of temperature programming (not

described in this report), miniaturized systems for "in-field" analysis, among others. Even presenting several advantages, the technique may not yet have proved to be as efficient and robust as conventional LC because the equipment is more susceptible than conventional HPLC to external conditions such as temperature oscillation, bubbles in the mobile phase, and mechanical vibration.

Moreover, this area requires the miniaturization of the whole chromatographic instrumentation, including columns, pumps, sample introduction, detectors, fittings, among others —an essential point to be improved for the growth of LC miniaturization— highlighting the decrease in the physical dimensions and columns' particle diameter and stationary phase thickness. Developments and improvement have been significantly growing with packed, monolithic, and open tubular (PLOT and WCOT) columns being utilized in several areas, including omics science, food chemistry, medicine, bioanalytical chemistry, and even analyzing small molecules that is a promising trend in miniaturized LC. Packed capillary columns are by far the most popular mode of miniaturized columns. These columns are commercially available from several companies and present excellent performance, reproducibility, and easy to transfer methods from HPLC, U-HPLC, and other variations as superficially porous columns. Monolithic capillary columns are still commercially scarce, and not yet as available as packed ones. Although being the most popular column type in GC, open tubular columns (WCOT and PLOT) did not yet reach the interest of large companies; these columns are not commercially available for LC. This fact occurs even considering that all theories on miniaturized column efficiency demonstrate that OT columns are much superior to the equivalent filled columns. Even so, a large number of research groups worldwide dedicate considerable efforts to prepare their OT-LC columns, aiming to improve their robustness, efficiency, and showing their superior performance, before they become commercially available. Since the initial development of miniaturized LC up to present, detectors have been much improved to achieve higher analytical sensitivity. Mass spectrometric-based detectors are now the most effective, selective, sensitive, and promising coupling candidate for miniaturized LC systems, for both quantitative and qualitative analysis. Nowadays, MS miniaturization is also being reported with particular emphasis on specific ionization and desorption interfaces including nano and low flow ESI, ambient pressure ionization sources (DART, DESI and others), and, more recently, the successful adaptation of the traditional GC-MS electron ionization (EI) source to miniaturized LC-EI-MS.

Overall, it can be concluded and projected that significant advances are still necessary to strengthen and improve the LC miniaturization, particularly in the niche of open tubular LC-MS. This work highlighted the current and future trends and perspectives of miniaturized LC columns. Besides that, recent capillary-LC and nano-LC applications were selected, presented, and discussed, emphasizing their coupling to mass spectrometry.

CRediT authorship contribution statement

Karen Mejía-Carmona: Writing - original draft, Writing - review & editing. **Juliana Soares da Silva Burato:** Writing - original draft, Writing - review & editing. **João Victor Basolli Borsatto:** Writing - original draft, Writing - review & editing. **Ana Lúcia de Toffoli:** Writing - original draft, Writing - review & editing. **Fernando Mauro Lanças:** Conceptualization, Writing - review & editing, Funding acquisition.

Acknowledgments

This research project was financed in part by the Coordenação de Aperfeiçoamento de Pessoal de Nível Superior - Brasil (CAPES) - Finance Code 001. The authors are grateful to FAPESP (Grants 2017/02147-0, 2015/15462-5, and 2014/07347-9) and CNPq (307293/2014-9) for the financial support provided.

References

[1] C. Eduardo, D. Nazario, B.H. Fumes, M. Ribeiro, F.M. Lanças, Chapter 13 - Miniaturized Column Liquid Chromatography, Elsevier Inc., 2018. https://doi.org/10.1016/B978-0-12-812792-6/00013-3.
[2] A.L. de Tofolli, E.V.S. Maciel, C.E.D. Nazario, F.M. Lanças, Liquid Chromatography, Packed Capillary, in: P. Worsfold (Editor), Encycl. Anal. Sci., third ed, Elsevier, NY, 2019, pp. 182–191.
[3] S.C. Lam, E. Sanz Rodriguez, P.R. Haddad, B. Paull, Recent advances in open tubular capillary liquid chromatography, Analyst 144 (2019) 3464–3482. https://doi.org/10.1039/c9an00329k.
[4] J. Šesták, D. Moravcová, V. Kahle, Instrument platforms for nano liquid chromatography, J. Chromatogr., A 1421 (2015) 2–17. https://doi.org/10.1016/j.chroma.2015.07.090.
[5] C.G. Horvath, B.A. Preiss, S.R. Lipsky, Fast liquid chromatography: an investigation of operating parameters and the separation of nucleotides on pellicular ion exchangers, Anal. Chem. 39 (1967) 1422–1428. https://doi.org/10.1021/ac60256a003.
[6] T. Tsuda, M. Novotny, Band-broadening phenomena in microcapillary tubes under the conditions of liquid chromatography, Anal. Chem. 50 (1978) 632–634. https://doi.org/10.1021/ac50026a023.
[7] T. Tsuda, M. Novotny, Packed microcapillary columns in high performance liquid chromatography, Anal. Chem. 50 (1978) 271–275. https://doi.org/10.1021/ac50024a026.
[8] K. Hibi, D. Ishii, I. Fujishima, T. Takeuchi, T. Nakanishi, Studies of open tubular micro capillary liquid chromatography. 1. The development of open tubular micro capillary liquid chromatography, J. High Resolut. Chromatogr. 1 (1978) 21–27. https://doi.org/10.1002/jhrc.1240010106.
[9] D. Isshi, K. Asai, K. Hibi, T. Jonokuchi, M. Nagaya, A study of micro-high-performance liquid chromatography, J. Chromatogr. 144 (1977) 157–168.
[10] M.V. Novotny, Development of capillary liquid chromatography: a personal perspective, J. Chromatogr., A 1523 (2017) 3–16. https://doi.org/10.1016/j.chroma.2017.06.042.
[11] G. Desmet, S. Eeltink, Fundamentals for LC miniaturization, Anal. Chem. 85 (2013) 543–556. https://doi.org/10.1021/ac303317c.
[12] C.E.D. Nazario, M.R. Silva, M.S. Franco, F.M. Lanças, Evolution in miniaturized column liquid chromatography instrumentation and applications: an overview, J. Chromatogr., A 1421 (2015) 18–37. https://doi.org/10.1016/j.chroma.2015.08.051.
[13] C. Fanali, L. Dugo, P. Dugo, L. Mondello, Capillary-liquid chromatography (CLC) and nano-LC in food analysis, TrAC - Trends Anal. Chem. 52 (2013) 226–238. https://doi.org/10.1016/j.trac.2013.05.021.
[14] N. Tanaka, D.V. McCalley, Core-shell, ultrasmall particles, monoliths, and other support materials in high-performance liquid chromatography, Anal. Chem. 88 (2016) 279–298. https://doi.org/10.1021/acs.analchem.5b04093.
[15] J.W. Jorgenson, Capillary liquid chromatography at ultrahigh pressures, Annu. Rev. Anal. Chem. 3 (2010) 129–150. https://doi.org/10.1146/annurev.anchem.1.031207.113014.
[16] M.F. Wahab, D.C. Patel, R.M. Wimalasinghe, D.W. Armstrong, Fundamental and practical insights on the packing of modern high-efficiency analytical and capillary columns, Anal. Chem. 89 (2017) 8177–8191. https://doi.org/10.1021/acs.analchem.7b00931.
[17] F.M. Lanças, J.C. Rodrigues, S.S. de Freitas, Preparation and use of packed capillary columns in chromatographic and related techniques, J. Sep. Sci. 27 (2004) 1475–1482. https://doi.org/10.1002/jssc.200401853.
[18] F. Svec, Y. Lv, Advances and recent trends in the field of monolithic columns for chromatography, Anal. Chem. 87 (2015) 250–273. https://doi.org/10.1021/ac504059c.
[19] L.S. Ettre, M.J.E Golay and the invention of open-tubular (capillary) columns, J. High Resolut. Chromatogr. Chromatogr. Commun. 10 (1987) 221–230.
[20] T. Tsuda, K. Hibi, T. Nakanishi, T. Takeuchi, D. Ishii, Studies of open-tubular micro-capillary liquid chromatography. II. Chemically bonded octadecylsilane stationary phase, J. Chromatogr. 158 (1978) 227–232. https://doi.org/10.1016/S0021-9673(00)89969-0.
[21] T.J. Causon, R.A. Shellie, E.F. Hilder, G. Desmet, S. Eeltink, Kinetic optimisation of open-tubular liquid-chromatography capillaries coated with thick porous layers for increased loadability, J. Chromatogr., A 1218 (2011) 8388–8393. https://doi.org/10.1016/j.chroma.2011.09.047.
[22] E. Guihen, J.D. Glennon, Recent highlights in stationary phase design for open-tubular capillary electrochromatography, J. Chromatogr., A 1044 (2004) 67–81. https://doi.org/10.1016/j.chroma.2004.05.107.
[23] R.-N.N. Li, Y.-N.N. Wang, M.-H.H. Peng, X.-Y.Y. Wang, G.-S.S. Guo, Preparation and application of porous layer open tubular capillary columns with narrow bore in liquid chromatography, Chin. J. Anal. Chem. 45 (2017) 1865–1873. https://doi.org/10.1016/S1872-2040(17)61057-0.
[24] D.A. Collins, E.P. Nesterenko, B. Paull, Porous layer open tubular columns in capillary liquid chromatography, Analyst 139 (2014) 1292–1302. https://doi.org/10.1039/c3an01869e.

[25] S. Forster, H. Kolmar, S. Altmaier, Synthesis and characterization of new generation open tubular silica capillaries for liquid chromatography, J. Chromatogr., A 1265 (2012) 88–94. https://doi.org/10.1016/j.chroma.2012.09.054.

[26] S. Forster, H. Kolmar, S. Altmaier, Preparation and kinetic performance assessment of thick film 10-20 µm open tubular silica capillaries in normal phase high pressure liquid chromatography, J. Chromatogr., A 1315 (2013) 127–134. https://doi.org/10.1016/j.chroma.2013.09.059.

[27] T. Hara, S. Futagami, S. Eeltink, W. De Malsche, G.V. Baron, G. Desmet, Very high efficiency porous silica layer open-tubular capillary columns produced via in-column sol-gel processing, Anal. Chem. 88 (2016) 10158–10166. https://doi.org/10.1021/acs.analchem.6b02713.

[28] J.J. van Deemter, F.J. Zuiderweg, A. Klinkenberg, Longitudinal diffusion and resistance to mass transfer as causes of nonideality in chromatography, Chem. Eng. Sci. 5 (1956) 271–289. https://doi.org/10.1016/0009-2509(56)80003-1.

[29] J.C. Giddings, Reduced plate height equation: a common link between chromatographic methods, J. Chromatogr., A 13 (1964) 301–304.

[30] J.H. Knox, J.F. Parcher, Effect of column to particle diameter ratio on the dispersion of unsorbed solutes in chromatography, Anal. Chem. 41 (1969) 1599–1606. https://doi.org/10.1021/ac60281a009.

[31] J.C. Gildings, Comparison of theoretical limit of separating speed in gas and liquid chromatography, Anal. Chem. 37 (1965) 60–63. https://doi.org/10.1021/ac60220a012.

[32] H. Poppe, Some reflections on speed and efficiency of modern chromatographic methods, J. Chromatogr. A (1997) 3–21. https://doi.org/10.1016/S0021-9673(97)00376-2.

[33] G. Desmet, D. Clicq, P. Gzil, Geometry-independent plate height representation methods for the direct comparison of the kinetic performance of LC supports with a different size or morphology, Anal. Chem. 77 (2005) 4058–4070. https://doi.org/10.1021/ac050160z.

[34] J. Billen, G. Desmet, Understanding and design of existing and future chromatographic support formats, J. Chromatogr., A 1168 (2007) 73–99. https://doi.org/10.1016/j.chroma.2007.07.069.

[35] G. Desmet, D. Cabooter, K. Broeckhoven, Graphical data representation methods to assess the quality of LC columns, Anal. Chem. 87 (2015) 8593–8602. https://doi.org/10.1021/ac504473p.

[36] T. Hetzel, D. Loeker, T. Teutenberg, T.C. Schmidt, Characterization of the efficiency of microbore liquid chromatography columns by van Deemter and kinetic plot analysis, J. Sep. Sci. 39 (2016) 3889–3897. https://doi.org/10.1002/jssc.201600775.

[37] T. Hetzel, C. Blaesing, M. Jaeger, T. Teutenberg, T.C. Schmidt, Characterization of peak capacity of microbore liquid chromatography columns using gradient kinetic plots, J. Chromatogr., A 1485 (2017) 62–69. https://doi.org/10.1016/j.chroma.2017.01.018.

[38] K. Broeckhoven, D. Cabooter, F. Lynen, P. Sandra, G. Desmet, The kinetic plot method applied to gradient chromatography: theoretical framework and experimental validation, J. Chromatogr., A 1217 (2010) 2787–2795. https://doi.org/10.1016/j.chroma.2010.02.023.

[39] S. Bruns, T. Müllner, M. Kollmann, J. Schachtner, A. Höltzel, U. Tallarek, Confocal laser scanning microscopy method for quantitative characterization of silica monolith morphology, Anal. Chem. (2010) 6569–6575. https://doi.org/10.1021/ac100909t.

[40] S. Bruns, U. Tallarek, Physical reconstruction of packed beds and their morphological analysis: core-shell packings as an example, J. Chromatogr., A 1218 (2011) 1849–1860. https://doi.org/10.1016/j.chroma.2011.02.013.

[41] S. Bruns, J.P. Grinias, L.E. Blue, J.W. Jorgenson, U. Tallarek, Morphology and separation efficiency of low-aspect-ratio capillary ultrahigh pressure liquid chromatography columns, Anal. Chem. 84 (2012) 4496–4503. https://doi.org/10.1021/ac300326k.

[42] F. Gritti, A stochastic view on column efficiency, J. Chromatogr., A 1540 (2018) 55–67. https://doi.org/10.1016/j.chroma.2018.02.005.

[43] D.T.-T. Nguyen, D. Guillarme, S. Rudaz, J.L. Veuthey, Fast analysis in liquid chromatography using small particle size and high pressure, J. Sep. Sci. 29 (2006) 1836–1848. https://doi.org/10.1002/jssc.200600189.

[44] T.R. Covey, B.A. Thomson, B.B. Schneider, Atmospheric pressure ion sources, Mass Spectrom. Rev. 28 (2009) 870–897. https://doi.org/10.1002/mas.20246.

[45] F. Rigano, P.Q. Tranchida, P. Dugo, L. Mondello, High-performance liquid chromatography combined with electron ionization mass spectrometry: a review, TrAC - Trends Anal. Chem. 118 (2019) 112–122. https://doi.org/10.1016/j.trac.2019.05.032.

[46] R.E. Majors, Developments in HPLC column packing design, LCGC N. Am. 24 (2006) 8–15.

[47] R.E. Majors, Sub-2- µm porous particles — where do we go from Here ? LCGC N. Am. 23 (2005) 1248–1255.

[48] M. Franc, J. Sobotníková, P. Coufal, Z. Bosáková, Comparison of different types of outlet frits in slurry-packed capillary columns, J. Sep. Sci. 37 (2014) 2278–2283. https://doi.org/10.1002/jssc.201400434.

[49] A.J. Santos-Neto, K.E. Markides, P.J.R. Sjöberg, J. Bergquist, F.M. Lancas, Capillary column switching restricted-access media-liquid chromatography-electrospray ionization-tandem mass spectrometry system for simultaneous and direct analysis of drugs in biofluids, Anal. Chem. 79 (2007) 6359–6367. https://doi.org/10.1021/ac070671g.

[50] A.J. Chetwynd, A. David, A review of nanoscale LC-ESI for metabolomics and its potential to enhance the metabolome coverage, Talanta 182 (2018) 380–390. https://doi.org/10.1016/j.talanta.2018.01.084.

[51] J.P. Grinias, R.T. Kennedy, Advances in and prospects of microchip liquid chromatography, TrAC - Trends Anal. Chem. 81 (2016) 110–117. https://doi.org/10.1016/j.trac.2015.08.002.

[52] A. Celma, J.V. Sancho, N. Salgueiro-González, S. Castiglioni, E. Zuccato, F. Hernández, L. Bijlsma, Simultaneous determination of new psychoactive substances and illicit drugs in sewage: potential of micro-liquid chromatography tandem mass spectrometry in wastewater-based epidemiology, J. Chromatogr., A 1602 (2019) 300–309. https://doi.org/10.1016/j.chroma.2019.05.051.

[53] H. Yin, K. Killeen, The fundamental aspects and applications of Agilent HPLC-Chip, J. Sep. Sci. 30 (2007) 1427–1434. https://doi.org/10.1002/jssc.200600454.

[54] L.E. Blue, J.W. Jorgenson, 1.1µm Superficially porous particles for liquid chromatography. Part II: column packing and chromatographic performance, J. Chromatogr., A 1380 (2015) 71–80. https://doi.org/10.1016/j.chroma.2014.12.055.

[55] F.S. Semaan, A.J.D.S. Neto, F.M. Lanças, É.T. Gomes Cavalheiro, Rapid HPLC-DAD determination of furosemide in tablets using a short home-made column, Anal. Lett. 38 (2005) 1651–1658. https://doi.org/10.1081/AL-200065813.

[56] H.S. Berg, K.E. Seterdal, T. Smetop, R. Rozenvalds, O.K. Brandtzaeg, T. Vehus, E. Lundanes, S.R. Wilson, Self-packed core shell nano liquid chromatography columns and silica-based monolithic trap columns for targeted proteomics, J. Chromatogr., A 1498 (2017) 111–119. https://doi.org/10.1016/j.chroma.2017.03.043.

[57] Y. Guan, L. Zhou, Z. Shang, Dry-packed capillary columns for micro HPLC, J. High Resolut. Chromatogr. 15 (1992) 434–436. https://doi.org/10.1002/jhrc.1240150706.

[58] J.C. Rodrigues, F.M. Lanças, Preparation of packed capillary columns using supercritical carbon dioxide on cyclone-type slurry reservoir, J. Chromatogr., A 1090 (2005) 172–177. https://doi.org/10.1016/j.chroma.2005.06.074.

[59] W. De Malsche, H. Eghbali, D. Clicq, J. Vangelooven, H. Gardeniers, G. Desmet, Pressure-driven reverse-phase liquid chromatography separations in ordered nonporous pillar array columns, Anal. Chem. 79 (2007) 5915–5926. https://doi.org/10.1021/ac070352p.

[60] G. Tóth, T. Panić-Janković, G. Mitulović, Pillar array columns for peptide separations in nanoscale reversed-phase chromatography, J. Chromatogr., A 1603 (2019) 426–432. https://doi.org/10.1016/j.chroma.2019.06.067.

[61] C. Salmean, S. Dimartino, 3D-Printed stationary phases with ordered morphology: state of the art and future development in liquid chromatography, Chromatographia 82 (2019) 443–463. https://doi.org/10.1007/s10337-018-3671-5.

[62] K.B. Lynch, J. Ren, M.A. Beckner, C. He, S. Liu, Monolith columns for liquid chromatographic separations of intact proteins: a review of recent advances and applications, Anal. Chim. Acta 1046 (2019) 48–68. https://doi.org/10.1016/j.aca.2018.09.021.

[63] E.P. Nesterenko, Liquid Chromatography : Monolithic Columns, third ed., Elsevier Inc., 2018. https://doi.org/10.1016/B978-0-12-409547-2.13991-5.

[64] J.L. Dores-Sousa, A. Fernández-Pumarega, J. De Vos, M. Lämmerhofer, G. Desmet, S. Eeltink, Guidelines for tuning the macropore structure of monolithic columns for high-performance liquid chromatography, J. Sep. Sci. 42 (2019) 522–533. https://doi.org/10.1002/jssc.201801092.

[65] M.B. Espina-Benitez, J. Randon, C. Demesmay, V. Dugas, Development of a new in-line coupling of a miniaturized boronate affinity monolithic column with reversed-phase silica monolithic capillary column for analysis of cis-diol-containing nucleoside compounds, J. Chromatogr., A 1597 (2019) 209–213. https://doi.org/10.1016/j.chroma.2019.04.002.

[66] T. Hong, X. Yang, Y. Xu, Y. Ji, Recent advances in the preparation and application of monolithic capillary columns in separation science, Anal. Chim. Acta 931 (2016) 1–24. https://doi.org/10.1016/j.aca.2016.05.013.

[67] Z.-N. Qin, Q.-W. Yu, R.-Q. Wang, Y.-Q. Feng, Preparation of polymer monolithic column functionalized by arsonic acid groups for mixed-mode capillary liquid chromatography, J. Chromatogr., A 1547 (2018) 21–28. https://doi.org/10.1016/j.chroma.2018.03.007.

[68] C. Aydoğan, A. Gökaltun, A. Denizli, Z. El-Rassi, Organic polymer-based monolithic capillary columns and their applications in food analysis, J. Sep. Sci. 42 (2019) 962–979. https://doi.org/10.1002/jssc.201801051.

[69] R.N. Echevarría, S. Keunchkarian, J. Villarroel-Rocha, K. Sapag, M. Reta, Organic monolithic capillary columns coated with cellulose tris(3,5-dimethylphenyl carbamate) for enantioseparations by capillary HPLC, Microchem. J. 149 (2019) 104011. https://doi.org/10.1016/j.microc.2019.104011.

[70] L.Y. Zhao, Q.Y. Zhu, X.Q. Zhang, Y.J. Chen, L. Mao, H.Z. Lian, X. Hu, Preparation and analytical application of novel thiol-functionalized solid extraction matrices: from mesoporous silica to hybrid monolithic capillary column, Talanta 189 (2018) 517–526. https://doi.org/10.1016/j.talanta.2018.07.034.

[71] Q. Luo, G. Yue, G.A. Valaskovic, Y. Gu, S.L. Wu, B.L. Karger, On-line 1D and 2D porous layer open tubular/LC-ESI-MS using 10-µm-i.d. poly(styrene-divinylbenzene) columns for ultrasensitive proteomic analysis, Anal. Chem. 79 (2007) 6174–6181. https://doi.org/10.1021/ac070583w.

[72] R. Knob, C. Kulsing, R.I. Boysen, M. Macka, M.T.W. Hearn, Surface-area expansion with monolithic open tubular columns, TrAC - Trends Anal. Chem. 67 (2015) 16–25. https://doi.org/10.1016/j.trac.2014.12.004.

[73] P. Kubáň, P.K. Dasgupta, C.A. Pohl, Open tubular anion exchange chromatography. Controlled layered architecture of stationary phase by successive condensation polymerization, Anal. Chem. 79 (2007) 5462–5467. https://doi.org/10.1021/ac070690q.

[74] X. Wang, C. Cheng, S. Wang, M. Zhao, P.K. Dasgupta, S. Liu, Nanocapillaries for open tubular chromatographic separations of proteins in femtoliter to picoliter samples, Anal. Chem. 81 (2009) 7428–7435. https://doi.org/10.1021/ac901265t.
[75] L. Peng, M. Zhu, L. Zhang, H. Liu, W. Zhang, Preparation and evaluation of 3 m open tubular capillary columns with a zwitterionic polymeric porous layer for liquid chromatography, J. Sep. Sci. 39 (2016) 3736–3744. https://doi.org/10.1002/jssc.201600535.
[76] C. Aydoğan, Chiral separation and determination of amino acid enantiomers in fruit juice by open-tubular nano liquid chromatography, Chirality (2018) 1–6. https://doi.org/10.1002/chir.23006.
[77] M.J.E. Golay, Vapor phase chromatography and the telegrapher's equation, Anal. Chem. 29 (1957) 928–932. https://doi.org/10.1021/ac60126a019.
[78] M.J.E. Golay, Discussion of the Results with Three Experimental Gas-Liquid Chromatographic Columns, Perkin-Elmer Corp., Norwalk, Connecticut, 1956.
[79] C.F. Poole, Gas chromatography system constant database over an extended temperature range for nine open-tubular columns, J. Chromatogr., A 1590 (2019) 130–145. https://doi.org/10.1016/j.chroma.2019.01.028.
[80] V.L. Leal, M.R. da Silva, F.M. Lanças, Avanços recentes na miniaturização de colunas para cromatografia líquida, Sci. Chromatogr. 9 (2017) 117–133. https://doi.org/10.4322/sc.2017.010.
[81] M.R. da Silva, O.K. Brandtzaeg, T. Vehus, F.M. Lanças, S.R. Wilson, E. Lundanes, An automated and self-cleaning nano liquid chromatography mass spectrometry platform featuring an open tubular multi-hole crystal fiber solid phase extraction column and an open tubular separation column, J. Chromatogr., A 1518 (2017) 104–110. https://doi.org/10.1016/j.chroma.2017.08.071.
[82] M. Zhu, L. Zhang, Z. Chu, S. Wang, K. Chen, W. Zhang, F. Liu, Preparation and evaluation of open-tubular capillary columns modified with metal-organic framework incorporated polymeric porous layer for liquid chromatography, Talanta 184 (2018) 29–34. https://doi.org/10.1016/j.talanta.2018.02.010.
[83] M.A. Ahmed, B.M.B. Felisilda, J.P. Quirino, Recent advancements in open-tubular liquid chromatography and capillary electrochromatography during 2014–2018, Anal. Chim. Acta (2019). https://doi.org/10.1016/j.aca.2019.08.016.
[84] Y. Yang, P. Xiang, H. Chen, Z. Zhao, Z. Zhu, S. Liu, On-column and gradient focusing-induced high-resolution separation in narrow open tubular liquid chromatography and a simple and economic approach for pico-gradient separation, Anal. Chim. Acta 1072 (2019) 95–101. https://doi.org/10.1016/j.aca.2019.04.008.
[85] K. Grob, G. Grob, New approach to capillary columns for gas chromatography, J. Chromatogr. 347 (1985) 351–356.
[86] K. Grob, Making and Manipulating Capillary Columns for Gas Chromatography, Dr. Alfred Hüthig Verlag, 1986.
[87] B.X. Mayer, E. Lorbeer, A fused silica capillary column coated with a medium polar stationary phase for HTGC, J. High Resolut. Chromatogr. 18 (1995) 504–506. https://doi.org/10.1002/jhrc.1240180811.
[88] B. Xu, N.P.E. Vermeulen, Fused silica capillary deactivation with D4 in the presence of oxygen, J. High Resolut. Chromatogr. Chromatogr. Commun. 9 (1989) 679–682.
[89] K. Göhlin, A. Buskhe, M. Larsson, Kinetic performance of open-tubular and packed columns in LC using the same stationary phase: immobilized polymethyloctadecylsiloxane, Chromatographia 39 (1994) 729–739. https://doi.org/10.1007/BF02274590.
[90] P.A. Bristow, J.H. Knox, Standardization of test conditions for high performance liquid chromatography columns, Chromatographia 10 (1977) 279–289. https://doi.org/10.1007/BF02263001.
[91] J.H. Knox, M.T. Gilbert, Kinetic optimization of straight open-tubular liquid chromatography, J. Chromatogr. 186 (1979) 405–418.
[92] J.C. Giddings, Dynamics of Chromatography; Part I: Principles and Theory, Dekker, Marcel, New York, 1965.
[93] K.B. Lynch, A. Chen, S. Liu, Miniaturized high-performance liquid chromatography instrumentation, Talanta 177 (2018) 94–103. https://doi.org/10.1016/j.talanta.2017.09.016.
[94] L. Yi, P.D. Piehowski, T. Shi, R.D. Smith, W.J. Qian, Advances in microscale separations towards nanoproteomics applications, J. Chromatogr., A 1523 (2017) 40–48. https://doi.org/10.1016/j.chroma.2017.07.055.
[95] L.E. Blue, E.G. Franklin, J.M. Godinho, J.P. Grinias, K.M. Grinias, D.B. Lunn, S.M. Moore, Recent advances in capillary ultrahigh pressure liquid chromatography, J. Chromatogr., A 1523 (2017) 17–39. https://doi.org/10.1016/j.chroma.2017.05.039.
[96] S. Fanali, Nano-liquid chromatography applied to enantiomers separation, J. Chromatogr., A 1486 (2017) 20–34. https://doi.org/10.1016/j.chroma.2016.10.028.
[97] R.E. Wilson, A. Jaquins-Gerstl, S.G. Weber, On-column dimethylation with capillary liquid chromatography-tandem mass spectrometry for online determination of neuropeptides in rat brain microdialysate, Anal. Chem. 90 (2018) 4561–4568. https://doi.org/10.1021/acs.analchem.7b04965.
[98] S. Liu, J. Peng, H. Zhang, X. Li, Z. Liu, X. Kang, M. Wu, R. Wu, Preparation of organic-silica hybrid monolithic columns via crosslinking of functionalized mesoporous carbon nanoparticles for capillary liquid chromatography, J. Chromatogr., A 1498 (2017) 64–71. https://doi.org/10.1016/j.chroma.2017.03.067.
[99] C.A. Klein, CANCER: the metastasis cascade, Science 321 (2008) 1785–1787. https://doi.org/10.1126/science.1164853.
[100] M. Yu, S. Stott, M. Toner, S. Maheswaran, D.A. Haber, Circulating tumor cells: approaches to isolation and characterization, J. Cell Biol. 192 (2011) 373–382. https://doi.org/10.1083/jcb.201010021.
[101] L. Liu, K. Yang, X. Zhu, Y. Liang, Y. Chen, F. Fang, Q. Zhao, L. Zhang, Y. Zhang, Aptamer-immobilized open tubular capillary column to capture circulating tumor cells for proteome analysis, Talanta 175 (2017) 189–193. https://doi.org/10.1016/j.talanta.2017.07.041.
[102] T. Vehus, H. Roberg-Larsen, J. Waaler, S. Aslaksen, S. Krauss, S.R. Wilson, E. Lundanes, Versatile, sensitive liquid chromatography mass spectrometry-Implementation of 10 μm OT columns suitable for small molecules, peptides and proteins, Sci. Rep. 6 (2016) 1–10. https://doi.org/10.1038/srep37507.
[103] P. Xiang, Y. Yang, Z. Zhao, M. Chen, S. Liu, Ultrafast gradient separation with narrow open tubular liquid chromatography, Anal. Chem. 91 (2019) 10738–10743. https://doi.org/10.1021/acs.analchem.9b02190.
[104] P. Xiang, Y. Yang, Z. Zhao, A. Chen, S. Liu, Experimentally validating open tubular liquid chromatography for a peak capacity of 2000 in 3 h, Anal. Chem. 91 (2019) 10518–10523. https://doi.org/10.1021/acs.analchem.9b01465.
[105] K. Murtada, F. de Andrés, Á. Ríos, M. Zougagh, A simple poly(styrene-co-divinylbenzene)-coated glass blood spot method for monitoring of seven antidepressants using capillary liquid chromatography-mass spectrometry, Talanta 188 (2018) 772–778. https://doi.org/10.1016/j.talanta.2018.06.059.
[106] A.M. King, I. Grant, P.D. Rainville, G. Isaac, M. Coen, I.D. Wilson, R.S. Plumb, Capillary ultra performance liquid chromatography–tandem mass spectrometry analysis of tienilic acid metabolites in urine following intravenous administration to the rat, J. Chromatogr. B 1087–1088 (2018) 142–148. https://doi.org/10.1016/j.jchromb.2018.04.034.
[107] F. Rigano, A. Albergamo, D. Sciarrone, M. Beccaria, G. Purcaro, L. Mondello, Nano liquid chromatography directly coupled to electron ionization mass spectrometry for free fatty acid elucidation in mussel, Anal. Chem. 88 (2016) 4021–4028. https://doi.org/10.1021/acs.analchem.6b00328.
[108] A.L. Capriotti, G. Caruso, C. Cavaliere, R. Samperi, S. Ventura, R. Zenezini Chiozzi, A. Laganà, Identification of potential bioactive peptides generated by simulated gastrointestinal digestion of soybean seeds and soy milk proteins, J. Food Compos. Anal. 44 (2015) 205–213. https://doi.org/10.1016/j.jfca.2015.08.007.
[109] J. Alcántara-Durán, D. Moreno-González, B. Gilbert-López, A. Molina-Díaz, J.F. García-Reyes, Matrix-effect free multi-residue analysis of veterinary drugs in food samples of animal origin by nanoflow liquid chromatography high resolution mass spectrometry, Food Chem. 245 (2018) 29–38. https://doi.org/10.1016/j.foodchem.2017.10.083.
[110] D. Moreno-González, J. Alcántara-Durán, S.M. Addona, M. Beneito-Cambra, Multi-residue pesticide analysis in virgin olive oil by nanoflow liquid chromatography high resolution mass spectrometry, J. Chromatogr., A 1562 (2018) 27–35. https://doi.org/10.1016/j.chroma.2018.05.053.
[111] M. Carrera, J.M. Gallardo, S. Pascual, Á.F. González, I. Medina, Protein biomarker discovery and fast monitoring for the identification and detection of Anisakids by parallel reaction monitoring (PRM) mass spectrometry, J. Proteom. 142 (2016) 130–137. https://doi.org/10.1016/j.jprot.2016.05.012.
[112] M.D.M. Contreras, D. Arráez-Román, A. Fernández-Gutiérrez, A. Segura-Carretero, Nano-liquid chromatography coupled to time-of-flight mass spectrometry for phenolic profiling: a case study in cranberry syrups, Talanta 132 (2015) 929–938. https://doi.org/10.1016/j.talanta.2014.10.049.
[113] Y. Wang, S. Ma, Y. Chen, L. Zhang, J. Ou, Y. Shen, M. Ye, Thiol-radical-mediated polymerization for preparation of POSS-containing polyacrylate monoliths in capillary liquid chromatography, Talanta 190 (2018) 62–69. https://doi.org/10.1016/j.talanta.2018.07.061.
[114] S. Ma, H. Zhang, Y. Li, Y. Li, N. Zhang, J. Ou, M. Ye, Y. Wei, Fast preparation of hybrid monolithic columns via photo-initiated thiol-yne polymerization for capillary liquid chromatography, J. Chromatogr., A 1538 (2018) 8–16. https://doi.org/10.1016/j.chroma.2018.01.028.
[115] C. Qi, H. Jiang, J. Xiong, B. Yuan, Y. Feng, On-line trapping/capillary hydrophilic-interaction liquid chromatography/mass spectrometry for sensitive determination of RNA modifications from human blood, Chin. Chem. Lett. 30 (2019) 553–557. https://doi.org/10.1016/j.cclet.2018.11.029.
[116] C. Aydoğan, Z. El Rassi, MWCNT based monolith for the analysis of antibiotics and pesticides in milk and honey by integrated nano-liquid chromatography-high resolution orbitrap mass spectrometry, Anal. Methods 11 (2019) 21–28. https://doi.org/10.1039/c8ay02173b.
[117] N. Albekairi, A. Aqel, Z.A. ALOthman, Simultaneous capillary liquid chromatography determination of drugs in pharmaceutical preparations using tunable platforms of polymethacrylate monolithic columns modified with octadecylamine, Chromatographia 82 (2019) 1003–1015. https://doi.org/10.1007/s10337-019-03739-4.
[118] M.R. Gama, M.L. Lee, C.B.G. Bottoli, Preparation of an organic monolithic column based on carboxyethyl acrylate for capillary liquid chromatography, Sep. Sci. Plus. 1 (2018) 597–602. https://doi.org/10.1002/sscp.201870031.
[119] M. Han, W. Li, R. Chen, Y. Han, X. Liu, T. Wang, H. Guo, X. Qiao, Amino acid and ionic liquid modified polyhedral oligomeric silsesquioxane-based hybrid monolithic column for high-efficiency capillary liquid chromatography, J. Chromatogr., A 1572 (2018) 82–89. https://doi.org/10.1016/j.chroma.2018.08.045.
[120] L. Narciso Meirelles, T. Silva Campos, Z. Rodriguez, R. Hernandez, F. Svec, Z. Zajickova, "Single-pot" approach towards the preparation of alkyl and polyfluoroalkyl organo-silica monolithic capillaries for reversed-phase liquid chromatography, J. Sep. Sci. 41 (2018) 3669–3676. https://doi.org/10.1002/jssc.201800688.
[121] K. Chen, L. Zhang, W. Zhang, Preparation and evaluation of open-tubular capillary column combining a metal–organic framework and a brush-shaped polymer for liquid chromatography, J. Sep. Sci. 41 (2018) 2347–2353. https://doi.org/10.1002/jssc.201800121.

Capítulo 5

Investigation of the applicability of silica-graphene hybrid materials as stationary phases for capillary liquid chromatography

BORSATTO, João V. B.; MACIEL, Edvaldo V. S.; LANÇAS, Fernando M. Investigation of the applicability of silica-graphene hybrid materials as stationary phases for capillary liquid chromatography. **Journal of Chromatography A**, *[S. l.]*, v. 1685, p. 463618, 2022. DOI: 10.1016/j.chroma.2022.463618. Disponível em: https://linkinghub.elsevier.com/retrieve/pii/S0021967322008093.

Journal of Chromatography A 1685 (2022) 463618

Contents lists available at ScienceDirect

Journal of Chromatography A

journal homepage: www.elsevier.com/locate/chroma

Investigation of the applicability of silica-graphene hybrid materials as stationary phases for capillary liquid chromatography

João V.B. Borsatto[a], Edvaldo V.S. Maciel[a,b], Fernando M. Lanças[a,*]

[a] Laboratory of Chromatography, Institute of Chemistry at Sao Carlos, University of Sao Paulo, P.O Box 780, Sao Carlos 13566590, Brazil

ARTICLE INFO

Article history:
Received 1 June 2022
Revised 1 August 2022
Accepted 27 October 2022
Available online 29 October 2022

Keywords:
Capillary liquid chromatography
Graphene oxide
Hybrid materials
Orthogonality
SiGO-C18ec

ABSTRACT

Graphene and graphene-derived substances are cutting-edge materials receiving increasing attention in the analytical chemistry field. Graphene oxide sheets bonded to amino silica particles functionalized with octadecyl (C18) groups and endcapped, also known as SiGO-C18ec, have been successfully employed as extraction phases and in analytical columns associated with conventional liquid chromatography (LC). In this work, SiGO-C18ec particles of 3, 5, and 10 µm nominal id were employed to pack capillary LC columns (100 mm long x 0.3 mm id), and their performance in the gradient mode was evaluated and compared. A 3 µm C18 capillary LC column (50 x 0.3 mm) was used as a reference column. Eight analytes having different polarities and topological surface areas were selected as a probe in this study: carbofuran clomazone, hexazinone, carbamazepine, citalopram, clomipramine, desipramine, and ochratoxin A. Studies about orthogonality were performed to investigate the orthogonality between the SiGO-C18ec and C18 phases. Among the SiGO-C18ec phases investigated, the column packed with 5 µm SiGO-C18ec particles presented the best peak capacity (29) in 15 min.

Additionally, the performance of the columns packed with 5 µm SiGO-C18ec particles overcame the performance of the C18 columns used. Significant orthogonality was found between C18 and SiGO-C18ec packed columns; however, no significant differences were found between columns packed with SiGO-C18ec particles of different diameters.

1. Introduction

Graphene and graphene-derived materials have received significant attention due to their unique surface characteristics in the last two decades. Graphene materials are composed of long and flat leaves with a high surface area. The presence of aromatic rings allows oxidation of the surface, which favors the binding of ligands to modify the physical-chemistry surface characteristics. Due to this characteristic, graphene oxide materials called the attention of analytical chemists to evaluate their potential use in the sensor and extraction phase areas [1,2]. Graphene oxide derivatives were reported to have also applicability in solid-phase extraction (SPE). Fumes and Lanças quantified parabens contaminants in water samples by using a syringe packed with graphene oxide coated on silica particles as an SPE cartridge [3]. Online applications of the same phase were also proposed and validated in our research group. For instance, Da Silva and coworkers have employed a needle sleeve coated with β-cyclodextrin-graphene oxide-silica (SiGO-βCD) to perform an automated online sample preparation-LC analysis [4]. Online in-tube solid-phase microextraction (in-tube SPME) was also explored using graphene oxide bonded to silica particles. De Toffoli and coworkers have used amino silica functionalized with graphene oxide sheets (SiGO) particles in an extraction column to quantify target triazines in water samples [5]. Medija-Carmona and Lanças employed SiGO, endcapped graphene oxide silica particles ($SiGO_{ec}$), and endcapped octadecyl silane-graphene oxide silica particles (SiGO-C18ec) to quantify xanthine in coffee beverages [6]. Owing to the verified high applicability of these graphene-derived materials to produce high quality and selectivity online SPE extraction columns in our research group [3,5–7], their applicability as a stationary phase for LC analytical columns was considered. A particular phase highlights itself for the application in analytical columns, the SiGO-C18ec.

The use of graphene and graphene oxide was already employed and studied by other authors such as Qu and coworkers [8], which produced a capillary LC column coated with graphene oxide sheets. In addition, Zang and coworkers [9] investigated the retention mechanism of graphene bound to silica particles and SiGO phases. These authors propose that the retention mechanism of this sta-

* Corresponding author.
E-mail address: flancas@iqsc.usp.br (F.M. Lanças).
[b] Department of Chemistry, Clemens Schöpf Institute, Technical University of Darmstadt, Darmstadt 64287, Germany

https://doi.org/10.1016/j.chroma.2022.463618
0021-9673/

tionary phase is based on mixed-mode retention by π-π interactions, hydrophobic interactions, and hydrogen bonding [9].

Packing them in capillary columns is an excellent strategy to work and investigate new candidates for stationary phases. The reduced volume of the capillary LC column hardware allows the packing bed to use a minimal amount of stationary phase - in the scale of a few milligrams. Capillary chromatography is a way to establish itself as a powerful chromatography technique that presents the same performance of conventional scale but with a large economy of mobile phase solvents. Another advantage of the capillary scales is the optimized coupling to electrospray ionization sources once the flow rate reduction increases the ionization efficiency [10–13]. Though the capillary scale presents advantages, it is essential to highlight its limitations, especially concerning column evaluation. Gritti already demonstrated that certain combinations of specific column diameters and particle diameters might result in low efficient columns [14].

Performance and selectivity are considered the two main issues when evaluating different stationary phases. The most established performance parameters investigations are still based on the van Deemter curves [15], applicable in isocratic modes. In gradient modes, the kinetic plots recently became a powerful strategy to investigate gradient performance [16–18], though they are not a novelty [19]. Kinetic plots usually comprise one parameter of column performance in function of a parameter of time (for instance, resolution versus analysis time). Other combinations are possible, such as peak capacity (n) in the function of the flow rate, which is intercorrelated to the analysis time. Relevant considerations are determining selectivity, retention factor (k), selectivity factor (α), and orthogonality. The retention factor is significant in comparing columns in the isocratic mode because its calculation is quite simple and does not demand additional experiments. The gradient retention factor (k') presents a different calculation than the isocratic retention factor parameter and depends on a series of experiments performed in gradient mode to determine k'. The selectivity factors are based on the calculation of the retention factor for two peaks (consecutive or not). Finally, the orthogonality evaluation is not based on a parameter but on a graphical representation method. To obtain an orthogonality plot, the retention times of two different columns are distributed on the axis, and the coordinate of each data point to the retention time of the same compound in each column is considered. Another critical aspect to investigate in new stationary phases is the changing in the morphology according to the composition of the mobile phase [20,21]. Although there is no evidence that it may occur in SiGO-C18ec particles, it is relevant to investigate whether the mobile phase composition affects the graphene oxide sheets morphology or not, especially because the selectivity of the phase could be changed.

This study evaluated the performance and orthogonality of SiGO-C18ec particles of different diameters in capillary liquid chromatography. Once this phase is still in the developmental stage, we intend to bring some light to this challenge. To do that, a multiclass set of compounds were selected. Furthermore, gradient separation mode was chosen, and the peak capacity and peak capacity at kinetic performance limits were assessed to compare the performance of columns packed with particles of different sizes. In addition, the orthogonality among the SiGO-C18ec phases and C18 was evaluated.

2. Material and methods

2.1. Reagents and analytical standards

Solvents and solutions: LC grade Acetonitrile (MeCN), Methanol (MeOH), Isopropanol (IPA), Toluene, Hydrochloric acid 37% (HCl), and Tetrahydrofuran (THF) was acquired from Tedia (Fairfield, US). MS-grade high-purity (> 98%) Formic Acid (FA) was purchased from Honeywell Fluka (Seelze, DE). Deionized ultra-pure water (H_2O) used in this work was in-lab produced by a Milli-Q® synthesis Millipore system (Burlington, US).

For the synthesis of graphene oxide (GO), SiGO, and SiGO-C18ec: graphite powder (< 20 µm), potassium permanganate 99% ($KMnO_2$), sodium nitrate 99% ($NaNO_3$), N-hydroxisuccinimide 97% (NHS), dimethylformamide (DMF), trimethylchlorosilane (TMCS), and 1-ethyl-3-(3-dimethyl aminopropyl) carbodiimide hydrochloride (EDC) were purchased from Sigma-Aldrich (St. Louis, US). Both sulfuric acid 98% (H_2SO_4) and imidazole 98% AR-grade acquired from Mallinckrodt (Paris, FR), Hydrogen peroxide 30 % (H_2O_2) from Synth (Diadema, BR), Hydrazine/Water 80% from Merck (Darmstadt, DE), and chlorodimethyl-n-octadecylsilane (C18) 95% from Alfa Aesar (Ward Hill, US). For use as supporting material, aminopropyl silica (Si) from different particle diameters – 3, 5, and 10 µm – was provided by Sigma-Aldrich (St. Louis, US). C18 particles of 3 µm were acquired from Chromatorex (Fuji-Silysia, Kasugai, Japan).

The analytical standards of carbofuran clomazone, hexazinone, carbamazepine, citalopram, clomipramine, desipramine, and ochratoxin A were acquired from Sigma-Aldrich (St. Louis, US). Stock solutions for each compound were prepared in MeOH at a concentration level between 250 and 1000 mg/L and kept at -7 °C. Individual or mixed working solutions were at a concentration of 100 mg/L. The analytes were selected to cover a wide range of molecular mass and topological surface area (Fig. 1).

2.2. Analytical instrumentation

The LC system used was an Acquity M-Class LC coupled to a Xevo TQ S Micro MS from Waters (Milford, US). The LC-MS equipment is composed of a µ-binary solvent manager module, sample manager module, and trap-valve manager module. The mobile phase consisted of H_2O (A) and MeCN (B), both added with 0.1% of formic acid to enhance the positive electrospray (ESI) ionization process. A gradient mode was applied from 1 to 99% of B in 15 min, followed by 5 min at 99% of B. The column temperature was set at 35 °C, the injection volume was 0.05 µL, and the flow rate was between 1 and 7 µL/min, depending on the experiment. The ESI-MS parameters in positive ionization mode were a capillary voltage of 3.5 kV, a source temperature of 150 °C, desolvation gas (N_2) flow of 600 L/h, and desolvation temperature of 330 °C, collision gas (Ar) flow of 0.100 L/h. The experimental data were processed by MassLynx 4.2 software from Waters. The main parameters selected for use in the tandem MS experiments are presented in Table 1.

2.3. Synthesis of the stationary phases

The SiGO-C18ec material was synthesized as previously described by Fumes and Lanças [3,5,6,22]. The synthesis starts with the conversion of graphite powder into graphene oxide (GO) through Hummer's method with minor modifications [23]. In short, 1.0 g of graphite, 0.5 g $NaNO_3$, and 23 mL of H_2SO_4 were mixed inside a reaction flask and let stirring for 1 h into an ice bath. After 3.0 g of $KMnO_4$ was added, the reaction let stirring again, now for 10 h at room temperature, until the almost-black mixture turned into a brownish-like one. With the reaction flask placed again in the ice bath, 50 mL of H_2O was added carefully to avoid sudden enhancements in temperature. After that, an additional amount of 100 mL of H_2O was added, followed by 10 mL of H_2O_2 (30%), which was inserted and dropped carefully into the reaction, turning it into a yellow mixture. At this point, the reaction was let stir overnight to promote precipitation of our desired material – graphene oxide. The product was centrifuged at 5040

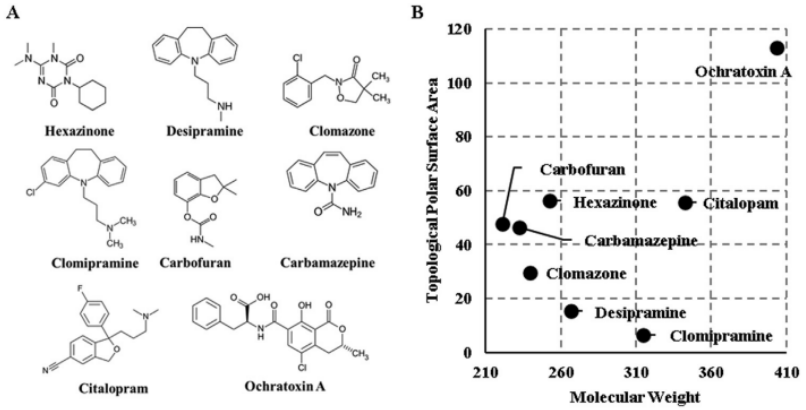

Fig. 1. (A) Molecular structure representation of the compounds used in this work. (B) Topological surface area and molecular weight of the compounds used in this work.

Table 1
MRM ionic transition and MS instrumental parameters employed for detecting the compounds.

	1st Monitored Transition				2nd Monitored Transition			
Compounds	Precursor Ion (m/z)	Product Ion (m/z)	Collision Energy (V)	Cone Voltage (V)	Precursor Ion (m/z)	Product Ion (m/z)	Collision Energy (V)	Cone Voltage (V)
Carbofuran	222.04	123.01	10	12	222.04	165.09	34	12
Clomazone	239.93	89.19	46	50	239.93	124.96	16	50
Hexazinone	253.25	171.07	12	40	253.25	70.98	34	40
Carbamazepine	253	152	42	24	253	167	44	24
Citalopram	325	234	26	32	325	262	20	32
Clomipramine	315	86	18	24	315	227	42	27
Desipramine	267	193	42	22	267	208	24	22
Ochratoxin A	404	239	26	24	404	221	36	24

RCF for 10 min, washed five times with 5% (v/v) HCl solution, and subsequently washed with ultrapure water, centrifuged again, and finally lyophilized.

The next step consisted of covalently supporting the graphene oxide into the amino silica (Si) surface by forming a peptide bond between the oxygenated groups of GO and the amino group of the amino silica. The method chosen for this step was initially proposed by Liu et al. [24] Briefly, 40. 0 mg of GO and 100 mL of ultrapure water were added into a reaction flask and let sonicating for 1 h. So, 750 µL of an aqueous solution formed by 5 mol/L and 10 mol/L of NHS and EDC, respectively, was added, and the reaction let stirring for 1 h to activate the GO material. At last, 1.0 of amino silica (Si) was added, and the reaction was left to stir again for 4 h at room temperature. The product (SiGO) was filtered under vacuum, washed alternatively with MeOH and ultrapure water at least five times, and finally lyophilized again.

The last reaction step for producing the SiGO-C18ec stationary phase was performed under an N_2 atmosphere, using a two-necked reaction flask connected to a Friedrich condenser, where 400 mg of SiGO was mixed with 4.0 mL of dry toluene. Subsequently, 5 mg of imidazole dissolved in 400 µL of dry toluene and 40 mg of chlorodimethyl-n-octadecylsilane (C18) dissolved in 600 µL of dry toluene were added to the reaction. After, the reaction was left refluxing for approximately 8 h in an oil bath (55 °C). Then, the SiGOC18 particles were filtered and washed sequentially with toluene, MeOH, MeOH/H_2O (1:1), and MeOH again. Before starting the end-capping process, the product was left drying under 40 °C for approximately 48 h. The endcapping procedure consisted of the same steps for octadecylsilane-functionalization but changed the reagent C18 for 50 µL of TMCS.

2.4. Production of the chromatographic columns

Column hardware: The SiGO-C18ec LC columns were composed of 100 mm glass-lined stainless-steel tube (fused silica capillary covered by a stainless-steel tube) of 1/16 inches o.d. and 0.3 mm i.d. The frits were composed of a 1-2 mm glass wool filter disc of 1/16 inches diameter and 0.2 µm of porosity. The frits were assembled to the LC columns by a Valco set of unions, nuts, and ferrules for 1/16 inches tubing. The C18 column hardware is similar to the hardware previously cited but composed of a PEEKsil tube (fused silica capillary covered by a PEEK tube) of 50 and 0.3 mm i.d.

Column packing: 0.7 mg of each stationary phase was washed with 1 ml of acetone to remove non-bounded graphene sheets. After decantation, the supernatant was collected and discarded. The SiGO-C18ec particles were dried at room temperature for 24 h. The slurry-packing process was performed using a hydro-pneumatic pump DSHF-300 (Haskel, Burbank, USA) at 9000 kPa (900 bar) for 1 h, followed by 0.5 h of pressure re-equilibration. The packing solvent was ultra-pure water, while the SiGO-C18ec and C18 particles were suspended in a mixture of IPA:THF 4:1 before inserting in the packing chamber.

3. Results

3.1. Phase characteristics

SiGO-C18ec particles of 3, 5, and 10 µm were produced and evaluated in this work. Analyzing the SEM figures (Fig. 2A), it can be seen that the graphene oxide sheets were attached to the silica particle's surface, though with differences in the sheet format.

In the 3 µm particles, the graphene oxide sheets formed a rough structure such as crumpled paper. The 5 µm particles demon-

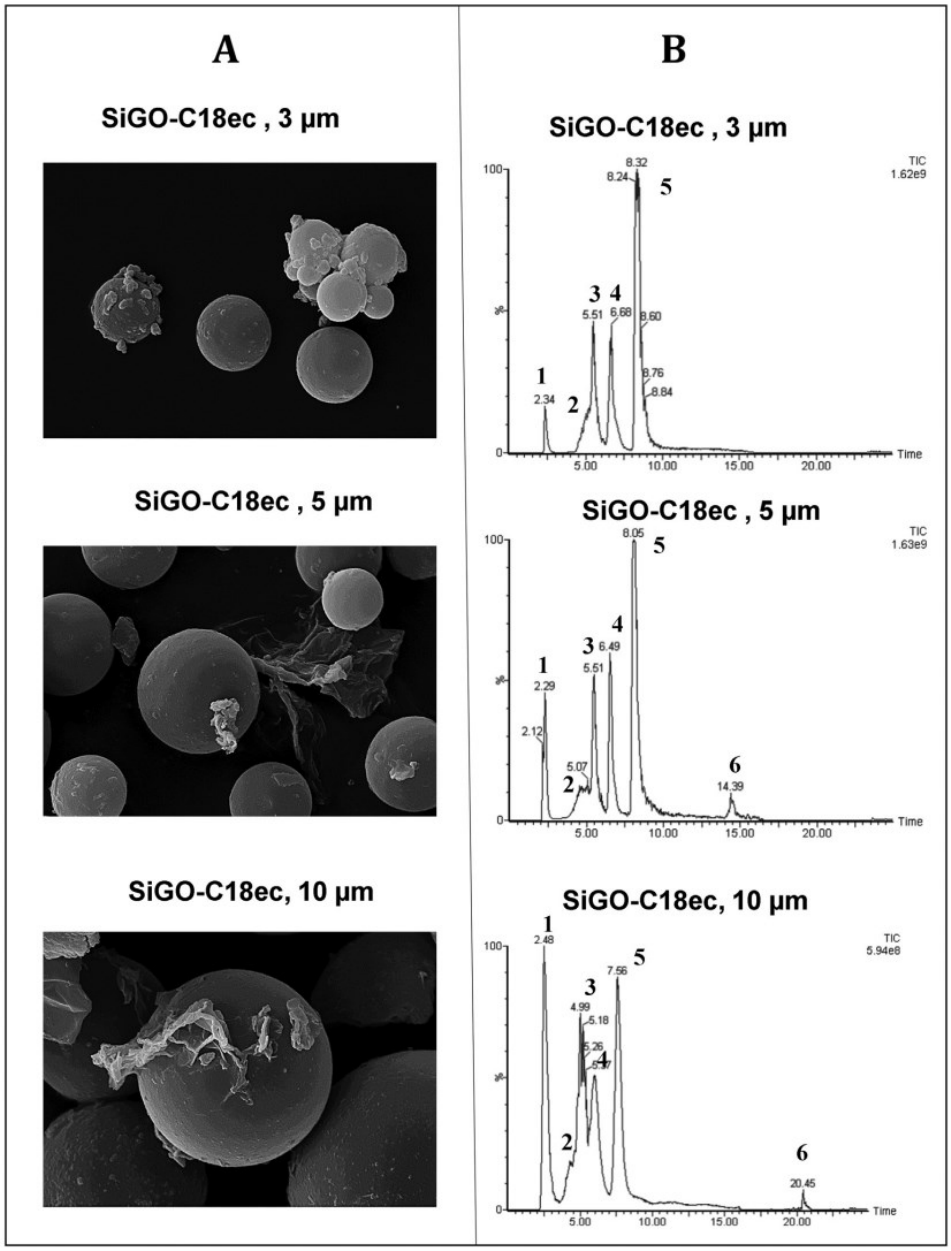

Fig. 2. SEM pictures of the SiGO-C18ec particles of 3, 5, and 10 µm id (A) and chromatograms (B)obtained using columns packed with SiGO-C18ec particles of 3, 5, and 10 µm. Separation conditions: flow rate of 5 µL/min, a gradient of 1 to 99% of B in 15 min, injection volume of 0.05 µL, and sample concentration of 100 µg/mL. (1) Non retained fraction, (2) co-elution of citalopram and desipramine, (3) clomipramine, (4) co-elution of hexazinone, carbamazepine, and carbofuran, (5) clomazone, and (6) ochratoxin A.

strated the same rough structure as graphene oxide sheets but with longer and flatter leaves present in approximately the same quantity. Finally, the 10 µm particles presented the flattest and most extended sheets as primary graphene oxide structures. In all three phases, free graphene oxide sheets were also present in the material—all were capable of retaining and separating the 8 compounds selected for this work (Fig. 2B).

3.2. Performance evaluation

The intermediate size particles (5 µm) were selected to perform the flow rate optimization study. 1, 3, 5, and 7 µL/min were the flow rates selected once they covered the entire operating range of the chromatographic system (system, column, and tubing) employed in this work. A flow rate of 1 µL/min produced a low signal-

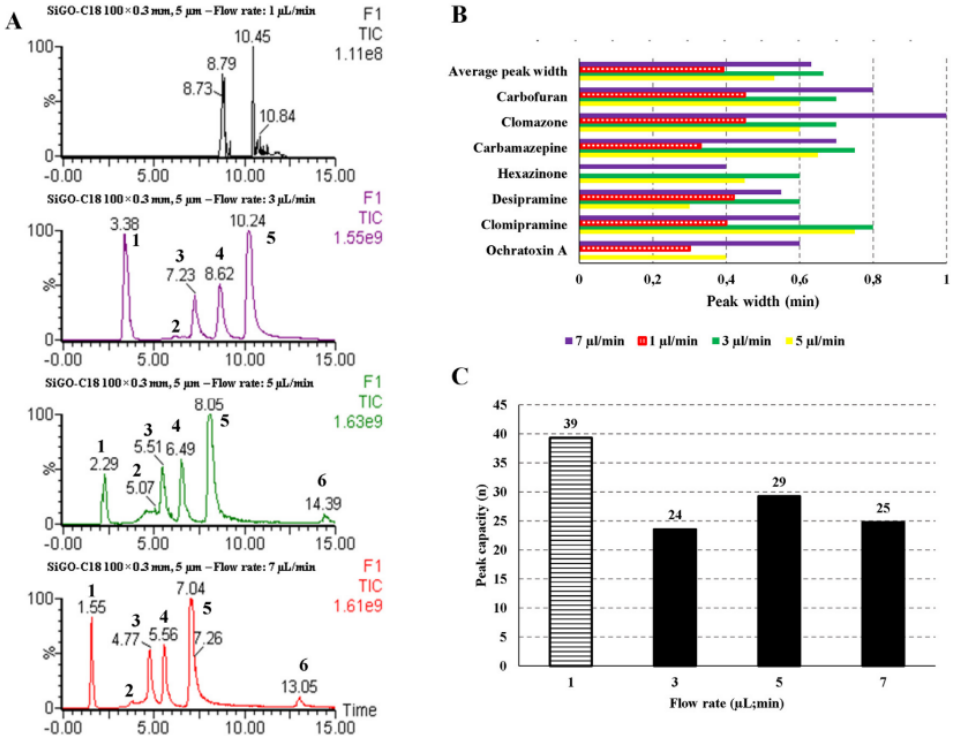

Fig. 3. (A) Chromatograms obtained at the column packed with SiGO-C18ec particles of 5 µm. at 1, 3, 5, and 7 µL/min. (B) The peak width of each compound in each flow rate was explored. (C) Peak capacity (n) at each flow rate was explored. Separation conditions: flow rate of 5 µL/min, a gradient of 1 to 99% of B in 15 min, injection volume of 0.05 µL, and sample concentration of 100 µg/mL. (1) Non retained fraction, (2) co-elution of citalopram and desipramine, (3) clomipramine, (4) co-elution of hexazinone, carbamazepine, and carbofuran, (5) clomazone, and (6) ochratoxin A.

to-noise ratio, making it challenging to distinguish the peak signal and the noise, while 7 µL/min nearly exceeded the maximum system pressure of 15.000 PSI.

Fig. 3A shows the chromatogram at each flow rate explored. For example, the flow rate of 1 µL/min resulted in small peaks due to the smallest signal-to-noise ratio (S/N) obtained at this flow (please notice the abundance scale on the right side of the figure). Therefore, the chromatographic parameters were also calculated for 1 µL/min and are presented alongside the parameters obtained for 3, 5, and 7 µL/min, but once they could have been affected by the low signal-to-noise ratio, they must be analyzed cautiously. For example, at 3 µL/min, the peak shape and signal were appropriate, but the last peak, corresponding to ochratoxin A, was not detected at the window, possibly due to the longitudinal diffusion.

On the other hand, 5 and 7 µL/min showed appropriate signal and peak shape. Fig. 3B shows the peak width value for each compound in each flow rate. Though the variation in the peak width was high, the 5 µL/min flow rate resulted in thinner peaks than the 3 and 7 µL/min flow rates. Fig. 3C represents the peak capacity (n) for the flow rates explored. It was observed that there is a similar peak capacity for 3, 5, and 7 µL/min flow rates in the range between 24 and 29 peaks in 15 min. For information on repeatability and robustness (page S-2) and the effect of the gradient curve shape on the retention time (page S-3), see the supplementary material.

3.3. Performance comparison

In conventional LC, the lower the diameter of the stationary phase, the higher the column performance [25]. However, in the SiGO-C18ec particles presented in this work, the particle diameter also affected the graphene distribution on the particle's surface. Because of that, it was essential to investigate the effect of this difference in the column performance and packing. Fig. 4A presents the peak width of each compound for each investigated column.

The SiGO-C18ec 10 µm particles resulted in broader peaks than the other columns, followed by the C18 3 µm as the second wider. The 5 µm SiGO-C18ec particles presented the thinnest peaks. When analyzing the maximum backpressure required in each column (Fig. 4B), it is seen that the 5 µm presented the highest values, even higher than the column packed with the 3 µm SiGO-C18ec particles. It indicates that the 3 µm particles resulted in a less compact packed bed than the 5 µm particles, oppositely to the expected. The peak capacity (n) was also compared for the same columns (Fig. 4C). The columns packed with SiGO-C18ec of 5 µm presented the highest peak capacity. The resolution between the citalopram and clomazone peaks was also compared (Fig. 4D), and the SiGO-C18ec 5 µm column presented the best resolution [26]. The separation mechanism was not studied for these particles.

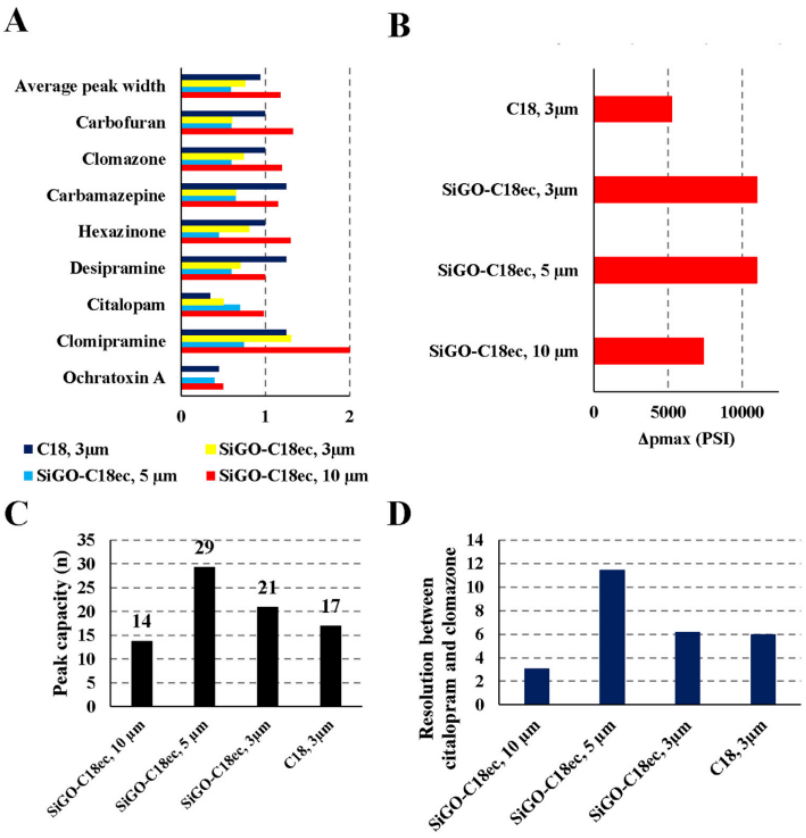

Fig. 4. (A) Comparison of peak width obtained using columns packed with SiGO-C18ec particles of 3, 5, and 10 µm and C18 3 µm. (B) Column pressure drop at column packed with SiGO-C18ec particles of 3, 5, and 10 µm and C18 3 µm. (C) Comparison of peak capacity (n) obtained using columns packed with SiGO-C18ec particles of 3, 5, and 10 µm and C18 3 µm. (D) Comparison of resolution between citalopram and clomazone in columns packed with SiGO-C18ec particles of 3, 5, and 10 µm and C18 3 µm. Separations conditions: flow rate of 5 µL/min, a gradient of 1 to 99% of B in 15 min, injection volume of 0.05 µL, and sample concentration of 100 µg/mL.

3.4. Orthogonality between SiGO-C18ec and C18

Selectivity is a critical factor in chromatography because it reflects the capability of the columns to work with different analytes. Orthogonality was used in this work to explore and compare the columns once orthogonality is related to the selectivity of each column. The normalized retention time (RT_{inorm}) was used to compare the column's orthogonality (see supplementary material page S-4 for equation details) [27]. In Fig. 5A, columns packed with SiGO-C18ec of 5 and 10 µm particles were compared. It is visible that there is an almost linear correlation between these columns.

When comparing the columns packed with SiGO-C18ec of 3 and 5 µm particles (Fig. 5B), the linear correlation between these columns was lower but also present. This suggests higher orthogonality between the column packed with 3 µm SiGO-C18ec and the column packed with 5 µm SiGO-C18ec when compared to the orthogonality of the same 5 µm SiGO-C18ec against the 10 µm SiGO-C18ec (Fig. 5A). This could be attributed to the graphene's sheet morphology differences between the 3 µm SiGO-C18ec and the 5 and 10 µm SiGO-C18ec particles (Fig. 2), though confirmation is still required. Compared to the C18 column, the 3 µm SiGO-C18ec column presented significative orthogonality, demonstrating that both phases have different selectivity (Fig. 5C). "Compared to the C18 column, the 3 µm SiGO-C18ec column presented significative orthogonality, demonstrating that both phases have different selectivity (Fig. 5C). We hypothesize that, although the particles were functionalized with C18 and further endcapped (supplementary material S4), residual amino groups could still be present in the particles and collaborate to the unique selectivity of the SiGO-C18ec phases."

The SiGO-C18ec 10 µm packed columns also presented significative orthogonality to the C18 stationary phase (Fig. 5D). The orthogonality between SiGO-C18ec 5 µm and C18 can be inferred by observing Fig. 5A–C.

4. Concluding remarks

This work evaluated the performance and selectivity of SiGO-C18ec phases in miniaturized liquid chromatography. C18 columns were used as references. It was observed that columns packed with the synthesized SiGO-C18ec particles could perform at least as well as the C18 columns in capillary liquid chromatography. The performance evaluation experiments demonstrated that the 5 µm SiGO-C18ec particles resulted in higher peak capacity and resolution columns. The same was concluded when comparing the peak capacity at the kinetic performance limit. The selectivity was evaluated by comparing the orthogonality between the columns. No significant differences in the orthogonality were found between the

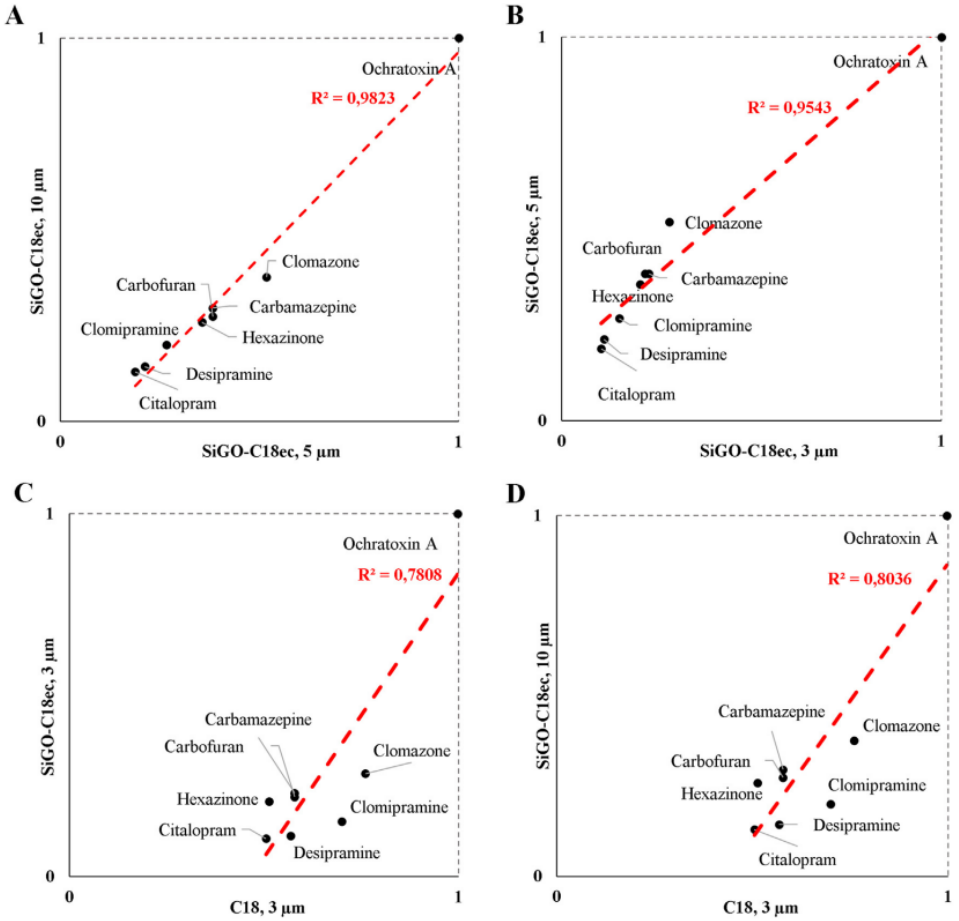

Fig. 5. Comparison of the normalized retention time (RT_{inorm}) between columns packed with particles (A) SiGO-C18ec 5 µm and SiGO-C18ec 10 µm, (B) SiGO-C18ec 3 µm and SiGO-C18ec 5 µm, (C) SiGO-C18ec 3 µm and C18 3 µm, and (D) SiGO-C18ec 10 µm and C18 3 µm. Retention time in the axis was compensated by subtracting the dead time. Separations conditions: flow rate of 5 µL/min, a gradient of 1 to 99% of B in 15 min, injection volume of 0.05 µL, and sample concentration of 100 µg/mL.

columns packed with SiGO-C18ec phases, though differences in the morphology of the graphene sheets were observed in the particles of different diameters. Compared to standard C18 columns, significative orthogonality was observed, demonstrating that the SiGO-C18ec columns have different selectivity compared to C18 columns.

In conclusion, the presented SiGO-C18ec particles are promising candidates as stationary phase in liquid chromatography, capable of being employed in a wide range of mobile phase compositions and presenting a selectivity different than C18, suggesting that it might be an alternative to C18 when a different selectivity is desirable.

Declaration of Competing Interest

The authors declare that they have no known competing financial interests or personal relationships that could have appeared to influence the work reported in this paper.

CRediT authorship contribution statement

João V.B. Borsatto: Conceptualization, Methodology, Data curation, Formal analysis, Writing – review & editing, Writing – original draft, Funding acquisition. **Edvaldo V.S. Maciel:** Conceptualization, Methodology, Data curation, Formal analysis, Writing – review & editing, Writing – original draft, Funding acquisition. **Fernando M. Lanças:** Conceptualization, Methodology, Data curation, Formal analysis, Writing – review & editing, Writing – original draft.

Acknowledgments

This research project was financed in part by the Coordination for the Improvement of Higher Education Personnel (CAPES – Brazil) - Finance Code 001. The authors are grateful to the São Paulo Research Foundation (FAPESP – Brazil, Grants 2019/22724-7, 2017/02147-0, 2015/15462-5, and 2014/07347-9) and the National Council for Scientific and Technological Development (CNPq – Brazil, 307293/2014-9; 308843/ 2019-3).

Supplementary materials

Supplementary material associated with this article can be found, in the online version, at doi:10.1016/j.chroma.2022.463618.

References

[1] X. Wang, B. Liu, Q. Lu, Q. Qu, Graphene-based materials: Fabrication and application for adsorption in analytical chemistry, J. Chromatogr. A 1362 (2014) 1–15, doi:10.1016/j.chroma.2014.08.023.

[2] Z.J Li, Q.F. Xia, Recent advances on synthesis and application of graphene as novel sensing materials in analytical chemistry, Rev. Anal. Chem. 31 (2012) 57–81, doi:10.1515/revac-2011-0039.

[3] B.H. Fumes, F.M. Lanças, Use of graphene supported on aminopropyl silica for microextraction of parabens from water samples, J. Chromatogr. A 1487 (2017) 64–71, doi:10.1016/j.chroma.2017.01.063.

[4] L.F. da Silva, D.A. Vargas Medina, F.M. Lanças, Automated needle-sleeve based online hyphenation of solid-phase microextraction and liquid chromatography, Talanta (2021) 221, doi:10.1016/j.talanta.2020.121608.

[5] A.L. de Toffoli, B.H. Fumes, F.M. Lanças, Packed in-tube solid-phase microextraction with graphene oxide supported on aminopropyl silica: determination of target triazines in water samples, J. Environ. Sci. Health Part B Pestic. Food Contam. Agric. Wastes 53 (2018) 434–440, doi:10.1080/03601234.2018.1438831.

[6] K. Mejía-Carmona, F.M. Lanças, Modified graphene-silica as a sorbent for in-tube solid-phase microextraction coupled to liquid chromatography-tandem mass spectrometry. Determination of xanthines in coffee beverages, J. Chromatogr. A 1621 (2020), doi:10.1016/j.chroma.2020.461089.

[7] A.L. de Toffoli, B.H. Fumes, F.M. Lanças, Packed in-tube solid phase microextraction with graphene oxide supported on aminopropyl silica: determination of target triazines in water samples, J. Environ. Sci. Health 53 (2018) 434–440 Part B., doi:10.1080/03601234.2018.1438831.

[8] Q. Qu, C. Gu, X. Hu, Capillary coated with graphene and graphene oxide sheets as stationary phase for capillary electrochromatography and capillary liquid chromatography, Anal. Chem. 84 (2012) 8880–8890, doi:10.1021/ac3023636.

[9] X. Zhang, S. Chen, Q. Han, M. Ding, Preparation and retention mechanism study of graphene and graphene oxide bonded silica microspheres as stationary phases for high performance liquid chromatography, J. Chromatogr. A 1307 (2013) 135–143, doi:10.1016/j.chroma.2013.07.106.

[10] T.R. Covey, BA. Thomson, B.B. Schneider, Atmospheric pressure ion sources, Mass Spectrom. Rev. 28 (2009) 870–897, doi:10.1002/mas.20246.

[11] D.A. Vargas Medina, E.V.S. Maciel, A.L. de Toffoli, F.M. Lanças, Miniaturization of liquid chromatography coupled to mass spectrometry, TrAC Trends Anal. Chem. 128 (2020) 115910, doi:10.1016/j.trac.2020.115910.

[12] D.A. Vargas Medina, E.V. Soares Maciel, A. Lúcia de Toffoli, F.M. Lanças, Miniaturization of liquid chromatography coupled to mass spectrometry. 2. Achievements on modern instrumentation for miniaturized liquid chromatography coupled to mass spectrometry, TrAC Trends Anal. Chem. (2020) 115910, doi:10.1016/j.trac.2020.115910.

[13] D.A. Vargas Medina, E.V.S. Maciel, F.M. Lanças, Miniaturization of liquid chromatography coupled to mass spectrometry. 3. Achievements on chip-based LC–MS devices, TrAC Trends Anal. Chem. 131 (2020) 116003, doi:10.1016/j.trac.2020.116003.

[14] F. Gritti, A stochastic view on column efficiency, J. Chromatogr. A 1540 (2018) 55–67, doi:10.1016/j.chroma.2018.02.005.

[15] J.J. van Deemter, F.J. Zuiderweg, A. Klinkenberg, Longitudinal diffusion and resistance to mass transfer as causes of nonideality in chromatography, Chem. Eng. Sci. 5 (1956) 271–289, doi:10.1016/0009-2509(56)80003-1.

[16] G. Desmet, D. Cabooter, K. Broeckhoven, Graphical data representation methods to assess the quality of LC columns, Anal. Chem. 87 (2015) 8593–8602, doi:10.1021/ac504473p.

[17] H. Eghbali, G. Desmet, Optimum kinetic performance of open-tubular separations in microfluidic devices, J. Sep. Sci. 30 (2007) 1377–1397, doi:10.1002/jssc.200600464.

[18] J. Billen, G. Desmet, Understanding and design of existing and future chromatographic support formats, J. Chromatogr. A 1168 (2007) 73–99, doi:10.1016/j.chroma.2007.07.069.

[19] H. Poppe, Some reflections on speed and efficiency of modern chromatographic methods, J. Chromatogr. A 778 (1997) 3–21, doi:10.1016/S0021-9673(97)00376-2.

[20] R.J. Vonk, A. Vaast, S. Eeltink, P.J. Schoenmakers, Titanium-scaffolded organic-monolithic stationary phases for ultra-high-pressure liquid chromatography, J. Chromatogr. A 1359 (2014) 162–169, doi:10.1016/j.chroma.2014.07.039.

[21] I. Nischang, O. Brüggemann, On the separation of small molecules by means of nano-liquid chromatography with methacrylate-based macroporous polymer monoliths, J. Chromatogr. A 1217 (2010) 5389–5397, doi:10.1016/j.chroma.2010.06.021.

[22] E.V.S. Maciel, A.L. de Toffoli, J. da S. Alves, F.M. Lanças, Multidimensional liquid chromatography employing a graphene oxide capillary column as the first dimension: determination of antidepressant and antiepileptic drugs in urine, Molecules 25 (2020) 1092, doi:10.3390/molecules25051092.

[23] W.S. Hummers, R.E. Offeman, Preparation of Graphitic Oxide, J. Am. Chem. Soc 80 (1958) 1339, doi:10.1021/ja01539a017.

[24] Q. Liu, J. Shi, J. Sun, T. Wang, L. Zeng, G. Jiang, Graphene and graphene oxide sheets supported on silica as versatile and high-performance adsorbents for solid-phase extraction, Angew. Chem. In. Ed. 50 (2011) 5913–5917, doi:10.1002/anie.201007138.

[25] M.F. Wahab, D.C. Patel, R.M. Wimalasinghe, D.W. Armstrong, Fundamental and practical insights on the packing of modern high-efficiency analytical and capillary columns, Anal. Chem. 89 (2017) 8177–8191, doi:10.1021/acs.analchem.7b00931.

[26] U.D. Neue, Theory of peak capacity in gradient elution, J. Chromatogr. A 1079 (2005) 153–161, doi:10.1016/j.chroma.2005.03.008.

[27] M. Gilar, P. Olivova, A.E. Daly, J.C. Gebler, Orthogonality of separation in two-dimensional liquid chromatography, Anal. Chem. 77 (2005) 6426–6434, doi:10.1021/ac050923i.

Capítulo 6

Application of an in-house packed octadecylsilica-functionalized graphene oxide column for capillary liquid chromatography analysis of hormones in urine samples

Maciel, Edvaldo V. S.; **Borsatto, João V. B.**; Mejia-Carmona, Karen; Lanças, Fernando M. Application of an in-house packed octadecylsilica-functionalized graphene oxide column for capillary liquid chromatography analysis of hormones in urine samples. **Analytica Chimica Acta**, *[S. l.]*, v. 1239, n. August 2022, p. 340718, 2023. DOI: 10.1016/j.aca.2022.340718. Disponível em: https://linkinghub.elsevier.com/retrieve/pii/S0003267022012892.

Analytica Chimica Acta 1239 (2023) 340718

Contents lists available at ScienceDirect

Analytica Chimica Acta

journal homepage: www.elsevier.com/locate/aca

Application of an in-house packed octadecylsilica-functionalized graphene oxide column for capillary liquid chromatography analysis of hormones in urine samples

EdvaldoV.S. Maciel [1], João V.B. Borsatto, Karen Mejia-Carmona [2], Fernando M. Lanças [*]

Laboratory of Chromatography, Institute of Chemistry at Sao Carlos, University of Sao Paulo, P.O Box 780, 13566590, Sao Carlos, Brazil

HIGHLIGHTS

- A synthesized graphene-based stationary phase for capillary liquid chromatography was presented.
- Preparation and chromatographic parameters of the packed analytical column are discussed.
- Different particle diameters (d_p) were assessed during the development of the column.
- Four hormones were separated, including dexamethasone, estradiol, estrone, hydrocortisone, and progesterone.
- One of the first reports of a graphene-based analytical column tested in a biological fluid.

GRAPHICAL ABSTRACT

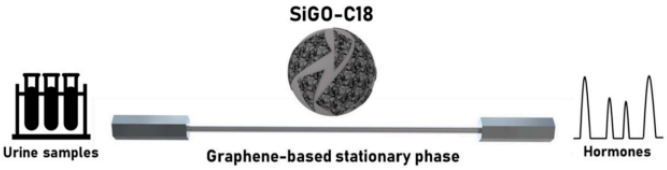

ARTICLE INFO

Keywords:
Capillary liquid chromatography
Stationary phase
Graphene-based materials
Packed column
Hormones
Urine samples

ABSTRACT

Graphene oxide-based LC stationary phases were developed and applied for separating hormones from urine using capillaryLC-MS/MS. Using two analytical approaches – direct injection and column-switching arrangement – it was possible to evaluate the chromatographic parameters and perform tests on the raw biological fluid. Two stationary phases (SPs) were produced, varying the amino silica support particle diameter (Si, 5, and 10 μm). Graphene oxide was covalently bonded to the surface of Si particles, and this material was functionalized by the insertion of octadecylsilica groups, generating the SiGO-C18. Infra-red spectroscopy assays revealed that both steps were successful – supporting GO onto Si and further C18 customization. Scanning electron microscopy showed spherical geometries with minor irregularities and narrow particle size distribution for the produced SPs. The GO-coating rate was higher on the Si particles of 10 μm. As a result, the 10 μm produced column reported better resolution, efficiency, and peak capacity. Therefore, this SiGO-C18 capillary column (100 mm × 0.32 mm i.d., 10 μm dp) was applied successfully in a column-switching method to separate hormones in urine. Linearity (R2 above 0.99), quantification limits (between 1.0 and 5 μg/L), and other figures of merit of the method were determined. It is worth mentioning that the SiGO-C18 capillaryLC column performed adequately, separating the

* Corresponding author.
E-mail address: flancas@iqsc.usp.br (F.M. Lanças).
[1] Present address: Clemens Schöpf Institute, Department of Chemistry, Technical University of Darmstadt, 64287 Darmstadt, Germany.
[2] Present address: Catalan Institute of Nanoscience and Nanotechnology (ICN2), CSIC & BIST, Campus UAB, Bellaterra, 08193 Barcelona, Spain.

https://doi.org/10.1016/j.aca.2022.340718
Received 5 August 2022; Received in revised form 7 December 2022; Accepted 9 December 2022
Available online 10 December 2022

target compounds in less than 6 min. We hope this work could significantly contribute to shedding some light on graphene-based materials as a promising class of stationary phase for miniaturized liquid chromatography.

Abbreviations

C18	octadecylsilica
CE	collision energy
CV	cone voltage
DoE	design of experiments
d_p	particle; diameter
EDC	1-ethyl-3-(3-dimethyl aminopropyl) carbodiimide hydrochloride;
FA	formic acid
FPP	fully porous particle
G	graphene
GBMs	graphene-based material
GO	graphene oxide;
IPA	isopropanol
MeCN	acetonitrile;
MeOH	methanol
MRM	multiple reaction monitoring
NHS	N-hydroxisuccinimide 97%
Si	amino sílica
SiGO	graphene oxide covalently supported onto amino silica
SiGO-C18	octadecyl silica functionalized graphene oxide onto amino silica
SP	stationary phase
SPP	superficial porous particle
TMS	trimethylchlorosilane

1. Introduction

Since the 1940s, scientists have been investigating the existence of **graphene** (**G**) as another carbon allotrope form. However, in 2004, Novoselov and coworkers isolated a single graphene sheet from pyrolytic graphite through a process known as mechanical exfoliation [1]. Graphene has a single-atom layer of sp^2 hybridized carbons on a hexagonal honeycomb lattice, sustained by solid in-plane σ bonds and an out-of-plane π-electron system [2]. This structural arrangement provides excellent mechanical resistance and flexibility [2]. Nowadays, graphene is one of the most tested materials for several goals principally because of its intrinsic characteristics such as good light transmittance (97.7) and thermal conductivity (5000 W/(mk)), high Young's modulus (1 TPa), and tensile breaking strength (135 GPa), and also a large specific surface area (2630 m2/g) [3]. Furthermore, due to the graphene π-electron system, electrons can move more straightforwardly than in graphite, providing excellent electrical conductivity with low resistivity and high electron mobility at room temperature (15.000 cm^2/v.s) [3]. These attractive properties have boosted graphene applications in many areas, such as energy storage, sensors, thermal interfaces, electronic circuits, catalysts, solar cells, and chemistry [3–8].

Graphene and related materials, particularly its precursor **graphene oxide (GO),** have been used as sorbents in analytical chemistry since 2011 [9,10]. As a result of the excellent extraction performance reported, the last decade has been marked by a considerable number of applications employing **graphene-based materials (GBMs)** in a broad range of sample preparation techniques [6]. On the other hand, quite a few papers were focused on assessing GBMs' potential as stationary phase (SP) for liquid chromatography (LC). However, their physicochemical properties suggest them as a promising candidate. For example, in addition to the large reactive surface area, G and GO can be chemically functionalized for customization – by inserting other reactive groups on their primary structure, mainly to improve chemical selectivity towards a specific class of target analytes. Furthermore, their excellent mechanical stability is a valuable characteristic of an LC stationary phase.

Furthermore, they can be obtained from a relatively easy and cost-effective process [11]. On the other hand, the G irregular morphology can be a weakness, curtailing its use as LC stationary phase. This occurs because packing the nanosheets in an LC column is challenging, especially for obtaining a highly homogenous and stable packed bed. Considering LC as an essential separation technique in analytical chemistry, it is normal to have many studies on improving chromatographic performance. One of the most explored strategies is the development of novel LC stationary phases (SPs) to achieve significant efficiency and faster analysis [12]. For example, analytical chemists currently count on a decent range of SPs, such as metal-organic frameworks, ionic liquids, mesoporous silica, polymers, cyclodextrins, and carbon-based materials [12–14]. For this latter, carbon nanotubes (single- and multi-walled), fullerene, and porous graphite have already been tested [15]. It is worth mentioning that these SPs are being investigated as alternatives to the well-recognized and commercially available octadecylsilica (C18), octyl silica (C8), amino (-NH2), cyano (CN), and phenyl-hexyl SPs. Although these traditional SPs have reported satisfactory results over the years, the desire for customized materials to better cope with specific classes of analytes with more selectivity encourages the "search" for novel stationary phases [12].

The current status of GBMs, a trend in carbonaceous material, suggests that they will potentially become a promising class of SP for LC. So far, some published works deserve mention in this topic: open-tubular capillaryLC columns coated with G and GO [16], octadecylsilica-functionalized GO particles [17], self-assembled GO-bonded silica LC columns [18], G- and GO-bonded silica SPs [19], GO-bonded silica functionalized with gold nanoparticles [20], graphene-modified quantum dots [21], and, graphene anchored onto core-shell SiO_2 particles [22]. In complement, Aydoğan and coworkers published interesting results on graphene-based monolithic LC columns. Such recent works have a different focus (monolith-based GO instead of our GO-based particles), though they reinforce the underdevelopment role of GBMs as LC stationary phases. Despite these positive contributions, the problems associated with graphene and graphene oxide morphology – their tendency of agglomeration and increased probability of clogging – still pose a challenge in wide-spreading the subject [19]. To overcome such downside, it is common to support GBMs onto the surface of other materials to produce more robust stationary phases capable of withstanding higher pressures [23]. An interesting approach is to covalently binding G or GO onto silica-based particles by a peptide bond. It is worth mentioning that more attention is required for evaluating the main chromatographic characteristics of these graphene-based LC columns, for example, by testing them in complex matrices instead of only employing standard analytical solutions.

Considering the subject as state-of-the-art in this niche of analytical chemistry, coming up with a study focused on producing, characterizing, and testing graphene-based LC stationary phases in a complex matrix might be a relevant contribution. Therefore, we present a study focusing on a novel **octadecylsilica-functionalized graphene oxide** supported **onto aminopropyl silica (SiGO-C18)** stationary phase for

capillaryLC-MS/MS analysis of hormones in urine samples. The target analytes were dexamethasone, estradiol, estrone, hydrocortisone, and progesterone. Of note, the stationary phase was end-capped to block residual silanol groups. The chromatographic resolution, efficiency, retention mechanism, and peak capacity were systematically evaluated to obtain a performance "footprint" for the SIGO-C18$_{ecp}$ LC column. A chemometric optimization and determination of essential validation parameters (linearity, precision, accuracy, selectivity, LOQs, and LOQs) were performed using the matrix-matched concept in free-of-hormones urine samples. To the best of our knowledge, this is the first time a graphene-based capillaryLC column was effectively employed and tested (as a proof-of-concept) in the separation of hormones in urine, a vital bio-fluid widely investigated by analytical (bio)chemists.

2. Methods

2.1. Reagents and standards

LC grade Acetonitrile (MeCN), Methanol (MeOH), Isopropanol (IPA), Toluene, Hydrochloric acid 37% (HCl), and Tetrahydrofuran (THF) were all acquired from Tedia (Fairfield, USA). MS-grade high-purity (>98%) formic acid (FA) was purchased from Honeywell Fluka (Seelze, DE). Deionized ultra-pure water (H2O) used in this work was in-lab produced by a Milli-Q® Millipore system (Burlington, USA). For obtaining GO, **SiGO (graphene oxide** supported **onto aminopropyl silica),** and SiGO-C18: graphite powder (<20 μm), potassium permanganate 99% ($KMnO_4$), sodium nitrate 99% (NaNO3), N-hydroxisuccinimide 97% (NHS), dimethylformamide (DMF), trimethylchlorosilane (TMS), and 1-ethyl-3-(3-dimethyl aminopropyl) carbodiimide hydrochloride (EDC) were purchased from Sigma-Aldrich (St. Louis, USA). In addition, both sulfuric acid 98% (H_2SO_4) and imidazole 98% AR-grade were provided by Mallinckrodt (Paris, FR), Hydrogen peroxide 30% (H_2O_2) from Synth (Diadema, BR), Hydrazine/Water 80% from Merck (Darmstadt, DE), and chloride-methyl-n-octadecylsilica (C18) 95% from Alfa Aesar (Ward Hill, USA). As supporting material, **aminopropyl silica (Si)** from different particle diameters – 5 and 10 μm – were acquired from Sigma-Aldrich (St. Louis, USA). Dexamethasone, estradiol, estrone, hydrocortisone, and progesterone high-purity analytical standards were purchased from Sigma-Aldrich (St. Louis, USA). Stock solutions of each hormone were prepared in MeOH at a concentration level of 1000 mg/L and kept at −7 °C. Finally, individual or mixed working solutions were prepared in (i) ultrapure water for evaluating fundamental chromatographic parameters of the SiGO-C18 capillary LC column and (ii) spiked urine samples for testing SiGO-C18 column performance in the separation of hormones.

2.2. Analytical instrumentation

The produced SPs were characterized by Fourier-transform infrared spectroscopy (FTIR) and scanning electron microscopy (SEM). The instruments used were an IRAffinity-1 infrared spectrophotometer from Shimadzu (Kyoto, JP), operating in 400–4000 cm^{-1} using KBr-based disks, and a LEE 440 scanning electron microscope from ZEISS-Leica (Cambridge, UK). The liquid chromatograph was an Acquity M-Class coupled to a mass spectrometer Xevo TQ S Micro from Waters (Milford, US). The LC-MS platform was equipped with the following modules: μ-binary solvent manager, sample manager, and trap-valve manager. Chromatographic separations were carried out using lab-made SiGO-C18 (100 × 0.32 mm) FPP 10 μm, SiGO-C18 (100 × 0.32 mm) FPP 5 μm, and a commercial Thermo Fisher Hypersil GOLD aQ C18 (100 × 0,32 mm) SPP 1.9 μm. It is worth mentioning that FPP stands out for fully porous particles and SPP for superficially porous particles. The mobile phase consisted of H_2O (A) and MeCN (B), combined according to the specific test (detailed information throughout the manuscript); in some cases, 0.1% of formic acid was employed as an additive to enhance the positive electrospray (ESI) ionization process. Other chromatographic parameters include column temperature, 35 °C; injection volume, 0.2 μL; and mobile phase flow rate, 4–12 μL/min (depending on the experiment). The MS parameters were: positive electrospray ionization (ESI+); capillary voltage, 3.5 kV; source temperature, 150 °C; desolvation gas, N_2, desolvation gas flow, 600 L/h; desolvation temperature, 330 °C; collision gas, Ar; collision gas flow, 0.100 mL/min. The experimental data were processed by MassLynx 4.2 software from Waters. Tandem MS parameters were obtained by direct infusion of the target hormones at 0.5 mL/min, diluted into the mobile phase (H_2O: MeCN, 80:20). Table S1, in the supplementary material, shows the ion transitions used in the multiple reaction monitoring mode (MRM), the respective collision energies (CE), and cone voltages (CV).

2.3. Stationary phases

Following Hummers' method, GO was obtained with minor modifications [24]. In short, 0.5 g of graphite powder, 25 mL of H_2SO_4, and 0.5 g of $NaNO_3$ were placed within a 250 mL round bottom flask and stirred for 120 min under an ice bath. Sequentially, 3.0 g of $KMnO_4$ was added gradually under continuous stirring and left for more than 60 min. After such a period, the ice bath was removed, the temperature was raised to 40 °C (assisted by an oil bath), and the reaction was left stirring overnight. The reaction mixture changed color from dark green to light brownish as time passed. After the reaction color changed, the flask was put back in the ice bath, and approx. 100 mL of H_2O was added under slow stirring. After, 5 mL of H_2O_2 30% was added carefully, using a Pasteur pipette, while the reaction color turned yellow. Later, the reaction was left resting (approx. 16 h) while GO turned into a brown precipitate. Finally, the supernatant was removed, GO was centrifuged at 5040 RCF for 20 min, washed several times with HCl 5% aqueous solution, and then washed with H_2O until pH 7. Sequentially, the reaction product was dispersed in water, sonicated for 30 min, and centrifuged at 1260 RCF for 20 min. Lastly, the GO precipitate was lyophilized.

For supporting GO onto Si surface, based on previous research group experiences for producing GBMs [25,26], two steps were modified: (i) replacement of bigger particles often used for sample preparation by aminopropyl silica particles (Si) of diameters suitable for chromatographic separation: 5 and 10 μm dp FPP, and (ii) use of the aqueous (or wet route) suggested by Liu et al. [27], instead of the organic route employing DMSO, as we already used in the past. Apart from that, every procedure step was similar. In short, 20 mg of GO, dispersed in 40 mL of ultrapure H_2O, was sonicated for 1 h. After, 375 μL of an aqueous solution containing 10 mol/L EDC and 5 mol/L NHS was prepared and left stirring for 30 min - aiming to activate the GO nanosheets – to favor the peptide bond formation between GO oxygenated groups and Si amino groups. After, 0.5 g of Si was added, and the reaction was left stirring at room temperature for 4 h. Then, the obtained solid (SiGO) was washed several times, alternating between MeOH and ultrapure H_2O. Finally, the solid was centrifuged at 5040 RCF for 20 min and lyophilized.

The last step was the functionalization of SiGO with C18 and subsequent end-capping for obtaining the desired material (SiGO-C18$_{edc}$) to be tested as an LC stationary phase. In short, 200 mg of SiGO dissolved in 2 mL of dry toluene, 2.5 mg of imidazole dissolved in 200 μL of dry toluene, and 20 mg of C18 dissolved in 300 μL of toluene were transferred to a two-necked flask coupled to a Friedrich condenser, under an N_2 atmosphere. The reaction mixture was left refluxing at approximately 50 °C for 5 h. After that period, the SiGO-C18 particles were vacuum filtered and washed several times in sequence with toluene, MeOH, MeOH/H_2O (50%), and MeOH. Finally, the reaction product was dried at 40 °C for 72 h. The stationary phase end-capping was performed in similar reaction conditions but replacing C18 with 50 μL of TMS – all other reagents and steps were the same. The final product, SiGO-C18$_{edc}$, was not lyophilized, only dried in an oven for 72 h at 40 °C. The supplementary material shows the process for obtaining the stationary phases – from GO to SiGO-C18 – in Fig S1.

2.4. Production of capillary columns

The in-lab made capillary LC columns were made of 100 mm glass-lined stainless-steel tubes (fused silica capillary covered by stainless steel tube) of 1/16 inches o.d. and 0.32 mm i.d. The frits were 1–2 mm glass wool filter discs (1/16 inches diameter and 0.2 μm porosity). The frit was placed into the tubes using a Valco 1/16 inches set of unions, nuts, and ferrules. To begin the packing process, 0.7 mg of each stationary phase was washed with 1 mL of acetone to remove the free GO nanosheets in the solution. Next, the precipitate (SiGO-C18 particles) was collected and dried at room temperature. Next, the slurry-packing process was performed using a hydro-pneumatic pump DSHF-300 (Haskel, Burbank, USA) at 9000 kPa (900 bar) for 1 h, followed by 30 min of pressure re-equilibration. The packing solvent was H_2O, while the SiGO-C18 particles were suspended in a mixture of IPA: THF 4:1 before being transferred to the packing chamber. More detailed information is provided in the supplementary material (FIG S2).

2.5. Separation of hormones in urine

After producing and performing some fundamental evaluation of the capillary LC columns, an actual application for separating hormones in urine samples was carried out, focusing on the analytical column that reported the best results. The authors herein consider that coming up with an application using the produced SiGOC18 capillaryLC column in a complex matrix such as human urine might reinforce its real applicability. In this stage, the capillaryLC-MS analytical system also included a SiGO in-house produced capillary extraction column for performing automated sample pre-treatment before chromatographic separation occurs in the developed SIGO-$C18_{ecp}$ LC column. In this context, a chemometric optimization using a full factorial design 2^4 with the center point replicated four times was conducted to investigate the influence of some analytical variables: urine pH (% formic acid), sample loading time, sample loading flow, and % MeCN in the loading mobile phase. The % of formic acid added to urine samples were 0.0, 2.5, and 5.0%; the loading times tested were 0.25, 1.63, and 3.00 min; the loading flow rates tested 5.0, 12.0, and 19.0 μL/min; and the % MeCN added to the loading mobile phase were 0.0, 15.0 and 30%. Table S2 (supplementary material) shows the experiments and combinations of values of the variables considered in this step. These variables were selected taking into account previously published works, assuming they could affect the analytical performance in similar approaches [28,29].

Although this work is focused on the fundamental evaluation of SiGO-C18 capillary columns in terms of chromatographic efficiency, selected figures of merit were studied to verify the quality of this work in a complex matrix (urine). Their evaluation was done following the International Conference on Harmonization (ICH) guideline Q2(R1) [30]. The parameters evaluated were selectivity, linearity, accuracy, precision (intra- and inter-day), recovery (%), limits of detection, and quantification (LOD and LOQ). During this step, we employed free-of-hormones urine samples as our representative matrix. The method selectivity was evaluated by comparing the chromatographic profiles among blank urine samples and the spiked ones to verify whether there is any interfering peak at the same retention time of each hormone. First, the LODs and LOQs were set as the concentration levels generating a signal-to-noise ratio of 3 and 10 times, respectively. Next, the linearity was assessed using spiked blank urine samples by applying the matrix-matched method. The analytical curve included six concentration levels evaluated in triplicate injections (5, 20, 40, 60, 80, and 100 μg L-1, n = 3). Accuracy was determined in three concentration levels (5, 40, and 80 μg L-1, n = 3) by comparing the theoretical value (C_t, theoretical concentration) with that experimentally reported accordingly with the linear equation (C_r, actual concentration) and expressed as recovery percent. Finally, precision was presented as relative standard deviation (RSD%) and evaluated at the same three concentration levels on the same day that linearity was evaluated (intra-day) and on a subsequent day (inter-day). Acceptation criteria considered accuracy between 70 and 110% and precision with RSD <20%. At last, the pre-concentration factors for each analyte were evaluated by injecting samples in the automated sample-prep-capillaryLC-MS system and the capillaryLC-MS instrument.

3. Results and discussion

3.1. Stationary phase characterization

The stationary phases' geometry interferes directly with the packing process, principally in forming a suitable and homogeneous packed bed that might modify the chromatographic performance. Spherical particles are ideal for producing high-efficient LC columns as the round shape generates compact unit cells, perfect for minimizing void volumes. Void volumes contribute to the analytes' molecular diffusion within the column. Another critical requirement for the stationary phase is a narrow range of particle diameters. Similar particles generate similar voids, while irregular particles generate irregular voids, maximizing undesirable molecular diffusion. Therefore, the morphology of aminopropyl silica particles was evaluated by scanning electron microscopy before the functionalization step with GO and C18. The photomicrographs depicting the aminopropyl silica particles showed a spherical geometry with minor irregularities (Fig. 1A) and a narrow particle size distribution (Fig. 1B).

Also, it is relevant to ensure that GO and C18 are chemically bound to the Si support. A simple and effective way to assess it is by confirming through FTIR that bonds between the Si particles and the binders (GO and C18) were formed (Fig. 2A). The bands in 800 and 1080 cm^{-1} refer to the Sil-OH bending vibration and Sil-O-Sil stretching vibration, respectively. The band at 1650 cm^{-1} is related to C═O bending vibration from a peptide bond, suggesting that GO was covalently supported onto the aminopropyl silica surface. The band at 3450 cm^{-1} indicates bending vibrations from the O–H bonds. Notably, this band presented 80% of transmittance in the Si and Si-GO spectra. However, on the SiGO-C18 particles, it is almost inexistent, suggesting the formation of the SiGO-C18 material, which decreased the presence of free oxygenated groups. Likewise, the sharp bands on 2928 and 2856 cm^{-1} can be associated with CH_2 and CH_3 bending vibration, indicating the formation of the SiGO-C18 functionalized material. Although the FTIR strongly indicates the formation of the SiGO-C18 material, the powder obtained is composed of different particles, as seen in Fig. 2B. A fraction of this material comprises Si particles not bonded to GO sheets, and a minor part comprises broken particles and free GO sheets. The scanning electron microscopy (SEM) pictures demonstrated that both particle diameters explored were coated partially by the GO sheets (Fig. 2C). Although both were coated, the difference in the coating yield was observed. The 5 μm Si particles presented some of the GO nanosheets formed compact structures similar to a "paper ball" on the surface of Si particles. However, they extended, and almost flat graphene GO nanosheets were bonded to the particles. The 10 μm particles presented the best coating of Si particles with GO nanosheets. The surface of 10 μm Si particles shows high coverage and flatter graphene sheets compared to the smallest ones.

3.2. Chromatographic evaluation

The SiGO-C18 capability to be employed as a packed LC stationary phase was evaluated by separating five hormones: dexamethasone, estrone, estradiol, hydrocortisone, and progesterone. Those compounds were selected because they present a similar main structure but different chemical ramifications. The SiGO-C18 stationary phase is demonstrated to retain and separate those compounds (Fig. 3). In the chromatograms of Fig. 3A and B (SiGO-C18 particles of 10 and 5 μm d_p), it is possible to see thinner peaks for the column packed with particles of 10 μm than for the one packed with particles of 5 μm. Additionally, the SiGO-C18

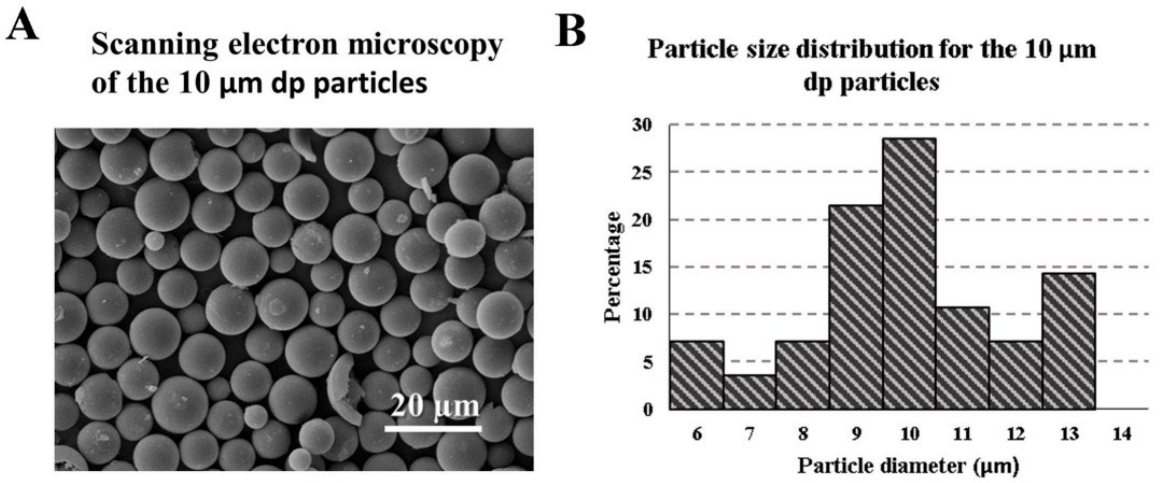

Fig. 1. (A) Photomicrography of the 10 µm dp Si particles. (B) Particle size distribution of the 10 µm dp Si particles.

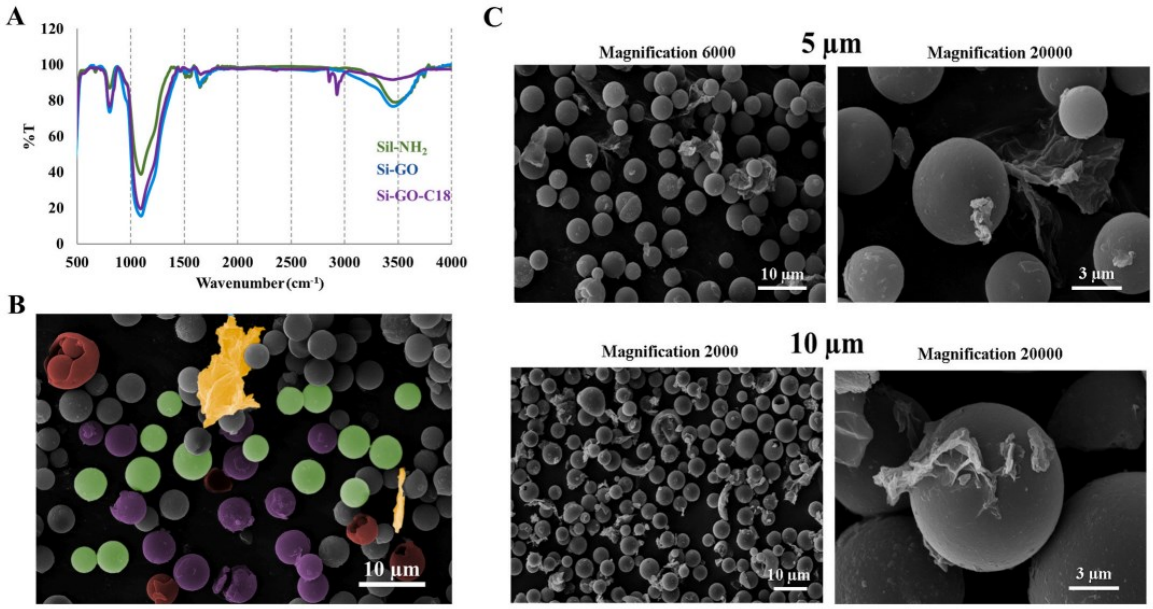

Fig. 2. (A) FTIR spectra of aminopropyl silica, Si (green), graphene oxide covalently supported onto aminopropyl silica, SiGO (blue), and octadecylsilica-functionalized graphene oxide covalently supported onto aminopropyl silica, SiGO-C18 (purple). (B) Photomicrograph of the 10 µm particles highlighting the bonded SiGO particles (purple), non-bonded Si particles (green), non-bonded GO (yellow), and broken particles (red). (C) Photomicrographs of SiGO-C18 particles of 5 µm and 10 µm with magnification to visualize the bulk and the individual particles. (For interpretation of the references to color in this figure legend, the reader is referred to the Web version of this article.)

column packed with particles of 10 µm is more retentive. Compared to a commercially available Thermo Fisher Hypersil GOLD aQ C18 column packed with particles of 1.9 µm, both in-lab produced SiGO-C18 columns presented thicker peaks but with the same retention order. An explanation for the more retentive behavior of the SiGO-C18 column (packed with 10 µm particles) is that, in this case, we achieved a better GO coating rate onto the Si surface. Therefore, in addition to hydrophobic interactions promoted by C18 groups – also observed in the commercially available C18 column – there are also interactions between the π-delocalized electron system from the GO and the cyclic structure of the hormones.

On the other hand, this interaction seems not strong enough to change the retention order among the different columns. Moreover, it is widely known that GO has some oxygen-containing groups pointing its planar nanosheets outwards and, despite participating in the peptide bonds formed with the Si, others can remain free, enhancing the polar character of the SiGO-C18 stationary phase. Another important characteristic to remember is that this secondary interaction promoted by

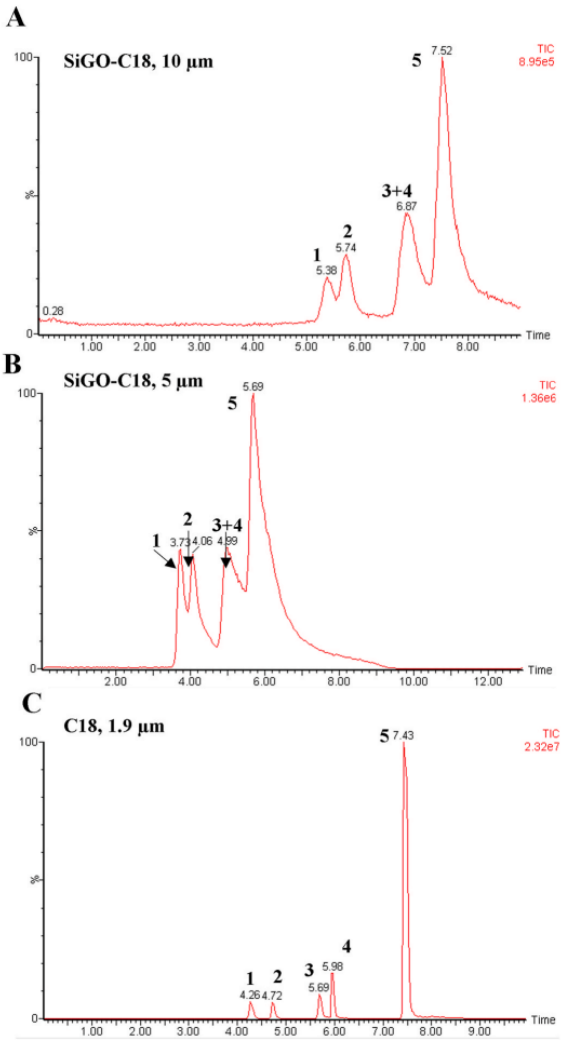

Fig. 3. Separation of (1) hydrocortisone, (2) dexamethasone, (3) estradiol, (4) estrone, and (5) progesterone in (A) SiGO-C18, 10 µm dp, (B) SiGO-C18, 5 µm dp, and (C) commercially available C18, 1.9 µm dp. The analyzes were performed in gradient mode with an initial concentration of 20% MeCN and a final concentration of 5% in 5.5 min. The flow rate was of 6 µL/min, the temperature was set at 30 °C, the standard sample spiked at a concentration of 75 µg/L, and the injection volume of 0.2 µL.

the GO structure seems to help better separate some matrix-interfering substances from the analytes. This occurrence can favor the ESI process and obtain a cleaner MS spectrum. This late phenomenon is better observed when the SiGO-C18 column was coupled with the SiGO extraction column, which provided us with suitable chromatographic separation and sample cleanup. This result is discussed in detail in the next section, 3.3.

It is essential to understand the effect of the retention time on its consequences in the increment of the bandwidth. Therefore, it is a meaningful comparison to assess how the particle size of mixed stationary phases influences column performance. This comparison is demonstrated using dexamethasone (Fig. 4A) and progesterone (Fig. 4B). Observing the results for dexamethasone, the column packed with SiGO-C18 particles of 10 µm d_p showed more attenuated band broadening than the column packed with particles of 5 µm d_p. Even in cases where the values of peak width in the dexamethasone plot are smaller for the column packed with particles of 5 µm than for the 10 µm, it is relevant to note that in proportion to the retention time, the column packed with 10 µm SIGO-C18 particles remain more efficient. Of note, the same conclusions were drawn for progesterone. The efficiency parameter is very objective in comparing the performance of chromatographic columns. Therefore, a comparison of the efficiency reported for columns packed with both particle diameters was performed (Fig. 4C). The column packed with particles of 10 µm showed higher efficiencies for the respective retention times than that one packed with 5 µm particles. The exception is the last point in the progesterone plot, where the column packed with 5 µm particles showed the higher efficiency. Resolution is another important parameter for evaluating performance and is directly related to efficiency. Both columns showed similar resolution in the analysis performed at 35% MeCN in the mobile phase. The only condition that resolution was higher on the column packed with 5 µm was in 65% MeCN, but still very close to the column packed with particles of 10 µm. The better-reported performance for the SiGO-C18 column packed with particles of 10 µm can be explained by two factors: (i) the higher GO coating rate for Si particles of 10 µm dp, and (ii) the profile of the column-packed bed, which is detailed discussed below (Fig. 4D).

The better GO coating rate on the surface of Si particles of 10 µm was discussed in the previous sections and Fig. 2C. The packed bed was investigated by analysis using 75% MeCN; almost no retention was observed in this case (Fig. 4D). Likewise, Fig. 4E confirms that the hormones were not retained in these conditions. They were eluted simultaneously in the dead time, and the difference in the retention time of the lesser and most retained compound was below 0.1 min. The SiGO-C18 column packed with particles of 10 µm presented a smaller bandwidth for all analytes, indicating that the packed bed is more homogeneous and superior to the one packed with 5 µm (Fig. 4F). This can occur because of some different characteristics: (i) 10 µm particles are larger and more prompt to form unit cells; (ii) the 10 µm particles are more compatible with the inner diameter of tubes (0.32 mm i.d.) used for producing the capillary columns, as demonstrated by Gritti [31].

Elution gradients are also widely exploited in LC separations. Unlike isocratic mode, in which the analyte is eluted constantly, in gradient mode, the analyte is retained at the head of the column until the % organic solvent in the mobile phase is sufficient to remove it from the stationary phase. Because of this, some parameters evaluated under isocratic conditions are incompatible with a gradient of elution. In this case, the peak capacity is the main factor for evaluating the performance of chromatographic separations employing an elution gradient. However, peak capacity is dependent on chromatographic efficiency. With this dependency in mind, analyses employing different flow rates were performed. Notably, the mobile phase flow rate is one of the main parameters affecting efficiency and will be explored in this section. For the less retained compound (dexamethasone, Fig. 5A), both analytical columns – packed with SiGO-C18 particles of 5 and 10 µm – presented similar retention for each flow rate explored. For progesterone (Fig. 5B), the column packed with particles of 10 µm was more retentive than its 5 µm counterpart at all flow rates explored. Compared to the commercial C18 column, the estrone was less retained in both SiGO-C18 LC columns (Fig. 5C). The peak width on both columns was compared to a commercial C18 column (Fig. 5D). The commercial C18 column presented lower peak broadening than both SiGO-C18 columns.

The SiGO-C18 column packed with particles of 10 µm presented lower band dispersion in all tested flow rates than the 5 µm, especially in the low flow rate region. These data show that SiGO-C18 stationary phases are adequately employed in gradient mode, applicable over a wide mobile phased flow range. The column packed with SiGO-C18 particles of 10 µm diameter showed superior performance. In elution gradient mode, the peak capacity is one of the main parameters to

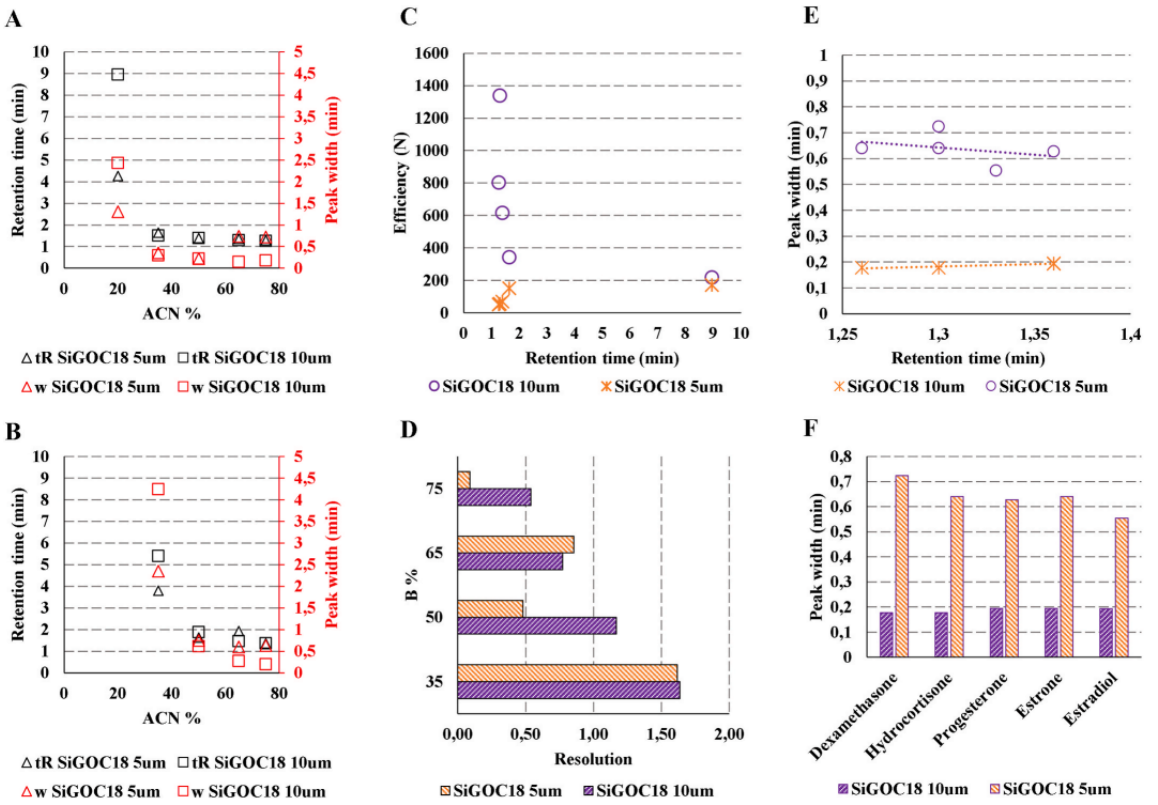

Fig. 4. (A) Retention time as a function of % MeCN for dexamethasone (at a flow rate of 12 μL/min). (B) Retention time as a function of % MeCN for progesterone (at a flow rate of 12 μL/min). (C) Chromatographic efficiency vs. retention time for dexamethasone. (D) Chromatographic resolutions between dexamethasone and progesterone for each % MeCN were explored. (E) Bandwidth as a function of retention time to hormones in no retentive conditions – 75% MeCN. (F) Bandwidth to the hormone series in no retentive condition. All the analyses were performed at a flow rate of 12 μL/min and 30 °C, sample concentration of 75 μg/L, and injection volume of 0.2 μL.

evaluate chromatographic performance. The column packed with SiGO-C18 particles of 10 μm presented more peak capacity than the column packed with particles of 5 μm. The peak capacity in the column packed with particles of 5 μm is approximately 50% smaller than its 10 μm counterpart (Fig. 5E). The causes of the superior peak capacity reported for the column packed with particles of 10 μm d_p over the column packed with the 5 μm ones are still unknown. Several factors can affect the peak capacity in the elution gradient, such as intrinsic properties of the analytes, stationary phase, and elution gradient conditions [32]. Keeping this in mind, the higher peak capacity of the 10 μm d_p SiGO-C18 column can only be stated accurately for the target hormones herein analyzed. Therefore, other classes of target analytes must be tested first to extend this statement. The resolution between dexamethasone and progesterone on both SiGO-C18 packed columns was compared to a commercial C18 column. The commercial column presented a higher resolution on flow rates below 8 μL/min than the SiGO-C18 columns. The column packed with SiGO-C18 particles of 10 μm presented a slightly higher resolution than the column packed with 5 μm SiGO-C18 particles. In the 8 μL/min, the three columns presented a similar resolution. Interestingly, at flow rates superior to 8 μL/min, the column packed with SiGO-C18 particles of 5 μm presented the highest resolution, and the commercial column the lowest one (Fig. 5F). This result demonstrated that, in gradient mode, the column packed with 5 μm SiGO-C18 particles may be suitable for operating at higher flow rates.

It is worth mentioning that despite the promising results reported in this work, the SiGO-C18 stationary phase and also the steps for producing such columns might be evaluated further. Although we were able to suitable separate the hormones using the SiGO-C18 columns (10 and 5 μm of particle), they showed lower overall performance when compared to the commercially available C18 column (except at flow rates ≤8 μL/min). Some reasons can explain this conclusion. One of the major facts favoring the higher efficiency of the commercial C18 column over the proposed ones, is informed in Fig. 3: while the commercial column utilized 1.9 μm (average) particles, our columns were packed with 5 and 10 μm (average) particles. Also, C18 columns have been optimized for a long time, possessing a well-defined theory about many aspects which contribute to producing highly efficient columns. For example, it is already known that capillary columns of RPLC (i.e., C18) are ideally packed by employing slurry solvents which promote agglomeration of particles instead of highly dispersed solutions. Accordingly, with Armstrong et al. [33], the combination between slurry solvent and intrinsic properties of the stationary phase is a crucial factor directly influencing the packing efficiency.

On the other hand, GBMs and, thereby, our SiGO-C18 stationary phase is still under developing materials with several possibilities of optimization, especially in terms of using it as an LC stationary phase, as not too much has been done so far towards this type of application. That said, it was already expected to see superior performance for the commercially available C18 column. Still, we demonstrated a similar performance of the SiGO-C18 column at low flow rates, which in our

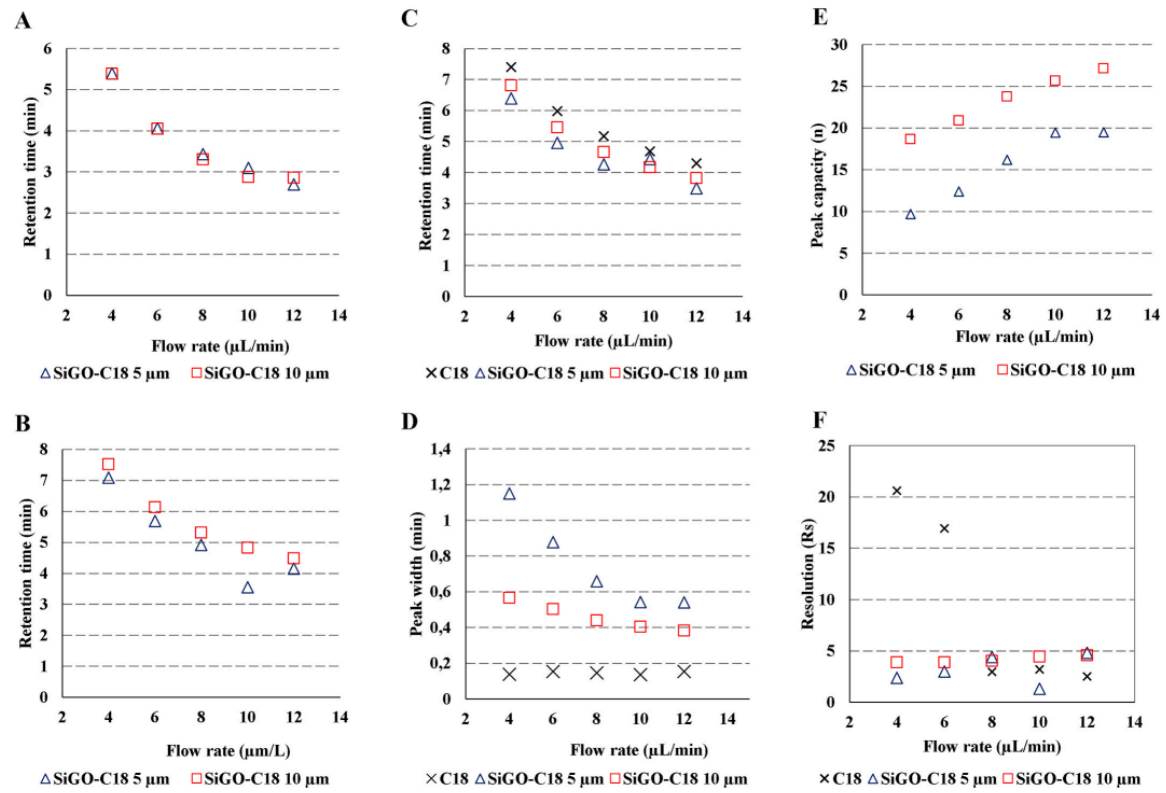

Fig. 5. (A) Retention time as a function of the flow rate for dexamethasone. (B) Retention time as a function of the flow rate for the progesterone. (C) Comparison of estrone retention time in the SiGO-C18 columns (open forms) with the commercial C18 column (black crosses). (D) Comparison of estrone's peak width in the SiGO-C18 columns (open forms) with commercial C18 column (black crosses). (E) Comparison of the peak capacity between the columns packed with 10 and 5 µm SiGO-C18 particles. (F) Comparison of the chromatographic resolution between dexamethasone and progesterone in the columns packed with 10 and 5 µm SiGO-C18 particles (open forms) and commercial C-18 column (black crosses). The analysis was performed in gradient mode with an initial concentration of 20% MeCN and a final concentration of 95% in 5.7 min. The temperature was 30 °C, the sample concentration of 75 µg/L, and the injection volume of 0.2 µL.

opinion, is already a promising result. Noteworthy, we synthesized the stationary phase and optimized the packing system for making capillary columns, and further tested them, while ref [17] used only 4.6 mm id columns, which are quite distinct from our columns. From our point of view, figuring out an ideal composition of slurry solvents for efficiently packing this SiGO-C18 or other GBMs might be a good starting point for improving the quality of these columns. Moreover, as already discussed by Gritti [31], finding the best combination between column ID and particle diameter could be another strategy for producing highly efficient columns packed with under-development stationary phases.

Most importantly, the focus was to demonstrate that the SiGO-C18 capillary column can represent an efficient alternative for separating target compounds in a complex matrix as human urine. However, it is crucial to remember that most published works on the same topic employ these newly developed columns in only standard mixtures [17–19,22]. Therefore, it does not represent, in some cases, the primary role of an LC column.

3.3. Applicability in urine samples

A design of experiments (DoE 2^4) was conducted to optimize the analytical conditions for the automated extraction and capillary-LC-MS determination of the hormones in urine. Pareto charts, response surfaces, and desirability functions were evaluated to obtain the best conditions. According to the Pareto chart (Figure S3A), the most significant variables were loading time (V1), loading flow (V2), and % formic acid added to urine samples (V3). It is worth mentioning that % of MeCN in the loading mobile phase had a no-significant effect on the method. Therefore, we opted for using only ultrapure water without MeCN as an additive in the subsequent steps. Although only cortisol is represented in the Pareto chart, it must be highlighted that the other four hormones reported similar behavior. According to Figure S3A, there is a positive effect on the method performance when the loading time is decreased, possibly because allowing urine samples to interact more time with the extraction column also increases the sorption of interfering substances. The addition of formic acid in the urine samples for altering the pH was done to optimize the ESI ionization efficiency of the hormones, as they can assume different charge states according to the sample pH. Once we used positive ESI, it was expected that adding formic acid would enhance our analytical response to the analytes, as seen from the Pareto chart. In addition, the variable loading flow exhibited a positive effect when increased, suggesting that a better interaction between hormones and the extraction column would be achieved at higher flow rates during the automated sample preparation step.

In the sequence, the response surfaces and desirability models show the interaction between two variables simultaneously and how they affect the method performance. This is useful in achieving an optimized condition for the variables, considering all hormones simultaneously. It is worth mentioning that the variable % MeCN in the loading mobile phase was removed from the experimental data, as it did not

significantly affect the method. However, as seen in Figure S.3B, there is a positive effect of diminishing loading time and increasing loading flow. At the same time, Figure S.3C shows an improvement in method performance when adding formic acid to the urine samples – decreasing its pH – and once again by adopting short loading times.

Furthermore, Figure S3D suggests a better condition when higher loading flow rates were combined with adding formic acid in the samples. Note that all these results corroborate with those already suggested by Pareto charts. Finally, the predicted values and the desirability function profiles were used to find a final optimized analytical condition for each variable in the multi-response experiments (Figure S4). So, by combining the DoE 2^4 and the desirability function, we were capable of obtaining a single optimized condition for the analytical method: 0.25 min of loading time, 19 μL min-1 of loading flow, urine samples acidified with 2.5% FA, and loading mobile phase without acetonitrile composed only of ultrapure water.

To evaluate the merits of this work, the most common figures of merit were determined and presented as follows. Figure S5 illustrates a representative chromatographic separation obtained for a spiked urine sample (75 μg/L) using the SIGO-C18ecp LC capillary column. As seen from (A), the MRM transition for each hormone is well-separated with adequate baseline and no interfering peaks at the retention times of the target analytes, indicating that the method is selective. The linearity was evaluated in six concentration levels from 5 to 100 μg/L for the hormones, and the reported determination coefficients (R2) were above 0.992, demonstrating an excellent linear tendency. Detection limits (S/N = 3) were between 0.05 and 2.0 μg/L, and quantification limits stood between 1.0 and 5 μg/L for all target analytes (S/N = 10). The method accuracy – measured by comparing three theoretical concentration levels for spiking samples with that obtained from the linear equation – showed values between 86.20 and 103.80%, which complied with the acceptance criteria. Intra- and inter-day precision expressed as RSD were 8.6–20% and 14–20%, respectively. Finally, the developed automated method's pre-concentration factor employing an online extraction column coupled with the SIGO-C18ecp analytical column reported good values between 4.5 and 8.2. Figure S5 (B) compares a chromatogram obtained using the online automated sample prep-capillaryLC-MS method and another acquired by direct injection of the same sample. As can be seen, there is a gain on the peak intensity of approx. 3-fold when using the automated sample prep approach. This can be explained by the capacity of the extraction column to pre-concentrating the hormones before injecting them into the analytical SiGO-C18 column. Table S3 in the supplementary material contains detailed information regarding the studied figures of merit.

4. Conclusions

A novel LC stationary phase using graphene oxide, further customized with octadecylsilica, has been applied to simultaneously determine five hormones in human urine. The chromatographic performance of the produced stationary phases was investigated considering several relevant factors: material characterization, packing process, efficiency, resolution, and applicability to an actual matrix. SEM Characterization assays were performed to measure the influence of Si particles' geometries in forming a homogeneous packed bed and, consequently, in the chromatographic separation. Spherical particles are ideal for producing highly efficient LC columns. The round shape generates compact unit cells, perfect for minimizing void volumes and widely recognized for enhancing the molecular diffusion of analytes. The photomicrographs of the aminopropyl silica particles showed a spherical geometry with minor irregularities (Fig. 1A) and narrow particle size distribution (Fig. 1B). The Si particles of 10 μm exhibited a higher GO coating rate, possibly because bigger particles collide more frequently with the free GO nanosheets while a coupling reaction occurs. FTIR spectra indicated that GO was covalently supported on the aminopropyl silica surface and successfully functionalized with C18 groups, resulting in the SiGO-C18 stationary phase.

In the sequence, some fundamental parameters for evaluating the performance of the SiGO-C18 capillary LC columns were evaluated in two conditions: (i) isocratic and (ii) elution gradient. In isocratic elution-based experiments, the column packed with 10 μm SiGO-C18 particles showed lower band broadening than the column packed with particles of 5 μm for all proportions of H2O: MeCN tested in the mobile phase. Therefore, the column packed with particles of 10 μm showed higher efficiencies for the respective retention times than the one packed with 5 μm particles. Furthermore, the low bandwidth reported by the column of 10 μm particles showed that a more homogeneous packed bed was formed. In this case, possibly the diameters of the large particles (10 μm) favor the formation of unit cells more efficiently, being more compatible with the column's inner diameter explored in this work (0.32 mm). The chromatographic resolution was similar for columns packed with 5 and 10 μm. In gradient elution-based experiments, both SiGO-C18 stationary phases are adequately employed in gradient mode, applicable to an extensive mobile phase flow rate range. Again, the column packed with SiGO-C18 particles of 10 μm diameter showed superior performance. In this case, this column had a 2-fold higher peak capacity than the one packed with particles of 5 μm. Interestingly, comparing both in-house made LC columns with the commercially available C18 showed comparable performance in flow rates at capillary scale (≥8 μL/min).

The capillary column packed with particles of 10 μm was applied further to separate five hormones in human urine using an automated sample-prep capillaryLC-MS approach. Although the SiGO-C18 column did not reach the highest chromatographic efficiency across the entire range of flow rates tested, it reached similar performance to the commercially available C18 column at a standard flow rate used in capillaryLC (e.g., 8 μl/min). It is worth keeping in mind that commercially available columns are optimized constantly and extensively, imposing a real challenge for new in-lab developed columns to reach precisely the same performance. On the other hand, this work shows that, despite the different performances, the SiGO-C18 column can be applied without significant concerns for separating compounds in human urine. Therefore, underscoring its real applicability and role as an LC analytical column. The leading figures of merit (linearity, LOQs, LODs, precision, accuracy, and pre-concentration factor) complied with the acceptance criteria of the ICH Q2(R1) guideline. Preliminary results showed that this SiGO-C18 stationary phase could be a promising alternative to the conventional stationary phase in capillary LC separations. It is worth mentioning that this work also demonstrated the separation of hormones present in "real" urine samples. This is an excellent aspect as, in several cases, in-house produced LC columns are just tested in standard mixtures of compounds, not considering the role they must play in routine analytical workflows.

CRediT authorship contribution statement

EdvaldoV.S. Maciel: Writing – original draft, Writing – review & editing. **João V.B. Borsatto:** Writing – original draft, Writing – review & editing. **Karen Mejia-Carmona:** Methodology, Resources. **Fernando M. Lanças:** Conceptualization, Funding acquisition, Project administration, Supervision, Writing – review & editing.

Declaration of competing interest

The authors declare here that they have no competing interest or personal relationships that could have influenced this work.

Data availability

Data will be made available on request.

Acknowledgment

The Fundação de Amparo à Pesquisa do Estado de São Paulo, FAPESP [Grant 2017/02147-0]; the Conselho Nacional de Ciência e Tecnologia, CNPq [Grant 308843/ 2019-3] and the Coordenação de Aperfeiçoamento de Pessoal de Nível Superior – Brasil, CAPES [Grant Finance Code 001] supported this work.

Appendix A. Supplementary data

Supplementary data to this article can be found online at https://doi.org/10.1016/j.aca.2022.340718.

References

[1] K.S. Novoselov, A.K. Geim, S.V. Morozov, D. Jiang, Y. Zhang, S.V. Dubonos, I. V. Grigorieva, A.A. Firsov, Electric field effect in atomically thin carbon films, Science 306 (2004) 666–669, https://doi.org/10.1126/science.1102896, 80.
[2] G. Yang, L. Li, W.B. Lee, M.C. Ng, Structure of graphene and its disorders: a review, Sci. Technol. Adv. Mater. 19 (2018) 613–648, https://doi.org/10.1080/14686996.2018.1494493.
[3] C. Simanjuntak, R. Siburian, H. Marpaung, Tamrin, Properties of Mg/graphite and Mg/graphene as cathode electrode on primary cell battery, Heliyon 6 (2020), e03118, https://doi.org/10.1016/j.heliyon.2019.e03118.
[4] N. Saba, M. Jawaid, Energy and environmental applications of graphene and its derivatives, in: Polym. Nanocomposites Energy Environ. Appl., Elsevier, 2018, pp. 105–129, https://doi.org/10.1016/B978-0-08-102262-7.00004-0.
[5] A. Nag, A. Mitra, S.C. Mukhopadhyay, Graphene and its sensor-based applications: a review, Sensors Actuators A Phys 270 (2018) 177–194, https://doi.org/10.1016/j.sna.2017.12.028.
[6] E.V.S. Maciel, K. Mejía-Carmona, M. Jordan-Sinisterra, L.F. da Silva, D.A. Vargas Medina, F.M. Lanças, The current role of graphene-based nanomaterials in the sample preparation arena, Front. Chem. 8 (2020), https://doi.org/10.3389/fchem.2020.00664.
[7] J.S. Lewis, T. Perrier, Z. Barani, F. Kargar, A.A. Balandin, Thermal interface materials with graphene fillers: review of the state of the art and outlook for future applications, Nanotechnology 32 (2021), 142003, https://doi.org/10.1088/1361-6528/abc0c6.
[8] T. Mahmoudi, Y. Wang, Y.-B. Hahn, Graphene and its derivatives for solar cells application, Nano Energy 47 (2018) 51–65, https://doi.org/10.1016/j.nanoen.2018.02.047.
[9] Y.-B. Luo, J.-S. Cheng, Q. Ma, Y.-Q. Feng, J.-H. Li, Graphene-polymer composite: extraction of polycyclic aromatic hydrocarbons from water samples by stir rod sorptive extraction, Anal. Methods 3 (2011) 92–98, https://doi.org/10.1039/C0AY00624F.
[10] Y.-B. Luo, Z.-G. Shi, Q. Gao, Y.-Q. Feng, Magnetic retrieval of graphene: extraction of sulfonamide antibiotics from environmental water samples, J. Chromatogr. A 1218 (2011) 1353–1358, https://doi.org/10.1016/j.chroma.2011.01.022.
[11] L. Sun, Structure and synthesis of graphene oxide, Chin. J. Chem. Eng. 27 (2019) 2251–2260, https://doi.org/10.1016/j.cjche.2019.05.003.
[12] K. Broeckhoven, G. Desmet, Advances and innovations in liquid chromatography stationary phase supports, Anal. Chem. 93 (2021) 257–272, https://doi.org/10.1021/acs.analchem.0c04466.
[13] J. Zhang, Z. Chen, Metal-organic frameworks as stationary phase for application in chromatographic separation, J. Chromatogr. A 1530 (2017) 1–18, https://doi.org/10.1016/j.chroma.2017.10.065.
[14] A.W. Sobańska, Emerging or underestimated silica-based stationary phases in liquid chromatography, Crit. Rev. Anal. Chem. (2020) 1–25, https://doi.org/10.1080/10408347.2020.1760782.
[15] S.R. Beeram, E. Rodriguez, S. Doddavenkatanna, Z. Li, A. Pekarek, D. Peev, K. Goerl, G. Trovato, T. Hofmann, D.S. Hage, Nanomaterials as stationary phases and supports in liquid chromatography, Electrophoresis 38 (2017) 2498–2512, https://doi.org/10.1002/elps.201700168.
[16] Q. Qu, C. Gu, X. Hu, Capillary coated with graphene and graphene oxide sheets as stationary phase for capillary electrochromatography and capillary liquid chromatography, Anal. Chem. 84 (2012) 8880–8890, https://doi.org/10.1021/ac3023636.
[17] X. Liang, S. Wang, S. Liu, X. Liu, S. Jiang, A novel octadecylsilane functionalized graphene oxide/silica composite stationary phase for high performance liquid chromatography, J. Separ. Sci. 35 (2012) 2003–2009, https://doi.org/10.1002/jssc.201200258.
[18] X. Liang, S. Liu, X. Song, Y. Zhu, S. Jiang, Layer-by-layer self-assembled graphene oxide/silica microsphere composites as stationary phase for high performance liquid chromatography, Analyst 137 (2012) 5237, https://doi.org/10.1039/c2an36091h.
[19] X. Zhang, S. Chen, Q. Han, M. Ding, Preparation and retention mechanism study of graphene and graphene oxide bonded silica microspheres as stationary phases for high performance liquid chromatography, J. Chromatogr. A 1307 (2013) 135–143, https://doi.org/10.1016/j.chroma.2013.07.106.
[20] X. Liang, X. Wang, H. Ren, S. Jiang, L. Wang, S. Liu, Gold nanoparticle decorated graphene oxide/silica composite stationary phase for high-performance liquid chromatography, J. Separ. Sci. 37 (2014) 1371–1379, https://doi.org/10.1002/jssc.201400005.
[21] Q. Luo, Z. Zhong, Y. Zheng, D. Gao, Z. Xia, L. Wang, Preparation and evaluation of a poly(N-isopropylacrylamide) derived graphene quantum dots based hydrophilic interaction and reversed-phase mixed-mode stationary phase for complex sample analysis, Talanta 224 (2021), 121869, https://doi.org/10.1016/j.talanta.2020.121869.
[22] H. Qian, W. Li, X. Wang, F. Xie, W. Li, Q. Qu, Simultaneous growth of graphene/mesoporous silica composites using liquid precursor for HPLC separations, Appl. Surf. Sci. 537 (2021), 148101, https://doi.org/10.1016/j.apsusc.2020.148101.
[23] R. Cong, M. Cheatham, C. Hollis, T. Hill, K. Bailey, K. Jackson, D. Mekap, B. Glad, P. Tyler, Z. Zhou, Fabrication of graphene-coated silica particles for polymer chromatography to quantify chemical composition distribution of polyolefin materials, Macromolecules 54 (2021) 7140–7146, https://doi.org/10.1021/acs.macromol.1c00912.
[24] W.S. Hummers, R.E. Offeman, Preparation of graphitic oxide, J. Am. Chem. Soc. 80 (1958), https://doi.org/10.1021/ja01539a017, 1339–1339.
[25] E.V.S. Maciel, B.H. Fumes, A.L. de Toffoli, F.M. Lanças, Graphene particles supported on silica as sorbent for residue analysis of tetracyclines in milk employing microextraction by packed sorbent, Electrophoresis 39 (2018) 2047, https://doi.org/10.1002/elps.201800051. –2055.
[26] K. Mejía-Carmona, F.M. Lanças, Modified graphene-silica as a sorbent for in-tube solid-phase microextraction coupled to liquid chromatography-tandem mass spectrometry. Determination of xanthines in coffee beverages, J. Chromatogr. A 1621 (2020), 461089, https://doi.org/10.1016/j.chroma.2020.461089.
[27] Q. Liu, J. Shi, J. Sun, T. Wang, L. Zeng, G. Jiang, Graphene and graphene oxide sheets supported on silica as versatile and high-performance adsorbents for solid-phase extraction, Angew. Chem. Int. Ed. 50 (2011) 5913–5917, https://doi.org/10.1002/anie.201007138.
[28] E.V.S. MacIel, K. Mejiá-Carmona, F.M. Lancas, Evaluation of two fully automated setups for mycotoxin analysis based on online extraction-liquid chromatography-TandemMass spectrometry, Molecules 25 (2020), https://doi.org/10.3390/molecules25122756.
[29] AL de Toffoli, E.V.S. Maciel, F.M. Lanças, Evaluation of the tubing material and physical dimensions on the performance of extraction columns for online sample preparation-LC–MS/MS, J. Chromatogr. A 1597 (2019) 18–27, https://doi.org/10.1016/j.chroma.2019.03.023.
[30] I.C. on Harmonisation, Validation of Analytical Procedures: Text and Methodology Q2(R1), 2005, p. 17.
[31] F. Gritti, A stochastic view on column efficiency, J. Chromatogr. A 1540 (2018) 55–67, https://doi.org/10.1016/j.chroma.2018.02.005.
[32] U.D. Neue, Theory of peak capacity in gradient elution, J. Chromatogr. A 1079 (2005) 153–161, https://doi.org/10.1016/j.chroma.2005.03.008.
[33] M.F. Wahab, D.C. Patel, R.M. Wimalasinghe, D.W. Armstrong, Fundamental and practical insights on the packing of modern high-efficiency analytical and capillary columns, Anal. Chem. 89 (2017) 8177–8191, https://doi.org/10.1021/acs.analchem.7b00931.

Capítulo 7

Online extraction followed by LC–MS/MS analysis of lipids in natural samples: a proof-of-concept profiling lecithin in seeds

Borsatto, João V. B.; Maciel, Edvaldo V. S.; Cifuentes, Alejandro; Lanças, Fernando M. Online Extraction Followed by LC–MS/MS Analysis of Lipids in Natural Samples: A Proof-of-Concept Profiling Lecithin in Seeds. **Foods**, *[S. l.]*, v. 12, n. 2, p. 281, 2023. DOI: 10.3390/foods12020281. Disponível em: https://www.mdpi.com/2304-8158/12/2/281

foods

MDPI

Communication

Online Extraction Followed by LC–MS/MS Analysis of Lipids in Natural Samples: A Proof-of-Concept Profiling Lecithin in Seeds

João V. B. Borsatto [1,2], Edvaldo V. S. Maciel [1,3], Alejandro Cifuentes [2,*] and Fernando M. Lanças [1]

[1] Laboratory of Chromatography, Institute of Chemistry at Sao Carlos, University of Sao Paulo, P.O. Box 780, Sao Carlos 13566590, Brazil
[2] Laboratory of Foodomics, Institute of Food Science Research (CIAL, CSIC), Nicolás Cabrera 9, 28049 Madrid, Spain
[3] Clemens Schöpf Institute, Department of Chemistry, Technical University of Darmstadt, 64287 Darmstadt, Germany
* Correspondence: a.cifuentes@csic.es

Abstract: Sample preparation is usually a complex and time-consuming procedure, which can directly affect the quality of the analysis. Recent efforts have been made to establish analytical methods involving minimal sample preparation, automatized and performed online with the analytical techniques. Online Extraction coupled with Liquid Chromatography–Mass Spectrometry (OLE–LC–MS) allows a fully connected extraction, separation, and analysis system. In this work, the lecithin profile was investigated in commercial sunflower, almonds, peanuts, and pistachio seeds to demonstrate that the concept of extraction, followed by the online analysis of the extract, could be applied to analyze this class of analytes in such complex solid matrices without a prior off-line solvent extraction step. The extraction phase gradient method was optimized. Two different analytical columns were explored, one being a conventional C18 (50 × 2.1 mm, 1.7 µm SPP) and the other a novel self-packed SIGO-C18ec (100 × 0.5, 5 µm FPP), which resulted in better separation. The analysis repeatability was investigated, and suggestions to improve it were pointed out. A characteristic ion with a m/z of 184, related to lysophosphatidylcholine structure, was used to identify the lecithin compounds. The temperature effect on the chromatograms was also explored. In short, it was found that the OLE–LC–MS approach is suitable for the analysis of lecithin compounds in seeds, being a promising alternative for lipidomics approaches in the near future.

Keywords: online sample preparation; OLE–LC–MS/MS; lipids; lecithin; SiGO-C18ec column; seeds; lipidomics

Citation: Borsatto, J.V.B.; Maciel, E.V.S.; Cifuentes, A.; Lanças, F.M. Online Extraction Followed by LC–MS/MS Analysis of Lipids in Natural Samples: A Proof-of-Concept Profiling Lecithin in Seeds. *Foods* **2023**, *12*, 281. https://doi.org/10.3390/foods12020281

Academic Editors: Luís Miguel Rodriguez-Alcalá, Lígia Pimentel and Susana Vidigal

Received: 16 November 2022
Revised: 23 December 2022
Accepted: 29 December 2022
Published: 7 January 2023

1. Introduction

Sample preparation online coupled with the analytical instrument (usually LC–MS (Liquid Chromatography–Mass Spectrometry) or GC–MS (Gas Chromatography–Mass Spectrometry)) is a trend in modern analytical chemistry [1,2], particularly useful in the qualitative and quantitative analysis of multi-analytes in complex matrices, such as natural products. Automating sample preparation and joining it to analytical methods can reduce analytical errors, labor, and the amount of solvents utilized, creating simple and environmentally friendly approaches [3–5]. The sample preparation, alongside human error and equipment problems, are the three primary sources of errors in most analytical methods [6]. In-tube SPME is an example of a technique widely used for online coupling sample extraction with LC, which requires minimal sample preparation or even no sample pre-processing before starting the automated procedure [7–10]. Nevertheless, when the sample is a solid, in-tube SPME cannot be used without a previous sample preparation step to convert the solid sample into a solution compatible with the technique. Online

extraction coupled with liquid chromatography (OLE–LC) is an exciting alternative for minimizing or suppressing this previous step, allowing the automated sample preparation of solid samples [11]. OLE–LC has been successfully applied to analyze natural and agro-products [12,13], soil samples [14,15], and other matrices [16–18]. To our knowledge, its applicability to the analysis of lipids in natural products has not been reported.

Lecithin is a general term given to amphiphilic lipid substances. Generally, it comprises a phospholipid connected to a glycerol group and different fatty acid groups; variations with groups such as glucose and cholesterol can also exist. In food industries, lecithin has been used with many purposes, such as an emulsifier, wetting agent, viscosity reduction, release agent, and in crystallization control [19,20]. In addition, it is a substance present in several natural sources [21], possessing a variety of fatty acids from source to source [22]. High-performance liquid chromatography coupled to MS has been an important tool for investigating polar and non-polar lipids [23,24]; supercritical fluid chromatography has also been applied [25] When an MS is unavailable, a derivatization process is often an option to analyze lipids by photodiode array (PDA) detection, owing to the lack of chromophores in the native lipids [26]. A review elaborated by Cajka and Fiehn summarizes the most relevant steps involved in lipid analysis. The report covered liquid chromatography, sample preparation, separation modes (such as reversed-phase LC, hydrophilic interaction chromatography, super-critical fluid chromatography, and two-dimensional liquid chromatography), mass spectrometry parameters, and data analysis [27]. Online approaches for the sample preparation of lipids have also been applied. For example, York and coworkers have developed a method to determine fat-soluble vitamins, mycotoxins, and hormones in hen egg yolk by sample cleanup by restricted access media coupled online to LC-MS [28]. Usually, lipids are analyzed in liquid chromatography (LC) with an octadecylsilane column (C18) or other more specialized columns [29–31]. The appropriate selection of a column stationary phase for lipids analysis is essential to avoid non-reversible binding between target compounds and the LC columns. Graphene oxide nanosheets covalently supported onto silica particles, chemically functionalized with octadecylsilica, and finally endcapped (SiGO-C18ec) is a promising solid material gaining new applications periodically. It has already been successfully applied as a sorbent for both extraction [32–34] and analytical columns [35]. Once OLE–LC can be considered a hybrid approach involving extraction and analytical steps, the SiGO-C18ec material can be considered worthy to be evaluated for this application.

This work aims to demonstrate that the OLE–LC–MS technique can be a promising tool for profiling lipid substances directly from a solid sample without non-automated and previous sample preparation. In addition, the effect of temperature on the analysis, repeatability, and column efficiency was also investigated.

2. Experimental

2.1. Chemicals, Samples, and Instrumentation

Chemicals: Chloroform (Avantor, Gliwice, Poland), formic acid (FA) (VWR International, Fontenay-sous-Bois, France), glass fiber filter 0.2 µm, lecithin refined standard 36,486 (ThermoFisher, GmbH, Karlsruhe, Germany), methanol (VWR international, Fontenay-sous-Bois, France), MilliQ water, line filter cartridge (Thermo scientific, Rockwood, USA), line filter hardware (Thermo scientific, Rockwood, NA, USA), 2-Propanol (VWR international, Fontenay-sous-Bois, France). Samples: almond seeds, pistachio seeds, peanut seeds, sunflower seeds.

LC Columns: C18 column of 50 × 2.1 mm and 1.7 µm superficially porous particles (SPP) (Phenomenex Inc., Torrance, NA, USA); SiGO-C18ec column prepared as described by Borsatto et al. [35], 100 × 0.5 mm and 5 µm fully porous particles (FPP) (details in Supplemental Materials Section S1), and silica particles 50–60 µm mesh (Sigma-Aldrich Co St. Louis, MO, USA). Instrumentation: Accela LC system composed of an auto-sampler and a column temperature controller, a quaternary pump, and a PDA detector (Thermo Electronic Corporation, San Jose, CA, USA) joined to a TSQ quantum access triple quadrupole

mass spectrometer (MS) fitted with an ESI source (Thermo Electronic Corporation, San Jose, CA, USA). Additionally, a cryogenic mill (Retsch, Haan, Germany) was used for grinding the seeds.

2.2. OLE System Assemble

First, the seeds are broken into pieces and mixed with silica in an Eppendorf in a ratio of 1:1 volume:volume. After that, it was macerated in a mill at room temperature until it formed a homogeneous-like powder with difficult differentiation between the silica particles and the seed material. Next, the lecithin refined standard powder was submitted to the same procedure before the analysis.

The OLE system assembly was: first, the line filter cartridge bottom (the part with the filter grade) was protected with a glass fiber filter of 0.2 µm. The filter was placed by pressing the upper part of the cartridge against the bottom part, cutting the filter in the middle. Next, the cartridge was opened again, and a small quantity of the mixture containing silica and the seed, just enough to partially cover the bottom of the cartridge (Figure 1A), was added. If an excess sample is added, the cartridge can be blocked. The addition of the sample to the cartridge is fast and takes less than one minute after the analyst acquires some practice. Next, the cartridge was placed in the line filter hardware in an inverse position and flushed with 100% water until the pressure stabilized (Figure 1B). After the pressure stabilization, the system was connected to the column inlet by the tubing, and the analysis started. For more details, see Supplemental Materials Section S2.

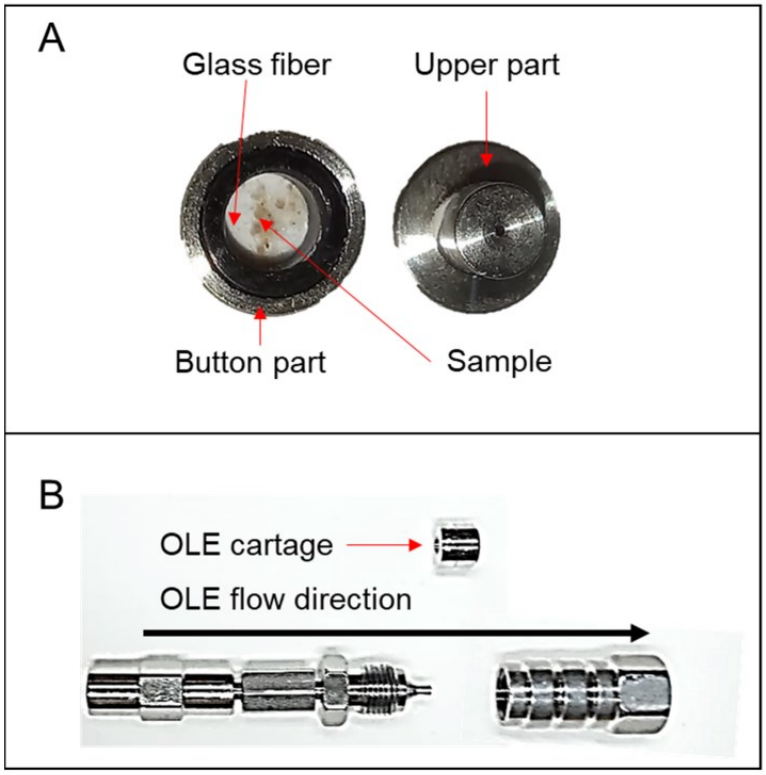

Figure 1. Set up of the analytical OLE system. (**A**) Example of OLE cartridge and the sample deposited on it. (**B**) Example of OLE hardware and flow direction during analysis.

2.3. OLE–LC–ESI–MS Analysis

The extraction method, in which the mobile phase work in the extraction and elution process, employed a quaternary gradient using water, methanol, chloroform, and 2-propanol, as described in Table 1. It is important to run the entire method presented in Table 1 to minimize the carry-over effect once the proportion of the organic solvents in the mobile phase to extract some compounds from the matrix could be different from the proportion of the organic solvents in the mobile phase to elute them from the column, causing this compound to accumulate in the column. For the C18 column, the employed flow rate was 0.3 mL/min, and for the SiGO-C18ec column, the flow rate varied between 0.2 and 0.15 mL/min. The temperature was kept constant at 30 °C, except for the experiments evaluating the influence of temperature variation. The MS method used a positive ESI with a skimmer offset voltage of 20 V, a full-scan mass range between 50 and 1200 m/z, a scan time of 1 s, and a collision voltage of 10 V.

Table 1. Time events of the quaternary gradient. The extraction and elution proceeded in a continuous flow.

Time	Water (0.1% FA) %	Methanol (0.1% FA) %	Chloroform %	2-Propanol %
0	100	0	0	0
10	0	100	0	0
20	0	10	90	0
30	0	10	0	90
35	0	10	0	90

3. Results and Discussion

3.1. Column Selection

The first step of this study was the column selection. Two columns, a standard commercial C18 and a self-packed SiGO-C18ec, were compared. Figure 2 shows typical chromatograms obtained in both columns: SiGO-C18eccolumn in Figure 2A and C18 column in Figure 2B. The SiGO-C18ec (Figure 2A) column presented a different selectivity than the commercial C18 column. It is worth mentioning that this selectivity difference between SiGO-C18ec and C18 was already observed for small molecules [35]. Due to these observations, it was decided to use the SiGO-C18ec column in the OLE–LC–MS experimental series aiming to profile lecithin in seeds. However, the SiGO-C18ec column presented some limitations that must be highlighted. The small inner diameter (0.5 mm) results in higher column backpressure that required an appropriate pumping system capable of withstanding high pressures, making the mobile phase flow through the system successfully. Within such a context, this characteristic demands operating at lower flow rates. Furthermore, the SiGO-C18ec particle is a new phase for LC, and its characteristics are not yet fully known, making it hard to propose the dominant separation mechanisms participating in the retention of the compounds. However, possible interactions between the analytes and the different types of π-bonding existing in the graphene oxide network and with the hydrophobic C18 chain has to be considered. Owing to the endcapping procedure executed during the stationary phase preparation, hydrophilic interactions on the silanol groups can be excluded (at least to a relevant extension).

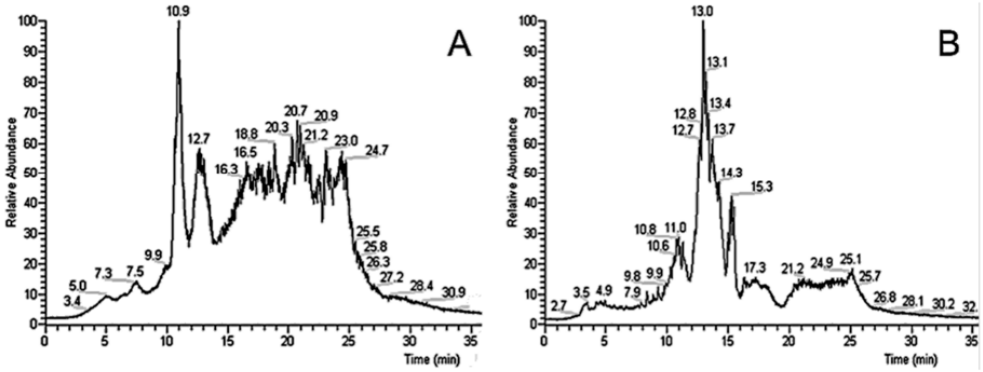

Figure 2. OLE–LC–MS analysis of sunflower seeds in quaternary gradient in (**A**) SiGO-C18ec (100 × 0.5, 5 µm FPP), at 0.2 mL/min and (**B**) C18 (50 × 2.1 mm, 1.7 µm SPP), at 0.3 mL/min. TIC chromatograms are in m/z range of 100 to 800. From 100% of H_2O (0.1% FA) to 100% of methanol (0.1% FA) in 10 min, followed by a linear gradient to 90% of chloroform and 10% of methanol (0.1% FA) in 10 min, and the last stem of a linear gradient of 90% of 2-propanol and 10% of methanol (0.1% FA) in 10 min, followed by more 5 min of isocratic 90% of 2-propanol and 10% of methanol (0.1% FA) at 30 °C.

3.2. Repeatability

Repeatability is an important parameter to be evaluated when proposing an analytical method or a new application for an existing analytical technique for quantitative and qualitative analysis. Figure 3 shows two sets of comparisons. Figure 3A,B shows the comparison of the OLE–LC–MS separation of sunflower seeds in a C18 column, and Figure 3C,D show the comparison of the OLE–LC–MS separation of lecithin standard in a SiGO-C18ec column. Note that the signal intensity for both pairs of repetitions is similar, suggesting that the amount of sample placed in the holder was similar. However, the peak shapes in the pairs of chromatograms are slightly different, although it is possible to do a straightforward correlation between peaks inside the same pair of replicates. The main explanation for this observation is related to the eddy diffusion phenomena. When the sample is placed into the extraction cartridge, and the mobile phase flows through it, some voids could be formed, and the analytes disperse themselves in those regions. Once the formation of the voids is random and varies from sample to sample and cartridge to cartridge, it affects the repeatability. Once the target of this work was not quantitative, no attempt was made to improve the repeatability, but further investigation into the cartridge packing conditions would undoubtedly improve this factor. The literature shows the possibility of operating OLE–LC–MS quantitatively [36].

3.3. Temperature Selection

Temperature is an essential variable in the extraction of compounds from a complex matrix (e.g., natural seeds). To evaluate how the temperature was affecting the extraction performance in the OLE–LC–MS experiments, a C18 column was used once the SiGO-C18ec phase characteristics were not yet fully known. Therefore, the temperature variation could affect the separation mechanism of the SiGO-C18ec column and produce bias in the observation of the effect of the temperature in the OLE–LC–MS analysis. Figure 4 shows the OLE–LC–MS analysis at three different temperatures, 30, 40, and 50 °C. Minimal changes between the chromatogram profile and the MS intensity can be seen. So, it was decided to proceed with further experiments at 30 °C once the SiGO-C18 column had already been operating at this temperature.

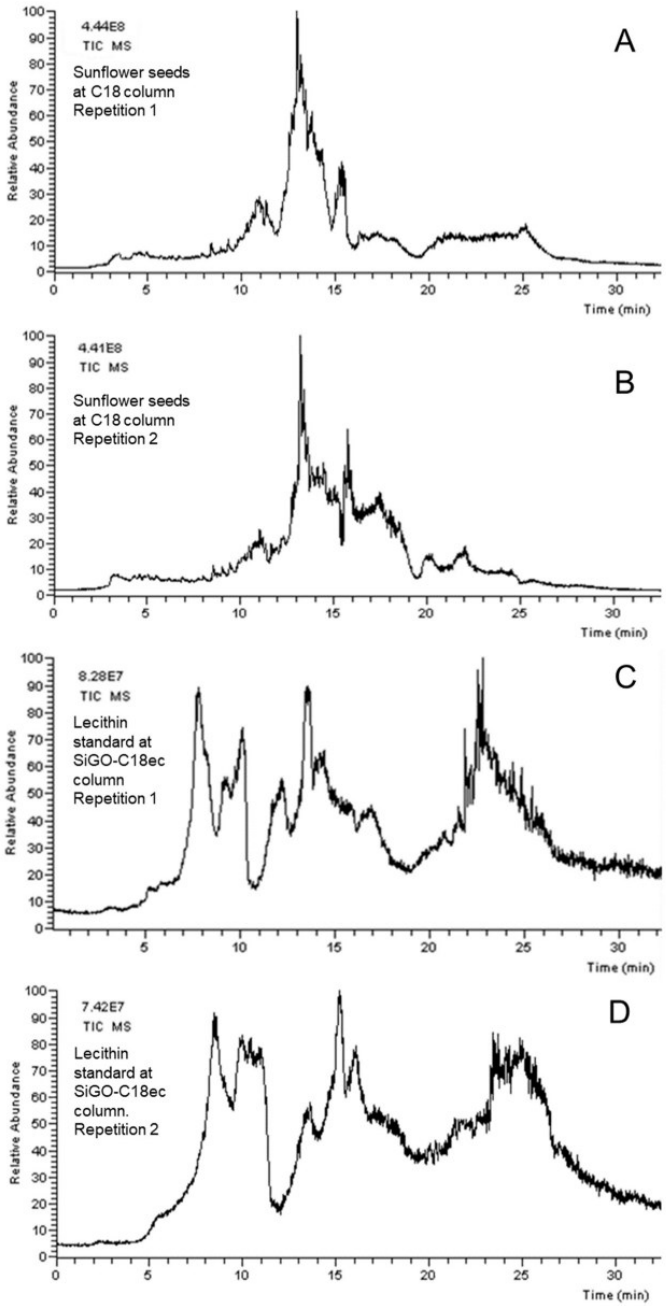

Figure 3. Repetitions of OLE–LC–MS analysis. Sunflower seeds in C18 column, 100 × 2.1, 1.9 SPP, at 0.3 mL/min (**A**,**B**) and lecithin standard in SiGO-C18ec, 100 × 0.5, 5 FPP, at 0.15 mL/min (**C**,**D**) in quaternary gradient going from 100% of H_2O (0.1% FA) to 100% of methanol (0.1% FA) in 10 min, followed by a linear gradient to 90% of chloroform and 10% of methanol (0.1% FA) in 10 min, and the last stem of a linear gradient of 90% of 2-propanol and 10% of methanol (0.1% FA) in 10 min, followed for more 5 min of isocratic 90% of 2-propanol and 10% of methanol (0.1% FA) at 30 °C. TIC chromatograms in m/z range of 50 to 1200.

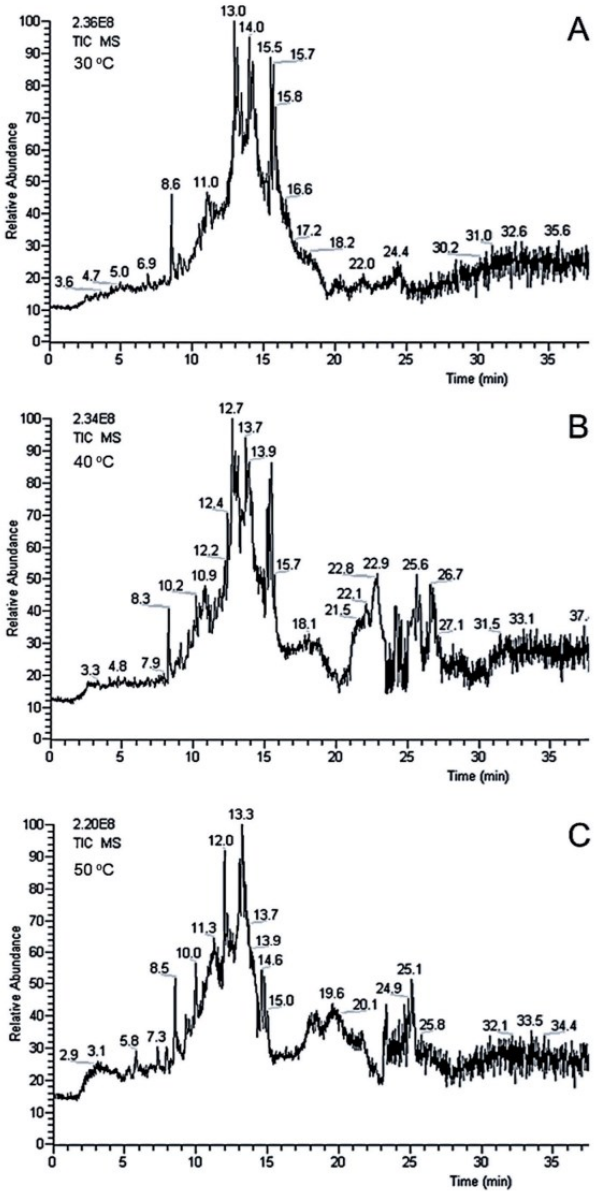

Figure 4. OLE–LC–MC analysis at (**A**) 30 °C, (**B**) 40 °C, and (**C**) 50 °C in the C18 column, 100 × 2.1, 1.9 SPP, at 0.3 mL/min. Quaternary gradient going from 100% of H_2O (0.1% FA) to 100% of methanol (0.1% FA) in 10 min, followed by a linear gradient to 90% of chloroform and 10% of methanol (0.1% FA) in 10 min, and the last stem of a linear gradient of 90% of 2-propanol and 10% of methanol (0.1% FA) in 10 min, followed for more 5 min of isocratic 90% of 2-propanol and 10% of methanol (0.1% FA) at 30 °C. TIC chromatograms in m/z range of 50 to 1200.

3.4. Lecithin Profile in Seeds Samples

As a proof of the potential application of the OLE–LC–MS approach to the online extraction–separation analysis of lipids in natural products, four different seeds were used: almond, peanut, pistachio, and sunflower. Lecithins were identified based on the characteristic ion at m/z = 184, related to the lysophosphatidylcholine structure in the

molecule [37]. Comparing the retention time and the MS spectra between the sample under study and the lecithin standard were also used to identify the investigated lecithin. Once a low-resolution triple quadrupole mass analyzer was used, confirming the identity of the fatty acids' fragments composing each lecithin structure was pretty challenging. Figure 5 shows the chromatograms obtained from the lecithin standard, the samples, and the blank (OLE cartridge containing only the glass fiber filter and silica particles). Although the blank sample shows some peaks, the blank chromatogram presents lower intensity than the samples' chromatograms. Consequently, it did not interfere in the observation of the peaks of the major compounds, but minor compounds in the sample might be suppressed. This can be confirmed by combining the MS spectra signals in this range and verifying that the characteristic lecithin MS spectrum could be visualized with no interference (the m/z signal recorded in the blank sample is displayed in the Supplemental Materials Section S3). A possible explanation for this signal on the blank sample can be attributed to a potential carry-over effect provoked by the non-reversible bonding of some compounds from the samples to the column. This effect should be investigated in further work. However, when the retention time was higher than 18 min, the MS spectra observed became more complex, with several peaks presenting relative intensity closer to the base peak. When comparing the chromatograms in Figure 4, all samples presented a similar chromatogram, especially in the region having chloroform in the mobile phase (between 10 to 20 min).

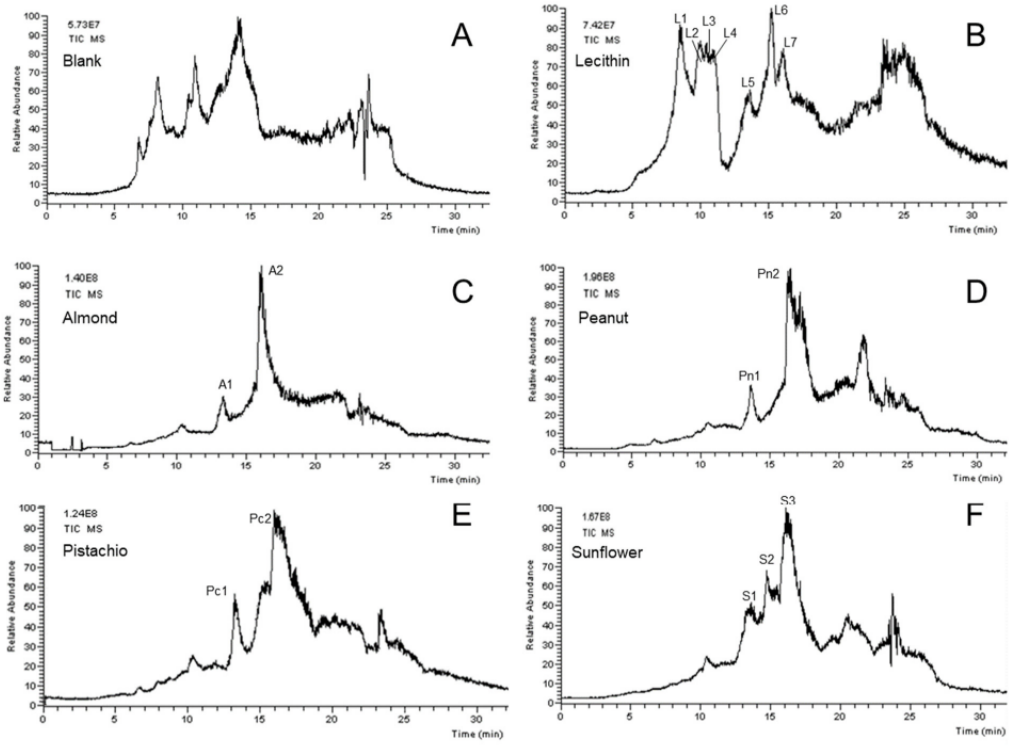

Figure 5. Comparison of the chromatograms obtained from (**A**) blank, (**B**) lecithin standard, (**C**) almond, (**D**) peanut, (**E**) pistachio, and (**F**) sunflower. Quaternary gradient going from 100% of H_2O (0.1% FA) to 100% of methanol (0.1% FA) in 10 min, followed by a linear gradient to 90% of chloroform and 10% of methanol (0.1% FA) in 10 min, and the last stem of a linear gradient of 90% of 2-propanol and 10% of methanol (0.1% FA) in 10 min, followed for more 5 min of isocratic 90% of 2-propanol and 10% of methanol (0.1% FA) at 30 °C. SiGO-C18ec (100 × 0.5, 5 FPP), at 0.15 mL/min. TIC chromatograms in m/z range of 50 to 1200.

Table 2 shows the retention time, the m/z values observed for each sample, and the lecithin standard when chloroform was present in the mobile phase. For the complete table with all lecithins observed in the lecithin standard, see the Supplemental Materials Section S4. Seven lecithins were observed in the lecithin analytical standard, 2 in almond (A1 and A2), 2 in peanut (Pn1 and Pn2), 2 in pistachio (Pc1 and Pc2), and 3 in sunflower (S1, S2, and S3). Although the MS spectra observed were slightly different for each kind of seed, they presented a similar pattern compared to the lecithin standard and the characteristic ion m/z = 184, which confirms lecithin's presence in the samples. Although the retention time and MS pattern presented similarities for all investigated samples, due to the complexity of the samples, it is challenging to confirm that they are the same substance. The sample identification step could be much improved by using a higher-resolution mass analyzer, including minor lecithins that could be co-eluted and were not investigated in this work. Despite these noticed drawbacks, the proposed approach demonstrates the possibility of automating a relevant step of the analysis of complex samples in difficult matrices, such as lipids in unprocessed seeds. This may provide an incentive for more studies expanding the focus on the qualitative analysis of other seeds or different solid complex matrices, using the fully automated online concept.

Table 2. Comparison of m/z values obtained in each retention time from a lecithin standard and from seed samples.

Lecithin Standard		Almond		Peanut		Pistachio		Sunflower	
tR	**m/z (+)**	**tR**	**m/z (+)**	**tR**	**m/z (+)**	**tR**	**m/z (+)**	**tR**	**m/z (+)**
13.6	184	13.3	184	13.3	184	13.3	184	13.5	184
			339		339				207
	575		577		577		575		575
	601		601		603		599		599
					643				
	758		758		760		758		758
	782		784		784		784		784
15.2	184					15	184	14.8	184
	306								207
							365		
									491
	575						575		575
	599						601		599
							617		615
	758						758		758
	782						784		782
	842								
									877
							883		
							919		
									935
16	184	16.1		16		16.3		16.2	184
	313								207
	575		577		577		577		575
	599								
			603		603		603		603
									615
	758								
	782								
			881		881		881		881
					882				
			905		905		905		904
					907				

4. Conclusions

This work demonstrated that OLC–LC–MS is a technique that can be applied for online extraction–analysis of lecithin from seeds. Furthermore, it is a promising technique for performing direct lipids analysis in solid matrices. The SiGO-C18ec column was more suitable for this application in this approach than the conventional C18 column. Additionally, it is the first reported separation performed in the SiGO-C18ec column using chloroform and 2-propanol in the mobile phase, demonstrating that this column is an alternative when a less-polar mobile phase is required. Finally, although the repeatability obtained in this work was not as good as desired for quantitative analysis, the literature shows that this potential drawback can be overcome when desired. Shortly, the results obtained in this work prompted us to investigate the described approach further to perform lipidomic studies using this OLE–LC–MS approach.

Supplementary Materials: The following supporting information can be downloaded at: https://www.mdpi.com/article/10.3390/foods12020281/s1, Supplementary Material.

Author Contributions: Conceptualization, J.V.B.B.; methodology J.V.B.B.; investigation, J.V.B.B. and E.V.S.M.; resources, F.M.L. and A.C.; writing—original draft preparation, J.V.B.B.; writing—review and editing, J.V.B.B., E.V.S.M., F.M.L. and A.C.; supervision, F.M.L. and A.C.; project administration, F.M.L. and A.C.; funding acquisition, F.M.L. and A.C. All authors have read and agreed to the published version of the manuscript.

Funding: The authors are grateful for the financial support from (i) the Coordination for the Improvement of Higher Education Personnel (CAPES–Brazil, Finance Code 001 and Proc. 88887.695324/2022-00); (ii) the São Paulo Research Foundation (FAPESP–Brazil, Grants 2019/22724-7, 2017/02147-0; (iii) the National Council for Scientific and Technological Development (CNPq–Brazil, 307293/2014-9; 308843/ 2019-3; Proc. 142513/2019-9); and (iv) the Spanish Ministry of Science and Innovation (PID2020-113050RB-I00 project).

Institutional Review Board Statement: Not applicable.

Informed Consent Statement: Not applicable.

Data Availability Statement: The data are available from the corresponding author.

Conflicts of Interest: The authors declare no conflict of interest.

References

1. Wei, D.; Li, M.; King, K.W.; Yang, L. Online and Automated Sample Extraction. *Bioanalysis* **2015**, *7*, 2227–2233. [CrossRef] [PubMed]
2. Serra-Mora, P.; Moliner-Martínez, Y.; Molins-Legua, C.; Herráez-Hernández, R.; Verdú-Andrés, J.; Campíns-Falcó, P. Trends in Online Intube Solid Phase Microextraction. *Compr. Anal. Chem.* **2017**, *76*, 427–461. [CrossRef]
3. Fumes, B.H.; Andrade, M.A.; Franco, M.S.; Lanças, F.M. On-Line Approaches for the Determination of Residues and Contaminants in Complex Samples. *J. Sep. Sci.* **2017**, *40*, 183–202. [CrossRef] [PubMed]
4. de Toffoli, A.L.; Fumes, B.H.; Lanças, F.M. Packed In-Tube Solid Phase Microextraction with Graphene Oxide Supported on Aminopropyl Silica: Determination of Target Triazines in Water Samples. *J. Environ. Sci. Health. B* **2018**, *53*, 434–440. [CrossRef] [PubMed]
5. MacIel, E.V.S.; Mejiá-Carmona, K.; Lancas, F.M. Evaluation of Two Fully Automated Setups for Mycotoxin Analysis Based on Online Extraction-Liquid Chromatography-TandemMass Spectrometry. *Molecules* **2020**, *25*, 2756. [CrossRef] [PubMed]
6. Technical Analytical Methods Committee Briefs What Causes Most Errors in Chemical Analysis? *Anal. Methods* **2013**, *5*, 2914–2915. [CrossRef] [PubMed]
7. Moliner-Martinez, Y.; Ballester-Caudet, A.; Verdú-Andrés, J.; Herráez-Hernández, R.; Molins-Legua, C.; Campíns-Falcó, P. 14—In-Tube Solid-Phase Microextraction. In *Solid-Phase Extraction*; Poole, C.F., Ed.; Elsevier: Amsterdam, The Netherlands, 2020; pp. 387–427, ISBN 9780128169063.
8. Kataoka, H. In-Tube Solid-Phase Microextraction: Current Trends and Future Perspectives. *J. Chromatogr. A* **2021**, *1636*, 461787. [CrossRef]
9. Costa Queiroz, M.E.; Donizeti de Souza, I.; Marchioni, C. Current Advances and Applications of In-Tube Solid-Phase Microextraction. *TrAC Trends Anal. Chem.* **2019**, *111*, 261–278. [CrossRef]
10. Gou, Y.; Pawliszyn, J. In-Tube Solid-Phase Microextraction Coupled to Capillary LC for Carbamate Analysis in Water Samples. *Anal. Chem.* **2000**, *72*, 2774–2779. [CrossRef]

11. Ferreira, V.G.; Leme, G.M.; Cavalheiro, A.J.; Funari, C.S. Online Extraction Coupled to Liquid Chromatography Analysis (OLE-LC): Eliminating Traditional Sample Preparation Steps in the Investigation of Solid Complex Matrices. *Anal. Chem.* **2016**, *88*, 8421–8427. [CrossRef]
12. Assirati, J.; Rinaldo, D.; Rabelo, S.C.; da Silva Bolzani, V.; Hilder, E.F.; Funari, C.S. A Green, Simplified, and Efficient Experimental Setup for a High-Throughput Screening of Agri-Food by-Products—From Polar to Nonpolar Metabolites in Sugarcane Solid Residues. *J. Chromatogr. A* **2020**, *1634*, 461693. [CrossRef] [PubMed]
13. Cao, Y.; Liu, W.; Gong, X.; Yu, J.; Tu, P.; Li, J.; Song, Y. Online Pressurized Liquid Extraction Enables Directly Chemical Analysis of Herbal Medicines: A Mini Review. *J. Pharm. Biomed. Anal.* **2021**, *205*, 114332. [CrossRef]
14. Votani, A.; Chisvert, A.; Giokas, D.L. On-Line Extraction Coupled to Liquid Chromatographic Analysis of Hydrophobic Organic Compounds from Complex Solid Samples—Application to the Analysis of UV Filters in Soils and Sediments. *J. Chromatogr. A* **2020**, *1610*, 460561. [CrossRef]
15. Maciel, E.V.S.; Lanças, F.M. A Cartridge-Based Device for Automated Analyses of Solid Matrices by Online Sample Prep–Capillary LC-MS/MS. *Anal. Bioanal. Chem.* **2022**, *414*, 2725–2737. [CrossRef] [PubMed]
16. Xu, X.; Li, T.; Zhang, K.; Cao, Y.; Liu, L.; Zhang, S.; Tu, P.; Song, Y.; Zhao, Y.; Li, J. Direct Flavonoid-Focused Chemical Comparison among Three Epimedium Plants by Online Liquid Extraction-High Performance Liquid Chromatography-Tandem Mass Spectrometry. *Molecules* **2021**, *26*, 1520. [CrossRef] [PubMed]
17. Qian, Z.-M.; Chen, L.; Wu, M.-Q.; Li, D.-Q. Rapid Screening and Characterization of Natural Antioxidants in Polygonum Viviparum by an On-Line System Integrating the Pressurised Liquid Micro-Extraction, HPLC-DAD-QTOF-MS/MS Analysis and Antioxidant Assay. *J. Chromatogr. B Anal. Technol. Biomed. Life Sci.* **2020**, *1137*, 121926. [CrossRef]
18. Wang, F.; Cheng, L.; Cao, Y.; Wei, Q.; Tong, C.; Shi, S. Online Extraction and Enrichment Coupling with High-speed Counter-current Chromatography for Effective and Target Isolation of Antitumor Anthraquinones from Seeds of Cassia Obtusifolia. *J. Sep. Sci.* **2022**, *45*, 938–944. [CrossRef]
19. Bot, F.; Cossuta, D.; O'Mahony, J.A. Inter-Relationships between Composition, Physicochemical Properties and Functionality of Lecithin Ingredients. *Trends Food Sci. Technol.* **2021**, *111*, 261–270. [CrossRef]
20. Deng, L. Current Progress in the Utilization of Soy-Based Emulsifiers in Food Applications—A Review. *Foods* **2021**, *10*, 1354. [CrossRef]
21. Alhajj, M.J.; Montero, N.; Yarce, C.J.; Salamanca, C.H. Lecithins from Vegetable, Land, and Marine Animal Sources and Their Potential Applications for Cosmetic, Food, and Pharmaceutical Sectors. *Cosmetics* **2020**, *7*, 87. [CrossRef]
22. Fernandes, G.D.; Alberici, R.M.; Pereira, G.G.; Cabral, E.C.; Eberlin, M.N.; Barrera-Arellano, D. Direct Characterization of Commercial Lecithins by Easy Ambient Sonic-Spray Ionization Mass Spectrometry. *Food Chem.* **2012**, *135*, 1855–1860. [CrossRef]
23. Alves, E.; Simoes, A.; Domingues, M.R. Fruit Seeds and Their Oils as Promising Sources of Value-Added Lipids from Agro-Industrial Byproducts: Oil Content, Lipid Composition, Lipid Analysis, Biological Activity and Potential Biotechnological Applications. *Crit. Rev. Food Sci. Nutr.* **2021**, *61*, 1305–1339. [CrossRef]
24. Alves, E.; Domingues, M.; Domingues, P. Polar Lipids from Olives and Olive Oil: A Review on Their Identification, Significance and Potential Biotechnological Applications. *Foods* **2018**, *7*, 109. [CrossRef] [PubMed]
25. Yang, Y.; Liang, Y.; Yang, J.; Ye, F.; Zhou, T.; Gongke, L. Advances of Supercritical Fluid Chromatography in Lipid Profiling. *J. Pharm. Anal.* **2019**, *9*, 1–8. [CrossRef]
26. Dogra, R.; Kumar, M.; Kumar, A.; Roverso, M.; Bogialli, S.; Pastore, P.; Mandal, U.K. Derivatization, an Applicable Asset for Conventional HPLC Systems without MS Detection in Food and Miscellaneous Analysis. *Crit. Rev. Anal. Chem.* **2022**, 1–21. [CrossRef] [PubMed]
27. Cajka, T.; Fiehn, O. Comprehensive Analysis of Lipids in Biological Systems by Liquid Chromatography-Mass Spectrometry. *TrAC Trends Anal. Chem.* **2014**, *61*, 192–206. [CrossRef] [PubMed]
28. York, J.L.; Magnuson, R.H.; Schug, K.A. On-Line Sample Preparation for Multiclass Vitamin, Hormone, and Mycotoxin Determination in Chicken Egg Yolk Using LC-MS/MS. *Food Chem.* **2020**, *326*, 126939. [CrossRef]
29. Siejak, P.; Smułek, W.; Nowak-Karnowska, J.; Dembska, A.; Neunert, G.; Polewski, K. Bird Cherry (Prunus Padus) Fruit Extracts Inhibit Lipid Peroxidation in PC Liposomes: Spectroscopic, HPLC, and GC–MS Studies. *Appl. Sci.* **2022**, *12*, 7820. [CrossRef]
30. Liu, Y.; Wang, Y.; Hao, Z.; Pan, L. HPLC Method for Separation of Cannabidiol Hemp Seed Oil with Skin Lipids and Tandem HRMS Technology for Characterization of a Chemical Marker. *Cosmetics* **2021**, *8*, 108. [CrossRef]
31. Lagutin, K.; Mackenzie, A.; Bloor, S.; Scott, D.; Vyssotski, M. HPLC-MS, GC and NMR Profiling of Bioactive Lipids of Human Milk and Milk of Dairy Animals (Cow, Sheep, Goat, Buffalo, Camel, Red Deer). *Separations* **2022**, *9*, 145. [CrossRef]
32. de Toffoli, A.L.; Lanças, F.M.; de Toffoli, A.L.; Maciel, E.V.S.; Fumes, B.H.; Lanças, F.M. The Role of Graphene-Based Sorbents in Modern Sample Preparation Techniques. *J. Sep. Sci.* **2018**, *41*, 288–302. [CrossRef] [PubMed]
33. Mejía-Carmona, K.; Lanças, F.M. Modified Graphene-Silica as a Sorbent for in-Tube Solid-Phase Microextraction Coupled to Liquid Chromatography-Tandem Mass Spectrometry. Determination of Xanthines in Coffee Beverages. *J. Chromatogr. A* **2020**, *1621*, 461089. [CrossRef] [PubMed]
34. Qu, Q.; Gu, C.; Hu, X. Capillary Coated with Graphene and Graphene Oxide Sheets as Stationary Phase for Capillary Electrochromatography and Capillary Liquid Chromatography. *Anal. Chem.* **2012**, *84*, 8880–8890. [CrossRef]
35. Borsatto, J.V.B.; Maciel, E.V.S.; Lanças, F.M. Investigation of the Applicability of Silica-Graphene Hybrid Materials as Stationary Phases for Capillary Liquid Chromatography. *J. Chromatogr. A* **2022**, *1685*, 463618. [CrossRef] [PubMed]

36. Liu, W.; Song, Q.; Yan, Y.; Liu, Y.; Li, P.; Wang, Y.; Tu, P.; Song, Y.; Li, J. Integrated Approach for Confidence-Enhanced Quantitative Analysis of Herbal Medicines, Cistanche Salsa as a Case. *J. Chromatogr. A* **2018**, *1561*, 56–66. [CrossRef] [PubMed]
37. Liebisch, G.; Drobnik, W.; Lieser, B.; Schmitz, G. High-Throughput Quantification of Lysophosphatidylcholine by Electrospray Ionization Tandem Mass Spectrometry. *Clin. Chem.* **2002**, *48*, 2217–2224. [CrossRef] [PubMed]

Capítulo 8

Applicability and limitations of a capillary-LC column-switching system using hybrid graphene-based stationary phases

Borsatto, João Victor Basolli; Maciel, Edvaldo Vasconcelos Soares; Cifuentes, Alejandro; Lanças, Fernando Mauro. Applicability and Limitations of a Capillary-LC Column-Switching System Using Hybrid Graphene-Based Stationary Phases. **Molecules**, *[S. l.]*, v. 28, n. 13, p. 4999, 2023. b. DOI: 10.3390/molecules28134999. Disponível em: https://www.mdpi.com/1420-3049/28/13/4999.

molecules

MDPI

Article

Applicability and Limitations of a Capillary-LC Column-Switching System Using Hybrid Graphene-Based Stationary Phases

João Victor Basolli Borsatto [1,2], Edvaldo Vasconcelos Soares Maciel [1,3], Alejandro Cifuentes [2,*] and Fernando Mauro Lanças [1,*]

[1] Laboratory of Chromatography, Institute of Chemistry at Sao Carlos, University of Sao Paulo, P.O. Box 780, Sao Carlos 13566590, Brazil; jvictorborsatto@usp.br (J.V.B.B.); daltoniqsc@gmail.com (E.V.S.M.)
[2] Laboratory of Foodomics, Institute of Food Science Research (CIAL, CSIC), Nicolás Cabrera 9, 28049 Madrid, Spain
[3] Clemens Schöpf Institute, Department of Chemistry, Technical University of Darmstadt, 64287 Darmstadt, Germany
* Correspondence: a.cifuentes@csic.es (A.C.); flancas@iqsc.usp.br (F.M.L.)

Abstract: Graphene oxide sheets fixed over silica particles (SiGO) and their modification functionalized with C18 and endcapped (SiGO-C18ec) have been reported as sorbents for extraction and analytical columns in LC. In this study, a SiGO column was selected as the extraction column and a SiGO-C18ec as the analytical column to study the applicability and limitations of a column-switching system composed exclusively of columns packed with graphene-based sorbents. Pyriproxyfen and abamectin B1a were selected as the analytes, and orange-flavored carbonated soft drinks as the matrix. The proposed system could be successfully applied to the pyriproxyfen analysis in a concentration range between 0.5 to 25 µg/mL presenting a linearity of R^2 = 0.9931 and an intra-day and inter-day accuracy of 82.2–111.4% (RSD < 13.3%) and 95.5–99.8% (RSD < 12.7%), respectively. Furthermore, the matrix composition affected the area observed for the pyriproxyfen: the higher the concentration of orange juice in the soft drink, the higher the pyriproxyfen the signal observed. Additionally, the SiGO extraction column presented a life use of 120 injections for this matrix. In contrast, the proposed system could not apply to the analysis of abamectin B1a, and the SiGO-C18ec analytical column presented significant tailing compared to a similar approach with a C18 analytical column.

Keywords: capillary liquid chromatography; graphene-based materials; packed column; column switching; direct injection; SiGO; SiGO-C18ec

Citation: Borsatto, J.V.B.; Maciel, E.V.S.; Cifuentes, A.; Lanças, F.M. Applicability and Limitations of a Capillary-LC Column-Switching System Using Hybrid Graphene-Based Stationary Phases. *Molecules* **2023**, *28*, 4999. https://doi.org/10.3390/molecules28134999

Academic Editors: Gavino Sanna and Petr Bednar

Received: 12 May 2023
Revised: 15 June 2023
Accepted: 19 June 2023
Published: 26 June 2023

1. Introduction

Graphene and graphene-based materials are used in diverse analytical chemistry applications [1–3]. These materials have also been receiving increasing attention in sample preparation and liquid chromatography (LC) in the last decade. Graphene-based phases can be present in different ways. Fe_3O_4 magnetic particles containing graphene [4] or graphene oxide [5], graphene-based aerogels [6,7] and hydrogels [8,9], and graphene-based material fixed on silica particles [10–12] are examples of how these materials can be produced. Other possibilities of application for graphene-based materials are summarized in recent reviews [13–15].

Applications in separation science are as diverse as the possibilities of graphene-based material compositions [16–18]. Techniques such as stir bar sorptive extraction [16,19], solid-phase extraction [10,20], fiber solid-phase microextraction [20,21], in-tube solid-phase microextraction [12,22], and others [1,23,24] are examples of graphene-based material applications in sample preparation techniques. A particular focus can be given to column-switching methods coupled with LC or miniaturized LC because they minimize the steps

of sample preparation procedures [25,26]. Sample preparation errors are one of the three most predominant sources of error in analytical chemistry [27]. Among the graphene-based phases applied to column-switching, graphene oxide sheets fixed to amino-silica particles (SiGO) and graphene oxide sheets fixed to amino-silica particles functionalized with C18 and endcapped (SiGO-C18ec) can be highlighted. These phases have been successfully applied in environmental, biological, and food analysis [28,29]. For example, extraction columns (also known as pre-concentration columns) packed with SiGO-C18ec particles have been applied with success in studies of pesticides in sugarcane spirits [30], mycotoxin separation in beverages [31], and xanthines in coffee beverages [32]. Examples of their application in a column-switching setup containing SiGO particles in the extraction column are the determination of β-lactams from environmental water samples [33], pesticides in sugarcane spirits [30], and resolution of antidepressant and antiepileptic drugs in urine [34].

Graphene-based materials have also been explored as packing material for analytical columns in LC [28]. Graphene sheets fixed to silica particles [35,36], graphene oxide sheets fixed to silica particles functionalized with C18 [37,38], graphene sheets fixed to silica particles modified with gold nanoparticles [39], and cellulose-coated reduced oxide sheets fixed to silica particles [40] are examples of some materials that have been applied as stationary phases in liquid chromatography. Columns packed with the SiGO-C18ec phase have been successfully used in quantitative analyses of hormones in urine samples [41]. A recent study compared a SiGO-C18ec with a commercial C18 column, both packed capillary LC columns operating in reverse-phase LC [42]. It was observed that SiGO-C18ec phases present different selectivity from C18 phases. Once graphene-based columns are applicable as both extraction and analytical columns in column-switching mode, it is possible to presume that a column-switching system composed of only graphene-based columns could be viable. This work evaluates the applicability and limitations of a column-switching system consisting exclusively of columns packed with graphene-based stationary phases. To the best of our knowledge, no work has described the use of a column-switching system composed exclusively of graphene-based packed columns in any application, and this a vacancy to be investigated. For this study, a SiGO column was selected as the extraction column and a SiGO-C18ec as the analytical column. In addition, pyriproxyfen and abamectin B1a were selected as analytes, and orange-flavored carbonated soft drinks as a matrix. Orange soft drink, are an interesting matrix to evaluate this proposed column-switching system. Though this matrix is complex and presents solid material in suspension, it can also be directly injected in the column-switching system without pretreatment. Pyriproxyfen and abamectin B1a are insecticides employed to control several pest species in diverse cultures. They have been selected as model analytes for this study because quantitative analysis has already been reported in the literature for both compounds in orange and orange by-product samples [43,44]. The leading figures of merit were evaluated, including linearity, accuracy, and precision of the calibration curve, the matrix effect, and the column life-use parameters. A comparison of the peak shape with a C18 analytical column is presented.

2. Results and Discussion

2.1. Selection of the Analytes

Pyriproxyfen and abamectin B1a are pesticides from two distinct chemical classes, which present different structures (Figure 1).

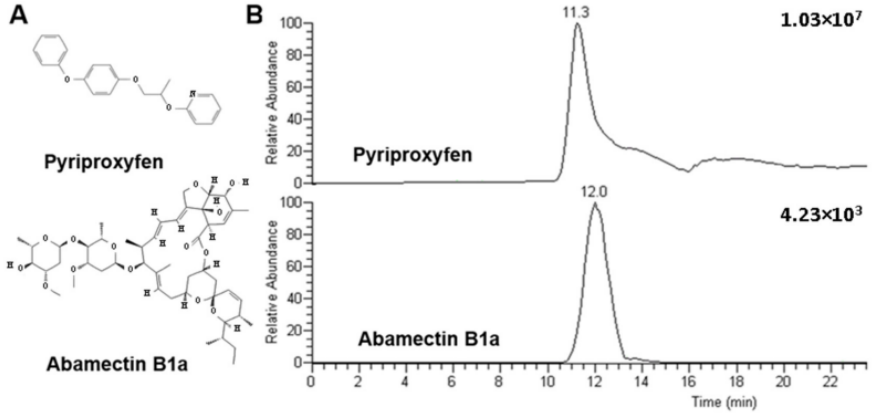

Figure 1. Structure of the analytes evaluated (**A**) and chromatograms obtained in the column-switching method described (**B**). Separation conditions: loading time of 3 min at 50 µL/min, linear gradient from 50% to 100% B in 15 min followed by an additional 5 min of 100% of B; 100 µL of the sample at a concentration of 10 µg/mL of each analyte was injected.

Pyriproxyfen mainly comprises aromatic rings and abamectin B1a by aliphatic chains (Figure 1A). Despite these structural differences, pyriproxyfen and abamectin B1a presented closed retention times in the column-switching system composed of the columns packed with SiGO and SiGO-C18ec (Figure 1B). The similarity in the retention time indicated that both analytes were similarly retained in the proposed column-switching system. This characteristic was important to evaluate whether the proposed column-switching system, composed exclusively of columns packed with graphene-based phases, is multipurpose or not. If the system demonstrated successful quantitative analysis for only one of the analytes, it would suggest its limitations as a multipurpose system. Conversely, if it provided suitable quantitative analysis for both compounds, further investigation would be necessary to confirm the multipurpose capabilities of the system. Because of the characteristics mentioned above, these compounds were selected for this study. In addition, the gradient method was optimized to ensure the elution of the monitored compounds and to elute non-monitored compounds that could stay retained in the columns and reduce the life use of the devices (Section 2.6 details the life-use aspects of these columns). Figure 1B depicts two other pieces of evidence: (i) the pyriproxyfen MRM chromatogram presents a more intense signal than the abamectin 1Ba MRM chromatogram; and (ii) the pyriproxyfen MRM chromatogram presents a more pronounced tail, which is almost not present in the abamectin B1a chromatogram.

2.2. Loading Method

The first variable evaluated for this study was the loading flow rate. The loading flow rate directly affects the extraction of the analytes in the extraction column. Figure 2 shows the area and the relative standard deviation (% RSD) obtained for both evaluated compounds at 25, 50, and 100 µL/min loading flow rates.

The loading flow rate did not affect the area obtained for the pyriproxyfen (Figure 2A), but a reduction in the % RSD was observed with the decrease in the loading flow rate (Figure 2B). For the abamectin B1a, the 50 µL/min loading flow rate resulted in a higher area (Figure 2C) and lower relative % RSD (Figure 2D) than the other explored. Therefore, the 50 µL/min loading flow rate was selected to be used this study because it allowed for better extraction of both analytes from the matrix.

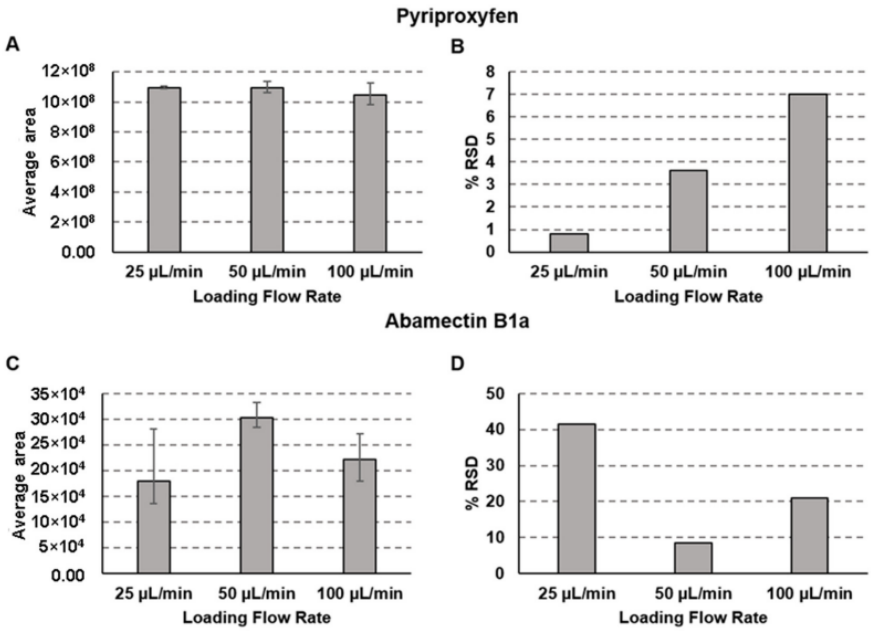

Figure 2. The area obtained with loading flow rates of 25, 50, and 100 µL/min (**A**) and % RSD for each loading flow rate (**B**) for pyriproxyfen and the area obtained with loading flow rates of 25, 50, and 100 µL/min (**C**) and % RSD for each loading flow rate (**D**) for abamectin B1a. Separation conditions: loading time of 3 min at 50 µL/min, linear gradient from 50% to 100% B in 15 min followed by an additional 5 min of 100% of B; 100 µL of the sample at a concentration of 10 µg/mL of each analyte was injected. The analyses were performed in triplicate for each flow rate, and the error bars represent the maximal and minimal values observed experimentally.

2.3. Linearity of the Calibration Curve

Calibration curves are the core of quantitative analysis [45]. The experimental data in Figure 3 shows that the column-switching method presented an excellent linearity for the study of pyriproxyfen, with $R^2 > 0.99$ (Figure 3A).

The % RSD for the pyriproxyfen analysis was lower than 12% for all the concentrations (Figure 3B). Both observations suggest that the experimental setup composed of a first column containing SiGO (extraction column) and a second column of SiGO-C18ec (analytical column) is suitable for analyzing pyriproxyfen in beverages consisting of orange juice. On the other hand, for abamectin B1a, the calibration curve did not present good linearity, with $R^2 < 0.47$ (Figure 3C), and gave high values for % RSD (Figure 3D). Based on that observation, it is possible to point out one of the limitations of the explored system: SiGO columns are not multipurpose, at least not at this point of development, and their application could still be limited. These limitations are already expected once graphene-derived columns are under early development. Usually, each kind of reverse-phase stationary phase has a specific range of operations. In some cases, it can be broad (C18, as an example) but limited in others (chiral phases, as an example). Although it demands much more investigation before a conclusion can be drawn, it seems that the graphene-based stationary phase can become one option for specific applications instead of a multipurpose phase.

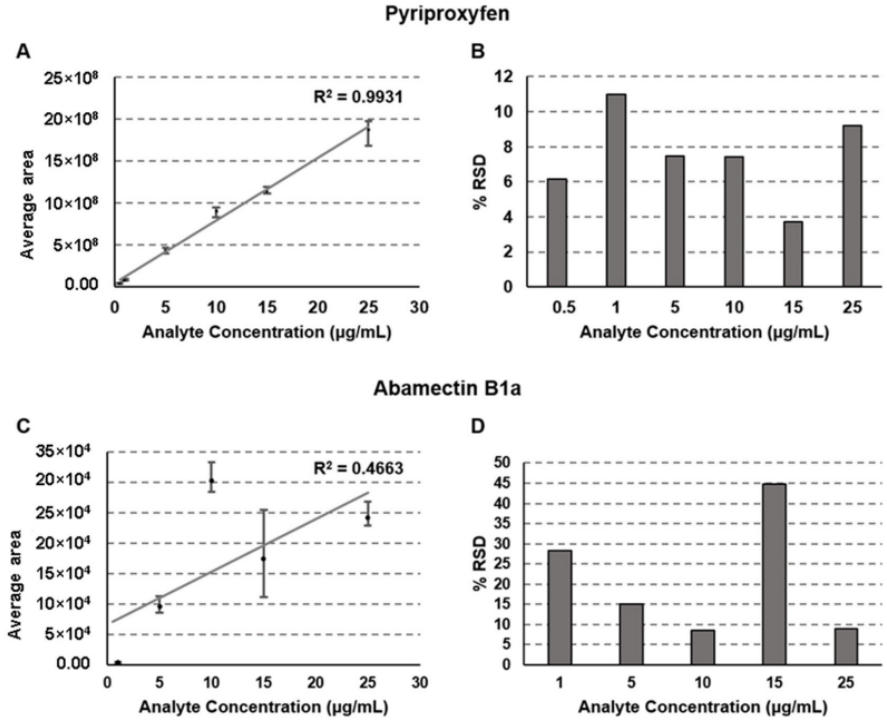

Figure 3. The calibration curve (**A**) and % RSD for each point of the calibration curve (**B**) for pyriproxyfen and the calibration curve (**C**) and % RSD for each point of the calibration curve (**D**) for abamectin B1a. Separation conditions: loading time of 3 min at 50 µL/min, linear gradient from 50% to 100% B in 15 min followed by an additional 5 min of 100% of B; 100 µL of the sample was injected. The analyses were performed in triplicate for each concentration and the error bars represent the maximal and minimal values observed experimentally.

2.4. Intra-Day and Inter-Day Accuracy and Precision

Accuracy and precision are other critical factors in quantitative analysis. For this work, the acceptance criteria were accuracy between 70–110% and precision with % RSD <20%; these values were based on previous work using graphene-based extraction or analytical columns [33,41]. Table 1 presents the accuracy and precision data obtained. For the pyriproxyfen analysis, the intra-day % RSD was lower than 20% for all the points and, in most determinations, lower than 10%.

The inter-day % RSD for this compound was 12.7%, 3.9%, and 2.9% for 2, 8, and 20 µg/mL concentrations, respectively. The intra-day accuracy for the analysis of the pyriproxyfen was between 82.2% and 111.4%, and the inter-day accuracy was between 95.5% and 99.8%. For the analysis of abamectin B1a, the proposed column-switching system was demonstrated not to be reliable. For this compound, obtaining intra-day and inter-day % RSD higher than 20% and accuracy in a wide range between 5.8% and 207% was typical. The observations stated in the last section are confirmed here. Graphene-based stationary phases are promising phases that can be used in a column-switching system, but their applications might not be multipurpose and present limitations.

Table 1. Intra-day and inter-day accuracy and precision (% RSD) obtained using the described column-switching system for both analytes. Separation conditions: loading time of 3 min at 50 µL/min, linear gradient from 50% to 100% B in 15 min followed by an additional 5 min of 100% of B; 100 µL of sample was injected.

Compound		**Pyriproxyfen**			**Abamectin B1a**		
Concentration (µg/mL)		**2**	**8**	**20**	**2**	**8**	**20**
Expected Area *		190,000,000	610,000,000	1,450,000,000	84,362	136,104	239,587
Day 1	Area	176,290,988	612,883,132	1,438,632,466	4899	120,972	274,393
	Intra-Day RSD %	5.8	7.8	3.1	172.8	22.6	9
	% Accuracy **	92.8	100.5	99.2	5.8	88.9	114.5
Day 2	Area	156,108,411	621,257,647	1,501,904,177	7836	99,444	378,336
	Intra-Day RSD %	8.9	13.3	3.3	96.1	31.3	3
	% Accuracy **	82.2	101.8	103.6	9.3	73.1	157.9
Day 3	Area	211,749,192	567,532,037	1,399,813,509	12,072	282,730	372,730
	Intra-Day RSD %	3.2	5.3	5.4	344.6	18.9	17
	% Accuracy **	111.4	93.0	96.5	14.3	207.7	155.6
Average Inter-Day Area		181,382,863	600,557,605	1,446,783,384	8269	167,715	341,820
Inter-Day RSD % ***		12.7	3.9	2.9	35.6	48.8	14
Inter-Day % Accuracy **		95.5	98.5	99.8	9.8	123.2	142.7

* Calculated based on the calibration curve. ** Accuracy is calculated based on the expected area from the calibration curve. *** Calculated based on the intra-day averages.

2.5. Matrix Effects

The matrix composition might affect the analytical signal (peak area, as an example) observed, interfering with the analysis. This is called the "matrix effect". Knowledge about the matrix effect is essential in most analysts' chromatography column-switching approach to extraction, especially when a sample pretreatment is not included in the analytical workflow before the injection step. To conduct this experiment, two commercial orange-flavored soft drinks with different proportions of orange juice in their compositions and spiked with pyriproxyfen in water were explored. Only pyriproxyfen was used to study the effect of the matrix. In the concentration of 2 µg/mL, the impact of the matrix was minimal. However, the analytes might have been better extracted in orange juice samples than pure water (Figure 4A).

The same trend was observed for the concentration of 8 µg/mL: the extraction in both samples containing orange juice was similar, and both were better than the aqueous sample (Figure 4B). For the 20 µg/mL solution, it is noted that the higher the percentage of orange juice in the matrix composition, the higher the area of the pyriproxyfen obtained (Figure 4C). These observations allow us to conclude that the matrix affects the extraction capability of the SiGO column, and this effect is more perceptible as the concentration of the analytes increases. These observations are even more visible in Figure 4D, which summarizes the average area obtained for the samples containing 2, 8, and 20 µg/mL of pyriproxyfen.

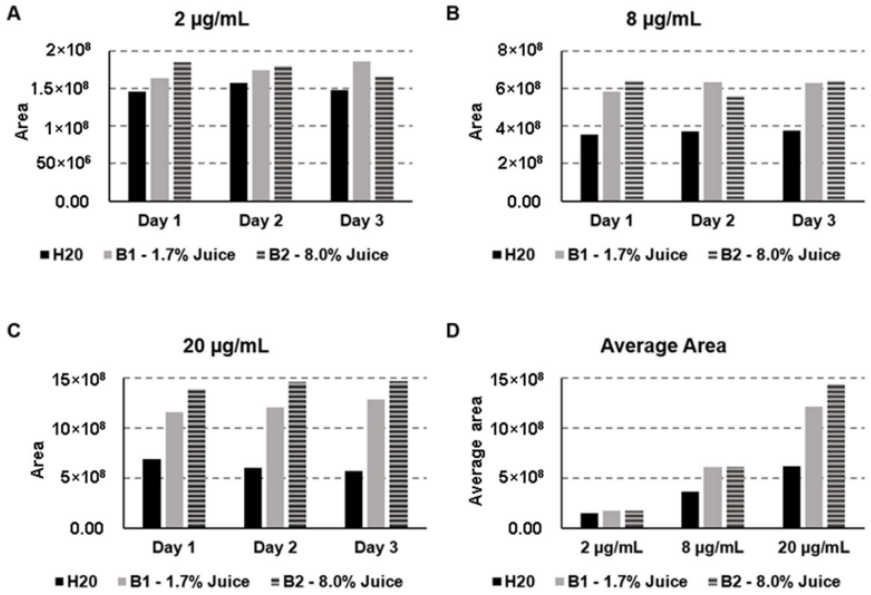

Figure 4. Matrix effect in the obtained area of pyriproxyfen for the 2 µg/mL (**A**), 8 µg/mL (**B**), 20 µg/mL (**C**), and a comparison of the average for the three concentrations (**D**). Separation conditions: loading time of 3 min at 50 µL/min, linear gradient from 50% to 100% B in 15 min followed by an additional 5 min of 100% of B; 100 µL of analytes were injected.

2.6. System Life Use

As yet, the life use of graphene-based columns is uncertain. In this study, we hope to bring some light to this aspect. The analyses were performed by injecting the sample without any preparation (despite adding 25% acetonitrile to keep the analytes soluble). After its hundredth analysis, the SiGO column (extraction column) presented for the first time a carry-over effect (Figure 5). Additionally, the column showed a blockage after about the 120th analysis. The column was washed in the back flush mode, removing the blockage, but the carry-over effect remained.

Additionally, after the washing, the column lost its repeatability compared to the previous separations. Therefore, the column was not considered helpful after this for this application. In contrast, although the SiGO-C18ec column (analytical) has an unknown life-use time, it has been used in uncountable separations (at least more than 300) and remains usable. It is essential to highlight that the SiGO-C18ec column used in this study has been used only as the analytical column, which may favor its durability.

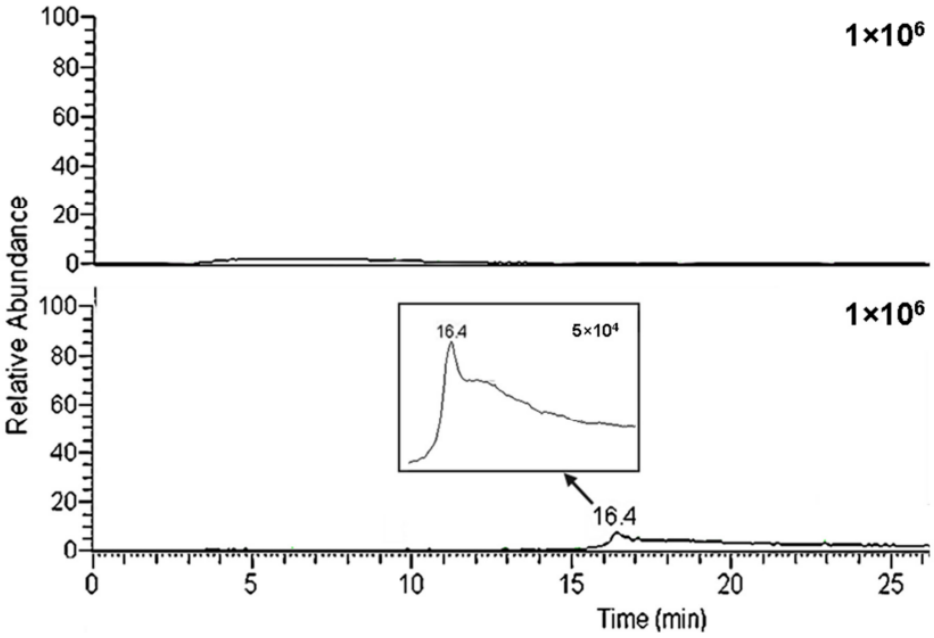

Figure 5. Blanks were obtained after 50 and 100 analyses performed in the same column. Separation conditions: loading time of 3 min at 50 µL/min, linear gradient from 50% to 100% B in 15 min followed by an additional 5 min of 100% B. No sample was injected.

2.7. Peak Shape Comparison with C18 Analytical Column

Another variable explored was the effect of the analytical column in the chromatograms obtained by the described column-switching method. The SiGO-C18ec (0.3 × 100 mm, 10 µm FPPs) column was compared to a C18 column (50 × 2.6 mm, 1.9 µm SPPs) using the same chromatographic method (Figure 6). For the abamectin B1a, it is clear that the C18 column resulted in thinner peaks than the SiGO-C18ec column for all the concentrations explored. No tail was observed for this compound in either column. However, a similar tailing was observed in both columns for the pyriproxyfen analysis, indicating that it may be caused in the SiGO extraction column. Although both columns presented tails for the pyriproxyfen peak, the tailing was higher (proportionally to the peak height) on the SiGO-C18ec column. In some separations using the SiGO-C18ec column, especially at concentrations $\geq$ 15 µg/mL, additional analysis was necessary to understand better and define when the tail ends and the baseline starts. One relevant highlight that must be taken into account here is the difference between the particle diameter and its porosity between the columns compared. The SiGO-C18ec is packed with 10 µm FPPs, while the C18 column is packed with 1.9 µm SPPs. Usually, reducing the particle diameter results in better performance, and reducing the particle core porosity does the same [46,47]. Additionally, as already mentioned, the SiGO-C18ec columns are in an early, underdevelopment stage, and their comparison to the well-established C18 columns needs to be conducted carefully. A positive affirmation about the SiGO-C18ec columns is that it is possible to confirm that it can be applied as a stationary phase and replace C18 columns occasionally. As a negative statement about the SiGO-C18ec columns, it is possible to affirm that it still demands several developments to be at a comparable stage with C18.

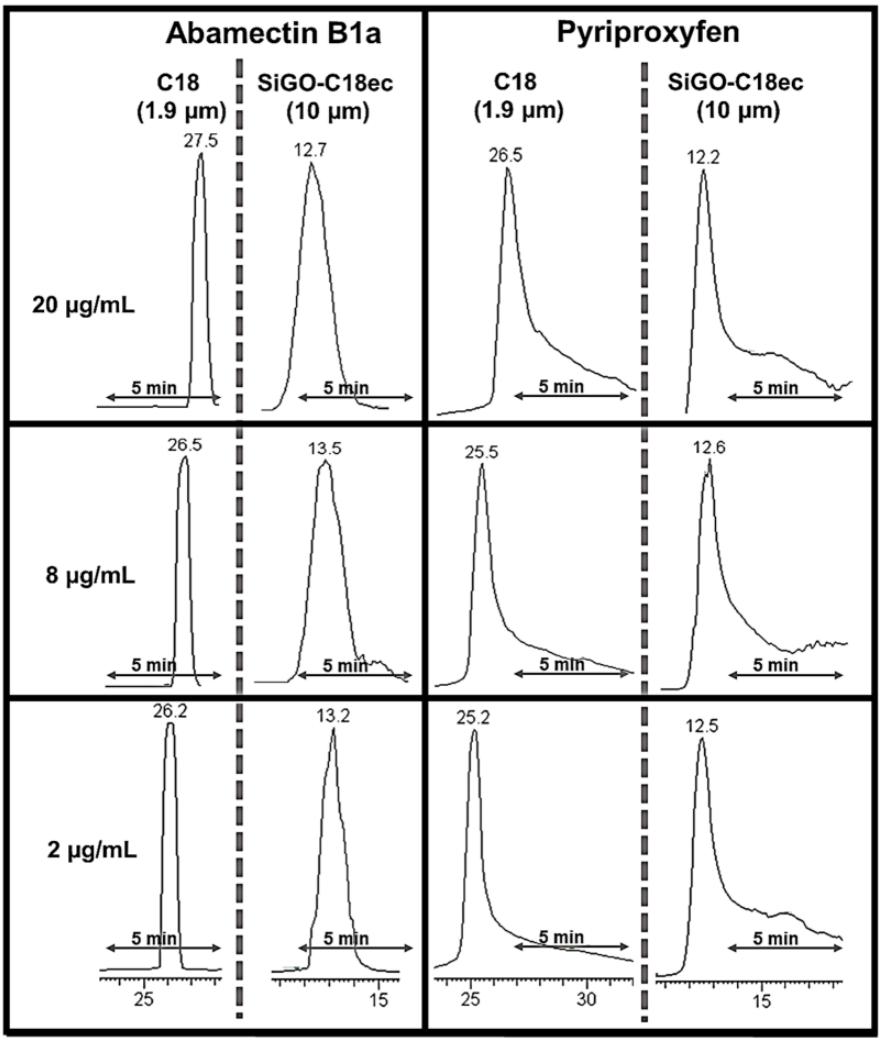

Figure 6. Comparisons of peak shape obtained for abamectin B1a and pyriproxyfen using C18 and SiGO-C18ec column as an analytical column in the column-switching system. Separation conditions: loading time of 3 min at 50 µL/min, linear gradient from 50% to 100% B in 15 min followed by an additional 5 min of 100% of B; 100 µL of analytes were injected.

The conclusions drawn via visual observation of peak shape were corroborated by analyzing the peak capacity performance parameter. In the proposed chromatographic method, the SiGO-C18ec column exhibited a peak capacity of six peaks in 15 min. In comparison, the C18 column demonstrated a peak capacity of 12 peaks under similar conditions, both at a concentration of 8 µg/mL. The peak capacity was determined at 13.4% of the peak height (equivalent to 4σ). However, the peak capacity observed in this study was lower than that reported in the literature for columns containing the same phase (SiGO-C18ec particles of 10 µm diameter). Notably, for hormone separation, a peak capacity of around 27 peaks in 15 min was reported [41], while for the separation of multiclass analytes, the reported peak capacity was 14 peaks in 15 min [42]. A comparison with other

graphene-based stationary phases revealed similar outcomes. For instance, a peak capacity of approximately 19 peaks in 8 min was obtained to separate aromatic compounds using a stationary phase composed of octadecylsilane-functionalized graphene oxide coated over silica particles [37]. In another study, separations of anilines utilizing graphene oxide coated over silica particles displayed an estimated peak capacity of 15 peaks in 12 min [36]. Additionally, a significantly higher result, estimating a peak capacity of 57 peaks in 18 min, was reported for separating alkylbenzenes using a stationary phase composed of octadecyl amine and serine-derived carbon dot-modified silica gel [48]. The estimated peak capacity reported in the above three instances was evaluated based on chromatograms available in the references.

3. Material and Methods

3.1. Reagents and Standards

LC-grade acetone, acetonitrile, and MS-grade high-purity (>98%) formic acid were purchased from VWR International (Fontenay-sous-Bois, France). Deionized ultrapure water (H_2O) was produced in the lab by a Milli-Q® Millipore system (Burlington, NJ, USA). The SiGO and SiGO-C18ec fully porous particles (FPPs) were produced as described by Maciel et al. [41]. The C18 column packed with 1.9 µm superficially porous particles (SPPs) was a Hypersil GOLD 50 × 2.1 mm (Thermo Electronic Corporation, San Jose, CA, USA). Pyriproxyfen and abamectin B1a were acquired from Cymit Chimica (Barcelona, Spain). The orange-flavored carbonated soft drinks comprising 8% orange juice (Kas Naranja, PepsiCo, Spain) and 1.7% (Schweppes Naranja, Schweppes, S.A. Spain) were both acquired in a local market.

3.2. Sample Preparation

The analytes' standards were solubilized to a 1000 µg/mL solution in pure acetone and then diluted to 100 µg/mL in 90% acetonitrile and 10% acetone solution. The 100 µg/mL pesticide solution produced the 0.5–25 µg/mL samples by spiking the analytes in the matrix. The samples comprised 25% organic fraction and 75% orange-flavored carbonated soft drinks. The soft drink with 8% orange juice in the composition spiked with the analytes was used for the calibration curves, accuracy and precision, and comparison with C18 column experiments. Solutions of 2, 8, and 20 µg/mL of each orange-flavored carbonated soft drink and water (25% organic and 75% water) were used to evaluate the matrix effect. The orange-flavored carbonated soft drinks were selected as the matrix because, although it is a complex matrix, it can be directly injected into the system without pretreatment.

3.3. Analytical Instrumentation

A liquid chromatography Accela LC system composed of an auto-sampler, a column temperature controller, and a quaternary pump (Thermo Electronic Corporation, San Jose, CA, USA) coupled with a TSQ Quantum Access triple-quadrupole mass spectrometer (MS) fitted with an electrospray ion (ESI) source (Thermo Electronic Corporation, San Jose, CA, USA) was used in this work. A 100 µL loop was placed in the injection valve. Analyses were carried out using lab-made SiGO and SiGO-C18ec columns prepared as described by Borsatto et al. [42], using 100 × 0.3 mm tubing and 5 µm SiGO FPPs and 10 µm SiGO-C18ec FPPs. The column-switching system was assembled as shown in Figure 7. The SiGO column (extraction column) was connected between the injection valve and the MS valve, and the SiGO-C18ec column was connected between the MS valve and the ESI inlet.

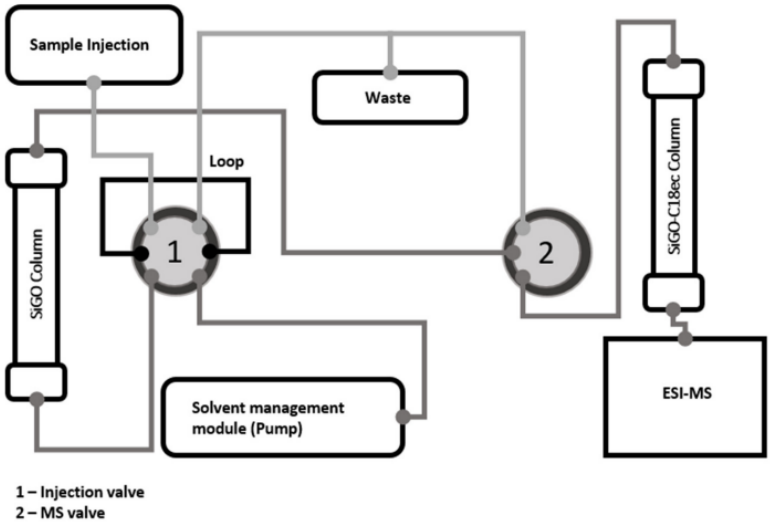

Figure 7. Scheme illustrating the column-switching system evaluated.

3.4. Analytical Methods

The mobile phase consisted of H_2O (A) and acetonitrile (B), both containing 0.1% of formic acid as an additive to enhance the positive electrospray (ESI) ionization process. In addition, a gradient method was used, as described in Table 2.

Table 2. HPLC column-switching events.

Event	Time	% B	Injection Valve Position	MS Valve Position
Pre-run	0 min	0%	Loading	Waste
Loading	0 to 3 min	0%	Inject	Waste
Gradient	3 to 18 min	50% to 100%	Inject	ESI-MS
Isocratic	18 to 23 min	100%	Inject	ESI-MS

An equilibration gradient drove the mobile phase composition back to 100% H_2O in 5 min, followed by an additional 10 min of constant 100% H_2O. The flow rate was kept constant at 50 µL/min, except for the loading flow rate experiment, in which 25 and 100 µL/min flows were also explored. The MS parameters were spray voltage of 4000 V, N_2 desolvation gas flow of 20 L/h, and capillary temperature of 400 °C. A multiple reaction monitoring (MRM) mode was used to observe the analytes. The quantifying transitions were 322 > 185 (collision energy of 20 V) for pyriproxyfen and 895 > 449 (collision energy of 40 V) for abamectin B1a. The qualifying transitions were 322 > 96 (collision energy of 40 V) for pyriproxyfen and 895 > 305 (collision energy of 70 V) for abamectin B1a.

4. Conclusions

This study investigated the applicability and limitations of a column-switching system composed exclusively of columns packed with graphene-based stationary phases. The samples of orange-flavored soft drinks with spiked analytes (25% of acetonitrile added to the samples) were directly injected without pretreatment or sample preparation. It was observed that the proposed column-switching system presented good linearity in the calibration curve and reasonable accuracy and precision (% RSD) for pyriproxyfen analysis, but not for abamectin B1a analysis. Furthermore, it demonstrated that this system could be applied to reliable quantitative analysis, but it is not multipurpose and presents limitations. The main restrictive factor was the limited capability of the SiGO extraction column to

retain some analytes well. It was also observed that the proportion of orange juice in the matrix composition affected the results.

Additionally, it was noted that the life use of the SiGO extraction column was about 120 injections in the explored conditions, blockages and carry-over effects being observed. In the last stage of this study, the analytical SiGO-C18ec column was compared with a commercial C18 column. It was noted that although the C18 column presented better performance with thinner peaks and less tail, owing to the much smaller particle size of the stationary phase, the SiGO-C18ec columns can be applied for the same use with no practical restriction. In short, graphene-based particles are promising stationary phases for liquid chromatography and can be applied in both dimensions of a column-switching system. Although columns packed with these materials have been finding current applications in LC, improvements are still needed to increase the range of applications and life use. If these phases keep being developed and optimized, soon it might become an additional solution for separation science applications. Optimizations in the injection process and the detection method could improve the sensibility and applicability of this system proposed and might be an interesting topic to be investigated in the future. Furthermore, ramifications of this work to investigate different analytes in the various matrix could lead to a better understanding of these phases and help to draw the boundary conditions for these systems.

Author Contributions: Conceptualization, J.V.B.B.; methodology, J.V.B.B.; investigation, J.V.B.B. and E.V.S.M.; resources, F.M.L. and A.C.; writing—original draft preparation, J.V.B.B.; writing—review and editing, J.V.B.B., E.V.S.M., F.M.L. and A.C.; supervision, F.M.L. and A.C.; project administration, F.M.L. and A.C.; funding acquisition, F.M.L. and A.C. All authors have read and agreed to the published version of the manuscript.

Funding: The authors are grateful for the financial support from (i) the Coordination for the Improvement of Higher Education Personnel (CAPES—Brazil, Finance Code 001 and Proc. 88887.695324/2022-00); (ii) the São Paulo Research Foundation (FAPESP—Brazil, Grants 2019/22724-7, 2017/02147-0); (iii) the National Council for Scientific and Technological Development (CNPq—Brazil, 307293/2014-9; 308843/2019-3; Proc. 142513/2019-9); and (iv) the Spanish Ministry of Science and Innovation (PID2020-113050RB-I00 project).

Institutional Review Board Statement: Not applicable.

Informed Consent Statement: Not applicable.

Data Availability Statement: Data will be made available on request.

Acknowledgments: The Technical University of Darmstadt—Germany, and the Alexander von Humboldt Foundation—Germany contributed to support this work.

Conflicts of Interest: The authors declare that they have no known competing financial interests or personal relationships that could have appeared to influence the work reported in this paper.

Sample Availability: Not applicable.

References

1. Joshi, D.J.; Koduru, J.R.; Malek, N.I.; Hussain, C.M.; Kailasa, S.K. Surface Modifications and Analytical Applications of Graphene Oxide: A Review. *TrAC Trends Anal. Chem.* **2021**, *144*, 116448. [CrossRef]
2. Justino, C.I.L.; Gomes, A.R.; Freitas, A.C.; Duarte, A.C.; Rocha-Santos, T.A.P. Graphene Based Sensors and Biosensors. *TrAC Trends Anal. Chem.* **2017**, *91*, 53–66. [CrossRef]
3. Huang, T.; Tang, X.; Luo, K.; Wu, Y.; Hou, X.; Tang, S. An Overview of Graphene-Based Nanoadsorbent Materials for Environmental Contaminants Detection. *TrAC Trends Anal. Chem.* **2021**, *139*, 116255. [CrossRef]
4. Li, X.; Li, S.; Bai, J.; Peng, Y.; Ning, B.; Shi, H.; Kang, W.; Zhou, H.; Gao, Z. Determination of Bisphenol A by High-Performance Liquid Chromatography Based on Graphene Magnetic Dispersion Solid Phase Extraction. *J. Chromatogr. Sci.* **2020**, *58*, 280–286. [CrossRef]
5. Zhang, L.; Zhang, Y.; Tang, Y.; Li, X.; Zhang, X.; Li, C.; Xu, S. Magnetic Solid-Phase Extraction Based on Fe_3O_4/Graphene Oxide Nanoparticles for the Determination of Malachite Green and Crystal Violet in Environmental Water Samples by HPLC. *Int. J. Env. Anal. Chem.* **2018**, *98*, 215–228. [CrossRef]

6. Hou, X.; Ding, R.; Yan, S.; Zhao, H.; Yang, Q.; Wu, W. ZrO_2 Nanoparticles and Poly(Diallyldimethylammonium Chloride)-Doped Graphene Oxide Aerogel-Coated Stainless-Steel Mesh for the Effective Adsorption of Organophosphorus Pesticides. *Foods* **2021**, *10*, 1616. [CrossRef]
7. Sun, H.; Feng, J.; Feng, J.; Sun, M.; Feng, Y.; Sun, M. Carbon Aerogels Derived from Waste Paper for Pipette-Tip Solid-Phase Extraction of Triazole Fungicides in Tomato, Apple and Pear. *Food Chem.* **2022**, *395*, 133633. [CrossRef]
8. Gao, Y.; Gao, M.; Chen, G.; Tian, M.; Zhai, R.; Huang, X.; Xu, X.; Liu, G.; Xu, D. Facile Synthesis of Covalent Organic Frameworks Functionalized with Graphene Hydrogel for Effectively Extracting Organophosphorus Pesticides from Vegetables. *Food Chem.* **2021**, *352*, 129187. [CrossRef]
9. Ligorio, C.; Vijayaraghavan, A.; Hoyland, J.A.; Saiani, A. Acidic and Basic Self-Assembling Peptide and Peptide-Graphene Oxide Hydrogels: Characterisation and Effect on Encapsulated Nucleus Pulposus Cells. *Acta Biomater.* **2022**, *143*, 145–158. [CrossRef]
10. Wang, N.; Lu, Y.; Cui, B. Preparation and Application of β-Cyclodextrin Functionalised Graphene Oxide-Grafted Silica Sorbents for Solid-Phase Extraction (SPE) of Polycyclic Aromatic Hydrocarbons from Fried Food Using a Box-Behnken Design. *Food Anal. Methods* **2021**, *14*, 1577–1589. [CrossRef]
11. Song, X.-L.; Lv, H.; Wang, D.-D.; Liao, K.-C.; Wu, Y.-Y.; Li, G.-M.; Chen, Y. Graphene Oxide Composite Microspheres as a Novel Dispersive Solid-Phase Extraction Adsorbent of Bisphenols Prior to Their Quantitation by HPLC–Mass Spectrometry. *Microchem. J.* **2022**, *172*, 106920. [CrossRef]
12. Sun, M.; Han, S.; Maloko Loussala, H.; Feng, J.; Li, C.; Ji, X.; Feng, J.; Sun, H. Graphene Oxide-Functionalized Mesoporous Silica for Online in-Tube Solid-Phase Microextraction of Polycyclic Aromatic Hydrocarbons from Honey and Detection by High Performance Liquid Chromatography-Diode Array Detector. *Microchem. J.* **2021**, *166*, 106263. [CrossRef]
13. Pei, J.; Ren, T.; Huang, Y.; Chen, R.; Jin, W.; Shang, S.; Wang, J.; Liu, Z.; Liang, Y.; Abd El-Aty, A.M. Application of Graphene and Its Derivatives in Detecting Hazardous Substances in Food: A Comprehensive Review. *Front. Chem.* **2022**, *10*, 894759. [CrossRef]
14. Hu, H.; Wen, W.; Ou, J. Z Construction of Adsorbents with Graphene and Its Derivatives for Wastewater Treatment: A Review. *Environ. Sci. Nano* **2022**, *9*, 3226–3276. [CrossRef]
15. Li, Y.; Lan, S.; Zhu, T. Recent Advances of Graphene-Based Sorptive Materials in Extraction: A Review. *TrAC Trends Anal. Chem.* **2021**, *142*, 116319. [CrossRef]
16. Manousi, N.; Kabir, A.; Zachariadis, G.A. Recent Advances in the Extraction of Triazine Herbicides from Water Samples. *J. Sep. Sci.* **2022**, *45*, 113–133. [CrossRef]
17. Musarurwa, H.; Tawanda Tavengwa, N. Recent Progress in the Application of PH-Responsive Polymers in Separation Science. *Microchem. J.* **2022**, *179*, 107503. [CrossRef]
18. Jiang, X.; Ruan, G.; Huang, Y.; Chen, Z.; Yuan, H.; Du, F. Assembly and Application Advancement of Organic-functionalized Graphene-based Materials: A Review. *J. Sep. Sci.* **2020**, *43*, 1544–1557. [CrossRef] [PubMed]
19. Zhou, J.; Wang, R.; Chen, Z. Stir Bar Sorptive Extraction with a Graphene Oxide Framework-Functionalized Stainless-Steel Wire for the Determination of Sudan Dyes in Water Samples. *Anal. Methods* **2019**, *11*, 2050–2056. [CrossRef]
20. Wang, X.; Han, Y.; Cao, J.; Yan, H. Headspace Solid-Phase-Microextraction Using a Graphene Aerogel for Gas Chromatography–Tandem Mass Spectrometry Quantification of Polychlorinated Naphthalenes in Shrimp. *J. Chromatogr. A* **2022**, *1672*, 463012. [CrossRef] [PubMed]
21. Pei, M.; Shi, X.; Wu, J.; Huang, X. Graphene Reinforced Multiple Monolithic Fiber Solid-Phase Microextraction of Phenoxyacetic Acid Herbicides in Complex Samples. *Talanta* **2019**, *191*, 257–264. [CrossRef]
22. de Toffoli, A.L.; Fumes, B.H.; Lanças, F.M. Packed In-Tube Solid Phase Microextraction with Graphene Oxide Supported on Aminopropyl Silica: Determination of Target Triazines in Water Samples. *J. Env. Sci. Health B* **2018**, *53*, 434–440. [CrossRef]
23. Sun, R.; Lu, F.; Yu, C.; Yang, Y.; Qiao, L.; Liu, A. Peanut Shells-Derived Biochars as Adsorbents for the Pipette-Tip Solid-Phase Extraction of Endocrine-Disrupting Phenols in Water, Milk and Beverage. *J. Chromatogr. A* **2022**, *1673*, 463101. [CrossRef] [PubMed]
24. Grajek, H.; Jonik, J.; Witkiewicz, Z.; Wawer, T.; Purchała, M. Applications of Graphene and Its Derivatives in Chemical Analysis. *Crit. Rev. Anal. Chem.* **2020**, *50*, 445–471. [CrossRef]
25. Costa Queiroz, M.E.; Donizeti de Souza, I.; Marchioni, C. Current Advances and Applications of In-Tube Solid-Phase Microextraction. *TrAC Trends Anal. Chem.* **2019**, *111*, 261–278. [CrossRef]
26. Ponce-Rodríguez, H.D.; Verdú-Andrés, J.; Herráez-Hernández, R.; Campíns-Falcó, P. Innovations in Extractive Phases for In-Tube Solid-Phase Microextraction Coupled to Miniaturized Liquid Chromatography: A Critical Review. *Molecules* **2020**, *25*, 2460. [CrossRef]
27. Technical Analytical Methods Committee Briefs What Causes Most Errors in Chemical Analysis? *Anal. Methods* **2013**, *5*, 2914–2915. [CrossRef] [PubMed]
28. Liang, X.; Hou, X.; Chan, J.H.M.; Guo, Y.; Hilder, E.F. The Application of Graphene-Based Materials as Chromatographic Stationary Phases. *TrAC Trends Anal. Chem.* **2018**, *98*, 149–160. [CrossRef]
29. Lanças, F.M.; Medina, D.A.V.; Pereira Dos Santos, N.G.; Sinisterra, M.J. Graphene-Based Sorbents for Modern Magnetic Solid-Phase Extraction Techniques. In *Analytical Applications of Functionalized Magnetic Nanoparticles*; The Royal Society of Chemistry: London, UK, 2021; pp. 174–199.

30. dos Santos, N.G.P.; Maciel, E.V.S.; Mejía-Carmona, K.; Lanças, F.M. Multidimensional Capillary Liquid Chromatography-Tandem Mass Spectrometry for the Determination of Multiclass Pesticides in "Sugarcane Spirits" (Cachaças). *Anal. Bioanal. Chem.* **2020**, *412*, 7789–7797. [CrossRef]
31. MacIel, E.V.S.; Mejiá-Carmona, K.; Lancas, F.M. Evaluation of Two Fully Automated Setups for Mycotoxin Analysis Based on Online Extraction-Liquid Chromatography-TandemMass Spectrometry. *Molecules* **2020**, *25*, 2756. [CrossRef]
32. Mejía-Carmona, K.; Lanças, F.M. Modified Graphene-Silica as a Sorbent for in-Tube Solid-Phase Microextraction Coupled to Liquid Chromatography-Tandem Mass Spectrometry. Determination of Xanthines in Coffee Beverages. *J. Chromatogr. A* **2020**, *1621*, 461089. [CrossRef]
33. Maciel, E.V.S.; Vargas-Medina, D.A.; Lancas, F.M. Analyzes of β-Lactam Antibiotics by Direct Injection of Environmental Water Samples into a Functionalized Graphene Oxide-Silica Packed Capillary Extraction Column Online Coupled to Liquid Chromatography Tandem Mass Spectrometry. *Talanta Open* **2023**, *7*, 100185. [CrossRef]
34. Maciel, E.V.S.; de Toffoli, A.L.; da Silva Alves, J.; Lanças, F.M. Multidimensional Liquid Chromatography Employing a Graphene Oxide Capillary Column as the First Dimension: Determination of Antidepressant and Antiepileptic Drugs in Urine. *Molecules* **2020**, *25*, 1092. [CrossRef] [PubMed]
35. Liang, X.; Liu, S.; Song, X.; Zhu, Y.; Jiang, S. Layer-by-Layer Self-Assembled Graphene Oxide/Silica Microsphere Composites as Stationary Phase for High Performance Liquid Chromatography. *Analyst* **2012**, *137*, 5237. [CrossRef] [PubMed]
36. Zhang, X.; Chen, S.; Han, Q.; Ding, M. Preparation and Retention Mechanism Study of Graphene and Graphene Oxide Bonded Silica Microspheres as Stationary Phases for High Performance Liquid Chromatography. *J. Chromatogr. A* **2013**, *1307*, 135–143. [CrossRef] [PubMed]
37. Liang, X.; Wang, S.; Liu, S.; Liu, X.; Jiang, S. A Novel Octadecylsilane Functionalized Graphene Oxide/Silica Composite Stationary Phase for High Performance Liquid Chromatography. *J. Sep. Sci.* **2012**, *35*, 2003–2009. [CrossRef] [PubMed]
38. Borsatto, J.V.B.; Maciel, E.V.S.; Cifuentes, A.; Lanças, F.M. Online Extraction Followed by LC–MS/MS Analysis of Lipids in Natural Samples: A Proof-of-Concept Profiling Lecithin in Seeds. *Foods* **2023**, *12*, 281. [CrossRef]
39. Liang, X.; Wang, X.; Ren, H.; Jiang, S.; Wang, L.; Liu, S. Gold Nanoparticle Decorated Graphene Oxide/Silica Composite Stationary Phase for High-Performance Liquid Chromatography. *J. Sep. Sci.* **2014**, *37*, 1371–1379. [CrossRef]
40. Li, Y.; Li, Q.; Zhu, N.; Gao, Z.; Ma, Y. Cellulose Type Chiral Stationary Phase Based on Reduced Graphene Oxide@silica Gel for the Enantiomer Separation of Chiral Compounds. *Chirality* **2018**, *30*, 996–1004. [CrossRef]
41. Maciel, E.V.S.; Borsatto, J.V.B.; Mejia-Carmona, K.; Lanças, F.M. Application of an In-House Packed Octadecylsilica-Functionalized Graphene Oxide Column for Capillary Liquid Chromatography Analysis of Hormones in Urine Samples. *Anal. Chim. Acta* **2023**, *1239*, 340718. [CrossRef]
42. Borsatto, J.V.B.; Maciel, E.V.S.; Lanças, F.M. Investigation of the Applicability of Silica-Graphene Hybrid Materials as Stationary Phases for Capillary Liquid Chromatography. *J. Chromatogr. A* **2022**, *1685*, 463618. [CrossRef] [PubMed]
43. Ferrer, C.; Martínez-Bueno, M.J.; Lozano, A.; Fernández-Alba, A.R. Pesticide Residue Analysis of Fruit Juices by LC–MS/MS Direct Injection. One Year Pilot Survey. *Talanta* **2011**, *83*, 1552–1561. [CrossRef] [PubMed]
44. by Liquid Chromatography–Electrospray Tandem Mass Spectrometry. *J. Chromatogr. A* **2003**, *992*, 133–140. [CrossRef]
45. Lee, T.D. Introduction to Modern Liquid Chromatography, Third Edition. *J. Am. Soc. Mass. Spectrom.* **2011**, *22*, 196. [CrossRef]
46. González-Ruiz, V.; Olives, A.I.; Martín, M.A. Core-Shell Particles Lead the Way to Renewing High-Performance Liquid Chromatography. *TrAC Trends Anal. Chem.* **2015**, *64*, 17–28. [CrossRef]
47. Blue, L.E.; Jorgenson, J.W. 1.1μm Superficially Porous Particles for Liquid Chromatography. Part II: Column Packing and Chromatographic Performance. *J. Chromatogr. A* **2015**, *1380*, 71–80. [CrossRef]
48. Zhao, C.; Yan, S.; Liu, J.; Xiong, Z.; Zhao, L. Octadecylamine and Serine-Derived Carbon Dots-Modified Silica Gel for Reversed Phase/Hydrophilic Interaction Liquid Chromatography. *Microchem. J.* **2022**, *183*, 107987. [CrossRef]

Capítulo 9

Conclusão e perspectivas futuras

O estudo sobre o comportamento da fase de SiGO-C18ec em colunas analíticas de cromatografia líquida (LC) representa uma interessante contribuição científica, uma vez que esse tipo de material era pouco explorado nesse contexto. Os resultados alcançados durante o doutorado indicaram que a aplicação de SiGO-C18ec em LC pode ser bem-sucedida. O desenvolvimento de novos materiais para a cromatografia líquida é de importância fundamental para os avanços no campo da química analítica. A cromatografia é uma técnica amplamente utilizada na análise e separação de substâncias em diversas áreas, como farmacologia, biologia, química ambiental, entre outras. Nesse contexto, a utilização de fases estacionárias derivadas de grafeno tem se destacado como uma possibilidade interessante para ampliar o leque de opções disponíveis para LC. Dentre os principais resultados obtidos que apontam nessa direção, colunas de SiGO-C18ec apresentaram seletividade diferente em relação às colunas convencionais de C18 para LC, apontando que essas colunas poderiam ser utilizadas em aplicações nas quais as colunas empacotadas com C18 não são capazes de realizar separações adequadas. No que diz respeito a métodos analíticos, as colunas empacotadas com SiGO-C18ec puderam ser utilizadas tanto em análises quantitativas quanto qualitativas. Embora ainda não seja uma fase multipropósito, ou seja, adequada para uma ampla gama de compostos, os resultados obtidos indicam que ela pode ser aplicada com sucesso em análises específicas, como a quantificação de pesticidas em refrigerantes e biomarcadores em urina, bem como na análise qualitativa de lecitinas em sementes.

Diante dos resultados obtidos, pode-se afirmar que a SiGO-C18ec representa uma alternativa promissora para a cromatografia líquida. No entanto, ainda são necessários estudos adicionais para aprimorar a performance desse material e ampliar sua aplicabilidade em diferentes tipos de análises. Nesse sentido, é possível que futuros estudos possam ser direcionados para o desenvolvimento de fases estacionárias derivadas de grafeno capazes de oferecer uma melhor seletividade e versatilidade em termos de aplicação.

De forma específica, pode-se apontar três possíveis ramificações dessa tese: (i) otimização do empacotamento SiGO-C18ec; (ii) investigação de outras fases de grafeno nas mesmas condições exploradas nessa tese; (iii) diversificação de aplicação das fases de SiGO-C18ec.

A primeira ramificação desses estudos compreende a otimização do empacotamento da fase de SiGO-C18. Usualmente, o empacotamento é feito por meio de um procedimento no qual partículas de fase estacionária são suspensas em uma solução e então empurradas para a coluna através de uma bomba de alta pressão. O empacotamento de uma coluna capilar é um

processo delicado. Para fases como C18, quanto mais aglomeradas as partículas estiverem na suspensão da solução que precede o empacotamento, melhor será a performance da coluna resultante. Já para alguns tipos de fase normal, quanto mais dispersas na solução de empacotamento, melhor será a coluna empacotada. A aglomeração de partículas de fase estacionária na suspensão pré-empacotamento depende das forças eletroestáticas de superfície. Essas interações eletroestáticas podem ser controladas a partir da proporção entre os solventes que compões a solução de suspensão de partículas de fase estacionária. Realizar um estudo sistemático para a otimização do empacotamento de partículas de SiGO-C18ec pode resultar num aumento de performance dessas colunas, uma vez que essas características ainda são desconhecidas.

A segunda ramificação do estudo envolve a investigação de outras fases de grafeno utilizáveis nas mesmas condições exploradas no processo de estudo da fase SiGO-C18ec, em especial, submetê-las à mesma serie experimental do artigo apresentado no capítulo 5. Isso é interessante, pois variar a composição da fase estacionária pode resultar em diferenças nas seletividades da coluna e então apontar uma ou um conjunto de fases que também podem ser promissoras para LC e submetê-las a análises mais aprofundadas. Exemplos de fases que poderiam ser avaliadas nessas condições são partículas de óxido de grafeno funcionalizadas com β-ciclodextrina e óxido de grafeno funcionalizadas com líquidos iônicos.

Por fim, a terceira ramificação a ser explorada é a diversificação da aplicação das fases de SiGO-C18ec, com vistas a ampliar o seu uso em novas áreas de pesquisa. Foi demostrado que as partículas de SiGO-C18ec não é uma fase multipropósito, mas que pode ser eficientemente utilizada para a análise de diversos compostos. Estudos sistemáticos visando expandir a gama de substâncias analisadas por esse tipo de coluna pode ajudar a desenhar as condições de contorno da aplicação de SiGO-C18ec em LC.

Anexo I

Trabalhos publicados

Artigos completos publicados em periódicos internacionais

1. **Borsatto, João Victor Basolli**; Maciel, Edvaldo Vasconcelos Soares; Cifuentes, Alejandro; Lanças, Fernando Mauro. Applicability and Limitations of a Capillary-LC Column-Switching System Using Hybrid Graphene-Based Stationary Phases.

   MOLECULES. Fator De Impacto (2021 Jcr): 4,9270, V.28, P.4999 - , 2023.

2. Maciel, Edvaldo V.S.; **Borsatto, João V.B**.; Mejia-Carmona, Karen; Lanças, Fernando M. Application of an in-house packed octadecylsilica-functionalized graphene oxide column for capillary liquid chromatography analysis of hormones in urine samples.

   ANALYTICA CHIMICA ACTA. Fator de Impacto (2021 JCR): 6,9110, v.1239, p.340718 - , 2023.

3. **Borsatto, João V. B.**; Maciel, Edvaldo V. S.; Cifuentes, Alejandro; Lanças, Fernando M. Online Extraction Followed by LC-MS/MS Analysis of Lipids in Natural Samples: A Proof-of-Concept Profiling Lecithin in Seeds.

   FOODS. Fator de Impacto (2021 JCR): 5,5610, v.12, p.281 - , 2023.

4. Da Silva Burato, Juliana Soares; **Basolli Borsatto, João Victor**; Lanças, Fernando Mauro. Practical aspects of preparation, optimization, and evaluation of poly(styrene-divinylbenzene)porous-layer open tubular (PLOT) columns for capillary liquid chromatography.

   TALANTA. Fator de Impacto (2021 JCR): 6,5560, v.253, p.124106 - , 2023.

5. **Borsatto, João V. B**.; Lanças, Fernando M. Recent Trends in Graphene-Based Sorbents for LC Analysis of Food and Environmental Water Samples.

   MOLECULES. Fator de Impacto (2021 JCR): 4,9270, v.28, p.5134 - , 2023.

6. **Borsatto, João V.B.;** Maciel, Edvaldo V.S.; Lanças, Fernando M. Investigation of the applicability of silica-graphene hybrid materials as stationary phases for capillary liquid chromatography.

JOURNAL OF CHROMATOGRAPHY A. Fator de Impacto (2021 JCR): 4,6010, v.1685, p.463618 - , 2022.

7. Vargas Medina, Deyber Arley; Burato, Juliana Soares Da Silva**; Borsatto, João Victor Basolli**; Lanças, Fernando Mauro. Porous layer open tubular nano liquid chromatography directly coupled to electron ionization mass spectrometry.

   JOURNAL OF CHROMATOGRAPHY A. Fator de Impacto (2021 JCR): 4,6010, v.1674, p.463143 - , 2022.

8. Medina, Deyber Arley Vargas; Pereira Dos Santos, Natalia Gabrielly; Da Silva Burato, Juliana Soares; **Borsatto, João Victor Basolli**; Lanças, Fernando Mauro. An overview of open tubular liquid chromatography with a focus on the coupling with mass spectrometry for the analysis of small molecules.

   JOURNAL OF CHROMATOGRAPHY A. Fator de Impacto (2021 JCR): 4,6010, v.1641, p.461989 - , 2021.

9. Vargas Medina, Deyber Arley; **Bassolli Borsatto, João Victor**; Maciel, Edvaldo Vasconcelos Soares; Lanças, Fernando Mauro. Current role of modern chromatography and mass spectrometry in the analysis of mycotoxins in food.

   TRAC-TRENDS IN ANALYTICAL CHEMISTRY. Fator de Impacto (2021 JCR): 14,9080, v.135, p.116156 - 156, 2021.

10. Maciel, Edvaldo Vasconcelos Soares; Vargas Medina, Deyber Arley; **Borsatto, João Victor Bassolli;** Lanças, Fernando Mauro. Towards a universal automated and miniaturized sample preparation approach.

    SUSTAINABLE CHEMISTRY AND PHARMACY. Fator de Impacto(2021 JCR): 5,4640, v.21, p.100427 - , 2021.

11. Mejía-Carmona, Karen; Soares Da Silva Burato, Juliana**; Basolli Borsatto, João Victor**; Lúcia De Toffoli, Ana; Lanças, Fernando Mauro. Miniaturization of liquid chromatography coupled to mass spectrometry. 1. Current trends on miniaturized LC columns.

    TRAC-TRENDS IN ANALYTICAL CHEMISTRY. Fator de Impacto (2021 JCR): 14,9080, v.122, p.115735 - , 2019.

Trabalhos apresentados em eventos científicos

Borsatto, João Victor Basolli; Maciel, Edvaldo Vasconcelos Soares; Lanças, Fernando Mauro. Hybrid functionalization of spherical silica particles by graphene oxide and octadecylsilane applied to the chromatographic analysis of human biomarkers. Apresentado no 5th *International Conference on Applied Surface Science,* 2022, Palma de Maiorca, Espanha.